ALFRED-WEGENER-INSTITUT
HELMHOLTZ-ZENTRUM FÜR POLAR- UND MEERESFORSCHUNG

709
2017

Berichte
zur Polar- und Meeresforschung

Reports on Polar and Marine Research

Russian-German Cooperation: Expeditions to Siberia in 2016

Edited by
Pier Paul Overduin, Franziska Blender, Dmitry Y. Bolshiyanov, Mikhail N. Grigoriev, Anne Morgenstern and Hanno Meyer

HELMHOLTZ GEMEINSCHAFT

Die Berichte zur Polar- und Meeresforschung werden vom Alfred-Wegener-Institut, Helmholtz-Zentrum für Polar- und Meeresforschung (AWI) in Bremerhaven, Deutschland, in Fortsetzung der vormaligen Berichte zur Polarforschung herausgegeben. Sie erscheinen in unregelmäßiger Abfolge.

Die Berichte zur Polar- und Meeresforschung enthalten Darstellungen und Ergebnisse der vom AWI selbst oder mit seiner Unterstützung durchgeführten Forschungsarbeiten in den Polargebieten und in den Meeren.

Die Publikationen umfassen Expeditionsberichte der vom AWI betriebenen Schiffe, Flugzeuge und Stationen, Forschungsergebnisse (inkl. Dissertationen) des Instituts und des Archivs für deutsche Polarforschung, sowie Abstracts und Proceedings von nationalen und internationalen Tagungen und Workshops des AWI.

Die Beiträge geben nicht notwendigerweise die Auffassung des AWI wider.

Herausgeber
Dr. Horst Bornemann

Redaktionelle Bearbeitung und Layout
Birgit Reimann

Alfred-Wegener-Institut
Helmholtz-Zentrum für Polar- und Meeresforschung
Am Handeshafen 12
27570 Bremerhaven
Germany

www.awi.de
www.reports.awi.de

The Reports on Polar and Marine Research are issued by the Alfred Wegener Institute, Helmholtz Centre for Polar and Marine Research (AWI) in Bremerhaven, Germany, succeeding the former Reports on Polar Research. They are published at irregular intervals.

The Reports on Polar and Marine Research contain presentations and results of research activities in polar regions and in the seas either carried out by the AWI or with its support.

Publications comprise expedition reports of the ships, aircrafts, and stations operated by the AWI, research results (incl. dissertations) of the Institute and the Archiv für deutsche Polarforschung, as well as abstracts and proceedings of national and international conferences and workshops of the AWI.

The papers contained in the Reports do not necessarily reflect the opinion of the AWI.

Editor
Dr. Horst Bornemann

Editorial editing and layout
Birgit Reimann

Alfred-Wegener-Institut
Helmholtz-Zentrum für Polar- und Meeresforschung
Am Handeshafen 12
27570 Bremerhaven
Germany

www.awi.de
www.reports.awi.de

***T**itel: Die Küstenlinie am Kapp Mamontov Klyk (westliche Laptewsee) erodiert mehr als 5m pro Jahr. B. Juhls (AWI) auf dem Weg zu einem Bohrloch, in dem die Temperatur bis in 70m Tiefe beobachtet wird. (Foto: Trond Ryberg, Helmholtz-Zentrum Potsdam Deutsches GeoForschungsZentrum, 4. Sep. 2016)*

Cover: The cliffs at Cape Mamontov Klyk (western Laptev Sea) erode more than 5m per year. B. Juhls (AWI) walks along the clifftop to visit a borehole site where the temperature is monitored down to 70 m depth (Photo: Trond Ryberg, Helmholtz Centre Potsdam GFZ German Research Centre for Geosciences, Sep. 4, 2016)

Russian-German Cooperation: Expeditions to Siberia in 2016

Edited by

Pier Paul Overduin, Franziska Blender, Dmitry Y. Bolshiyanov, Mikhail N. Grigoriev, Anne Morgenstern and Hanno Meyer

Please cite or link this publication using the identifiers
hdl:10013/epic.51474 or http://hdl.handle.net/10013/epic.51474 and
doi:10.2312/BzPM_0709_2017 or http://doi.org/10.2312/BzPM_0709_2017

ISSN 1866-3192

Expeditions to Siberia in 2016

Spring Samoylov 03.04. – 28.04.2016

Summer Samoylov 03.07. – 21.09.2016

Coastal and Offshore Permafrost 21.08. – 14.09.2016

Seismicity 22.07. – 05.08.2016

Beenchime Salaatski Crater 10.07. – 30.07.2016

Keperveem, Chukotka 28.06. – 26.07.2016

Lake Satagay, Central Yakutia 27.08. – 09.09.2016

Chief scientists

Mikhail Grigoriev (MPI Yakutsk), Hanno Meyer (AWI Potsdam) Dmitry Bolshiyanov (AARI), Anne Morgenstern (AWI Potsdam), Svetlana Evgrafova (SIF Krasnojarsk), Georg Schwamborn (AWI Potsdam), Luidmila Pestryakova (North-Eastern Federal University – NEFU, Yakutsk), Ulrike Herzschuh (AWI Potsdam), Boris Biskaborn (AWI Potsdam)

Contents

1. Introduction

Paul Overduin [1], Anne Morgenstern [1], Franziska Blender [1], Hanno Meyer [1], Dmitry Y. Bolshiyanov [2], Mikhail N. Grigoriev [3,4]

[1] Alfred Wegener Institute Helmholtz Center for Polar and Marine Research, Potsdam, Germany

[2] Arctic and Antarctic Research Institute, St. Petersburg, Russia

[3] Melnikov Permafrost Institute, Siberian Branch, Russian Academy of Sciences

[4] Trofimuk Institute for Petroleum Geology and Geophysics, Siberian Branch, Russian Academy of Sciences

This report provides an overview of the study locations, scientific objectives and field activities of the joint Russian-German expeditions to Siberia in 2016, which investigated the biology, geology, geomorphology, coastal dynamics, ecology and paleoenviroment of study sites spanning a region that extends 1300 km from north to south and 1500 km from west to east. Russian-German scientific cooperation in the Siberian periglacial realm has a long tradition with yearly expeditions to Yakutia and the Siberian Arctic since 1993. An expedition to the Lena River Delta in 1998 was the first in the series of annual joint Russian-German expeditions LENA within the framework of the Russian-German Cooperation SYSTEM LAPTEV SEA, supported by the research ministries of both countries. This first expedition laid the foundation for the establishment of a permafrost observatory on Samoylov Island in the central Lena Delta and the operation of a research station, which has been serving as a scientific and logistical base for the LENA expeditions ever since. Permafrost conditions, micrometeorology, trace gas exchange, biology, and many other parameters are monitored at long-term measurement sites on the island and have been providing important data for the expeditions and the research community as a whole, for example through publication via data portals such as PANGAEA (https://www.pangaea.de/) or integration into international data bases, such as the Global Terrestrial Network for Permafrost (GTN-P; http://gtnp.arcticportal.org/).

In 2016, the LENA expedition covered the period from April to September. It was coordinated by Prof. Dr. Hans-Wolfgang Hubberten (Alfred Wegener Institute Helmholtz Center for Polar and Marine Research - AWI, Potsdam), Prof. Dr. Dmitry Bolshiyanov (Arctic and Antarctic Research Institute - AARI, St. Petersburg) and Dr. Mikhail N. Grigoriev (Mel'nikov Permafrost Institute, Siberian Branch, Russian Academy of Sciences – MPI SB RAS, Yakutsk) and led by Dmitry Bolshiyanov and Waldemar Schneider. Besides Samoylov Island, field sites included other locations within the Lena River Delta and adjacent to it, such as Cape Mamontov Klyk, Kurungnakh Island, Sobo-Sise Island, Bykovsky Peninsula, Muostakh Island, and Beenchime crater. Participants are listed in Tab. 1.-1.

The expedition LENA 2016 is described in chapters 2 to 4. Chapter 2 summarizes the activities on and near Samoylov Island during spring and summer. The Research Station Samoylov Island is operated by the Trofimuk Institute for Petroleum Geology and Geophysics, Siberian Branch, Russian Academy of Sciences (IPGG SB RAS), and provided a logistics staging base, laboratories for field work and accommodation for the scientists, technicians and students. Chapter 3 reports on all field activities in the wider Lena Delta region (not restricted to Samoylov Island and surroundings). These include a ship-based field campaign (21 August - 16 September, 2016) to study coastal and offshore permafrost led by Paul Overduin (AWI) and Mikhail Grigoriev (MPI). Furthermore, a river ship was used (June 28 to August 2, 2016) between Yakutsk and the Lena Delta (lead: D. Bolshiyanov, AARI) to study the geomorphology of the Lena River valley. The seismicity of the Laptev rift was explored by a 10-person team (7 Russians, 3 Germans) between July 22 and August 5, 2016. The bedrock and environmental history of the Beenchime Salaatski Crater was studied between July 10 and 31, 2016 by a 7-person team (4 German and 3 Russian scientists) lead by Georg Schwamborn (AWI). The activities of this research team are summarized in Chapter 4.

In addition to these activities, which belong to the expedition LENA 2016, field work was also conducted by two Russian-German expeditions to Central Yakutia and Chukotka. Keperveem in Chukotka was visited for the first time in this context by a 14-person team (7 Germans, 7 Russians) to study past and present vegetation dynamics near the Siberian boreal treeline. Field work took place between 28 June and 26 July, 2016. This expedition was lead by Luidmila Pestryakova (North-Eastern Federal University – NEFU, Yakutsk) and Ulrike Herzschuh (AWI). Chapter 5 summarizes the activities of the Keperveem expedition.

Finally, field activities took place in Central Yakutia (expedition “Yakutia 2016”) at Lake Satagay and its surroundings to study the short-term climate variability in an extreme continental environment. The expedition comprised 7 Russian and 2 German participants (lead: Boris Biskaborn, AWI Potsdam) and took place between August 27 and September 9, 2016. These acitivies are summarized in Chapter 6.

This report contains short contributions of the participants. The authors are responsible for content and correctness.

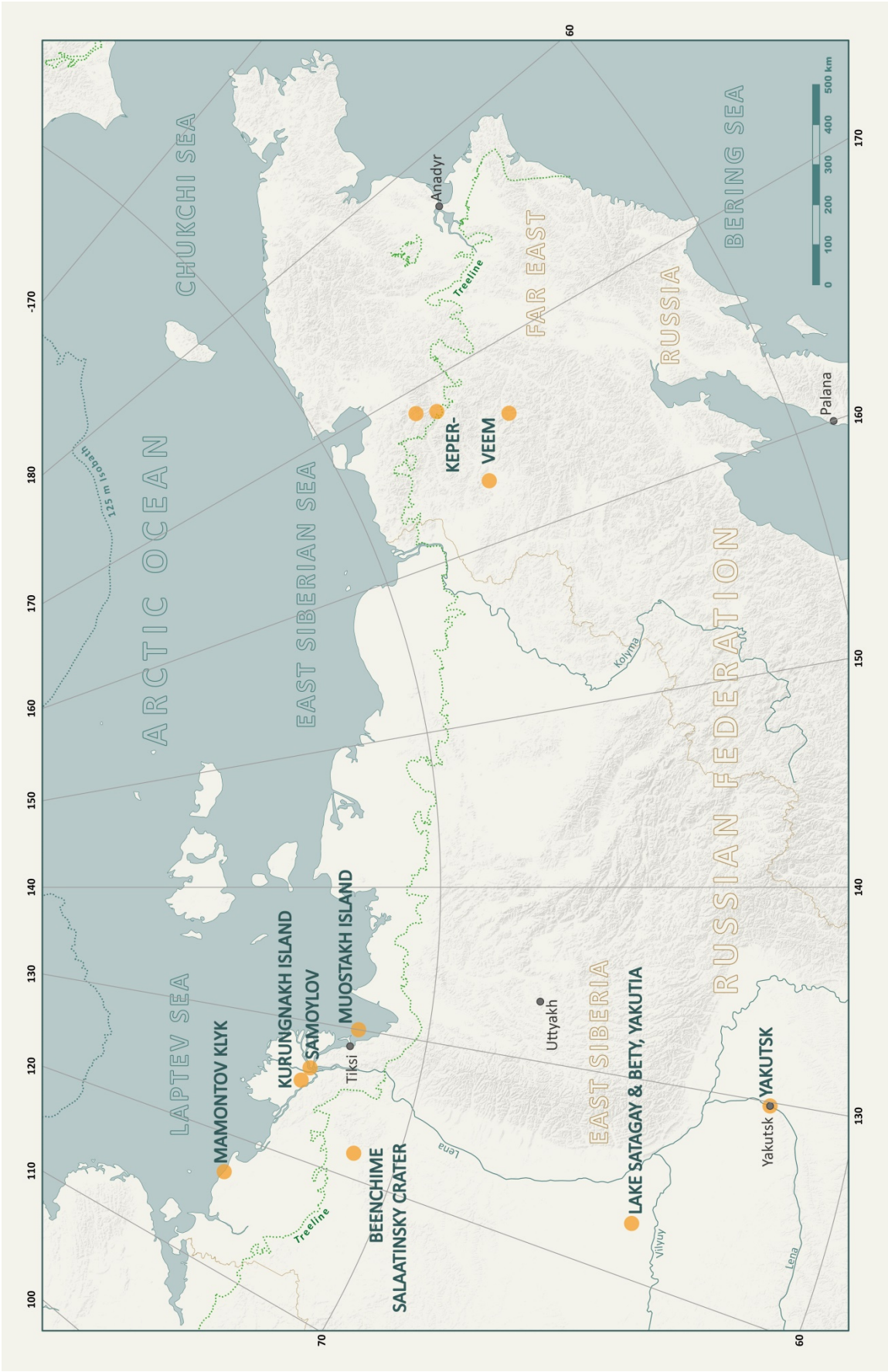

Figure 1.-1: Overview map of the study regions of the 2016 expeditions to Siberia (map compiled by Sebastian Laboor, AWI)

Expedition Lena 2016 – Participants and schedule

The spring expedition of „Lena 2016“ was lead by Mikhail Grigoriev (MPI Yakutsk) and Hanno Meyer (AWI Potsdam) from 3 April to 29 April, 2016. In total, a group of 16 participants (5 German and 11 Russian, Fig. 1.-2) took part in the “Lena 2016” spring campaign. The expedition group started in Berlin, St. Petersburg and Moscow and reached Tiksi from Moscow via Yakutsk by airplane. From Tiksi, the transfer to and back from the Samoylov research station was performed by trucks on the frozen Lena River.

Figure 1.-2: Group picture of the participants of the spring campaign „Lena 2016“ (photo: Martin Werner)

Summer activities in the Samoylov area were subdivided into three expedition parts: The **July** field work was led by Dmitry Bolshiyanov (AARI) and Anne Morgenstern (AWI Potsdam) from 3 to 31 July, 2016. The **August** field work was led by Svetlana Evgrafova (SIF Krasnojarsk) from 31 July to 3 September, 2016. The final expedition part (**September** field work) from 4 to 30 September, 2016 involved only two people, both from Germany.

Figure 1.-3: Group picture of the participants of the July campaign „Lena 2016“ part 1 (photo: Günter Stoof)

Figure 1.-4: Group picture of the participants of the July campaign „Lena 2016“ part 2 (photo: Günter Stoof)

Figure 1.5: Group picture of the participants of the August campaign „Lena 2016“ (photo: Günter Stoof)

Table 1.-1: Participant List Expedition Lena 2016

№	Participant	Institute	Period	Days
	Spring Samoylov	**03.04.16 to 28.04.16**		
1	Ekaterina Abramova	LDR	06.04.16 - 26.04.16	21
2	Nikita Bobrov	SPbSU	06.04.16 - 26.04.16	21
3	Dmitry Bolshiyanov	AARI	06.04.16 - 19.04.16	14
4	Alexander Derevyagin	MSU	06.04.16 - 26.04.16	21
5	Irina Fedorova	AARI	06.04.16 - 26.04.16	21
6	Mikhail Grigoriev	MPI	06.04.16 - 26.04.16	21
7	Sergey Krylov	SPbSU	06.04.16 - 26.04.16	21
8	Lars Kutzbach	UHH	06.04.16 - 26.04.16	21
9	Georgi Maksimov	MPI	06.04.16 - 26.04.16	21
10	Alexander Maslov	MPI	06.04.16 - 26.04.16	21
11	Hanno Meyer	AWI	06.04.16 - 26.04.16	21
12	Stepan Romanov	SPbSU	06.04.16 - 26.04.16	21
13	Waldemar Schneider	AWI	06.04.16 - 19.04.16	14
14	Peter Schreiber	AWI	06.04.16 - 26.04.16	21
15	Martin Werner	AWI	06.04.16 - 26.04.16	21

№	Participant	Institute	Period	Days
	Summer Samoylov	**03.07.16 to 21.09.16**		
1	Ekaterina Abramova	LDR	07.07.16 - 29.08.16	54
2	Viktor Alekseev	ZIN	07.07.16 - 31.07.16	25
3	Inna Alekseenko	AARI	02.08.16 - 29.08.16	28
4	Lutz Beckebanze	UHH	30.08.16 - 19.09.16	21
5	Christina Biasi	UEF	18.07.16 - 31.07.16	14
6	Dmitry Bolshiyanov	AARI	30.06.16 - 31.07.16	32
7	Jean-Louis Bonne	AWI	30.08.16 - 19.09.16	21
8	Niko Bornemann	AWI	07.07.16 - 31.07.16	25
9	Svetlana Evgrafova	SIF	02.08.16 - 29.08.16	28
10	Denis Fadeev	IPGG	10.07.16 – 30.07.16	20
11	Alexey Fage	IPGG	10.07.16 – 30.07.16	20
12	Irina Fedorova	AARI	18.07.16 - 31.07.16	13
13	Larisa Frolova	KFU	07.07.16 - 31.07.16	25
14	Guido Grosse	AWI	18.07.16 - 31.07.16	14
15	Johanna Kerttula	UEF	07.07.16 - 31.07.16	25
16	Christian Knoblauch	UHH	07.07.16 - 31.07.16	25
17	Miron Makushin	SPbSU	07.07.16 - 31.07.16	25
18	Maija Marushchak	UEF	07.07.16 - 17.07.16	11
19	Vera Meyer	AWI	02.08.16 - 29.08.16	28
20	Anne Morgenstern	AWI	18.07.16 - 31.07.16	14
21	Oleg Novikov	SIF	07.07.16 - 29.08.16	54
22	Vyacheslav Polyakov	AARI	02.08.16 - 29.08.16	28
23	Sergey Pravkin	AARI, SPbSU	30.06.16 - 31.07.16	32
24	Justine Ramage	AWI	18.07.16 - 10.08.16	24
25	Thorsten Riedel	AWI	02.08.16 - 29.08.16	28
26	Cornelia Ruhland	UHH	07.07.16 - 31.07.16	25
27	Olga Rusalimova	ISSA	10.07.16 – 30.07.16	20
28	Waldemar Schneider	AWI	07.07.16 - 29.08.16	54
29	Peter Schreiber	AWI	07.07.16 - 17.07.16	11
30	Alexander Schütt	UHH	07.07.16 - 31.07.16	25
31	Günter Stoof	AWI	07.07.16 - 29.08.16	54
32	Andrei Sementsov	IPGG	10.07.16 – 20.07.16	10
33	Leonid Tsibizov	IPGG	10.07.16 – 30.07.16	20
34	Carolina Voigt	UEF	07.07.16 - 31.07.16	25
35	Christian Wille	UHH	07.07.16 - 31.07.16	25
36	Anja Wotte	UC	02.08.16 - 29.08.16	28
37	Timofey Yeltsov	IPGG	10.07.16 – 30.07.16	20
	Days in total			1272

№	Participant	Institute	Period	Days
	Krater Beenchime	**10.07.16 to 30.07.16**		
1	Christoph Manthey	UP	13.07.16 - 26.07.16	14

2	Nikolai Oparin	DPMGI	13.07.16 - 26.07.16	14
3	Maria Oshchepkova	DPMGI	13.07.16 - 26.07.16	14
4	Ulli Raschke	MfN	13.07.16 - 26.07.16	14
5	Georg Schwamborn	AWI	13.07.16 - 26.07.16	14
6	Lutz Schirrmeister	AWI	13.07.16 - 26.07.16	14
7	Anatoly Zhuravlev	DPMGI	13.07.16 - 26.07.16	14
№	**Participant**	**Institute**	**Period**	**Days**
	Cruise	**21.08.16 to 14.09.16**		
1	Mikhail Grigoriev	MPI	24.08.16 - 11.09.16	15
2	Bennet Juhls	AWI	24.08.16 - 11.09.16	15
3	Paul Overduin	AWI	24.08.16 - 11.09.16	15
4	Trond Ryberg	GFZ	24.08.16 - 11.09.16	15
5	Matthias Winkel	GFZ	24.08.16 - 11.09.16	15
№	**Participant**	**Institute**	**Period**	**Days**
	Seismicity	**22.07.16 to 05.08.16**		
1	Boris Baranov	SIO	22.07.16 – 05.08.16	15
2	Wolfram Geissler	AWI	22.07.16 – 05.08.16	15
3	Stepan Gukov	YGS	22.07.16 – 05.08.16	15
4	Christian Haberland	AWI	22.07.16 – 05.08.16	15
5	Frank Krueger	UP	22.07.16 – 05.08.16	15
6	Dmitri Peresypkin	YGS	22.07.16 – 05.08.16	15
7	Sergey Petrunin	YGS	22.07.16 – 05.08.16	15
8	Sergey Shibaev	YGS	22.07.16 – 05.08.16	15
9	Rustam Tuktarov	YGS	22.07.16 – 05.08.16	15
10	Daniel Vollmer	UP	22.07.16 – 05.08.16	15

Table 1.-2: List of participating institutes and universities

AARI	Arctic and Antarctic Research Institute, St. Petersburg, Russian Federation
AWI	Alfred Wegener Institute Helmholtz Centre for Polar and Marine Research, Bremerhaven and Potsdam, Germany
DPMGI	Laboratory of Geodynamics and Regional Geology, Diamond and Precious Metal Geology Institute, Siberian Branch Russian Academy of Sciences, Yakutsk, Russian Federation
GFZ	Helmholtz Centre Potsdam – GFZ German Research Centre for Geosciences, Potsdam, Germany
IPGG	Trofimuk Institute for Petroleum Geology and Geophysics, Siberian Branch, Russian Academy of Sciences, Russian Federation
ISSA	Institute of Soil Sciences and Agrochemistry, Novosibirsk, Russian Federation
KFU	Kazan Federal University, Kazan, Russian Federation
LDR	Lena Delta Reserve, Tiksi, Russian Federation
MfN	Museum für Naturkunde, Leibniz Institute for Evolution and Biodiversity Science, Berlin, Germany
MPI	Melnikov Permafrost Institute, Siberian Branch, Russian Academy of Sciences, Yakutsk, Russian Federation

MSU	Department of Geography, Lomonosov Moscow State University, Moscow, Russian Federation
NEFU	North-Eastern Federal University, Yakutsk, Russian Federation
SIF	Sukachev Institute of Forest, Siberian Branch, Russian Academy of Sciences, Krasnoyarsk, Russian Federation
SIO	P. P. Shirshov Institute of Oceanology, Russian Academy of Sciences, Moscow, Russian Federation
SPbSU	Saint Petersburg State University, St. Petersburg, Russian Federation
UC	University of Cologne, Institute of Geology and Mineralogy, Cologne, Germany
UEF	Department of Environmental and Biological Sciences, University of Eastern Finland, Kuopio, Finland
UHH	University of Hamburg, Institute of Soil Science, Hamburg, Germany
UP	Institute of Earth and Environmental Science, Potsdam University, Potsdam, Germany
YGS	Yakutsk Branch Geophysical Survey, Russian Academy of Sciences, Yakutsk and Tiksi, Russian Federation
ZIN	Zoological institute of the Russian Academy of Sciences, St. Petersburg, Russia

Acknowledgements

The success of the expedition LENA 2016 would not have been possible without the support of the Russian and German organizing institutions, funding agencies, authorities and individual people. In particular, we would like to express our appreciation to the staff of the Research Station Samoylov Island, the Lena Delta Reserve, the Tiksi Hydrobase, and Arctica GeoCenter.

2. RESEARCH STATION SAMOYLOV ISLAND

2.1. Isotopic composition of the snow cover on Samoylov Island and its modification in spring

Hanno Meyer [1], Alexander Dereviagin [2]

[1] Alfred Wegener Institute Helmholtz Center for Polar and Marine Research, Potsdam, Germany

[2] Department of Geography, Lomonosov Moscow State University

Fieldwork period April 03 to April 29, (Samoylov Island)

Scientific background, objectives and methods

The objective of the stable isotope group with Alexander Dereviagin (MSU Moscow) and Hanno Meyer (AWI Potsdam) is to better understand the recent hydrology in the Northeast Siberian Arctic by using stable water isotopes. The research comprises continuous sampling of precipitation and snow, ice, rivers, lakes, ponds on various timescales (from event-basis to annually repeated samplings). This years' focus will be the transformation of snow in spring due to precipitation events, evaporation/sublimation, snow melt and runoff. Therefore, the fieldwork included a detailed and repeated sampling of snow profiles to monitor the spatial and temporal changes in its snow characteristics as well as its isotope geochemical composition on Samoylov Island.

We focused on understanding the spatial characteristics of a seasonal snow cover likely related to site-specific characteristics such as small differences in topography in the polygonal tundra (polygon wall vs. center) as well as the temporal changes of the snow cover in spring prior to and during the snow melt. Detailed descriptions of the snow properties including the thermal regime and density are accompanied by laboratory analyses of stable water isotope modifications in snow. This field work is in close relationship to an earlier study that was carried out in spring 2013.

Furthermore, the ice cover on local polygonal ponds and lakes was drilled with an ice drill Kovacs Mark III and at certain positions the active layer was cored. All these coring positions are indicative of the respective freezing processes since last fall and winter that are archived in the lake, pond or active layer ice. We aim to assess the differential freezing processes (shallow pond, deep pond, active layer) in the periglacial realm of Samoylov Island with stable water isotopes. Additionally, frost cracking events and their subsequent filling with snow melt have been monitored and, if possible, sampled to better understand the formation of recent ice wedges on Samoylov Island.

For a detailed snow survey and research on processes involved in snow build up and decay including snow metamorphism (recrystallization of snow) in the period preceding

snow melt (April 2016) a snow-covered low-center polygon has been selected. The profile was marked every meter by numbered poles (from 0 to 25). At the profile the following working steps were carried out: 1. measurements of snow cover thickness (every meter); 2. Detailed descriptions of the snow cover (ca. every second meter); 3. snow sampling (both for snow density and for isotope geochemical composition); 4. measurements of snow temperatures; 5. bore hole drilling.

The ca. 25 m long snow profile LD16-SP-1 was selected on 7 April and sampled on 8/9 April, 2016 in exact E-W direction (Fig. 2.1.-1). The sampling site is identical to LD13-SP-8 from the Lena 2013 campaign and situated at N 72°22.233' and between E 126°28.923'' and E 126°28.956''.

Figure 2.1.-1: The sampled snow profile LD-16-SP

The polygon is located at the first river terrace of the Olenyokskaya branch and has a diameter of about 20 m. In the center the polygon comprises of a frozen polygonal pond. The width of this frozen pond is about 18 m and, according to coring results (LD-16-BH-1A), its water depth is about 35-40 cm. The height of polygon rims is elevated about 30-35 cm above the level of the frozen pond. The width of polygon rims is of about 2-3 m. The vegetation cover at the surface of rims has a thickness of 3-8 cm and is composed mostly of mosses, herbaceous shrubs (Carex, Salix), sedges and lichens.

The snow depth in this profile varied between 11 cm (on the polygon rim) and 54 cm, with a mean snow depth of 41.8cm. The mean density of the complete snow profile (sampled with a liner tube) yielded 290 kg m^{-3}, but varying between 174 and 363 kg m^{-3} at different positions in the profile. More detailed snow density studies of the different layers of the snow profile with a 100 cm^3 tube yielded higher values (mean density 335 kg m^{-3}), but this largely excluded the depth hoar, which fell into pieces when using the snow density tube. Therefore, the measurements with the 100 cm^3 tube likely overestimate the density in the

profiles. The snow temperature ranged between -20 and -28°C with less negative temperatures and less variability on the polygon walls, which is characterized by a generally thinner snow cover than in the polygon centers, where more snow accumulates.

The snow transect was resampled on 15 April, 2016 for a second time (as LD16-SP-2). The snow characteristics remained almost unchanged since no new precipitation occurred and the temperatures remained well below zero degrees. The snow depth in this profile varied between 10 cm and 57 cm, with a mean snow depth of 42.2 cm. The snow density sampled with a 100 cm^3 tube yielded a mean density of 346 kg m^{-3}.

On 22 April, 2016, the snow transect was sampled for a third time (as LD16-SP-3).
At this time, the snow depth in this profile varied between 10 cm and 51 cm, with a mean snow depth of 39.7 cm. The snow density sampled with a 100 cm^3 tube yielded a mean density of 340 kg m^{-3}. In addition, mean density of the complete snow profile taken with a liner tube) yielded 327 kg m^{-3}, but varying between 252 and 402 kg m^{-3} at different positions in the profile.

The same snow transect was sampled on 26 April, 2016 for a last time, after a strong increase of the air temperatures close to 0°C as well as a rain event on 25 April, 2016 (LD16-SP-5). Densities and temperatures were measured at only 5 (instead of 10) profiles. The snow density sampled with a 100 cm^3 tube yielded a higher mean density of 428 kg m^{-3}. The snow depth in this profile varied between 9 cm and 53 cm, with a mean snow depth of 38.8 cm.

The measurements of the snow cover thickness using measuring tape and stainless steel sounding rod (“schup”) were carried out four times in study period: 7.04.2016 (SP-1); 15.04.2016 (SP-2); 22.04.2016 (SP-3); 26.04.2016 (SP-5). Table A 2.1.-1 in the Appendix presents the results of these measurements.

Detailed descriptions of the snow cover were carried out along vertical profiles across the complete snow cover at the markers (every meter). The determination of shape, size of snow crystals and the hardness of snow in different layers of snowpack was carried out with the help of a snow description chart provided by the WSL Institute for Snow and Avalanche Research SLF, Davos, Switzerland (Fig. 2.1.-2).

Figure 2.1.-2: Snow description chart (Institute for Snow and Avalanche Research, Davos, Switzerland)

In the vertical snow profiles and at the surface, following types of snow were differentiated: fresh snow, loose snow, compact snow, snow crust (hard packed snow), sublimation snow (Fig. 2.1.-3), depth hoar (Fig. 2.1.-4).

Figure 2.1.-3: Feather-like crystals of sublimation snow at the surface of the snow cover.

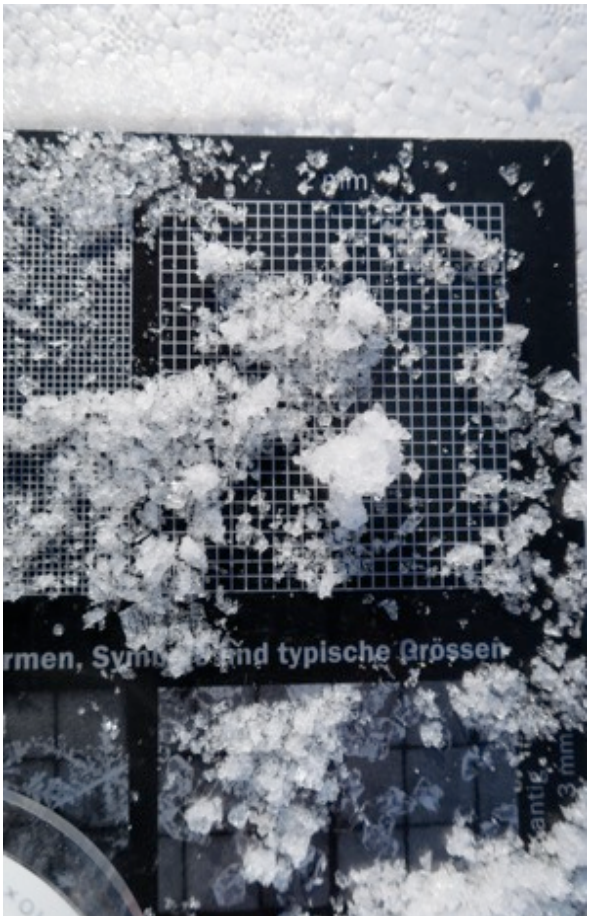

Figure 2.1.-4: Depth hoar crystals

Snow sampling was carried out in the vertical profiles across the snowpack (Fig. 2.1.-5). At each sampling point, different layers in the snowpack were described regarding the different types of snow, crystal sizes and forms and density.

For determining the snow density, we used a special cylinder with an exact volume of 100 cm^3. Further density measurements were carried out for the complete snowpack for every meter of the profile by means of a liner plastic tube with a diameter of 59 cm. Samples were weighed with a balance Kern EMB 1200-1 with Δ = 0.1 g and their respective densities determined. The mean snow density yielded 290 kg m^{-3} varying between 174 and 363 kg/ m^3. After density measurements, the samples were packed in plastic pockets for stable isotope analysis and then stored in thermoboxes for further transportation to Germany.

Fig. 2.1.-5: Points of snow sampling in vertical profiles (LD-16-SP-3)

For the measurements of snow temperatures, a digital thermometer Omnitherm Pt 100-L was used. The snow temperature varied in general between -14 and -28°C between 7 April and 23 April, 2016, with strong daily variations. Less negative and less variable temperatures were observed on the polygon walls, which is characterized by a generally thinner snow cover than in the polygon centers, where more snow accumulates.

Wind redistribution of snow formed a big snow patch close to the Samoylov station. Here, a snow depth of about 2.4 m was measured. At this position, a 235 cm long snow profile was cored on 17 April, 2016 (Figure 2.1.-6) with a Kovacs Mark III ice corer, briefly described and packed for transport. This snow profile should contain the snow fallen since the beginning of the winter, most likely with some major wind drift events in the record. Comparing isotope analyses of this core with recent precipitation events will reveal how much of the snow falling since last autumn will be captured in the snow pack.

Figure 2.1.-6: Snow core LD16-SP-4

Investigations of frost cracking (thermal contraction cracking) processes

Samples from snow above frost cracks (as potential source material for ice-wedge growth) have been taken in different geomorphological positions over the island. In total, 16 samples (labeled LD16-FCS-) have been taken. Depths of loose snow and depth hoar were monitored and both were sampled separately. The deepest frost crack was found on the floodplain. The depth of the frost crack was measured with a metal stick ”schup” (diameter ca. 1 cm) and reached more than 75 cm.

Further sampling

Four cores were retrieved during build-up of the fundament at the platform drill site, named Core I to IV (9 April 2016) and P4 (16 April 2016). These cores include the complete active layer and the topmost part of permafrost. Best sample material was selected for stable isotope analyses to study the refreezing of the active layer as well as the top layer of permafrost. For this purpose, one segment (0-88 cm) was taken from Core II, three segments (0-83, 83-154, 154-178 cm) from Core III, one segment (0-84 cm) from Core IV as well as 4 segments from core P4 (0-77, 77-140, 140-189, 189-214 cm).

Furthermore, coring at the shallow (35-40 cm deep) polygonal pond of snow profile LD16-SP-1 was carried out. LD16-BH-1A (0-39 cm) and -1B (0-37, 37-103 cm) are two twin cores of the complete pond ice in the polygon center. At meter 3.40 of the same snow profile, core LD16-BH-2 (0-66 cm) was recovered from the polygon wall and includes the complete active layer, which reached a thickness of 41 cm at this position. At meter 2.20 of the snow profile, core LD16-BH-3 (0-66 cm) was recovered from the polygon wall and includes the complete active layer, which reached a thickness of 41 cm at this position.

Further coring was performed at Shallow Lake, where two ice cores were retrieved. The core LD16-BH-5 (comprising 4 segments) was extracted at the rim of the lake where the lake was completely frozen to the bed with a lake ice thickness of 110 cm. The bottom segment BH-5-4 included frozen sediment. During the coring of LD16-BH-6 in the deeper central part of the shallow lake, a lake ice core (7 segments) with a total length of 233.5 cm was recovered. The core penetrated into the lake water, which rose in the borehole and froze the barrel of the Kovacs corer within less than a minute. Although it was later possible to free the core barrel from the borehole, it was no longer useable for further drilling. As a consequence, the preselected site LD16-BH-4 was not cored. All samples for stable isotope analyses are summarized in Table A 2.1.-2 in the Appendix.

2.2. ISOARC: Maintenance of the in-situ water vapour isotopic analyser

Jean-Louis Bonne [1], Martin Werner [1], Hanno Meyer [2], Sepp Kipfstuhl [1], Benjamin Rabe [1], Melanie Behrens [1]

[1] Alfred Wegener Institute Helmholtz Center for Polar and Marine Research, Bremerhaven, Germany

[2] Alfred Wegener Institute Helmholtz Center for Polar and Marine Research, Potsdam, Germany

Fieldwork period April 3 to April 29 and August 29 to September 19, 2016 (on Samoylov Island)

Objectives

The project ISOARC is supported by the AWI strategy fund and aims for understanding the water transport pathways in the Arctic with a focus on Northern Eurasia. The Picarro water vapour isotopic analyser, installed at Samoylov station in July 2015, records year-round continuous *in situ* atmospheric measurements. The specific humidity, as well as $H_2{}^{18}O$ and HDO, measurements of water vapour obtained in Samoylov, in combination with observations in the Arctic Ocean on-board Polarstern within the ISOARC project, and associated with a network of ground stations in Eurasian Arctic from collaborating institutes, provide a dataset covering an approx. 6,000 km transect of the eastern Arctic. This will allow for a quantitative assessment of the Eurasian Arctic water cycle, its isotopic variations and imprint in various climate archives. Moreover, the Samoylov water vapour isotope data will be paired with isotope measurements of precipitation samples collected in the nearby town of Tiksi and at the Samoylov station. The combination of these vapour and precipitation measurements enables to study the imprint of local climate conditions on stable isotope records.

In order to operate the instrument with maximal data coverage, regular maintenance is necessary. Some troubles with the calibration system were identified during the first winter operation of the instrument and had to be solved. Furthermore, some calibration experiments need to be done manually on site during field expeditions, as the Picarro isotopic analyzer will run mostly autonomously for several years.

Methods

The analyser is a Picarro brand L2140i Cavity Ring Down Spectrometer, operating with a custom-made calibration system (Fig. 2.2.-1). Ambient air is continuously pumped through a heated tube, with an inlet located at about 5 meters height above ground level. The analyser alternately measures either stable oxygen and hydrogen isotopes of ambient air sampled from the inlet or air coming from the calibration unit. For a better stability of the instrument, two independent calibration systems have been installed on the instrument. They allow measurements of liquid water standards from known isotopic values calibrated against VSMOW-SLAP international scale. The first system, later named vaporizer, consists in vaporizing the water standards at high temperature and mixing them with dry

air. Four standards of different isotopic composition can be measured with this system, each standard being potentially delivered by two independent water lines for a better resilience of the system. The second calibration system, later named bubbler, allows measurements of only one standard and consists of injecting dry air through a large amount of this liquid standard under controlled temperature and pressure environment, providing a humid air of theoretically known isotopic composition.

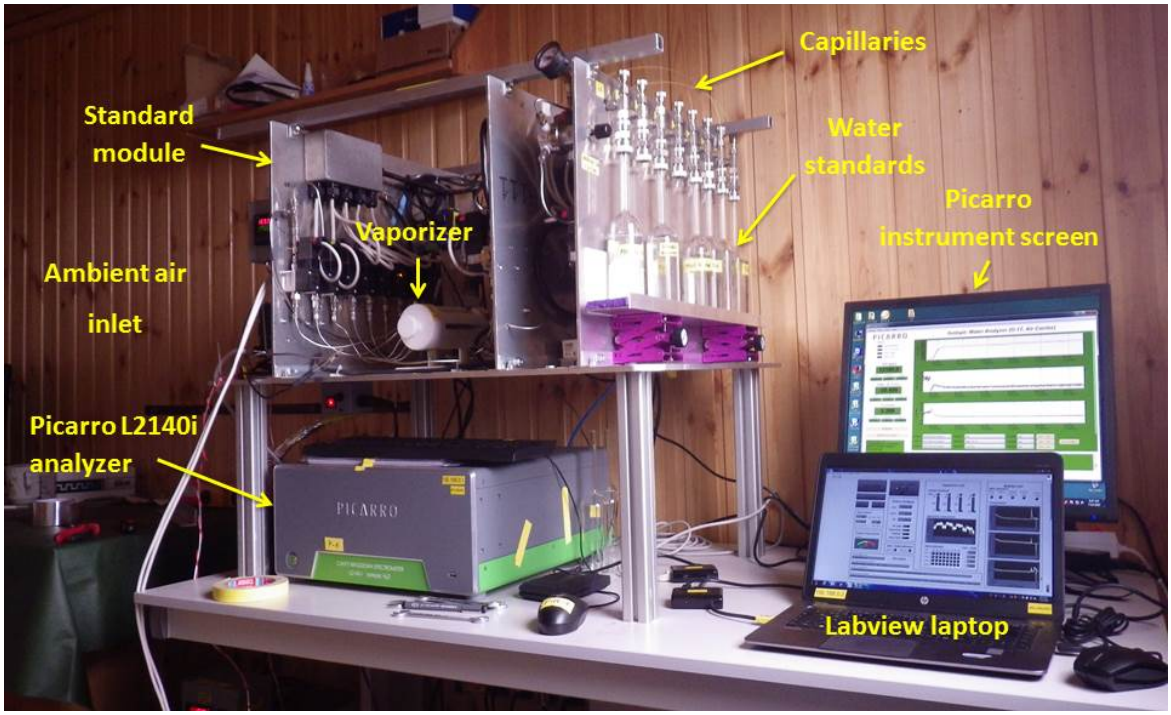

Figure 2.2.-1: The setup of the Picarro water isotope analyzer and the standard calibration module

In addition to the daily measurements of each standard to correct the drift of the analyser and calibrate the analyser to the VSMOW-SLAP scale, the sensitivity of the isotopic measurements to the humidity level also have to be corrected (Steen-Larsen et al. 2014, Bailey et al. 2015). This correction has to be determined experimentally by successive measurements of the standards at different humidity levels. To identify possible drift of this correction with time, this experiment is repeated during each maintenance mission. It cannot be performed remotely, due to necessary manual adjustments and the instabilities inherent to the injection of liquid standards during several hours.

The experience on field during the first summer and winter of operation depicted frequent instabilities in the use of the vaporizer, used in priority because it allows measurement of a range of different calibration standards. The liquid samples are indeed injected through glass capillaries, which have a tendency to clog frequently. Cutting the end of a clogged capillary generally solves the problem, but this operation has to be done manually by a person on site, and requires a permanent survey and frequent manipulations of the system, which are not always possible. For a better stability of the system, the program running the calibration system had to be adapted in 2016 in order that the typical calibration sequence allows the simultaneous use of both the bubbler and vaporizer. In order to prevent the capillaries from clogging, all liquid standards have been filtered, the bottles containing them were cleaned and the capillaries replaced. Several leaks have

also been identified and repaired during a complete leak test of the calibration system.

Aging of some metallic pieces subjected to high temperatures in the oven has also been observed. Those pieces had to be replaced, and the application of an anti-soldering paste should help prevent from fusion of those pieces. Routine maintenance of different consumables has also been done on site.

Preliminary results

The solutions brought during the maintenance missions did not completely solve the capillary clogging problem observed on the vaporizer. However, the use of the bubbler in addition to the vaporizer will assure stable measurement of at least one calibration standard on a daily basis (see typical calibration sequence on Fig. 2.2.-2). It was observed during the maintenance expedition that despite maintenance of the dry air generator used for the calibration units, the quality of the dry air produced is not as good as expected under summer conditions. This might result in a higher measurement uncertainty. A solution will have to be found for the next summer season.

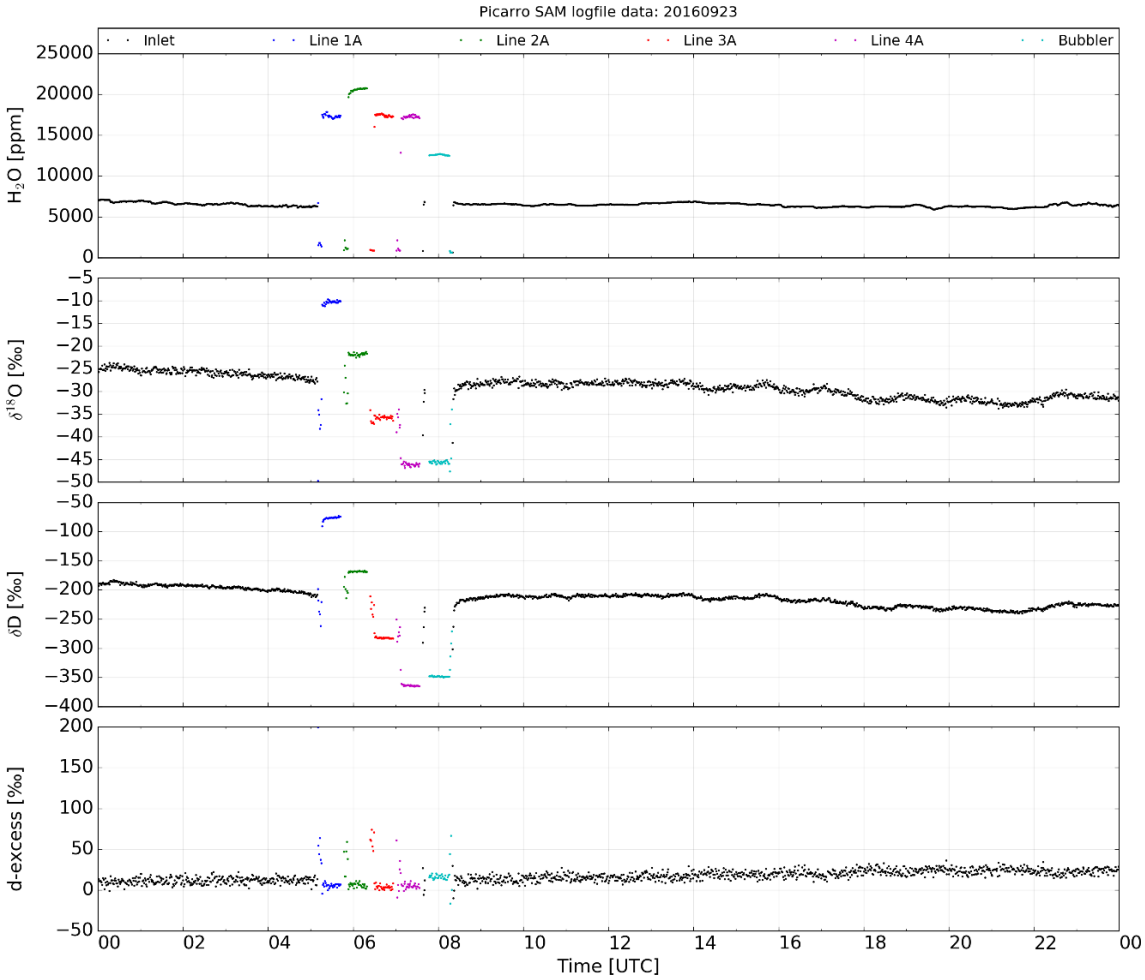

Figure 2.2.-2: Example of daily measurement sequence on 23-09-2016. From top to bottom, humidity in ppm, $\delta^{18}O$, δD and d-excess in ‰. Ambient air measurements are presented in black, measurements from the four isotopic standards on the vaporizer system in blue, green, red and purple, and measurement from the isotopic standard with the bubbler system in turquoise blue.

During summer 2016, the instrument has been running automatically. However, a problem of valves control on both calibrations systems led to several weeks of data gaps in July, before the adequate solution, which required intervention of a person on site, could be found. A similar problem already occurred in October 2015, this time linked with power supply troubles.

Humidity sensitivity experiments have been performed successfully for each standard both in April and September. Repeatability tests have depicted small variations of the response at a daily time scale, contrary to previous tests, which would indicate a higher uncertainty in the measurements at the very low humidity levels down to 1000 ppm water vapour in ambient air that were frequently reached during winter.

Even though some technical difficulties linked to measurements in a remote station without a responsible scientist permanently on site arose during the first year of operation, continuous observations of water vapour isotopic composition have been obtained with high data coverage since the installation of the analyser. The comparison of observations with ECHAM5-wiso outputs of vapour isotopic composition has shown the ability of the model to reproduce most of variability observed at the synoptic time scale, despite significant biases in the vapour isotopic composition (see Fig. 2.2.-3). These biases could give interesting hints about the atmospheric processes that the model does not simulate correctly.

The experience acquired from measurements in winter conditions on Samoylov Island is also precious for future deployment of similar instruments in Antarctica.

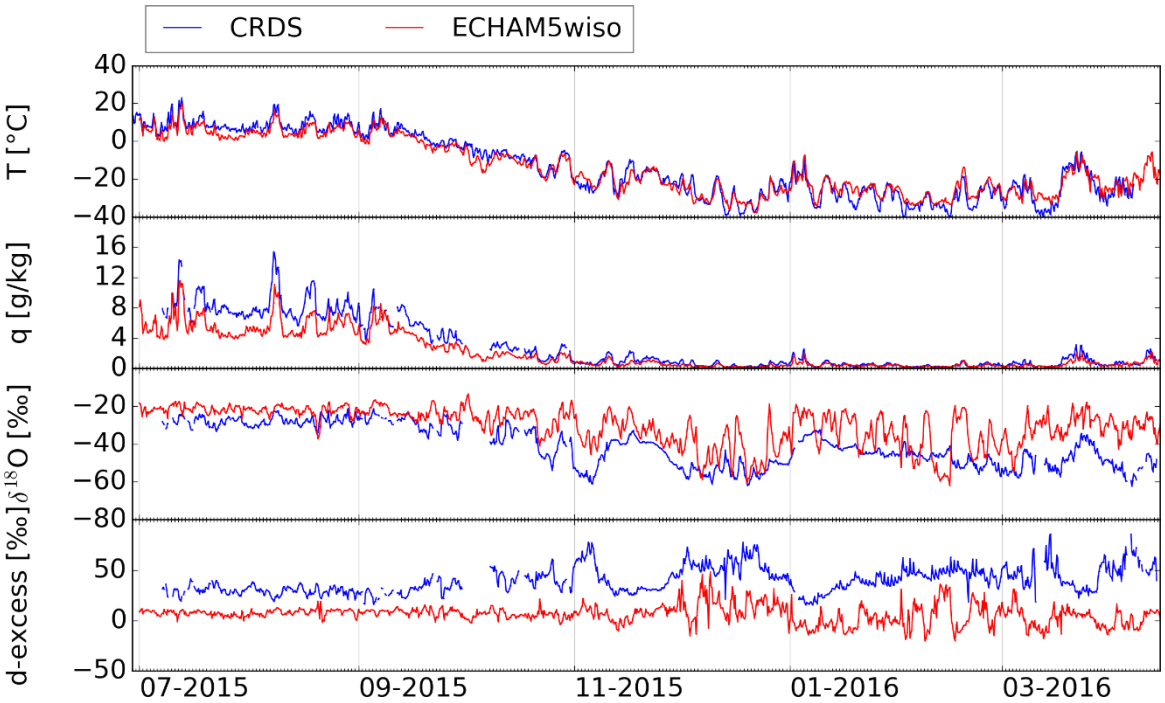

Figure 2.2.-3: Observations (blue) and ECHAM5wiso (red) outputs in Samoylov, at a 6 hours' resolution, from June 29th, 2015 to April 15th, 2016. Downwards: temperature in °C, humidity in ppm, $\delta^{18}O$ and d-excess in ‰. The humidity levels reached during winter are within the detection limits of the analyzer. Despite a good temperature simulation, significant biases in humidity and vapor isotopic composition are depicted. The strong synoptic variations on simulated isotopic

composition in winter might be linked to inability of the model to simulate very low amounts of vapor. Most seasonal and synoptic variations are however well simulated.

2.3. Heat and water budget of permafrost landscape on spatial and temporal scales – Installation of new infrastructure of the Samoylov observatory (ACROSS framework)

Peter Schreiber [1], Niko Bornemann [1], Julia Boike [1]

[1] Alfred Wegener Institute Helmholtz Center for Polar and Marine Research, Potsdam, Germany

Fieldwork period	April 03 to April 29, July 07 to July 31, 2016 (Samoylov, Kurungnakh and Sardakh Island)

Objectives

Monitoring of climate, active layer and permafrost thermal regime has been ongoing on the island of Samoylov since 1998 (Boike et al., 2013). In the framework of road map project Advanced Remote Sensing – Ground-Truth Demo and Test Facilities (ACROSS) a new field observatory is under construction on the island. Therefore, a new 10 m tower was installed in April. A wooden platform was built next to the new tower, which will support the new climate controlled field lab container. These new installations are connected to the Samoylov research base with a wooden boardwalk and 220V power lines. This infrastructure serves as a platform for several ongoing as well as new research projects.

Methods

New Instruments

Due to the new buildings of the Samoylov research station, a higher snow depth was observed in the area of the 27m deep borehole (temperature measurement). Consequently, changes in the temperature regime were observed. The borehole was instrumented in summer 2006. In summer 2016, the borehole site was equipped with an automatic snow monitoring station using a T-rack, an ultrasonic snow depth sensor (SR50A, Campbell) and one air temperature sensor (T109, Campbell) housed in a radiation shield. (Fig. 2.3.-1)

New Infrastructure

New Research Tower (Fig. 2.3.-2): to ensure a long-time stability of the new 10m research tower in permafrost ground, the following scheme was used. Four iron pipes were installed into the ground (in boreholes, drilled to 3.15 m depth) and connected with massive channel backstays to create a leveled surface as main basis. To ensure a possibility to adapt to future changes in the sensible ground, an adjustable setup of the tower to the described fundament was designed. Two bracing rings in different distances to the tower were drilled deeply into the ground and attached to the tower for extra strength during high wind speed conditions. The above ground fundament installation was

finally painted white to reduce radiative warming and thawing of the ground. For working safety, a security ladder was installed. Instruments can be mounted up to a height of at least 12 m (using extensions) above ground from 2017 on.

Platform for field lab (Fig. 2.3.-2, behind the tower): a wooden platform (19.50 m²) was installed on wooden stilts app. 60 cm above ground. The distance to the tower is no longer than 17 m, which is necessary for connection the closed path eddy covariance measurement devices from the new field lab to the tower. The igloo shaped field lab is planned to be installed in 2017.

Maintenance

The already established instrumentation on soil, thermal and hydrologic dynamic and micrometeorology was controlled and data retrieved. Some sensors were replaced by calibrated devices. Power supply was controlled and repaired if necessary. The metrological station on Kurungnakh (2010) was deinstalled, all instruments and installation infrastructure was carried back to Samoylov. The area of the investigation site was properly recultivated.

Overview of ongoing research stations

In this section, the stations, metadata and coordinates maintained by our group are listed in Tables 2.3.-1 to 2.3.-3.

Table 2.3.-1: List of running measurements on Samoylov

Name	ID	Measurements	Start of Measurements	Lat, Long
Soil station 2002	SaSoil2002/ 2010	soil temperature, soil moisture, soil heatflux, snow depth	2002	72.374194 126.495889
27m borehole 2006	SaHole2006	soil temperature	2006	72.369444 126.476444
Weather station 2002	SaMet2002/ 2010	air temperature, radiation, soil temperature	2002	72.369944 126.480833
Soil station 2012	SaSoil2012	soil temperature, soil moisture, soil heatflux, soil thermal properties snow depth/ water level,	2012	72.374194 126.495889
Snow station 2012	SaSnow2012	soil temperature, snow depth, surface temperature, snow properties	2012	72.374194 126.495889
Snow station 2016	SaSnow2016	air temperature, snow depth	2016	72.369444 126.476444
Research Tower	SaTower2016	Several atmospheric parameters, installation planned for 2017	2016	72.37353 126.49490
Pond 2014	SaPond2014	water level, water temperature	2014	72.370083 126.483383
Pond M11	SaPond_M11	water level, water temperature	2011	72.370553 126.484489

MoloLake	SaLake2	water level, water temperature	2009	72.378417 126.496856
Banja2Lake	SaLake4	water level, water temperature	2009	72.368865 126.502040
BigReindeer	SaLake5	water level, water temperature	2011	72.381650 126.499193

Table 2.3.-2: List of running measurements on Kurungnakh

Name	ID	Measurements	Start of Measurements	Lat, Long
Discharge Station	KuQ1	discharge, water temperature	2013	72.294056 126.152139
Water level monitoring	KuLuckyLake 1	Water temperature, water level	2013	72.295440 126.160710

Table 2.3.-3: List of running measurements on Sardakh

Name	ID	Measurements	Start of Measurements	Lat, Long
100m borehole 2009	SdHole2009	soil temperature	2009	72.571556 127.241556

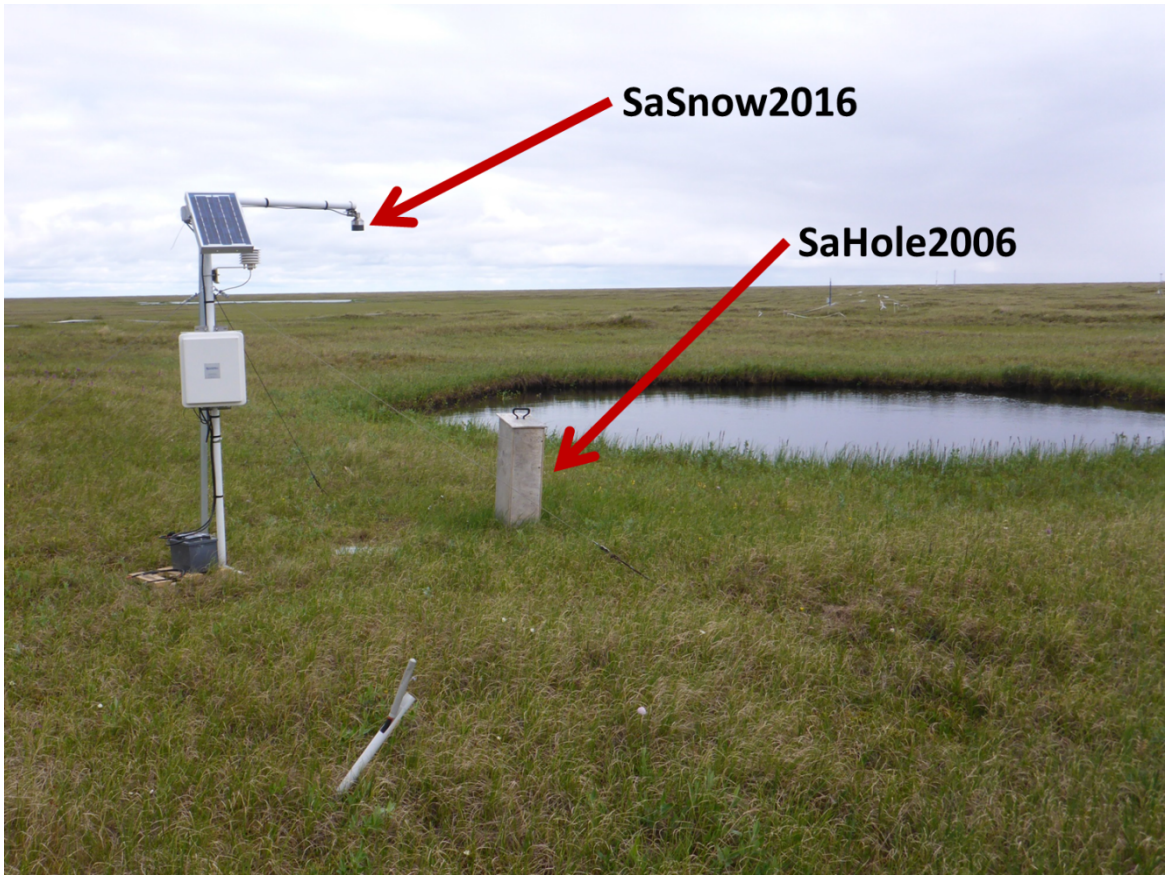

Figure 2.3.-1: Setup of the new snow depth measurement station (SaSnow2016) next to the 27m temperature borehole 2006 (SaHole2006)

Figure 2.3.-2: New ACROSS research infrastructure: wooden boardwark, 10 m tower, (SaTower2016). The wooden platform will be used as base for the climate controlled container. Samoylov research station is visible in the background.

2.4. Vertical Flux Measurements of Water, Carbon and Energy, AG Kutzbach, Universität Hamburg

Lars Kutzbach [1], Christian Wille [1], Lutz Beckebanze [1]

[1]Institute of Soil Science, Universität Hamburg, Hamburg, Germany

Fieldwork period July 7 to September 20, 2016 (Samoylov Island)

Objectives

The aim of the field work was to continue the long-term eddy covariance measurements of CH4, CO2, H2O and energy exchange from the land surface to the atmosphere at the polygonal river terrace of Samoylov Island. A continuation of this data series is important for analysing the inter-annual variability of these fluxes.

Methods

The flux measurements are based on the eddy-covariance method. Three-dimensional wind data from a sonic anemometer (Campbell Scientific CSAT3A) and concentrations of CH_4, CO_2, and H_2O from open-path (LI-COR LI-7500A, LI-7700) and closed-path gas analysers (LI-COR Li-7000, LGR FMA) are logged at a frequency of 20 Hz. The measurement height is 4.1 m. The footprint of the measurement covers the polygonal tundra within a radius of about 500 m around the tower. Further meteorological data (air temperature and relative humidity, solar and infrared radiation, wind speed and direction, barometric pressure, PAR radiation, precipitation) and soil data (temperature, volumetric water content, heat flux) are collected at the site.

Preliminary results

Meteorological, soil, and eddy-covariance data were logged continuously from September 2015 to July 2016. Due to technical problems, there exist several gaps in the gas concentration data. During the field work, necessary maintenance, calibration, and upgrade work was carried out. The processing of eddy-covariance raw data, and the quality control and gap-filling of fluxes will be finalised after the field work. Fig. 2.4.-1 shows preliminary meteorological and flux data from the period August 2015 – August 2016.

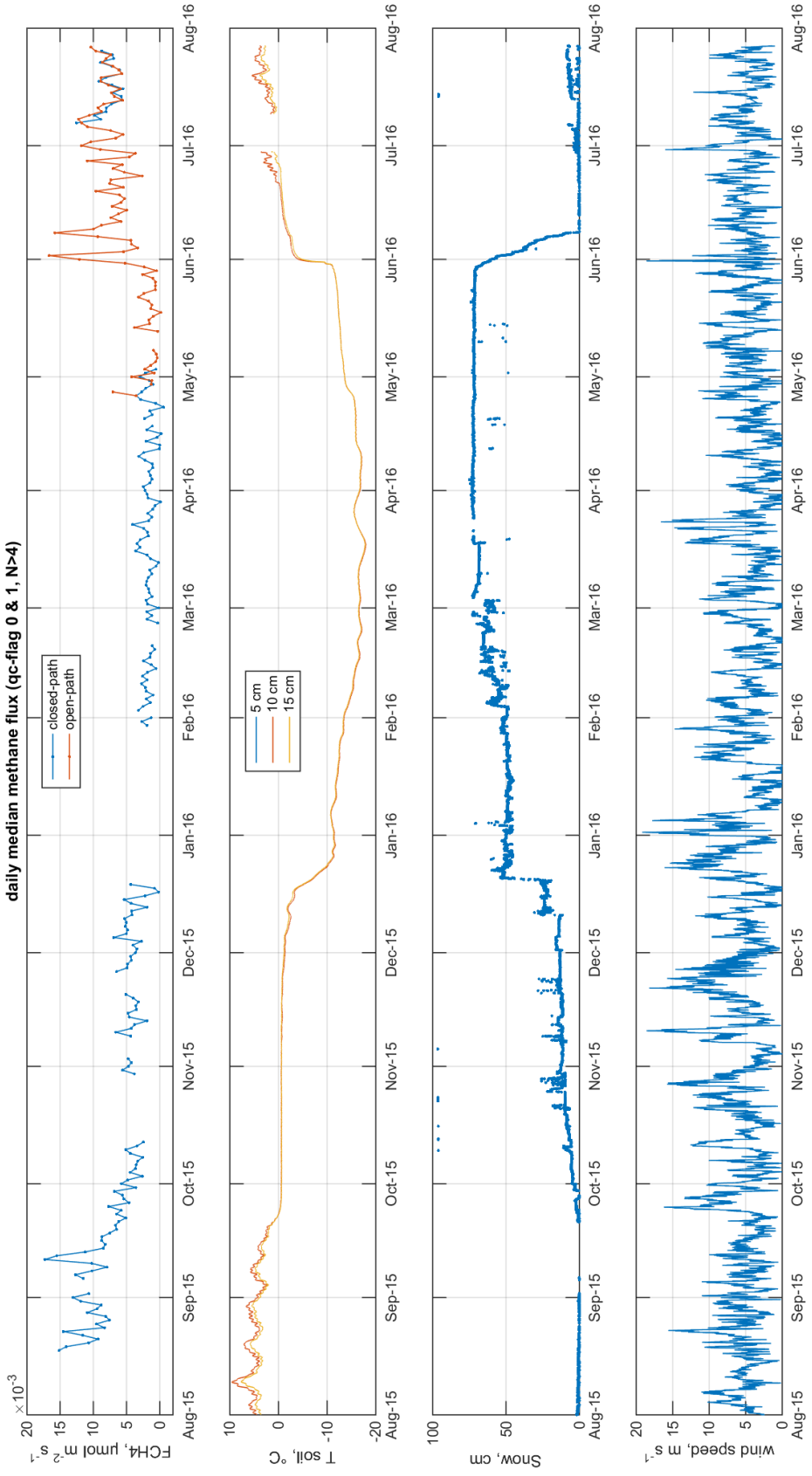

Figure 2.4.-1: Preliminary results from the period August 2015 – August 2016. From top to bottom: Daily median CH4 flux from open-path and closed-path gas analyzers; soil temperature at depth 5, 10 and 15 cm; snow height; wind speed.

2.5. Soil organic matter mineralization in thawing Yedoma deposits

Christian Knoblauch [1], Alexander Schütt [1], Cornelia Ruhland [1], Oleg Novikov [2], Svetlana Evgrafova [2], Eva-Maria Pfeiffer [1]

[1] Institute of Soil Science, Universität Hamburg, Hamburg, Germany

[2] V.N. Sukachev Institute of Forest, Siberian Branch, Russian Academy of Science, Krasnoyarsk, Russia

Fieldwork period July 2016 (Kurungnakh Island)

Objectives

A fundamental research question related to the impact of thawing permafrost on global change is, how fast the soil organic matter in the thawing permafrost can be mineralized to the greenhouse gases (GHG) carbon dioxide (CO_2) and methane (CH_4), and how much of these produced GHG will be released into the atmosphere. Current estimates on the degradability of thawing organic matter in permafrost are based on incubation studies, which are highly artificial and probably overestimate the GHG production under in situ conditions. In this respect, the organic matter rich Yedoma deposits are of particular interest because current research indicates that they contain substantial amounts of labile organic matter which will be the source for CO_2 and CH_4 after thaw. The basic research question is, how fast the thawed organic matter can be mineralized under in situ conditions to CO_2 and CH_4. This question was addressed by combining in situ flux measurements on Kurungnakh with incubations of recently thawed permafrost material from Kurungnakh.

Methods

Soil respiration measurements (CO_2 and CH_4 fluxes) were conducted at different sites on Kurungnakh (Table 2.5.-1), representing different stages of permafrost degradation by the closed chamber technique. Furthermore, soil samples from profiles of the sampling sites were taken to characterize the soil properties of the respective sampling sites (pH, C_{org}, C_{inorg}, N, $\delta^{13}C_{org}$, texture, etc.) and for soil incubations in the laboratories on Samoyloy. The soil incubations enable the comparison of in situ respiration fluxes with potential GHG productions from laboratory incubations.

Preliminary results

CH_4 and CO_2 fluxes were highly variable both in space and time. Highest CH_4 emissions were measured at sites K3 and K5 (Tab 2.5.-1) with maximum values of 53 mg m^{-2} d^{-1} and 63 mg m^{-2} d^{-1}, respectively at the 28th of July (Fig. 2.5.-1). Both CH_4 and CO_2 emission rates increased with increasing thawing depth and active layer temperature. CH_4 emissions were low or absent at sites with freshly thawed Ice Complex material but highest at those sites that contained substantial amounts of fresh surface vegetation, mixed into the eroded permafrost material. Anaerobic CH_4 production was detected in all of the incubated samples (sites K1 to K6) except for those from freshly thawed and not yet

relocated Yedoma material (K9). All un-vegetated sites were net sources for CO_2 with emission values about three orders of magnitude higher than those for CH_4.

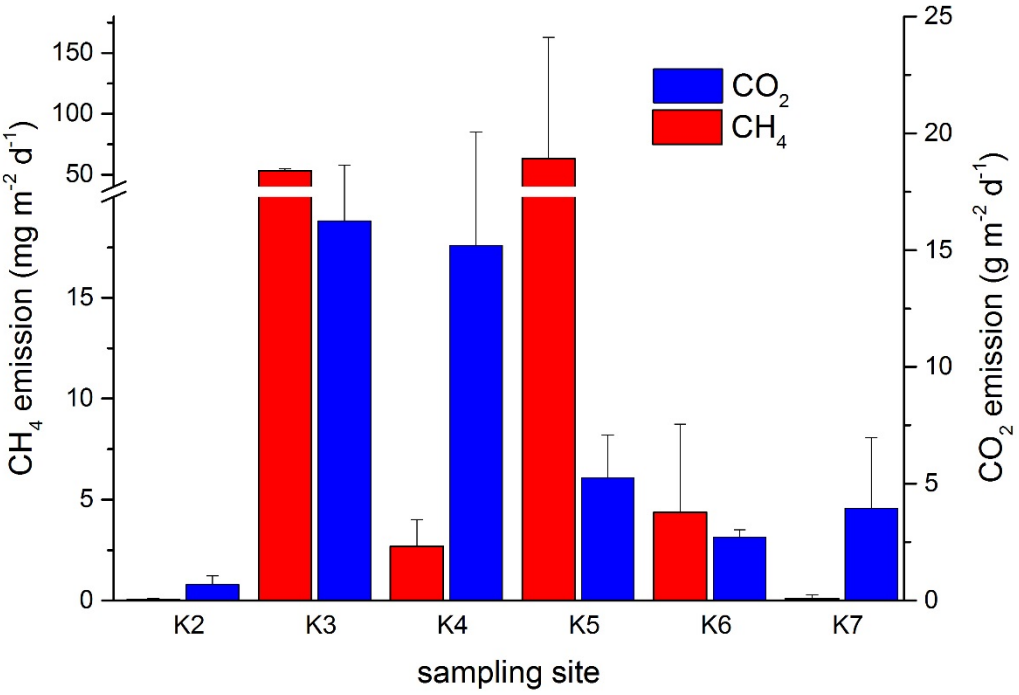

Figure 2.5.-1: CH_4 (red bars) and CO_2 fluxes (blue bars) at the sites K2 to K7 at July 28th 2016. Consider the different scales and unites of the y-axis.

Table 2.5.-1: Summary of soil sample sites on Kurungnakh and analyses conducted on Samoylov and planned for Germany.

Sampling Site	Position		Soil Sample Depth	Analysis conducted	Analysis planned
	N	E	cm		
Kur 1	72 20 21.1	126 17 45.0	0-50	GHG fluxes and production, pH, water content, LOI	C_{org}, C_{inorg}, N, $\delta^{13}C_{org}$, texture
Kur 2	72 20 20.4	126 17 34.5	0-42	GHG fluxes and production, pH, water content, LOI	C_{org}, C_{inorg}, N, $\delta^{13}C_{org}$, texture
Kur 3	72 20 20.4	126 17 34.5	0-43	GHG fluxes and production, pH, water content, LOI	C_{org}, C_{inorg}, N, $\delta^{13}C_{org}$, texture
Kur 4	72 20 20.4	126 17 31.6	0-42	GHG fluxes and production, pH, water content, LOI	C_{org}, C_{inorg}, N, $\delta^{13}C_{org}$, texture
Kur 5	72 20 19.5	126 17 28.8	0-20	GHG fluxes and production, pH, water content, LOI	C_{org}, C_{inorg}, N, $\delta^{13}C_{org}$, texture
Kur 6	72 20 20.3	126 17 29.1	0-17	GHG fluxes and production, pH, water content, LOI	C_{org}, C_{inorg}, N, $\delta^{13}C_{org}$, texture
Kur 7	72 20	126 17	0-24	GHG fluxes, pH, water	C_{org}, C_{inorg}, N,

	21.3	34.3		content, LOI	$\delta^{13}C_{org}$, texture
Kur 8	72 20 20.9	126 17 30.7	0-63	pH, water content, LOI	C_{org}, C_{inorg}, N, $\delta^{13}C_{org}$, texture
Kur 9	72 20 21.4	126 17 30.8	0-43	GHG fluxes and production, pH, water content, LOI	C_{org}, C_{inorg}, N, $\delta^{13}C_{org}$, texture
Kur 10	72 20 20.8	126 17 33.5	no samples	-	-
Kur 11	72 20 20.4	126 17 33.0	0-45	GHG fluxes, pH, water content, LOI	C_{org}, C_{inorg}, N, $\delta^{13}C_{org}$, texture

2.6. Influence of climate change on minerals in permafrost-affected soils

Cornelia Ruhland [1], Christian Knoblauch [1], Eva-Maria Pfeiffer [1]

[1] Institute of Soil Science, Universität Hamburg, Hamburg, Germany

Fieldwork period July 2016 (Samoylov and Kurungnakh Island)

Objectives

The aim of the current research is to investigate the effect of changing climate on minerals in permafrost-affected soils. Raising temperatures affect several processes in soils. Substances can be more easily dissolved, transported downstream and precipitated at another place. The main focus of the current work is on weathering of ferrous minerals but clay lessivation will also be considered. Furthermore, the surfaces of minerals sometimes indicate signs of thaw-freeze alternation, accumulation of certain mineral groups by frost weathering or mineral loss through weathering. Particular crystalline characteristics can indicate secondarily precipitated material. All these points are of interest and will be investigated with samples taken on Samoylov and Kurungnakh.

Methods

Samples were collected on Samoylov from two profiles of Holocene high-center polygons in the south-east and from one profile of a sand wedge in the south-west of the island (Table 2.6.-1). On Kurungnakh the samples were taken mainly from exposures of the ice complex in the eastern part of the island (Table 2.6.-2). Furthermore, the Pleistocene Lena sands below the Ice Complex were sampled. All samples will be analyzed by pedogenic and mineralogical methods.

Preliminary results

No preliminary results are available pending arrival of samples in Germany.

Table 2.6.-1: Sampling sites on Samoylov for soil mineralogical analyses

Sampling site	Posititon	Number of samples	Sample type	Analysis planned
S1	N 7222036 E 12628469	8	mineral soil sample	pH, conductivity, SEM, Microprobe, C/N, Fe/Mn
S2	N 7222042 E 12628427	8	mineral soil sample	pH, conductivity, SEM, Microprobe, C/N, Fe/Mn
S3	N 7222296 E 12627392	6	mineral soil sample	pH, conductivity, SEM, Microprobe, C/N, Fe/Mn

Table 2.6.-2: Sampling sites on Kurungnakh for soil mineralogical analyses

Sampling site	Posititon	Number of samples	Sample type	Analysis planned
K1	N 7220209 E 12617291	4	mineral soil sample	pH, conductivity, SEM, Microprobe, C/N, Fe/Mn
K2	N 7220233 E 12617339	3	mineral soil sample	pH, conductivity, SEM, Microprobe, C/N, Fe/Mn
K3	N 7220236 E 12617363	3	mineral soil sample	pH, conductivity, SEM, Microprobe, C/N, Fe/Mn
K4	N 7220239 E 12617371	6	mineral soil sample	pH, conductivity, SEM, Microprobe, C/N, Fe/Mn
K5	N 7220233 E 12617334	4	mineral soil sample	pH, conductivity, SEM, Microprobe, C/N, Fe/Mn
K6	N 7220198 E 12617438	1	mineral soil sample	pH, conductivity, SEM, Microprobe, C/N, Fe/Mn
K7	N 7220208 E 12617448	4	mineral soil sample	pH, conductivity, SEM, Microprobe, C/N, Fe/Mn

2.7. Yedoma: an overlooked source of N_2O from the Arctic?

Christina Biasi [1], Maija Marushchak [1], Carolina Voigt [1], Johanna Kerttula [1]

[1] Department of Environmental and Biological Sciences, University of Eastern Finland, Kuopio, Finland

Fieldwork period 3.7.-31.7.2016 (Samoylov Island, Kurungnakh Island)

Objectives

Yedoma soils are known to be very vulnerable towards carbon release but not yet investigated in terms of N_2O production. This is surprising, since they are rich in nitrogen and several soil and environmental conditions of Yedoma soils are highly suitable for N_2O production (e.g. high nutrient levels, low C/N ratio, eroded surfaces lacking plants, labile organic matter; permafrost thawing). The objective of this study was to explore the potential of Yedoma deposits to emit N_2O. We aimed at quantifying the emissions rates and analyze the spatial variability. We hypothesize that Yedoma soils are a yet overlooked, significant source of N_2O from the Arctic. In line with this major objective, multiple components of the N cycle were assessed, which have not yet been addressed from Yedoma deposits before. Inter-linked C dynamics in Yedoma were studied by our cooperation partner from same sites and soil samples (Dr. Christian Knoblauch, University of Hamburg).

Methods

On Kurungnakh Island, we quantified N_2O emissions *in situ* with the closed chamber technique, from surfaces with varying moisture content and vegetation cover, including Holocene cover, Yedoma deposits, and Yedoma mixed with more recent organics. The sites were located along transect on a Yedoma outcrop expanding from the top of the Yedoma plain down to the Lena river. For comparison, measurements were conducted on the exposed Holocene deposits on the Lena river bank on the Samoylov island (Table 2.7.-1, Fig. 2.7.-1). Total number of studied surfaces was 8 (n=5) and the fluxes were determined twice from all of them during the measurement campaign. Soil and water samples were taken from the same plots where *in-situ* flux measurements were done. These samples will be analyzed for nutrient content, and basic physico-chemical characteristics at UEF. Additionally, nitrogen process rates (gross mineralization and nitrification rates) will be determined by the pool-dilution techniques. A subsample of soil was also suspended in RNA later for molecular microbial analysis to identify microorganisms involved in key nitrogen turnover processes. Laboratory incubation experiment will follow at UEF from exported soil samples to determine N_2O production potential and factors determining N_2O turnover.

Table 2.7.-1: Sampling sites for soil analyses related to N_20 production on Kurungnakh Island.

	Description	Location	Coordinates	Altitude, m
1	Vegetated yedoma plain with Holocene cover	Kurungnakh island	N 72°20'25.2, E 126°17'32.2	52
2	Wet, freshly thawn yedoma	Kurungnakh island	N 72°20'23.3, E 126°17'35.2	46
3	Drier yedoma	Kurungnakh island	N 72°20'24.6, E 126°17'37.5	38
4	Yedoma with mosses	Kurungnakh island	N 72°20'23.0, E 126°17'36.8	30
5	Yedoma with grasses	Kurungnakh island	N 72°20'22.3, E 126°17'38.7	23
6	Sandy beach receiving yedoma melt-waters	Kurungnakh island	N 72°20'20.9, E 126°17'46.2	11
7	Sandy Holocene deposits	Samoylov island	N 72°22'04.8, E 126°28'32.7	21
8	Peaty Holocene deposits	Samoylov island	N 72°22'04.8, E 126°28'32.7	21

Figure 2.7.-1: Pictures of the sites studied by UEF. A: Overview of the studied yedoma exposure and canyon, B: Vegetated yedoma plain, C: Wet, freshly thawn yedoma, D: Drier yedoma, E: Yedoma with mosses, F: Yedoma with grasses, G: Sandy beach receiving yedoma melt-waters, H: Sandy Holocene deposits, I: Peaty Holocene deposits

Collected samples

The following sample material was collected during the field campaign by UEF:

- ~800 gas samples for analysis of N_2O, CO_2 and CH_4 concentrations and following flux calculation
- 389 water samples for analysis of pH, DOC and nutrients
- 141 soil samples for basic physico-chemical analysis (particle density, pH, organic matter, total C&N, nutrients) and laboratory incubations exploring the nitrogen turnover processes related to N_2O production

Preliminary results

Since the gas samples were taken into glass vials for later analysis of N2O concentration by gas chromatography at UEF, and have not yet been exported, we do not have results on N_2O emission potential from Yedoma at the time of this report. Similarly, the bulk of the extracts and soil water samples will be analysed for chemical composition only after they arrive in Kuopio. However, nitrate concentrations were determined from a few samples by a simple chemical test kit which we brought to the field. These first analysis showed relatively low nitrate concentrations (0.0-0.6 mg N l^{-1}) in the samples which can indicate low rates of N mineralization and nitrification, which would imply that also N_2O fluxes are low. On the other hand, it can be a result of high N turnover, when produced nitrate is rapidly used by microbial processes, including denitrification, a key process responsible for N_2O production in soils. Forthcoming laboratory analyses in Kuopio and determination of the gross mineralization and nitrification case will reveal which is the case.

2.8. Field-based incubation experiment with "ancient" organic matter

Svetlana Evgrafova [1], Oleg Novikov [1], Janina Stapel [2]

[1] V.N. Sukachev Institute of Forest, Siberian Branch, Russian Academy of Science, Krasnoyarsk, Russia

[2] Helmholtz Centre Potsdam - GFZ German Research Centre for Geosciences

Fieldwork period July to August 2016 (Samoylov Island)

Objectives

Frozen organic material is a potential substrate for microbial decay and, as a consequence, carbon release into the atmosphere and hydrosphere. However, in permanently frozen ground soil organic matter could be preserved from decomposition not only by low temperatures but also limited the initial energy required microbial decomposers as well as soil properties (e.g. protection mechanisms acting in the soils). Climate change effects, especially those of increasing temperatures on ecosystem structure and function have been addressed by numerous laboratory studies and field-based experiments. Generally, all natural soil heating experiments have been conducted in tundra permafrost-dominated or forest permafrost-free environments in Northern America and Northern Europe (Peterjohn et al., 1993; Melillo et al., 2002). These experiments mainly were focused on the gas (CO_2, CH_4) exchange between the soil and the atmosphere. The main result of soil heating experiments on temperate forest (Kirschbaum, 2004) performed over more than 10 years is that there is an increasing flux of CO_2 to the atmosphere at the beginning of the experiment before the system reaches a new steady-state. This is explained by the presence of two "pool" of organic carbon, one is being more easily decomposed and more reactive and another one is more refractory.

Methods

To find out a microbial response and carbon gaseous forms release (CO_2, CH_4) from organic matter that has been permanently frozen, we placed it *in situ* condition in field-based incubation experiment set up on Samoylov island in a rim of ice-wedge polygon. Experiment design is described on Fig. 2.8.-1.

The experiment has been installed in August, 2015. During July-August, 2016 soil respiration (CO_2 and CH_4 fluxes) were measured by the closed chamber technique. In addition, soil samples as well as "ancient" organic matter samples were taken for properties characterisation (chemical and microbiological, bulk ^{14}C of "ancient" organic matter), supplement gas samples were taken during July-August for $\delta^{13}C$ measurement in laboratory at Institute of Forest, Krasnoyarsk.

Preliminary results

Air and soil temperature, and active layer profile are presented on Fig.2.8.-2. In field-based experiment mean season methane efflux from soil surface was 0.55±0.07 mg CH_4 m^{-2} h^{-1}; mean season methane efflux from plots without "ancient" organic material

(disturbance control) was 0.50±0.02 mg CH_4 m^{-2} h^{-1}. CO_2 emission measured by dark chambers did not differ in magnitude in all plots until beginning of August and then was approximately 1.5 times higher in plots containing organic material (Fig. 2.8.-3). We can preliminary conclude that input of "ancient" organic material immediately involves in methane-driving cycle, while heterotrophic part of microbial community needs some period for adaptation to chemical properties of introduced organic matter.

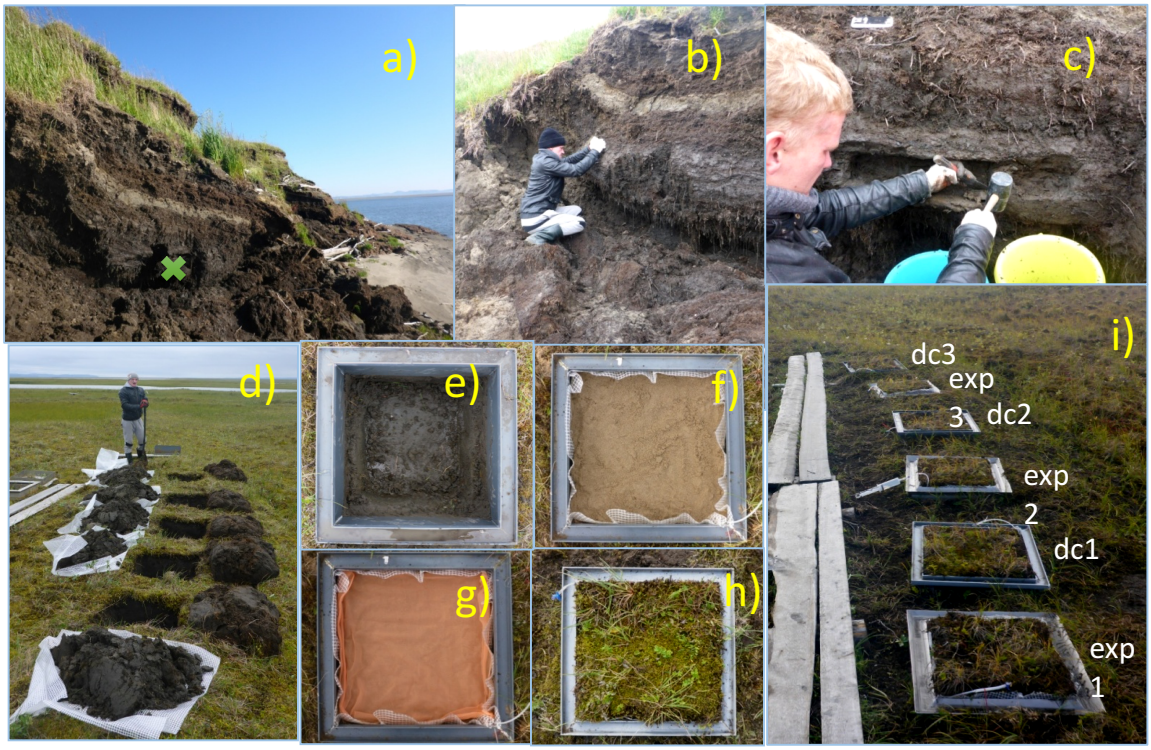

Figure 2.8.-1: Field-based incubation experiment set-up: a) Lena river bank of Samoylov Island, x – sampling place; b) removing of thawed part of organic material; c) sampling of frozen ("ancient") organic matter; d) experimental site preparation (digging holes up to permafrost table); e) permanent collar for chamber measurements installation; f) filling the hole with carbon-free sand; g) putting on the top of sand "ancient" organic material in polyester net bag (or polyester net bag without organic – disturbance control); h) placing on the top living ground cover (5 cm thickness); i) experiment view, exp1-3 – plots with "ancient" organic material, dc1-3 plots without organic material – disturbance control.

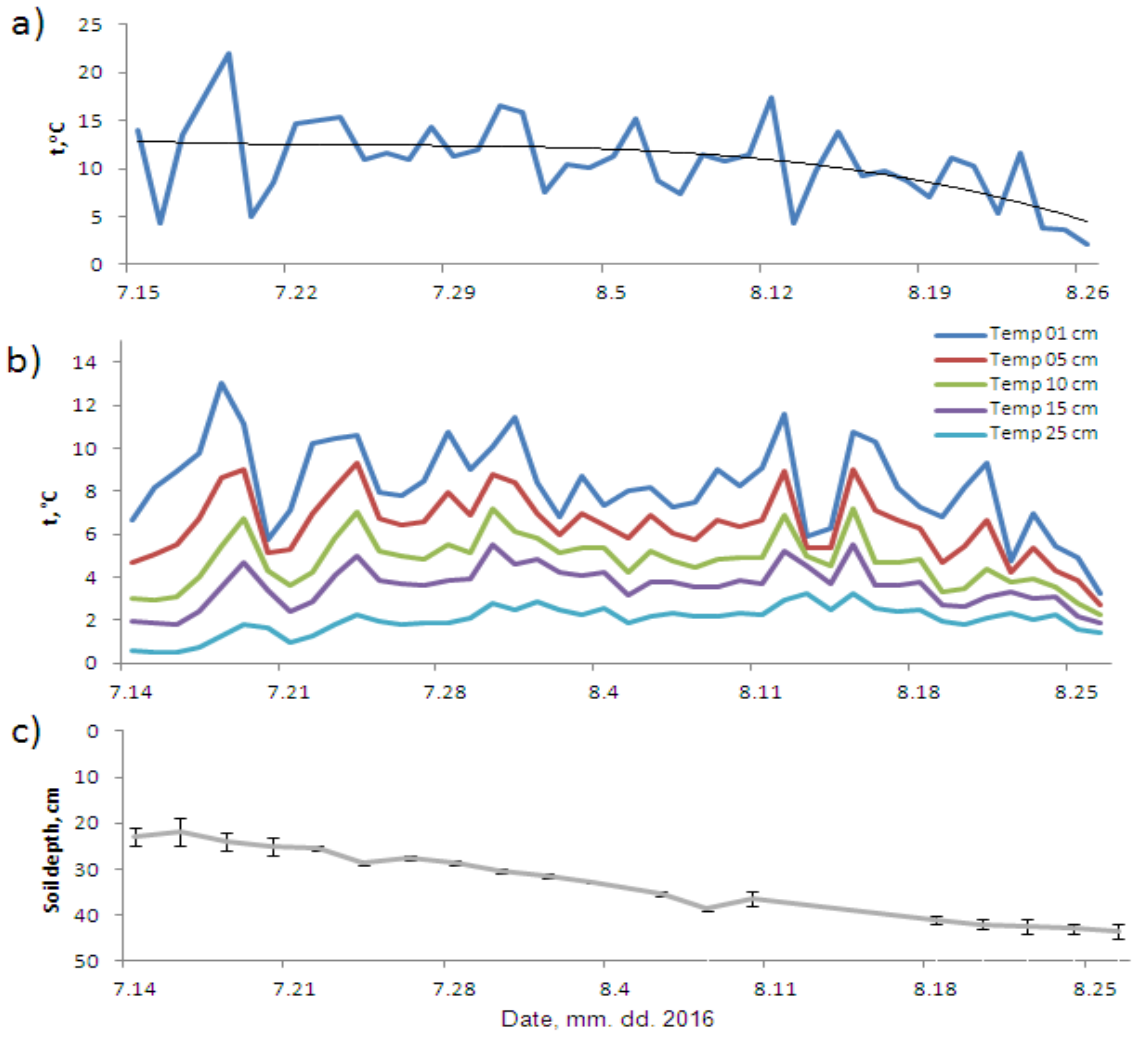

Figure 2.8.-2: Air (a) and soil (b) temperature, and active layer profile (c) of ice-wedge polygon rim where field-based experiment installed

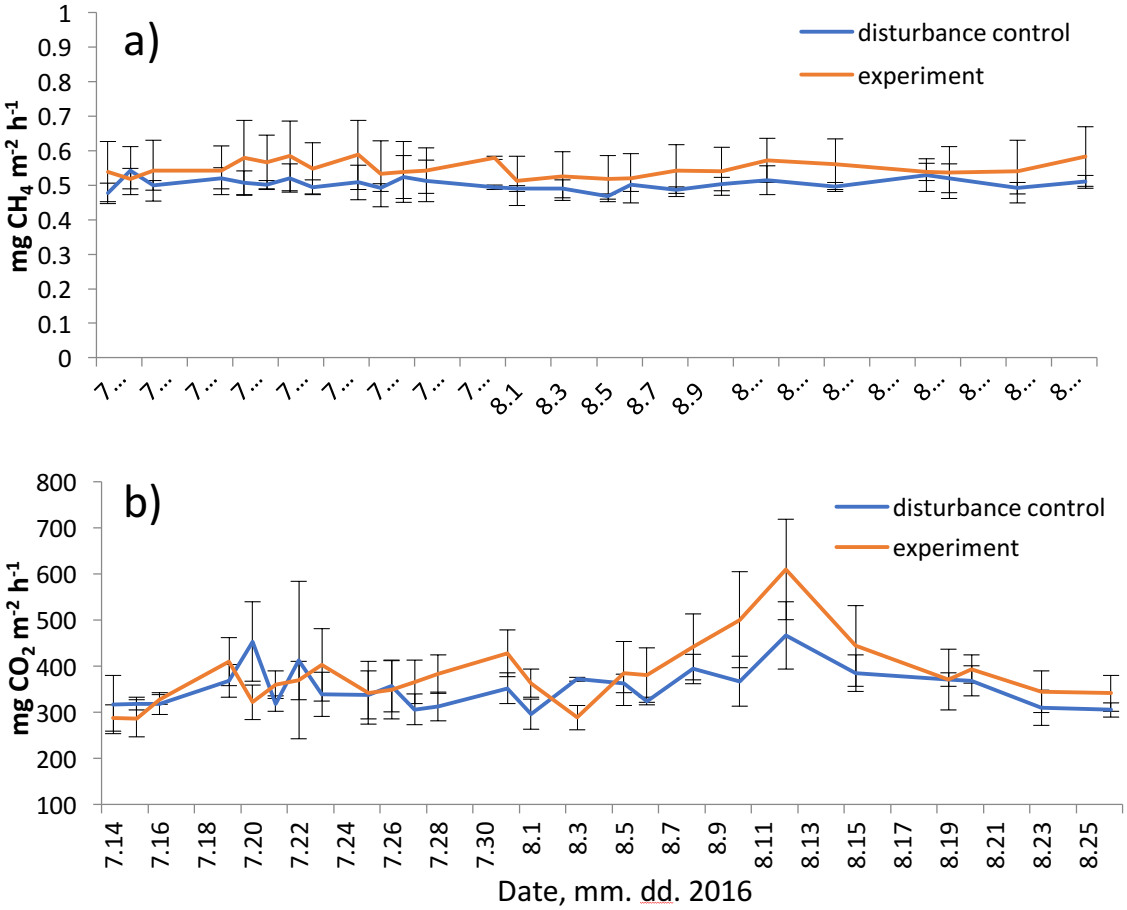

Figure 2.8.-3: CH_4 (a) and CO_2 (b) dynamics in field-based experiment

2.9. Quantification, isotopic and compositional analysis of dissolved and particulate carbon in the Lena and water bodies of its Delta

Vera Meyer [1], Thorsten Riedel [1], Gesine Mollenhauer [1]

[1] Dept. of Marine Geochemistry, Alfred Wegener Institute Helmholtz Center for Polar and Marine Research, Bremerhaven, Germany

Fieldwork period July 31 to August 31, 2016 (on Samoylov Island, Kurungnakh Island, Lena main channel)

Objectives

Understanding carbon cycling in permafrost landscapes is important to assess the climatic relevance of future permafrost thaw. Carbon export from Permafrost regions can occur via gas exchange or by river discharge as dissolved and particulate carbon (DIC, DOC and POC). Quantification combined with stable isotope analysis ($\delta^{13}C$ and compound-specific δD) and radiocarbon dating of DIC, DOC and POC can be used to estimate the contribution of fossil carbon pools to total export, determine organic matter sources and trace organic matter remineralization in the water bodies. It is known that both concentrations and radiocarbon composition of DOC and POC varies strongly over the season. Initial data also illustrate the seasonal trends in organic matter composition reflecting the relative contributions from the different sources within the Lena watershed.

In order to study the sources of carbon and the biogeochemical processes affecting carbon in Siberian rivers and lakes we collected water samples from thermokarst lakes and ponds on Samoylov and Kurugnakh, and from the Lena River main channel. For Lena 2016 the following sampling objectives were constituted:

1) Water samples from three depth profiles along a cross section of the Lena main channel once a week (4 times in total)
2) Water samples from a depth profile from North Lake (on Samoylov Island) and to sample its outflow stream and ponds adjacent to the lake (at least twice during the expedition).
3) Water samples from depth profiles of Lucky and Oval Lakes (Kurughnakh Island) and to sample the outflow systems. (at least twice during the expeditions)

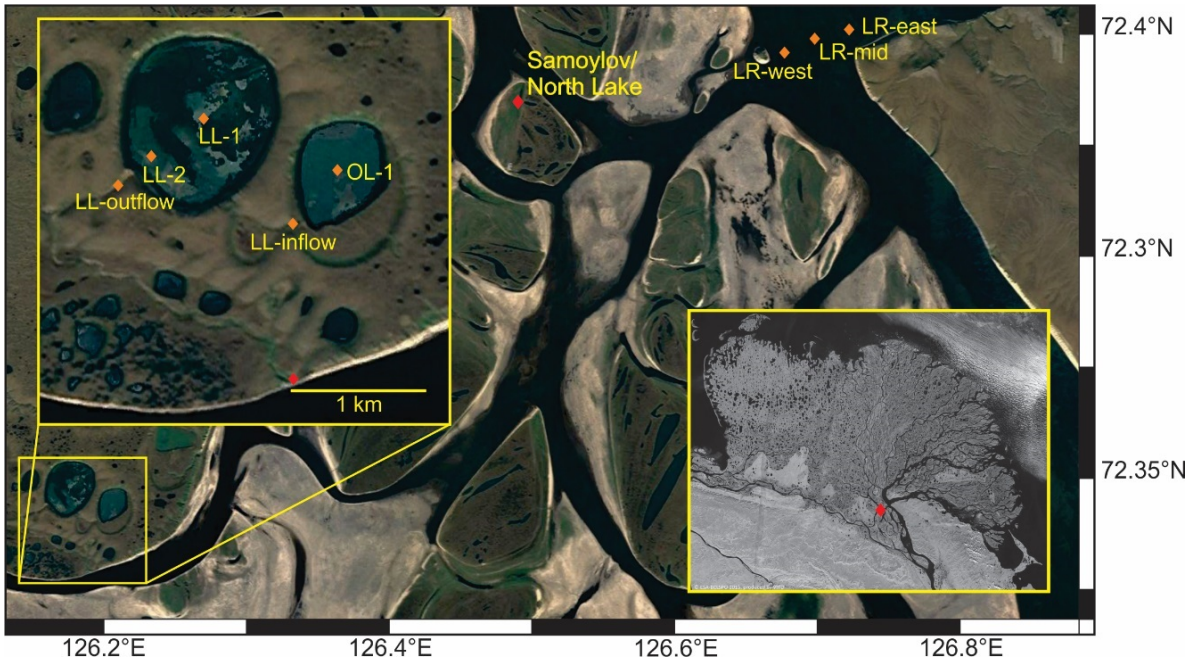

Figure 2.9.-1: Map of sampling locations in Lena Delta

Methods during field work

Lena river

Main channel

The Lena main channel was sampled along a cross-section close to Stolb Island (Fig. 2.9.-1). Along this transect three depth profiles were generated, each of them consisting of three sampling depths (near the surface, in the middle, near the bottom, see Table A 2.9.-1 in the Appendix). Water samples were taken using a 5L Niskin water sampler (General Oceanics, 1010). The device was equipped with a 30 m rope, a 1.5 kg iron weight and a 400 g drop messenger. At each sampling depth, the water sampler was deployed three to four times in order to obtain sample volumes of 15 L-20 L. The sampling depth was determined using a rope. The engine of the boat was switched off during the sampling procedure in order to facilitate a straight vertical immersion of the water sampler. Since it was intended to keep the sampling position rather constant the boat drove a few meters upstream after each deployment of the sampling device in order to correct for drift that had taken place while the engine had been shut down. Water samples for POC and DOC analysis were stored in plastic canisters (15-20L) until further processing in the laboratories on Samoylov Island. Moreover, amber glass bottles (4 ml and 330 ml) were filled for DIC analysis. Bottles were entirely filled with water in order to avoid entrainment of air in the headspace leading to gas exchange in the samples container. The Lena transect was sampled once a week and three times in total throughout the expedition. Due to logistical problems, it was not possible to repeat the procedure a fourth time. Due limited number of 330 ml amber bottles only the depth profile in the center of the channel was sampled once. All profiles were sampled three times with 4 ml amber vials.

Major Delta Channels

Additional sites at hydrographic profiles were sampled in the Trofimovskaya (1 location), Bykovskaya (1 location), Olenyokskaya (4 locations) and Tumatskaya (1 location) channels. At these sites, samples were taken by Irina Fedorova and colleagues at 0.6H (0.2H and 0.8H on occasions, see Table A 2.9.-1 in the Appendix) of the total water depth. These samples comprise 1 L of filtered water stored in plastic bottles as well as syringe filters.

River Transect

Surface water was additionally sampled at 20 locations (see Table A 2.9.-1 in the Appendix and Fig.2.9.-2) by G. Maximov along a river transect from Yakutsk to Samoylov. Along this transect, 1.5 L of surface water was sampled into plastic bottles and not treated further.

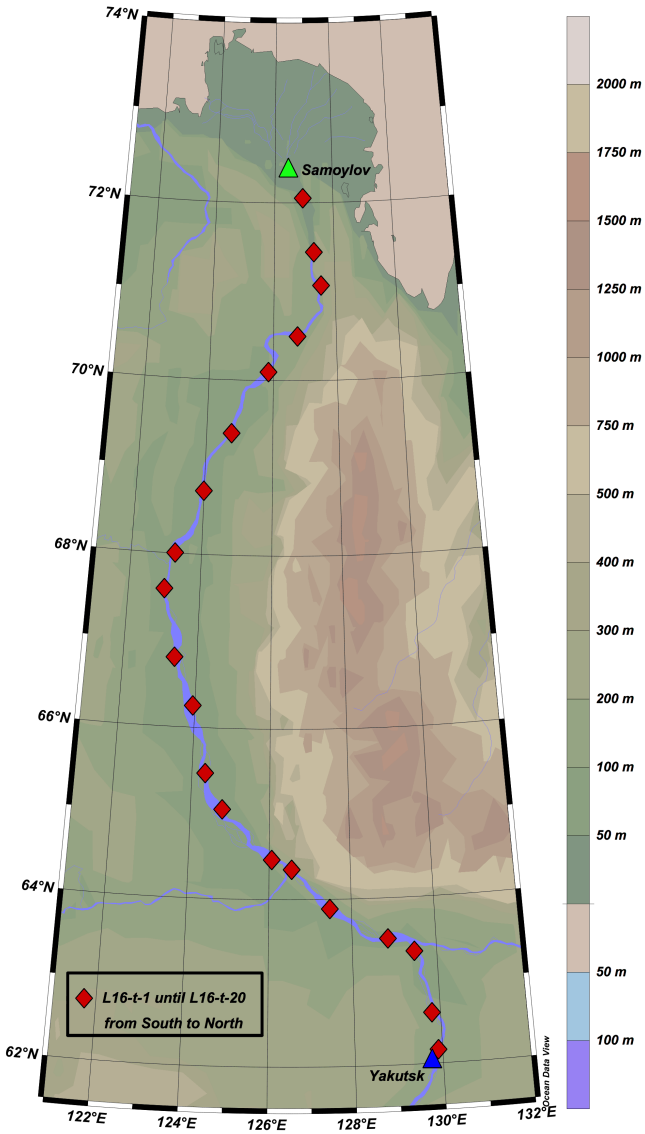

Figure 2.9.-2: Locations of sampling along river transect

Kurungnakh – Lucky and Oval Lakes

Lucky Lake and Oval Lake are neighboring thermokarst lakes which are connected through a small stream of 1 km length. The stream serves as outflow of Oval Lake and discharges into Lucky Lake. The entire lake-system ultimately drains into the Lena River via an outflow stream of Lucky Lake.

During the Lena 2016 expedition, water samples were collected from the two stream systems and from depth profiles on Oval Lake (1 profile) and Lucky Lake (2 profiles). Each profile comprised three sampling depths (see Fig. 2.9.-1). Each stream was sampled at one single location with visible water flow.

Sampling on the lakes was performed from a rubber boat using the same water sampler as on the Lena River. The water depth was measured with a labeled rope. Lucky Lake was sampled 100 m in front of the outflow and in the center. The sampling site on Oval Lake was in the center of the lake. In order to prevent drifting during the sampling procedure the boat was anchored with a heavy iron weight (ca. 10 kg). 15 L (samples for DOC and POC) were collected from each depth and stored in plastic canisters. Amber bottles (4 ml and 330 ml) were filled for DIC analysis. The streams were sampled at the surface by immersing the canisters (10 L) and amber bottles (4 ml and 330 ml) into the water. The sampling program was performed once during the expedition and was completed on two consecutive days. Logistical problems and bad weather conditions did not allow for a repetition of the entire procedure. Therefore, only the inflow and outflow streams as well as the central depth profile on Lucky Lake were sampled twice (repeated after 10 days). During the second campaign the streams were sampled with 15 L and the depth profile with 5 L per depth. Additionally, 4 ml amber vials were filled. Given the limited number of 330 ml amber bottles, large DIC samples were only taken once from the streams and along the central depth profile on Lucky Lake.

Samoylov – North Lake and adjacent ponds

On North Lake samples were obtained from one single depth profile consisting of two sampling depths (near the bottom and the surface) at the center of the lake. The outflow stream of North Lake was sampled at two locations (in the floodplain near the Lena and in proximity to the lake). Additionally, surface samples were taken from three polygonal ponds (1 m deep) situated on a north-south transect south of North Lake. Sampling of the lake and its outflow system for POC and DOC (15-20 L) as well as DIC (4 ml and 330 ml amber bottles) was performed according to the sampling protocol at Lucky Lake. Polygonal ponds were sampled at the rim by immersing canisters (sample volume: 15-20L) and amber glass bottles (4 ml and 330 ml).

Small DIC samples (4 ml amber vials) were taken from the depth profile, the upper part of the outflow and from one pond. The floodplain was not sampled. One large DIC sample (330 ml amber bottle) was taken from the pond. Due to the limited amount of amber bottles (330 ml) the other sites were not sampled.

The sampling procedure for 15-20 L canister was conducted twice during the expedition with the sampling campaigns being separated by a two-week interval. Sampling for DIC (4 ml vials) was only repeated once for the pond.

Filtration and sample treatment in the laboratories

Large samples (canisters) were filtered using glass fibre filters (Whatman, GF/F) of different diameters (142mm, 47mm and 25mm). The filtration volume for the 142 mm

filters was 6-20 L per sample, and 142 mm filters are intended for biomarker analyses of POM.120-180 ml were filtered using filters of 47 mm and 25 mm diameter (2-3 filters per sample, 60 ml for each filter). Small filters will be used for $\delta^{13}C$ and $\Delta^{14}C$ analyses of POC as well as POC determination. The filtrate from the small filters will be used for analyses of concentration, $\delta^{13}C$ and $\Delta^{14}C$ of DOC and was filled into 2-3 HDPE bottles (60ml each). 142 mm filters were wrapped in pre-combusted aluminium foil. Small filters (47 and 25 mm) were placed in combusted glass petri dishes. Filters and water samples were stored frozen. DIC samples were poisoned with 50 µl (4 ml vial) and 100 µl (330 ml bottles) of a saturated solution of $HgCl_2$ in distilled water and were stored at 4°C.

2.10. Carbon export form Siberian permafrost soils

Anja Wotte [1], Janet Rethemeyer [1]

[1] Organic Geochemistry and Radiocarbon Dating, University of Cologne, Cologne, Germany

Fieldwork period August 2016 (Samoylov Island and Kurungnakh Island)

Objectives

The overall objective of our investigations in the Lena Delta is to improve the understanding of organic carbon (OC) dynamics in Siberian permafrost soils. During the last years we focus on elucidating the quality of the organic matter stored in the active layer and its organo-mineral protection against microbial degradation (Höfle et al., 2013) as well as identifying the microbial community itself (Höfle et al., 2015) using lipid biomarker and radiocarbon analysis. The results of these studies revealed little protection of the organic matter by interaction with soil minerals thus suggesting a rapid microbial degradability even of several thousand-year-old OC in the active layer and transition zone. The microbial community - identified by bacteriohopanepolyols derived from soil bacteria - is strongly variable in the different structures of the polygonal tundra (rim, centre) and in different soil horizons mainly caused by differences in physical and chemical soil properties.

We now expanded our studies to obtain a complete picture of the OC carbon cycle in permafrost soils by the analysis of OC exports from the soils including dissolved and particulate organic carbon (DOC and POC) and carbon dioxide release from the soils by microbial respiration. Our preliminary unpublished results of DOC sampled near the permafrost table during Lena expedition 2014 suggest a broad range in ^{14}C age from 60 to 5560 yrs BP and strong differences between polygon rim's being much older than those collected in polygon centre's. This preliminary data set will be extended during the next years to obtain information on seasonal changes in DOC age and composition, respectively. During this year's expedition (Lena 2016), we collected for the first time microbial respired CO_2 using respirations chambers and molecular sieves to concentrate CO_2 for subsequent $^{14}CO_2$ analysis. These analyses are technically challenging but will give useful information on autotrophic and heterotrophic respiration (Biasi et al., 2014; Hicks Pries et al., 2013; Hicks Pries et al., 2015). We collected CO_2 samples at different geomorphological sites including a freshly eroded ice complex site.

Methods

During the Lena 2016 expedition we collected samples on Samoylov Island, part of the eastern terrace of the Lena River Delta, which is a late Holocene to modern delta floodplain, and on Kurungnakh Island, which is part of the third, late Pleistocene terrace, in August (Schirrmeister et al., 2011). DOC and POC samples were taken from four of our established polygonal sampling sites to continue our long-term investigations (Table 2.10.-1). Sampling from polygon rims was done from a soil pit using rhizons inserted horizontally into the soil above the permafrost table and from the polygon centres using

perforated steel tubes (1/8'' OD) inserted down to the frozen ground. Around 600 ml pore water were sampled at each location. The samples, which were taken with steel tubes, were filtered through glass fibre filters (GF/F, diameter 47 mm, Whatman). All samples were stored frozen in pre-cleaned 250 ml HDPE bottles.

Table 2.10.-1: DOC, POC and CO_2 samples collected for ^{14}C analysis

Site ID	Name	Latitude	Longitude	Sample material
Samoylov Island:				
FLP	Fish Lake Polygon	N 72.37278°	E 126.48512°	DOC, POC, $^{14}CO_2$
FLP2	Fish Lake Polygon 2	N 72.37220°	E 126.48920°	DOC, POC
TiP	Tim's Polygon	N 72.37407	E 126.49731°	DOC, POC, $^{14}CO_2$, sediment
Kurungnakh Island:				
KUP	Kurungnakh Polygon	N 72.32343°	E 126.22298°	DOC, POC
KUP2	Kurungnakh Polygon 2	N 72.32520°	E 126.26561°	DOC, POC, $^{14}CO_2$
K4	Icecomplex, mixed	N 72.33900°	E 126.29207°	$^{14}CO_2$, sediment
K7	Icecomplex, Baidzerakh	N 72.33924°	E 126.29302°	$^{14}CO_2$, sediment
KX	Icecomplex, Baidzerakh	N 72.33920°	E 126.29199°	$^{14}CO_2$, sediment

The CO_2 samples for ^{14}C analysis were also collected at our study sites on Samoylov and Kurungnakh Island to obtain a comprehensive data set (Table 2.10.-1). Additionally, we sampled CO_2 on exposed thermokarst mounds (Baydzherakhs) and freshly eroded ice complex sites on the eastern river shore of Kurungnakh Island to provide additional information for the studies by Christian Knoblauch and colleagues (University of Hamburg). At each site two to three replicate samples were collected. At some sites, we compare plots with vegetation und clipped plots from which the vegetation was removed about 3-7 days in advance (TiP: >1 year before). The clipping was done because the ^{14}C signature of the ecosystem respiration (without clipping) is indistinguishable from the atmospheric CO_2 (Hardie et al., 2005).

Figure 2.10.-1: Picture of our closed loop respiration chamber to which an infrared gas analyser, water traps, and the molecular sieve for CO_2 concentration are connected.

The CO_2 samples were collected between 12:30 and 18:00 using self-made, closed and dark respiration chambers similar to Hardie et al. (2005; diameter 23.5 cm, height ~15 cm, volume ~7 L), which was inserted >10 cm into the soil (Fig. 2.10.-1). The chambers were connected to an infrared gas analyser (IRGA, Licor 840A, Germany) for quantification of the CO_2 flux and to our new stainless-steel molecular sieve cartridges in which the CO_2 was trapped for ^{14}C analysis (Fig. 2.10.-1). The CO_2 desorption will be performed at the University of Cologne using vacuum systems.

Preliminary results

Fig. 2.10.-2 shows the variability of the CO_2 fluxes at the different study site. As expected, the CO_2 flux from the clipped soils (without vegetation) is lower compared to the soils with vegetation (Fig. 2.10.-2 A). The CO_2 flux from the sites with vegetation on Samoylov Island is highly variable in both, the centre and rim of the FLP polygon. It is much less variable in the clipped plots at all sites on Samoylov (FPL, TiP) and Kurungnakh Island (KUP2). The highest CO_2 fluxes were determined on the eroding ice complex on Kurungnakh Island, especially at the Baidzerkah hills (K7; Fig. 2.10.-2 B).

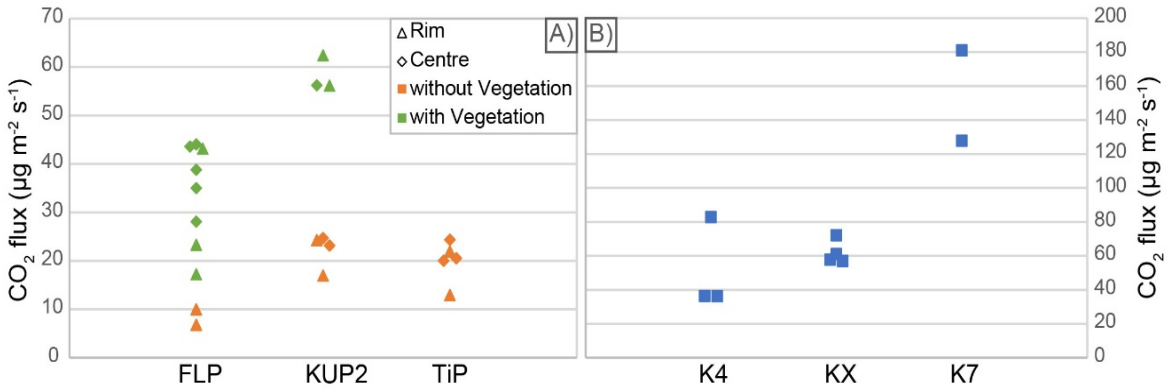

Figure 2.10.-2: Preliminary results of CO_2 fluxes determined at our study sites on A) Samoylov Island (FLP, TiP) and Kurungnakh Island (KUP2, K4, KX, K7), and B) on the eroding ice complex

All samples taken at the different study sites during our field campaign in August 2016 and the analyses that will be performed are listed in Table 2.10.-1 and Table 2.10.-2.

Table 2.10.-2: Sediment, poreater and CO_2 samples and their planned analyses. Sampling site coordinates are given in Table 2.10.-1. Abbreviations: R - rim, C - center

Sample ID	Depth (cm)	Sample type	Sampling purpose
Samoylov Island:			
16-FLP-R	30–32	porewater DOC+POC	^{14}C analysis
16-FLP-C	34	porewater DOC+POC	^{14}C analysis
FLP-R1–R3	---	CO_2 (3 replicates)	^{14}C and ^{13}C analysis
FLP-C1–C3	---	CO_2+ CH_4 (3+2 rep.)	^{14}C and ^{13}C analysis
FLP-R2+R3_oV	---	CO_2 (2 replicates)	^{14}C and ^{13}C analysis
FLP-Atm	---	CO_2	^{14}C and ^{13}C analysis
16-FLP2-R	34	porewater DOC+POC	^{14}C analysis
16-FLP2-C	32	porewater DOC+POC	^{14}C analysis
16-TiP-R	15	porewater DOC+POC	^{14}C analysis
16-TiP-C	35	porewater DOC+POC	^{14}C analysis
16-TiP_7-15	7–15	sediment	^{14}C analysis
TiP-C5+C6	---	CO_2 (2 replicates)	^{14}C and ^{13}C analysis
TiP-R15+R16	---	CO_2 (2 replicates)	^{14}C and ^{13}C analysis
Kurungnakh Island:			
16-KUP-R	32–35	porewater DOC+POC	^{14}C analysis
16-KUP-C	27–29	porewater DOC+POC	^{14}C analysis
16-KUP2-R	23	porewater DOC+POC	^{14}C analysis
16-KUP2-C	30	porewater DOC+POC	^{14}C analysis
KUP2-R1+R2	---	CO_2 (2 replicates)	^{14}C and ^{13}C analysis
KUP2-R2+R3_oV	---	CO_2 (2 replicates)	^{14}C and ^{13}C analysis
KUP2-C1	---	CO_2	^{14}C and ^{13}C analysis
KUP2-C1+C2_oV	---	CO_2 (2 replicates)	^{14}C and ^{13}C analysis
KUP2-Atm	---	CO_2	^{14}C and ^{13}C analysis
K4_0-3	0–3	sediment	^{14}C analysis
K4_6-11	6–11	sediment	^{14}C analysis
K4_14-18_OM	14–18	sediment	^{14}C analysis
K4_24-28	24–28	sediment	^{14}C analysis
K4_30-34_OM	30–34	sediment	^{14}C analysis
K4.1+3b	---	CO_2 (2 replicates)	^{14}C and ^{13}C analysis
K7_0-3	0–3	sediment	^{14}C analysis
K7_4-7	4–7	sediment	^{14}C analysis
K7_10-15	10–15	sediment	^{14}C analysis
K7.a+b	---	CO_2 (2 replicates)	^{14}C and ^{13}C analysis
KX_0-3	0–3	sediment	^{14}C analysis
KX_4-8	4–8	sediment	^{14}C analysis
KX_10-13	10–13	sediment	^{14}C analysis
KX_20-26	20–26	sediment	^{14}C analysis
KX_30-36	30–36	sediment	^{14}C analysis
KX_40-45	40–45	sediment	^{14}C analysis
KX.1+2b	---	CO_2+ CH_4 (2 replicates)	^{14}C and ^{13}C analysis

2.11. Sampling of Thermokarst and Thermoerosion Features to Characterize Soil Carbon Stocks, Ground Ice, and Surface Waters

Guido Grosse [1], Anne Morgenstern [1], Justine Ramage [1]

[1] Alfred Wegener Institute Helmholtz Center for Polar and Marine Research, Potsdam, Germany

Fieldwork period July 18-31, 2016 (Kurungnakh Island)

Objectives

With this field campaign, we continue our efforts to better understand the impacts of thermokarst and thermoerosion on landscape-scale soil carbon and hydrological dynamics. The studies conducted on Kurungnakh Island are a continuation of previous field studies on 1) drained thermokarst lake basins (DTLB) within the ERC PETA-CARB project (Sobo-Sise / Bykovsky Expedition 2014 and 2015, Yukechi expedition 2015) and previous NASA funded projects by Grosse conducted in various regions of Alaska and Siberia (Jones et al., 2012, Regmi et al 2012, Walter Anthony et al., 2014), 2) thermoerosional valleys (TEV) in the Laptev Sea region (Morgenstern, 2012, Morgenstern et al., in prep. a) and Yukon Territories of NW Canada, and 3) water characteristics in the Lena Delta (Polakowski, 2015, Morgenstern et al., in prep. b). The samples acquired during this field campaign will be used within several student thesis projects focusing on DOC characteristics of thermokarst lakes and their inlets and outlets (L. Polakowski), soil carbon stocks and dynamics of TEV (J. Ramage), and the characterization of DTLB drainage age, carbon storage, and surface properties (NN). Additional samples for these objectives were derived during the Sobo-Sise/Bykovsky Peninsula expedition in the eastern Lena Delta.

Methods

During the field campaign, several different methods were applied to derive permafrost soil, ground ice, and water samples from thermokarst and thermo-erosion affected landscape components on Kurungnakh Island.

In six DTLB (Fig. 2.11.-1) a central location was selected where a soil pit was dug by shovel to the bottom of the active layer. Then a permafrost core was hammer-cored using a core tube (1 basin) or drilled using a 3” diameter SIPRE permafrost corer (5 basins). The soils in the soil pit and the frozen core were described visually (soil characteristics, cryolithology, lithology, stratigraphy). Eventually the total depth of terrestrial peat overlying lake sediments was measured. From the soil pit, defined volumes of samples were cut with a knife and scissor or with a soil sampling tube. The frozen cores were cut in subsamples of 10 cm or sometimes shorter intervals if required by stratigraphic changes. Total depth reached for sampling varied between 80 and 158 cm. Samples will be analysed in the laboratory for soil carbon characteristics, granulometry, ground ice contents, and radiocarbon age of the basal terrestrial peat.

Figure 2.11.-1: Landsat-5 TM based map (bands 4-3-2) of Kurungnakh Island showing locations of sampled DTLB (red dots) and TEV (green dots)

For one TEV (Fig. 2.11.-1) we designed a transect sampling scheme consisting of three cross-profiles covering the upper, middle and lower reaches of the valley (Fig. 2.11.-2). Along these cross-profiles soil pits were excavated with a shovel and a permafrost core to one meter depth was drilled with a 3" diameter SIPRE permafrost corer. In the upper reaches, we cored 3 sites, in the middle reaches 5 sites, and in the lower reaches 3 sites, covering a wide range of TEV geomorphic conditions (Yedoma plateau, upper slope, lower slope, and valley bottom) with several sites each. Similar to the DTLB study, soils were described and sampled in the soil pits, and the frozen core was visually described accordingly (cryolithology, sedimentology, stratigraphy). Samples will be analysed in the laboratory for soil carbon characteristics and ground ice contents.

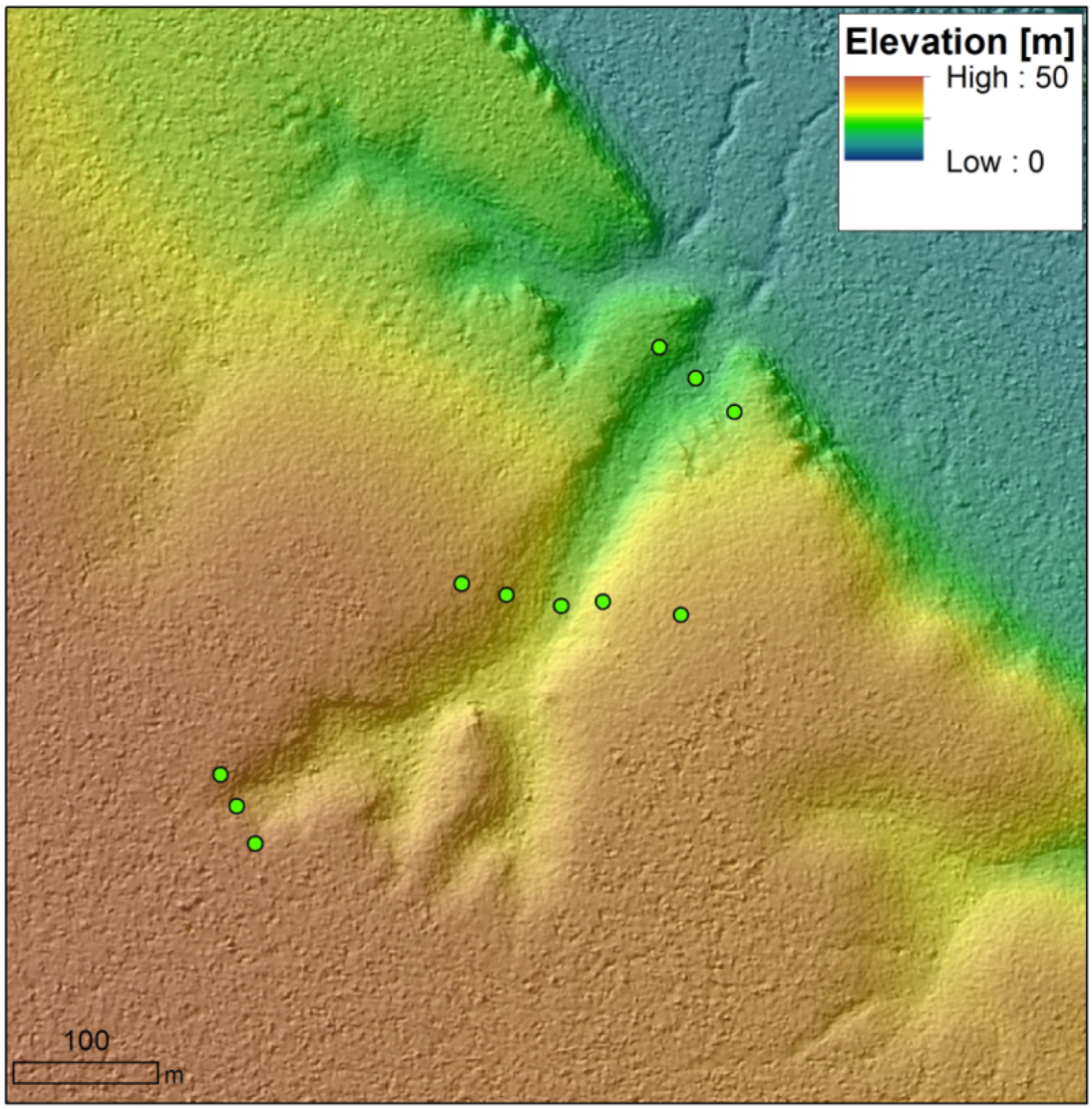

Figure 2.11.-2: Digital Elevation Map of TEV-1 and soil and permafrost sample locations. Elevation data based on WorldView-2 data (© DigitalGlobe; Stereo DEM produced by F. Günther).

During the entire campaign, samples of various surface waters, snow, and ground ice were collected strategically as well as opportunistically (Fig. 2.11.-3). Sampling included filling bottles with surface water (lakes, ponds, lake inlets and outlets, gully streams, Lena river) as well as using shovels or a hatchet to chip out pieces of snow from still existing snow patches or exposed ice wedges. At the sampling sites, water temperatures were measured and overall conditions of the water, weather, and time of the day were noted. In addition, ground ice encountered in permafrost cores drilled in DTLB and TEV was melted in the field station lab and filled in bottles for later analysis in the AWI Potsdam labs. From one core of a TEV pore water was extracted using rhizons in the field station lab after thawing of the core material. All derived water samples were measured in the field station lab for pH and electrical conductivity. Depending on the different analyses planned in the AWI Potsdam labs the water samples were divided into subsamples and pretreated (e.g. filtering, acidification).

Figure 2.11.-3: Sampling locations for surface water, snow, and ground ice, samples

Preliminary results

A total of six DTLB were sampled to a depth of 80 to 158 cm (Table A 2.11.-1 in the Appendix). The studied DTLB had different morphometric characteristics but all of them had clear evidence for lateral drainage, suggesting a catastrophic drainage event. Peat depths encountered ranged from 4 to 90 cm, suggesting significant different drainage ages. Overall, the active layer at the studied sites was rather shallow, ranging from 9 to 22 cm (Table A 2.11.-3 in the Appendix). Ground ice contents varied but DTLB with thicker peat appeared to have higher ice contents, consistent with a supposedly older drainage age and time for permafrost aggradation in the lake sediments.

A total of eleven sites were samples in one TEV down to a depth of 1 m (Table A 2.11.-2 in the Appendix). Organic layer thickness in the studied sites ranged from 4 to 30 cm. In 5 of the sites we encountered ice wedge ice starting at 62 to 107 cm depth. Active layer in the TEV ranged from 9 to 28 cm and there appears to be a correlation of active layer depth with slope angle and direction (Table A 2.11.-3 in the Appendix).

A total of 51 sites were sampled for water characteristics (Table A 2.11.-4 in the Appendix). Surface waters, i.e. waters from lakes, ponds, streams and the Lena river,

varied greatly in optical appearance (e.g. colour, turbidity) as well as in temperature at the time of sampling. The lowest temperatures (min. 0,2 °C) were measured at sites with active erosion of the permafrost, for example in the strongly eroding TEV-2, the highest (max. 15,9 °C) in the Lena River. pH values varied between 5,63 and 7,73 and electrical conductivity between 26 and 124 µS/cm.

2.12. Integrated non-invasive geophysical-soil studies of permafrost upper layer and aerial high-resolution photography

Leonid Tsibizov [1], Alexey Fage [1], Olga Rusalimova [2], Denis Fadeev [1], Vladimir Olenchenko [1], Igor Yeltsov [1], Vladimir Kashirtsev [1]

[1] Institute of Petroleum Geology and Geophysics, Siberian Branch, Russian Academy of Sciences, Akademgorodok, Russia

[2] Institute of Soil Sciences and Agrochemistry, Novosibirsk, Russia

Fieldwork period July 10 to July 30, 2016 (on Samoylov and Kurungnakh)

Objectives

The main objective is to define which features of upper layer in permafrost are detectable with non-intrusive geophysical methods. Initially it was suggested that integrated studies could be the key to clarification of some permafrost features. The reason for this assumption is obvious: different methods work in different physical domains therefore we could benefit from jointly using several of them. Accurate knowledge of upper layer geophysical image allows to clarify deeper structures with these methods. We used non-invasive geophysical methods to study areas with presumably different types of permafrost. We have also analyzed physical and chemical properties of soil samples. It is expected that the joint processing of geophysical data and soil properties will improve the accuracy of the interpretation of geophysical anomalies observed in permafrost. This knowledge could further transform into geophysical method that helps quickly determine upper layer parameters, affecting the biogeochemical processes in the active layer of the soil. Our goal is also to consider the way in which these methods could be used for upscaling of different sampling data.

This year expedition has also used UAV-based aerial imaging to acquire surface maps of extremely high resolution (5-7 cm/pixel). These images help us better understand the correlation between anomalies that we observe on our geophysical cross-sections and surface features. We also hope that different groups of scientists could benefit from this work and use these images in their studies.

Methods

We worked at four sites (Fig. 2.12.-1): site 1 is at the center of Samoylov island on the contact of wet polygonal tundra and dry sandy zone; site 2 is on alas slope on Kurunghakh island; site 3 is near the cliff of degrading ice complex on Kurungnakh island; site 4 is in vicinity of Samoylov station structures affected by diesel engine exhaust heat. Methods used:

1. High-resolution orthophoto (5-7 cm/pixel) and DEM (25-30 cm vertical resolution, 1x1 m grid) made with UAV.
2. 2-elevation (0.4 m and 1.15 m) magnetic survey (gradiometer GSMP-35g, base magnetic station MMPOS-2) with 1 m distance between profiles and about 10 cm

distance between neighbouring points along each profile due to continuous (10 Hz) measuring mode. Relative measurement errors of GSMP-35g (10 Hz) and base station MMPOS-2 (0.2 Hz) are less than 0.1 nT (http://www.gemsys.ca, http://www.magnetometer.ru). Total error depends on magnetic variation intensity (considering the necessity of interpolation due to low frequency of the base station) and magnitude of spatial gradient in measuring area (usually less than 5 nT/m) combined with positional accuracy (± 10 cm). We can estimate the total error as 1 nT for the most part of surveying area.

3. Electrical resistivity tomography (ERT): SibER-48 (http://nemfis.ru) at 20 cm step (1.5-meter penetration depth, very high resolution) and 5 m step (45 meters penetration depth).
4. Ground penetrating radar (GPR): SIR-3000 (http://www.geophysical.com) with 200 MHz antenna, 0.5 m distance between profiles, 5 mm between neighboring impulses along each profile due to continuous measuring mode, 60 ns measuring period (corresponding to about 2.8 m depth assuming median dielectric permittivity of section equal to 6), positional accuracy is ± 5 cm.
5. Electromagnetic sounding (EMS): multielectromagnetic profiler AEMP-14 (http://nemfis.ru).
6. Soil studies: a number of soil samples on each site and some soil samples at other locations characterized by different soil types and relief patterns. All soil pits were dug to the bottom of the active layer using shovel, afterwards a permafrost core was extracted using a metal tube and sledgehammer. Active layer was sampled according to its genetic soil horizons. Permafrost cores were taken in subsamples of 10 cm to the depth of 100 cm. The meso- and micro-relief, plant community and soils morphology were described visually at every soil sampling location. Sample analyses:
    - measurements in the field: fresh sample volume and weight, magnetic susceptibility - measured with kappameter KT-5 (absolute values are not precise due to the sample size (38 mm) smaller than kappameter working area (~ 65 mm),
    - laboratory studies: a number of physical and chemical properties (A 2.12.-2), including mid–near-infrared spectroscopic analysis (NIRS-MIRS) - a useful tool for characterizing the overall heterogeneity of soil chemical properties especially for total carbon and nitrogen, and it can be used without any preliminary calibration (Bornemann, 2011; Akroume et al., 2016); for a more detailed study of soil organic matter (SOM) thermogravimetric analysis of the quality of soil organic matter will be made (Siewert, 2002, 2004). The method allows to determine biodegradable (easily available for microbial transformations) component of SOM and recalcitrant (humified) component. Ratio of these components along with total carbon content and C to N ratio in soil play a key role in microbiological processes in soil and in particular regulating rate of decomposition of SOM and emission of greenhouse gases.
7. Temperature monitoring: autonomous temperature stations ASTM (IPGG SB RAS) with 10 temperature sensors (calibrated DS18B20 with accuracy of 0.06 C) at 0, 10, 20, 30, 40, 50, 60, 70, 80, 100 cm depth (A 2.12.-1).

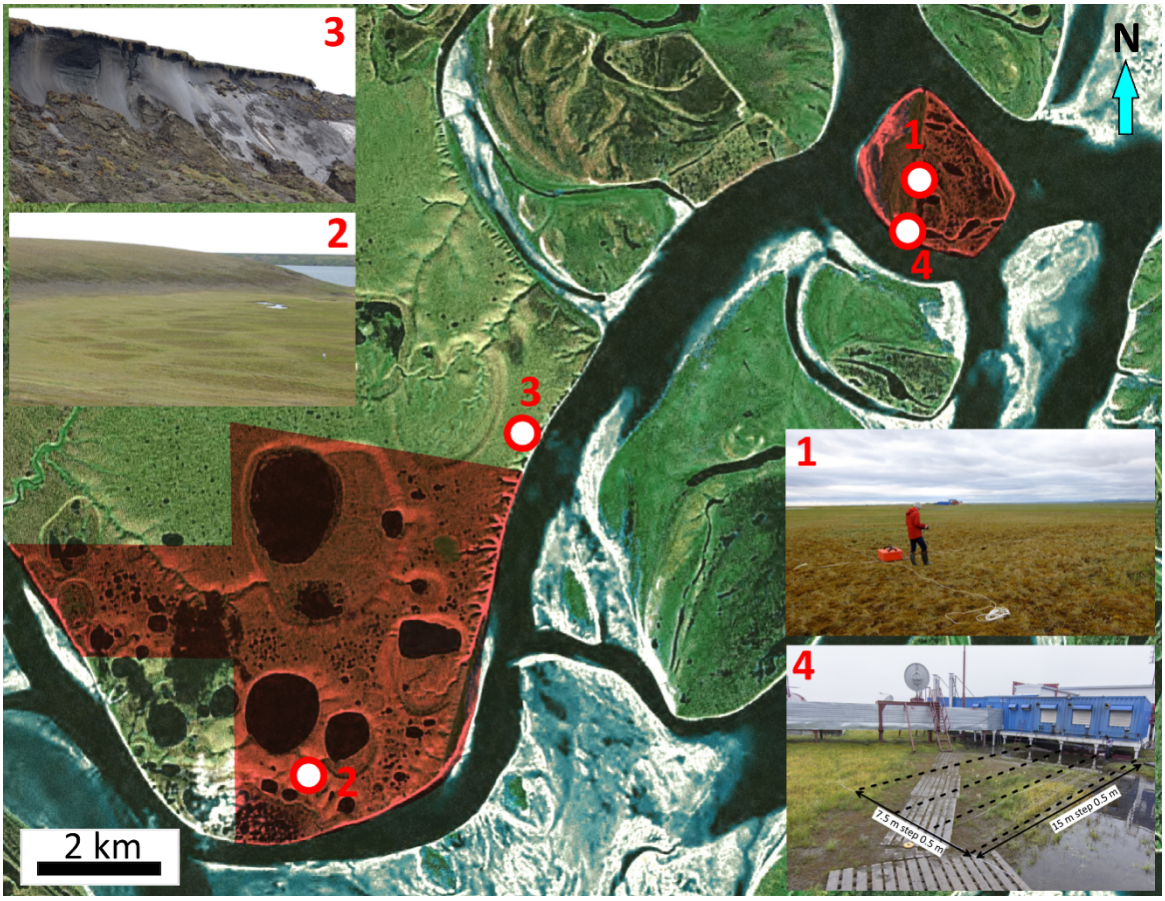

Figure 2.12.-1: Working sites map: 1 – area on Samoylov (magnetometry, ERT, GPR, EMS, sampling); 2 – area on alas slope on Kurungnakh (magnetometry, ERT, sampling, temperature monitoring); 3 – area on the top of the ice complex (magnetometry, sampling, temperature monitoring); 4 – area on Samoylov station ground (ERT, EMS); red areas – UAV orthophoto coverage

Preliminary results

Aerial orthophoto

34 km^2 of territory was covered. Resulting maps have resolution 3-7 cm/pixel (see Fig. 2.12.-2). Based on aerial photography digital elevation models (DEM) of Samoylov and Kurungnakh were built (see Fig. 2.12.-3 and 2.12.-4).

Figure 2.12.-2: Example of an orthophoto image (rubber boat can be clearly seen near the lake); resolution 5 cm/pixel

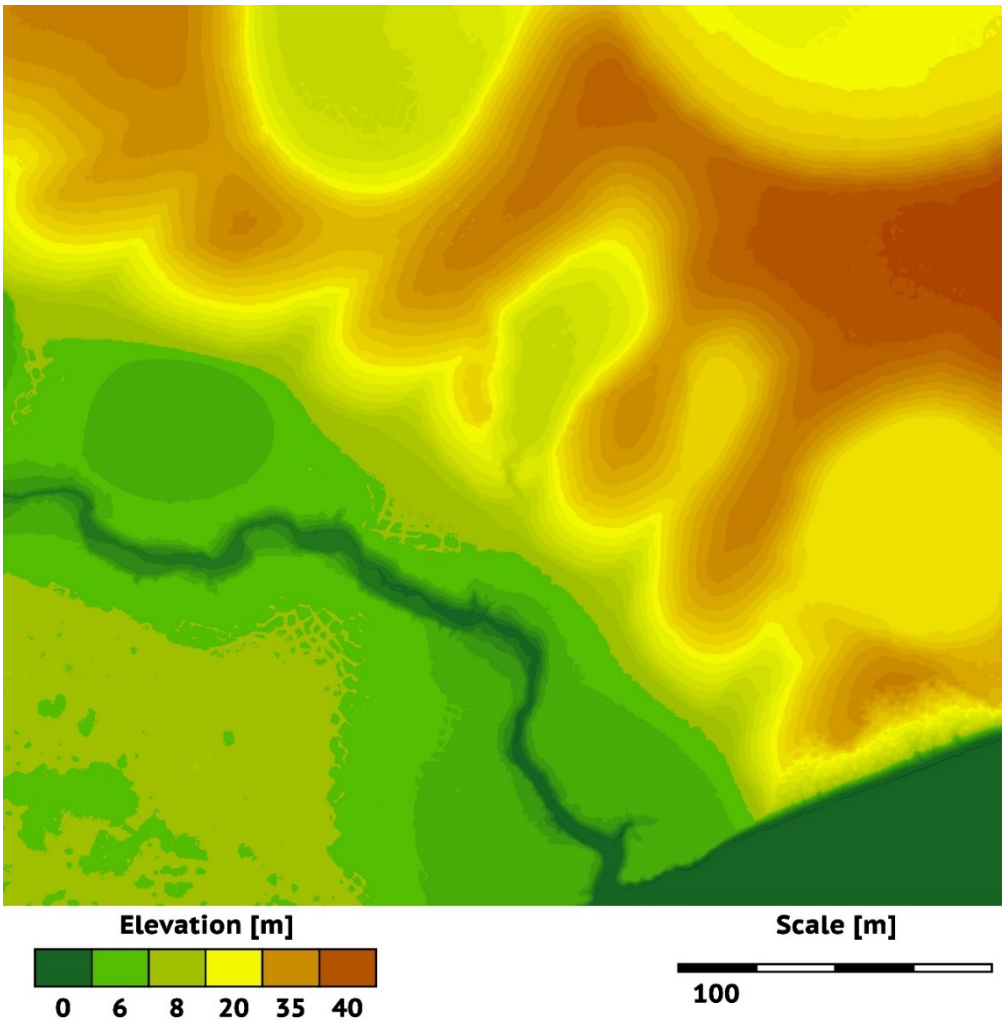

Figure 2.12.-3:. DEM sample of Kurunknakh island, orthographic projection

Figure 2.12.-4: DEM sample of Kurunknakh island sideview with surface texture; resolution of a base orthophoto image ~7 cm/pixel

Site 1 (Samoylov island)

Location (N 72.37602; E 126.47912): at the center of Samoylov island on the contact of wet polygonal tundra and dry sandy zone (Boike et al., 2012) was picked as a proving grounds for testing all available geophysical and soil methods. The site was chosen on the base of visible heterogeneity in plant and soil cover under conditions of subdued relief. Acquisition scheme overlaying aerial photo of the site is shown at Fig. 2.12.-5. Negative total magnetic field anomalies (Fig. 2.12.-5, right) spatially correlated to ice wedges (the effect was noticed by Hodgetts et al. (2011), which are also visible on ERT profile (Fig. 2.12.-6) as high-resistivity anomalies. Active layer bottom boundary and another deeper boundary are seen on GPR survey (Fig.2.12.-7). Ice wedges in GPR radargrams are seen as regions of weak signal reflection. No meaningful data was obtained with EMS presumably due to very high electrical resistivity of frozen ground and relatively thin thawed layer. Magnetic susceptibility of upper meter of the section is about $\cdot 10^{-3}$ SI (Fig. 2.12.-8), low values are usually related to high ice content. Survey spatial density allows us to build 3D magnetic and electrical models, compare data between geophysical methods and trace correlations of certain features in different physical domains.

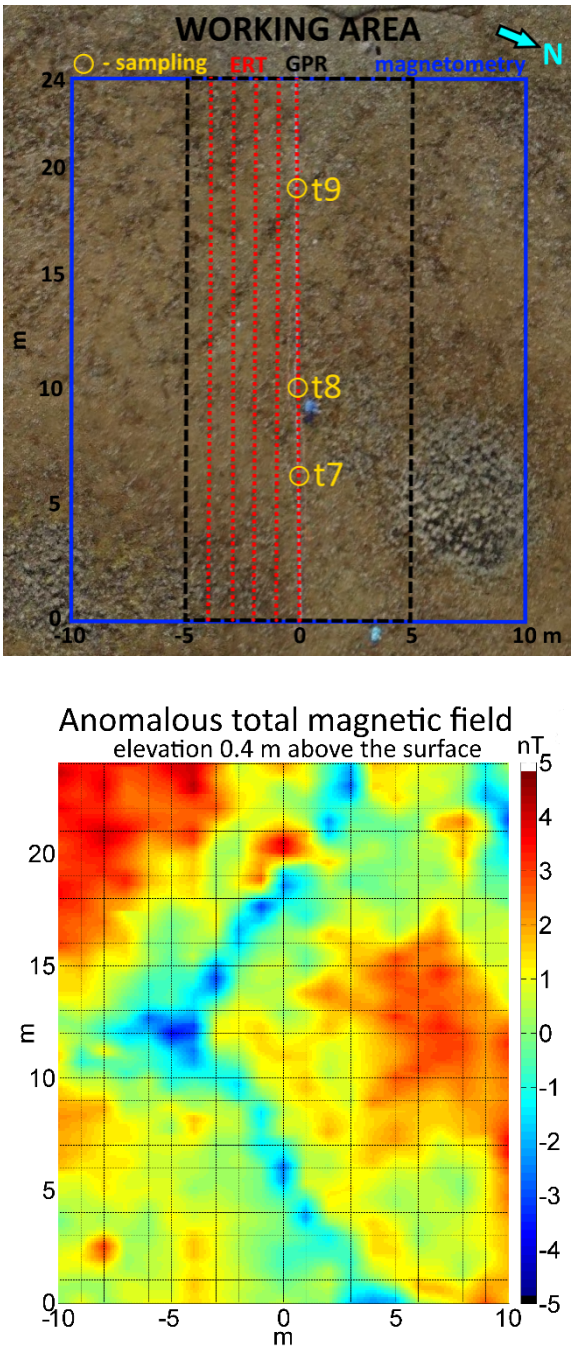

Figure 2.12.-5: Aerial photo with survey scheme. Left image: magnetic (blue line) and GPR (black dotted line) survey rectangles; ERT profiles (red dotted lines), sampling points (yellow circles). Anomalous total magnetic field (total error ± 1 nT) observed at elevation 0.4 ± 0.1 m (right): linear negative anomalies are spatially correlated to ice wedges (also visible on aerial photo)

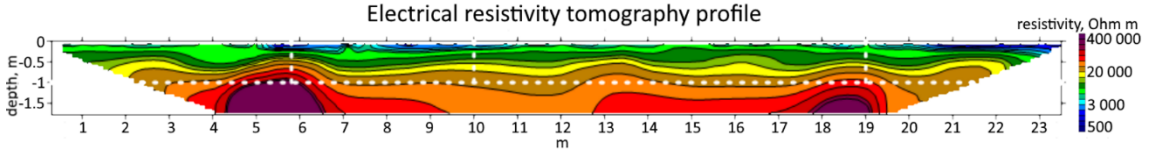

Figure 2.12.-6: Small-scale ERT profile at coordinate x = 0 m (Fig. 2.12.-5, left): ice wedges are visible at 6 and 19 meters over horizontal axis as high-resistivity anomalies

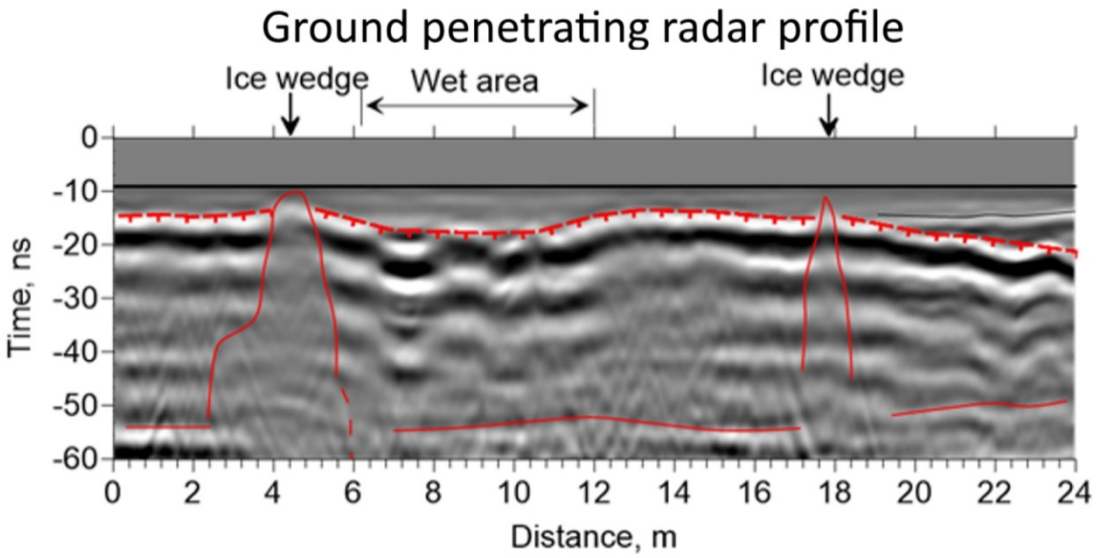

Figure 2.12.-7: Radargram along profile with coordinate x = 2.5 m (Fig. 2.12.-5, left). High-intensity reflecting boundary at time interval 10-20 ns is attributed to the bottom of the active layer (red dotted line); an unidentified boundary is shown with red line at 50-55 ns; vertical anomalies with lack of reflection at distances 4,5 m u 18 m (marked with red contours) are presumably related to ice wedges.

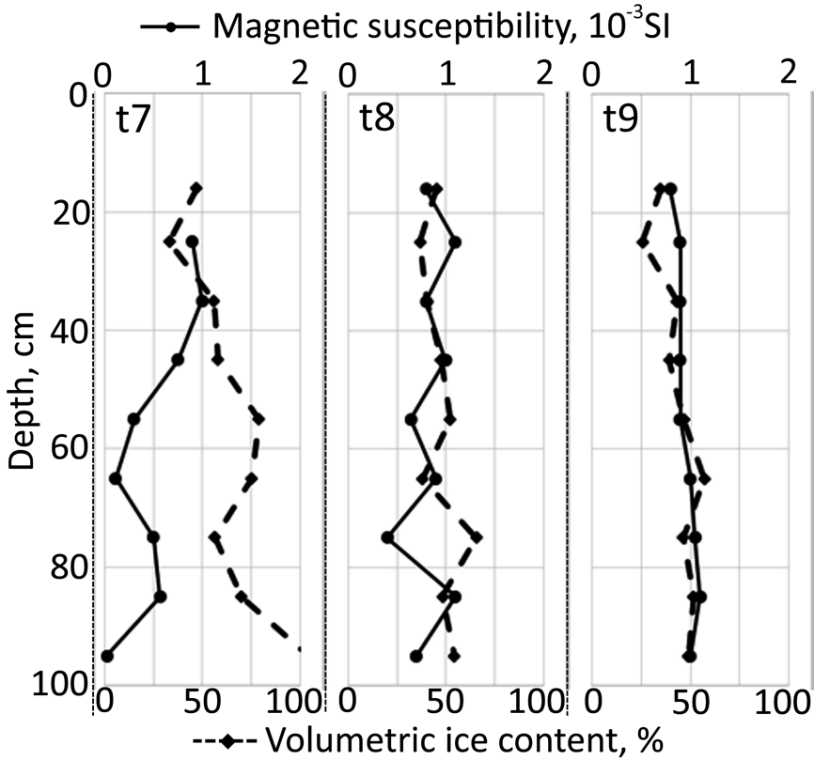

Figure 2.12.-8: Magnetic susceptibility and ice content of samples at three points along central profile with coordinate x = 0 m (Fig. 2.12.-5, left)

Site 2 (alas on Kurungnakh island)

Location (N 72.28972; E 126.18678): alas slope on Kurunghakh island. Acquisition scheme overlaying aerial photo of the site is shown at Fig. 2.12.-9. Presumably hidden ice wedges at south-eastern part of the area (outside of alas border) are discriminated with negative anomalies encircling positive anomalies. Positive linear anomaly of yet undefined origin with partly similar pattern is observed along alas border. Polygon rims (presumably also containing ice wedges) at north-western part of the area are seen as weak linear negative anomalies. Small-scale ERT shows resistivity decrease in central part of the profile (Fig. 2.12.-11), that is believed to be linked to increased thawed layer. Beyond that, upper part of the profile (left on Fig. 2.12.-11) shows relatively homogeneous medium while lower part (right on Fig. 2.12.-11) disjoints to regular structures of unclear origin. Magnetic susceptibility of frozen soil at the part of alas slope where positive magnetic anomaly is observed increases two-three times comparing to other points (Fig. 2.12.-12). Active layer thickness and organic matter content also increase at that zone. Soil sampling was made along a catena crossing alas from its raised edge to bottom. Three temperature stations are installed to compare temperature conditions outside, on the slope and at the bottom of the alas (Fig. 2.12.-9, A 2.12.-1).

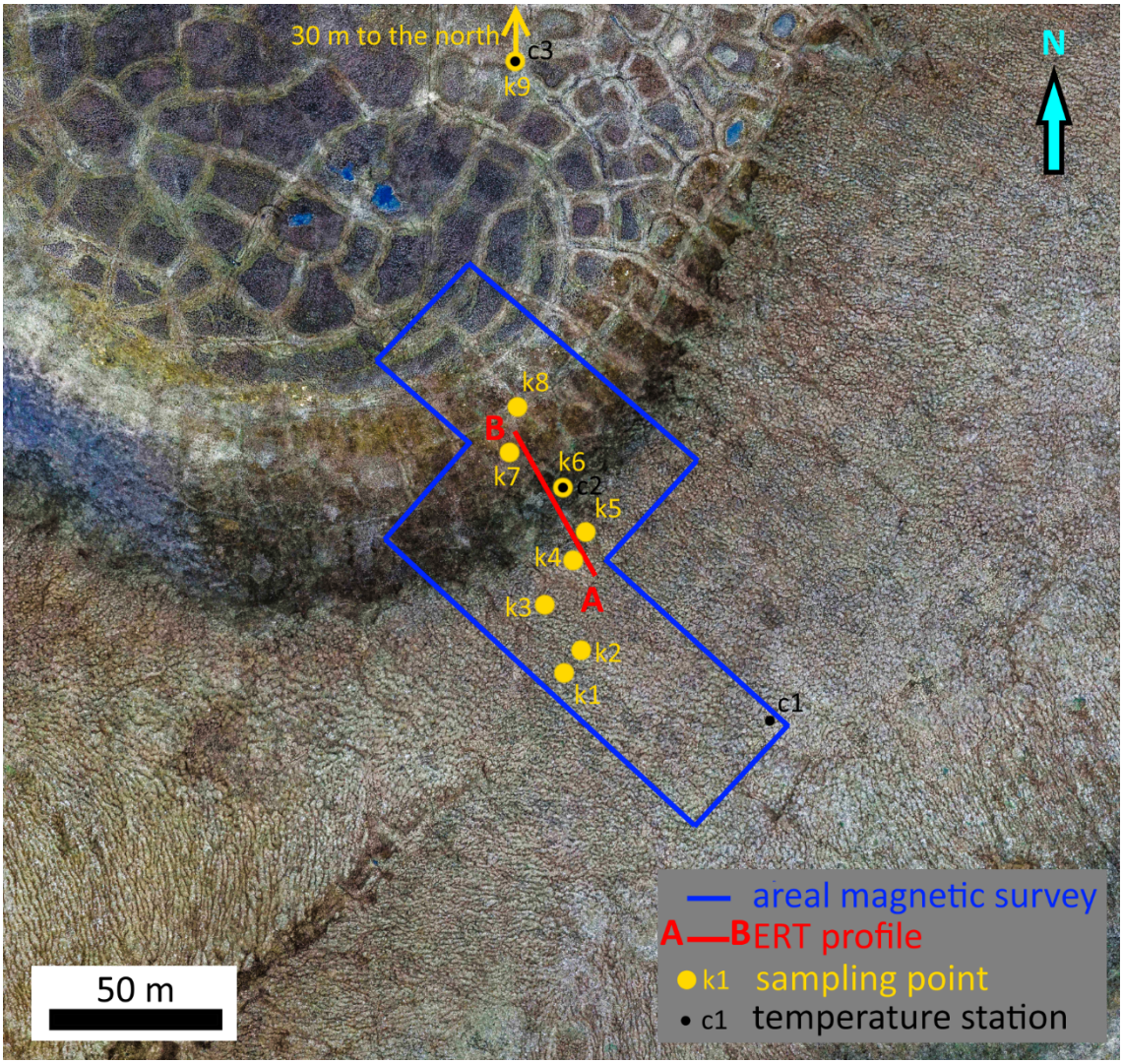

Figure 2.12.-9: Aerial photo with survey scheme overlaying: magnetic survey area boundary (blue line), ERT profile (red line), sampling points (yellow dots) and temperature station sites (black dots)

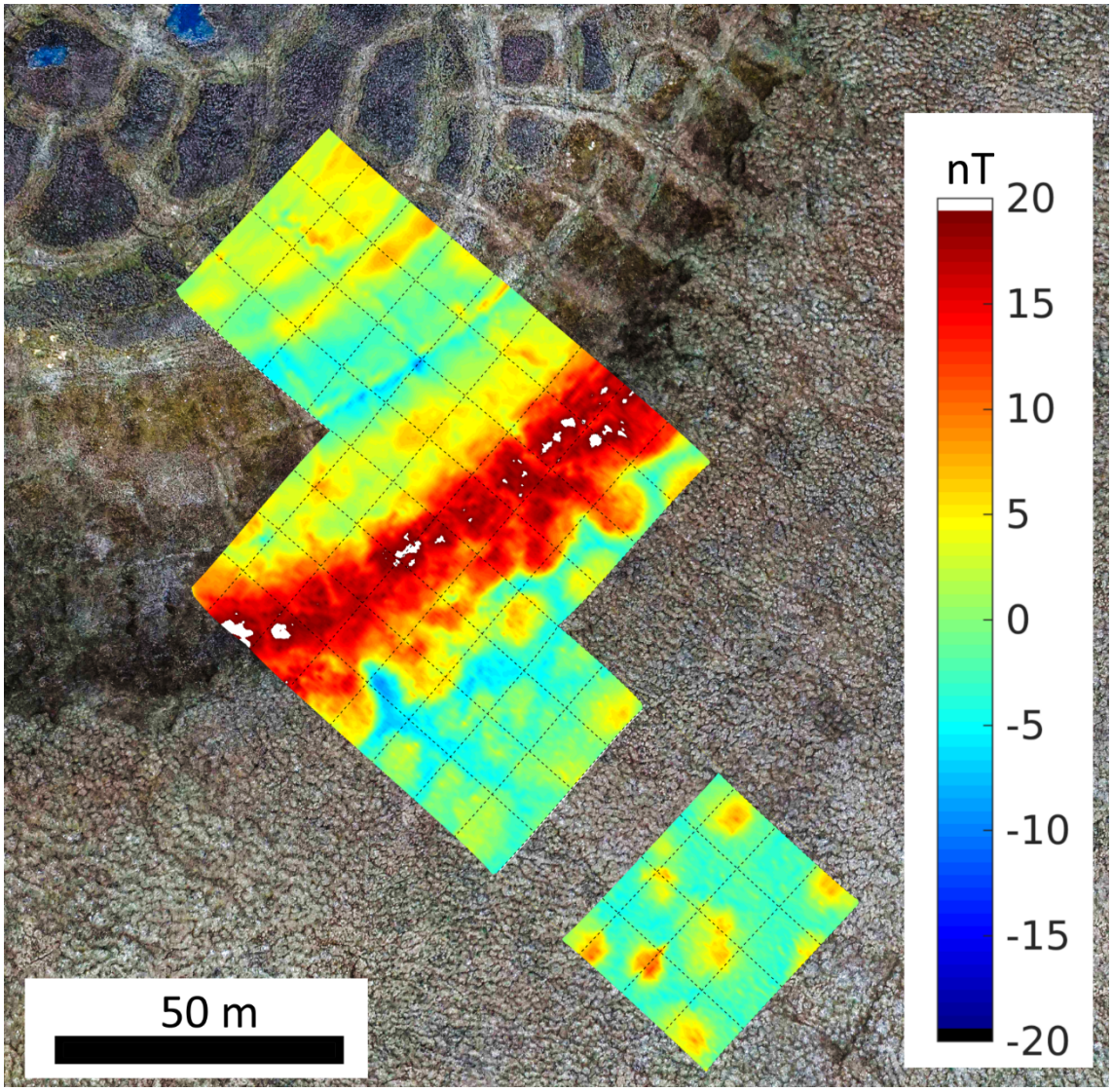

Figure 2.12.-10: Anomalous total magnetic field (total error ± 1 nT) observed at elevation 0.4 ± 0.1 m: presumably hidden ice wedges at south-eastern part of the area (outside of alas border) are easily discriminated; positive linear anomaly of undefined origin is observed along alas border)

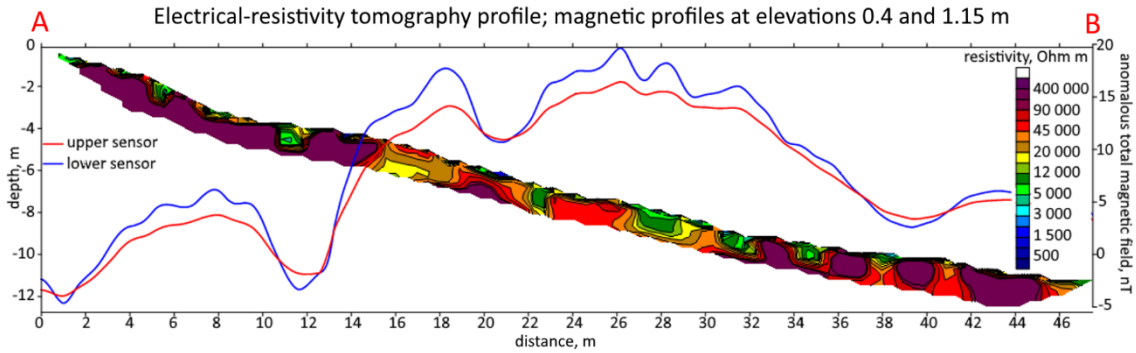

Figure 2.12.-11: Small-scale electrical resistivity profile (topography is taken from DEM model) and 2-elevation magnetic profile (interpolated data) crossing positive magnetic anomaly on the alas slope: relatively homogeneous high-resistivity medium in upper part, resistivity decrease in central part and disjointed pattern in lower part of the profile

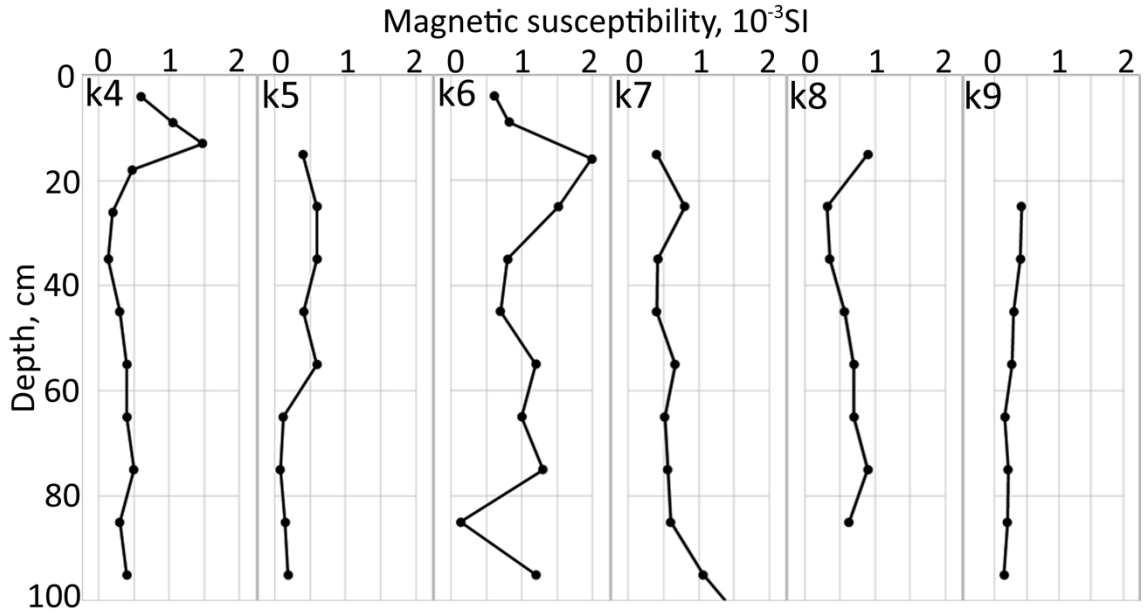

Figure 2.12.-12: Magnetic susceptibility of samples: k6 is located at the center of positive magnetic anomaly (Fig. 2.12.-10)

Site 3 (ice complex on Kurungnakh island)

Location (N 72.33983; E 126.29142): near the cliff on top of the ice complex on Kurungnakh island. Acquisition scheme overlaying satellite photo of the site is shown at Fig. 2.12.-13. Magnetic survey distinctively shows the structure of upper layer (Fig. 2.12.-14): negative anomalies are presumably related to ice wedges dividing medium. One can see difference in width and magnitude of these anomalies – we suggest that different types of ice wedges could be the source of it - according to Wetterich et al. (2008) the ice complex contains older wide and deep ice wedges in lower layers and younger thin ice wedges in upper layer. A thorough numerical modeling is required to answer the question if magnetic survey can discriminate these features. Beyond the magnetic survey, two temperature stations were installed: at distances 25 and 100 m from the current cliff position (Fig. 2.12.-13, A 2.12.-1) to observe eventual influence of ice complex degrading boundary on temperature of upper layer.

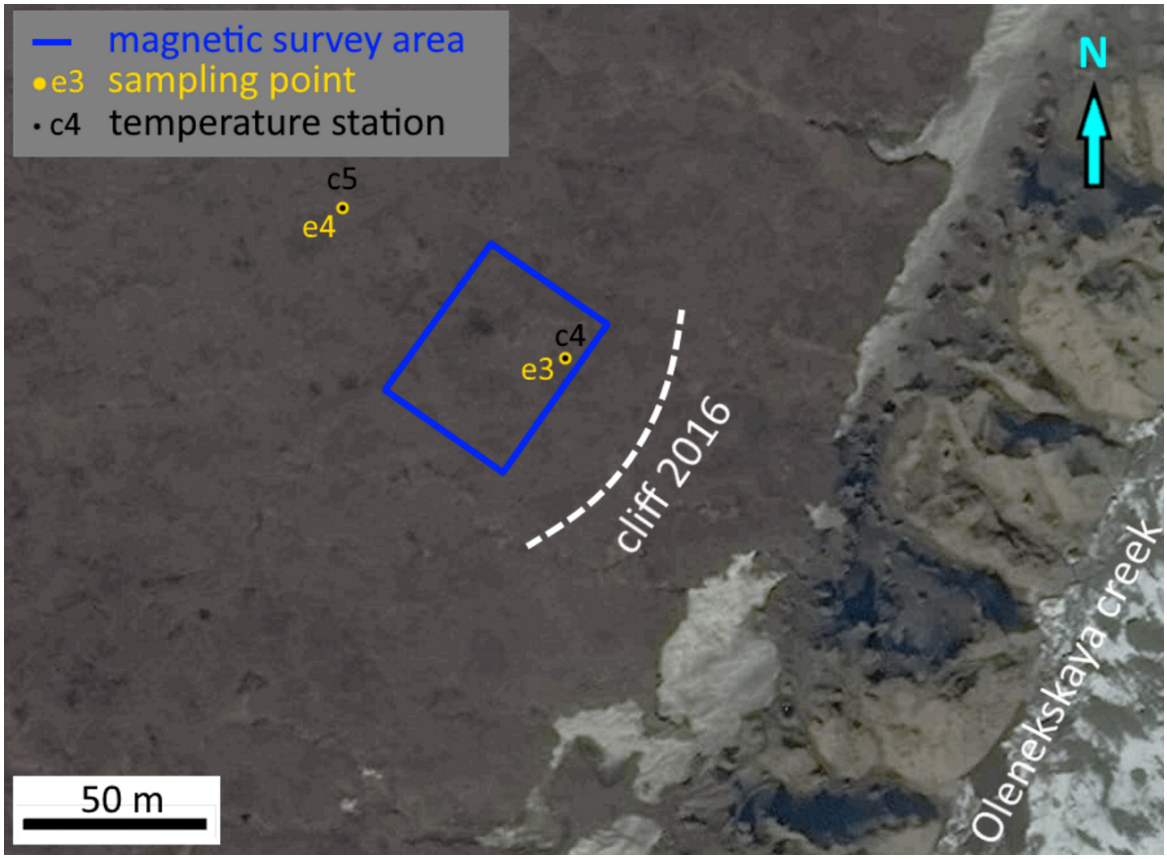

Figure 2.12.-13: Satellite photo with acquisition scheme: magnetic survey area boundary (blue line), sampling points (yellow dots) and temperature station sites (black dots); white dotted line approximately shows current position of degrading ice complex boundary

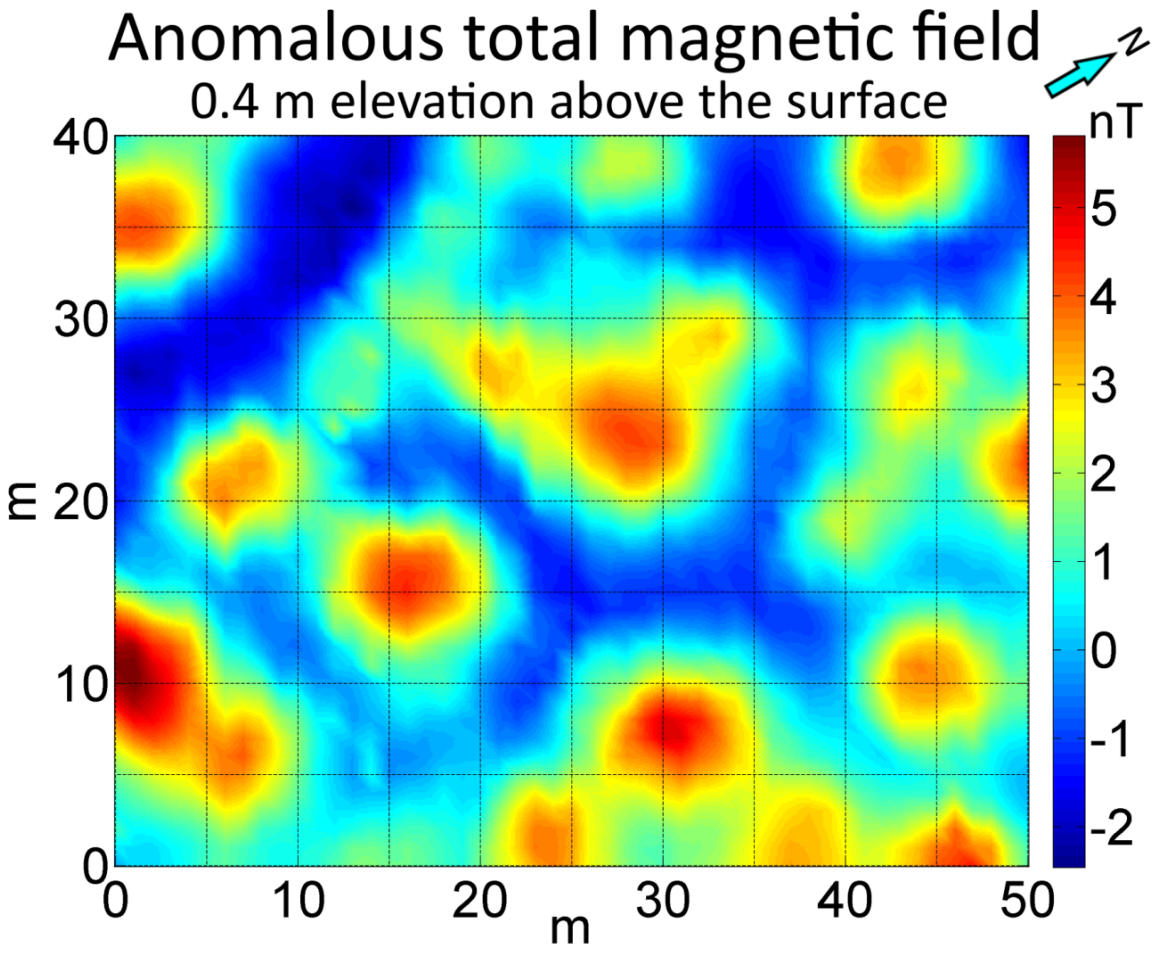

Figure 2.12.-14: Anomalous total magnetic field (total error ± 1 nT) observed at elevation 0.4 ± 0.1 m above the surface: negative anomalies are presumably linked to ice wedges (Wetterich et al., 2008)

Site 4 (area on Samoylov station ground)

Location (N 72.37011; E 126.47457): degrading area - the part of Samoylov station ground affected by station engine heating. Acquisition scheme overlaying photo of the site is shown at Fig. 2.12.-15. Small-scale ERT shows good correlation with direct measurements made by metal rod (Fig. 2.12.-15). EMS data is also in agreement with provided results, but resolution of the method is lower, than small-scale ERT. Obtained data shows that ERT and EMS could be useful in monitoring of active layer thickness. These methods can show upper layer structure in general and with due account of geophysical properties could clarify not only active layer thickness but such features as boundary sharpness and lateral inhomogenities of thawed zone.

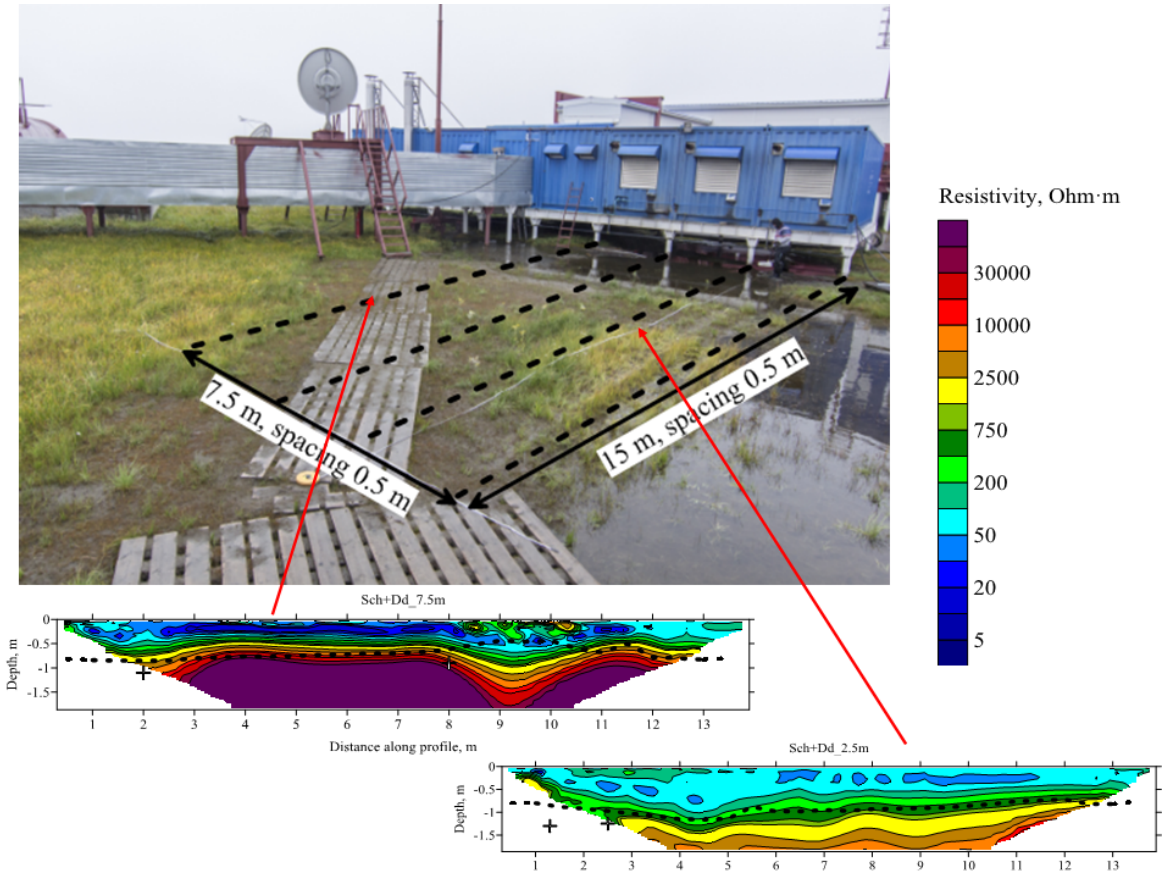

Figure 2.12.-15: Small-scale ERT profiles with marked active layer depth (black dotted line), local high-resistivity anomalies at shallow depth (at x = 8.5 – 11 m at upper picture) are originated by wooden pavement (its lower part is buried)

2.13. Zooplankton communities in the ice-covered lakes on Samoylov Island

Ekaterina Abramova [1]

[1] Lena Delta Reserve, Tiksi, Russia

Fieldwork period April – May 2016 on Samoylov Island

Objectives

Many pelagic fauna investigations in the Arctic regions have focused on summer-time processes in the freshwater ecosystems. However, our knowledge of the structure and functioning of zooplankton communities in tundra lakes during the long winter periods is poor. The winter conditions make the ice-covered lakes a unique environment for the water organisms. Firstly, the amount of light entering the lake is further reduced, completely decreasing the photosynthetic activity of algae. Secondly, the temperature, which affects all biological and chemical processes, is not much higher than the freezing point throughout the water column. And thirdly, the ice reduces gas exchange between the water and atmosphere and oxygen concentrations in the lakes should greatly decrease over the winter. Thus, the behavior of pelagic communities under the ice cover is very intriguing. During our studies in April-May 2016 we analyzed the species richness, population structure and life strategy of zooplankton in the ice-covered lakes on Samoylov Island at the end of the winter season.

Methods

In the total, we collected collected 26 zooplankton samples from five lakes on Samoylov Island during the spring expedition of 2016: Banya I – Banya III, South and Fish lakes. Single sampling stations were located approximately in the deepest part of each lake. A small Apstein net (opening diameter 20 cm, mesh size 100 µm) was used for zooplankton sampling. The net catches were made from holes drilled through the lake ice (Fig. 2.13.-1). The sampling interval in the different lakes varied between 5-7 days. Variabilities of water depth, ice thickness, temperature, pH, conductivity and oxygen concentrations are summarized in the Appendix in Table A 2.13.-1.

In addition to net samples, three ice cores were collected from Shallow Lake and two ice blocs were obtained from Fish Lake during the spring expedition. The ice was completely melted and water was filtered though a sieve with mesh size 63 µm.

Concentration, preservation (4% formalin or 100% ethanol) and processing of samples were made during the expedition at the Samoylov Island research station. Either the whole sample or parts of it were analyzed in a Bogorov chamber under Olympus SZX9 and BX60 stereomicroscopes. All adult organisms were determined to species level. Juvenile copepods were separated into copepodite stages and identified to species/genus level. Nauplii of the common Copepoda species were counted without species identification.

A laboratory experiment with common in Banya-II lake calanoida *Limnocalanus johanseni* Marsh, 1920 was carried out at the end of April. Ten adult females of this species were selected and placed separately into ten Petri dishes in 20 ml of water. The dishes were left standing in a refrigerator at 4°C for one week.

Figure 2.13.-1: Zooplankton sample collection during the winter expedition on Samoylov Island

Preliminary results

The winter pelagic fauna was impoverished and consisted of 25 species belonging to two phyla (Rotifera and Arthropoda) and juvenile stages of Copepoda. All organisms regularly encountered in the samples are listed in Appendix in Table A 2.13.-2. The highest species diversity (13 species) was found in Banya-I and Banya-III lakes. The species composition was dominated by Rotifera in both lakes. In Banya-II, Fish and South lakes the species richness was lower (7, 6 and 4 zooplankton species respectively). The number of Rorifera and Copepoda species in these lakes was almost equal (Table A 2.13.-2 in the Appendix).

The average total abundance of winter zooplankton comprised 4894 ind./m^3 in Banya-I lake. The lowest number of organisms we found in Banya-II, where the total abundance changed from 1132 to 2022 ind./m^3 during the period of investigation. Both pelagic communities were clearly dominated by Rotifera and young stages of Copepoda (Fig. 2.13.-2). The highest zooplankton richness (up to 10762 ind./m^3 on average) was recorded in Banya Lake-III with a maximum of 26610 ind./m^3 in the first week of May (Fig. 2.13.-2). Juvenile stages of *Cyclops kolensis* Lilljeborg, 1901 comprised about 60% from the total zooplankton abundance in that time. A similar situation was observed in South Lake, but the share of *C. kolensis* here was much higher: up to 95% of the total (5800 ind./m^3) number of organisms.

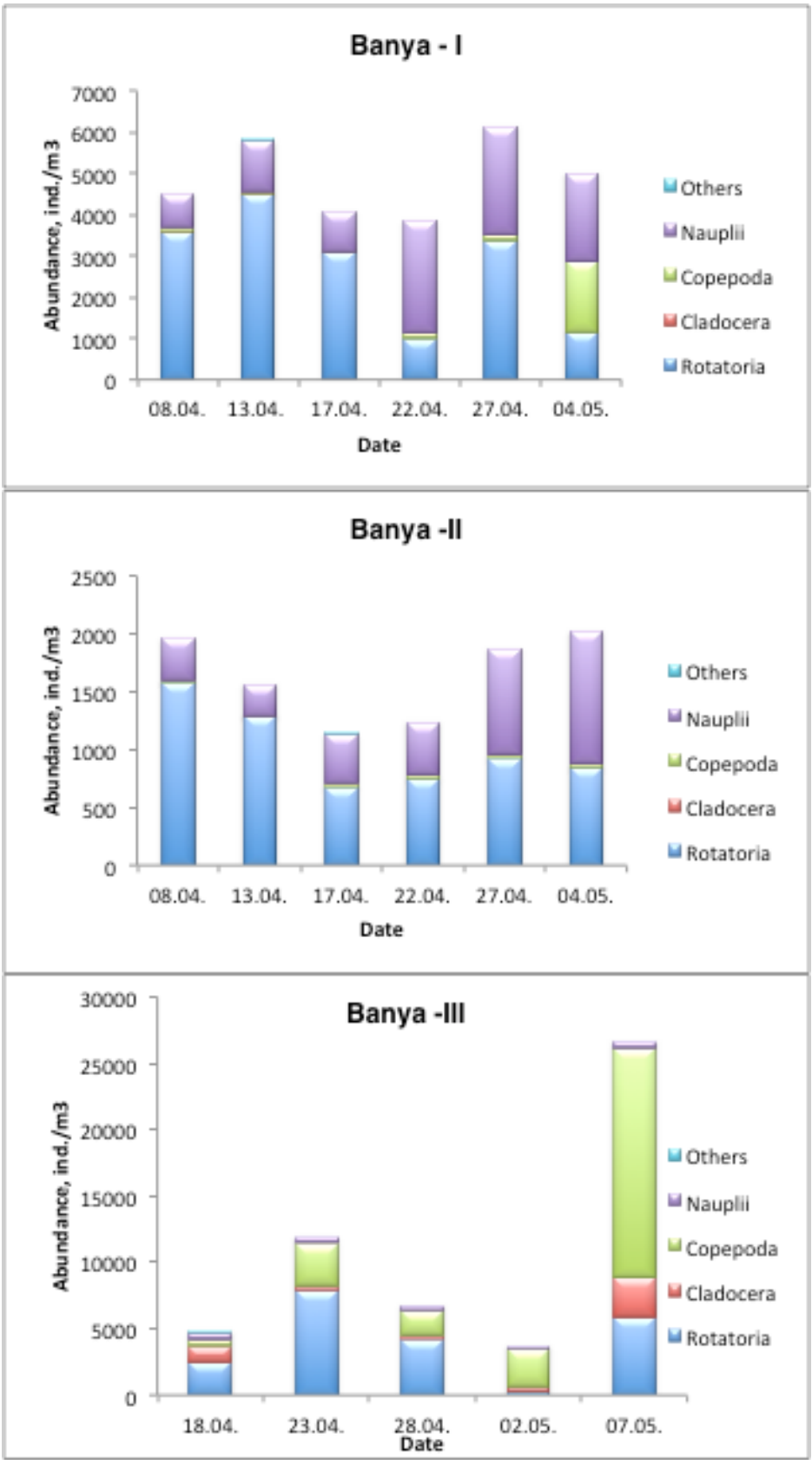

Figure 2.13.-2: The total zooplankton abundance variations and relative abundance (%) of common groups in three oxbow lakes (Banya-I, II and III) in April-May 2016

Our study revealed not a low species diversity of zooplankton at the end of winter, but we found comparatively high zooplankton abundance in the ice-coved lakes on Samoylov Island. It seems that common and abundant Rotifera: *Keratella cochlearis* (Gosse, 1851), *Kellicottia longispina* Kellicott, 1879 and *Polyarthra spp*. produced several new generations during the period of our observations. Some pelagic crustaceans also reproduced at the end of the winter, despite the harsh abiotic conditions at that time. For example, the population of *Eudiaptomus graciloides* (Lilljeborg, 1888) was dominated by adult males and females with egg sacs (4-6 eggs in sac) in April-May (Fig. 2.13.-3). The released eggs continued their development without delay and the number of free-swimming young stages of *E. graciloides* increased in the pelagic community of Fish Lake. The data obtained allow us to conclude that *E. graciloides* has at least two generations per year (summer and winter) in the tundra lakes of the Lena Delta.
The adult and larval stages dominated in the population of another copepod, *L. johanseni,* from Banya-II lake at the end of winter season. These crustaceans do not form egg sacks and females eject small-size eggs into the water one by one. The laboratory experiment with females of *L. johanseni* demonstrated quite high productivity. The number of eggs produced by various females varied from 22 to 76 eggs per week. The daily production was 7-8 eggs per female. The experiment confirms the 2-cycle life strategy of *L. johanseni* in the Delta Lena water ecosystems.

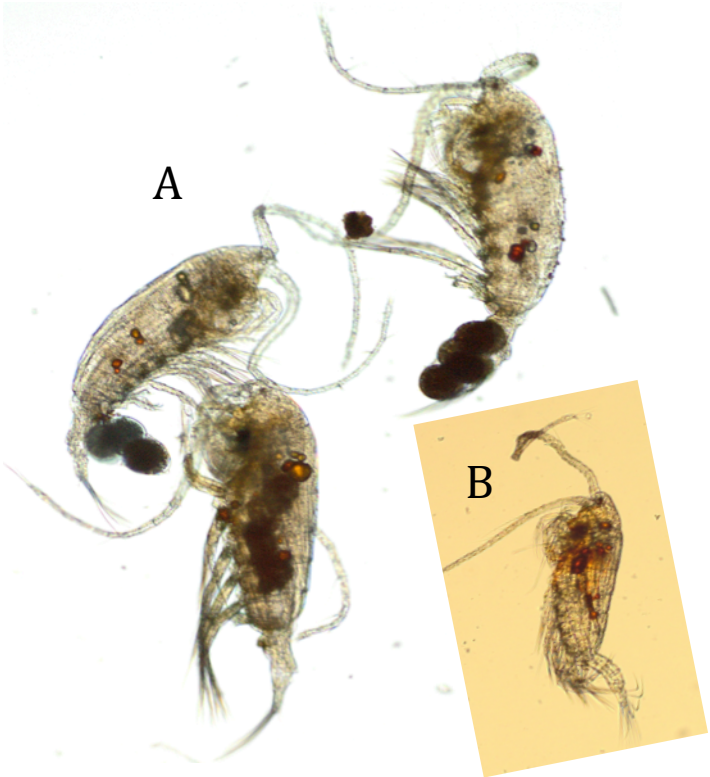

Figure 2.13.-3: Adult female, females with egg sacks (A) and male (B) of E. graciloides from Fish Lake collected in May 2016

The analysis of ice cores from shallow lakes revealed new information about the life strategies of some cyclopoid copepods in Arctic habitats. In the upper part of the cores we found mostly plant detritus and several representatives of Rotifera, Ostracoda, and Nematoda. In the lower part of one of the cores, 22 mature females of *Cyclops arcanus* Alekseev 1990 were discovered (Fig. 2.13.-3). It is the first recorded occurence of this

species in the Lena River region and it is the first record of the resting stages, presented by adult females frozen in ice. After thawing of the ice, the females were able to move actively. It is a new type of diapause among Copepoda that has not previously been described in the literature.

The many questions encountered during this study indicate that investigations into the winter zooplankton may reveal many significant phenomena below and within lake ice.

Acknowledgements
We would like to express gratitude for the opportunity to carry out field and laboratory work at the Samoylov Island research station (Siberian Branch of the Russian Academy of Sciences, Novosibirsk) and for the technical support provided. We would also like to thank Waldemar Schneider and Hanno Meyer (AWI, Potsdam), the Samoylov Island station team and all of our colleagues who helped with zooplankton sample collection.

2.14. Zooplankton investigations in summer 2016. Copepod speciation in Siberian Arctic: the case of the River Lena delta

Viktor Alekseev [1], Ekaterina Abramova [2]

[1] Zoological institute of the Russian Academy of Sciences, St. Petersburg, Russia

[2] Lena Delta Reserve, Tiksi, Russia

Fieldwork period July **-** August 2016 on Samoylov, Kurungnakh, America-Khaya, Tit-Ary and Sagastyr islands

Objectives

1. Our long-term observations of pelagic fauna from 11 lakes on Samoylov Island allowed us to identify 65 crustacean species. This number is comparable with the amount of pelagic crustaceans found in freshwaters of Iceland (Novichkova et. al., 2014). This similarity can probably be attributed to the paucity of collections rather than to distributional peculiarities. The number of zooplankton collections from the Lena Delta over last two decades is high compared to other areas at similar latitudes in Russia, and probably in the entire world. The main objectives of our research during the summer expedition of 2016 were (1) to continue our monitoring investigations of species diversity and seasonal to interannual variations of zooplankton abundance in the the various types of water ecosystems in the southern part of the Lena Delta; (2) to evaluate the different factors affecting the pelagic communities structure in this region; (3) to get information about the geographic distribution, biology and taxonomic status of Copepoda species inhabiting transitional zone between freshwater and marine ecosystems.

2. Periodical glaciation and de-glaciation of parts of the Arctic, along with temporal isolation of the great river watersheds, should have accelerated the rapid speciation process among aquatic organisms inhabiting affected parts of the circumpolar region. For the last glaciation cycle (about 10 000 years), this acceleration has been demonstrated, mainly for vertebrates, such as fishes of Coregonus genera, Amphibians and even mammalians (seals in large Eurasian Lakes), but poorly studied in invertebrates. Scientists believe that speciation in groups as ancient as the copepods or cladocerans is too slow to be observed on historical time scales within the Holocene. Recent molecular-genetic studies on some brackish water copepods revealed rapid speciation in the *Eurytemora affinis* group (Lee, 2000; Alekseev & Souissi 2011). Our study in the River Lena delta was conducted to test these hypotheses on continental species of cyclopoid and harpacticoid copepods.

Material

A total of 50 quantitative and qualitative samples of zooplankton were collected in July-August 2016 on Samoylov, Tit-Ary, America-Khaya, Kurungnakh and Sagastyr islands (Table A 2.14.-1 in the Appendix). Besides this, 9 quantitative zooplankton samples were

obtained from the brackish water area during marine expedition led by P. P. Overduin (Table A 2.14.-2 in the Appendix).
Additionally, from August 2-16 we collected and preliminarily studied 98 qualitative zooplankton samples in different waterbodies in the River Lena delta that included: 12 permanent lakes, 31 polygonal ponds, 14 swamps and about 50 temporary water bodies. We also studied the personal copepod collection of E. Abramova, sampled within the delta in the last 30 years. For sampling in lakes, we used a towel net (mesh size 100 µm, from bottom to surface), in other cases a handle net with mesh size 120 µm, (near shore, from 10 till 100 l filtered) was used. The live specimens were immediately picked from the samples in the laboratory and preserved in 95% ethanol for DNA searching or 2-4% formalin for analysis of external morphology.

Preliminary results

More than 15 cyclopoid species were found in the Lena delta (Abramova, 1996; Abramova & Tuschling, 2005). In some species, we found a set of morphological differences.

Eucyclops sp. (Fig. 2.14.-1)

Location: Tit-Ary Island. Biotope: A small permanent waterbody on top of a hill. Among macrophytes near the shore, water depth less than 0.3 m.
Morphological peculiarities: female. Robust body, brownish in color, maximal width near middle of thoracic part, total length without seta about 1 mm. Long antennas reach second free thoracic somite with narrow smooth hyaline plate at three distal segments. Basipodal segment of antennae at caudal side without long hairs on top. Coxal spine of swimming legs 4 homogeneously covered with long hairs on both sides. Caudal ramus about 4.5 times as long as wide, on lateral edges with long row of strong dents (30-35) that near lateral seta insertion seta like and several times longer others. The innermost setae 1.5-1.7 times as long as outermost or dorsal seta.
Taxonomical status: this form belongs to *speratus* group, but in several taxonomically relevant featurs such as furka construction and its armament; it could be a new species. Description of it is in preparation for a future publication.

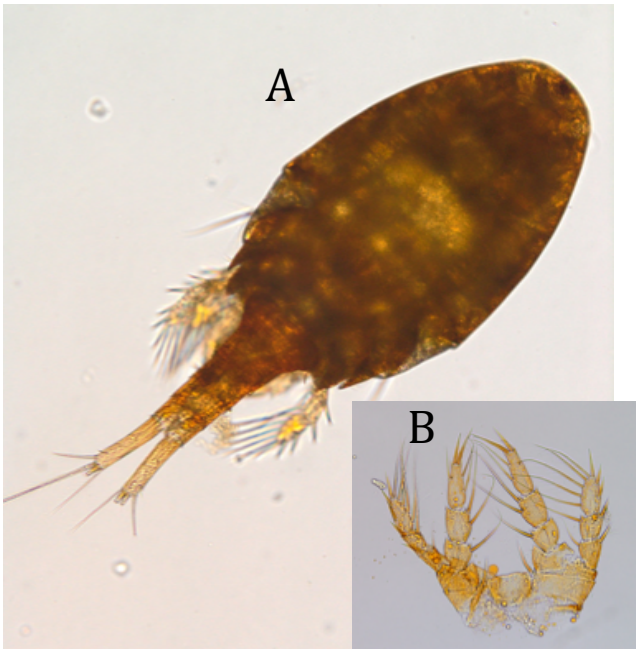

Figure 2.14.-1: Female of Eucyclops sp. (A) and her fourth pair of swimming legs (B)

Eucyclops cf. denticulatus

Location: Samoylov Island. Biotope: Oxbow lake –III, in open deep area.
Morphological peculiarities of female: body shape typical for genus, yellowish in color. Length about 0,9 mm. Antennules at 3 distal segments with well-developed hyaline plate not smooth but regular bracken edges. Caudal rami slightly divergent and narrow with long row of tiny dents along lateral side.
Taxonomical status: This form is close to the type description has no clear seen dents on hyaline plate of 3 distal segments of antennule. This detail of construction is very important and used in most identification keys for this genus. Possibly this reflects a long period of isolation of this population from the nominative form in Europe and can be evaluated as subspecies level of speciation.

Cyclops cf. kikuchi (Fig. 2.14.-2)

Location: Samoylov Island. Biotope: Pelagic of Banya- I and Banya-III lakes flooded annually by river waters during the spring flood.

Morphological peculiarities of this form: more narrow caudal rami (L/W=10 when in nominal form up to 8 only) and distal seta of endopodit of legs 4 reaches the distal ends of spines (the peculiarities not observed in type population from Europe as well as from the same form found in the Lena river). Taxonomical status. It is possibly a local form adapted to low temperature or a postglacial relict.

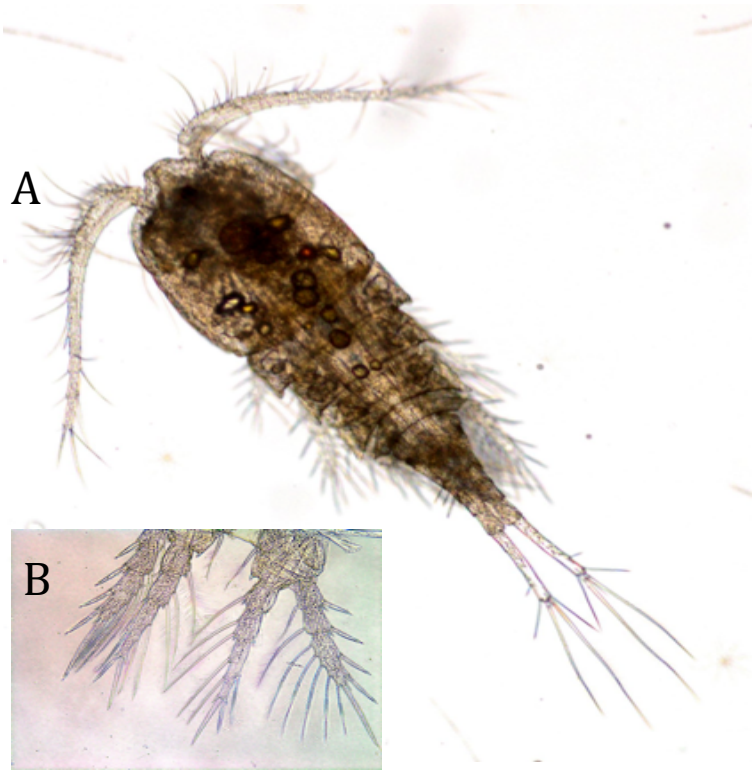

Figure 2.14.-2: Female of Cyclops kikuchi (A) and her fourth pair of the swimming legs (B)

Cyclops abyssorum group

Location: Samoylov Island.
Biotope: permanent shallow water bodies on the floodland and polygonal ponds of the first delta terrace.
Morphological peculiarities: in tundra waterbodies, we found several closely related forms that differed in furca proportion, along with the typical nominative form, inhabiting the Lena river itself.
The taxonomical status of this flock of forms is not clear now and needs both morphometrical and molecular-genetic analyses. To our mind this group could be a candidate for post-glacial speciation in Arctic and deserves more intensive study.

Preliminary conclusions

1. In thermokarst lakes of the Lena River Delta we found several cyclopids belonging to genera Eucyclops and Cyclops that morphologically differed from known co-genders. At least one (*Eucyclops sp.* 1) represents a new species for science and will be described soon (Alekseev & Abramova, in pr.). This species, to our mind, is an element of a more or less ancient faunistic complex of Beringia.
2. Two other forms are morphologically not so distinct from related specimens found in the River Lena itself. They differ in body sizes and length-to-width proportions in some taxonomically important structures, along with some other variations. The taxonomical value of these forms will be estimated later on after molecular-genetic study of their DNA.

3. Finally, a flock of species preliminary identified as *Cyclops abyssorum* group that includes at least 4 morphologically different forms of unclear status may also represent recent speciation. This group will be studied with statistically based morphological measurements and the DNA barcode method.

Acknowledgements

We would like to thank Waldemar Schneider and Paul Overduin from the Alfred Wegener Institute, Potsdam for cooperation, technical assistance and help in the field. We appreciated very much the chance to use the Samoylov Island research station (Siberian Branch of the Russian Academy of Sciences, Novosibirsk) for our studies.

2.15. Influence of geomorphological, lithological, and permafrost features on soil cover heterogeneity and evolution

Inna Alekseenko [1], Vyacheslav Polyakov [1], Dmitriy Bolshiyanov [1]

[1] Arctic and Antarctic Research Institute, Russian Federal Service for Hydrometeorology and Environmental Monitoring, St. Petersburg, Russia

Fieldwork period August, 1st till August, 31st, 2016 on Samoylov Island, Kurungnakh Island, Stolb Island, Tit-Ary Island, Arga-Bilir-Aryta Island

Objectives

It is well known that high latitude terrestrial ecosystems play a crucial part in the global carbon cycle (McGuire et al., 2012). Some estimates of carbon stores in circumpolar permafrost-affected soils (Hugelius et al., 2014) have shown that deltaic alluvium and Yedoma region deposits store significant amounts of total carbon with respect to circumpolar soils. However, there is a lack of observational evidence in these regions (Hugelius et al., 2014). Some detailed studies in the Lena River delta revealed a relationship between the quantity of stored soil organic carbon (SOC) and the geomorphological units of the delta (Siewert, Hugelius, 2015). It was shown that the highest content of SOC is observed in soils of the third (oldest) terrace whereas SOC was lowest in soils formed on modern floodplains and alluvial deposits, indicating that SOC content is strongly affected by landscape and geomorphology features. Similar observations were made on Samoylov Island, where different SOC contents in soils of Holocene river terrace and active floodplain were observed (Zubrzycki et al., 2013). Furthermore, there SOC content differs between polygon center and polygon rim wherever these smaller scale landscape features are found. Taking into consideration the complex geomorphological, lithological and permafrost structure of the whole Lena river delta region, a wide range of dissimilar soil types of different age might be studied. The field work described here colleted observations of soil profiles in relation to different landforms, various slope steepness and various parent materials in the Lena Delta.

Methods

Soil profiles were studied at different unique landscape positions. Several catenas were studied from the top to the bottom of the hills (or pingos) on different geomorphological units of the delta. At each soil pit or exposure, soil samples were taken from each genetic horizon within the active layer. Fig. 2.15.-1 demonstrates almost all sampling points except for soil profiles studied on Tit-Ary Island in the southern delta. An example of a permafrost-affected soil profile is given in the Fig. 2.15.-2. Some of the planned soil analyses are listed in Table 2.15.-1.

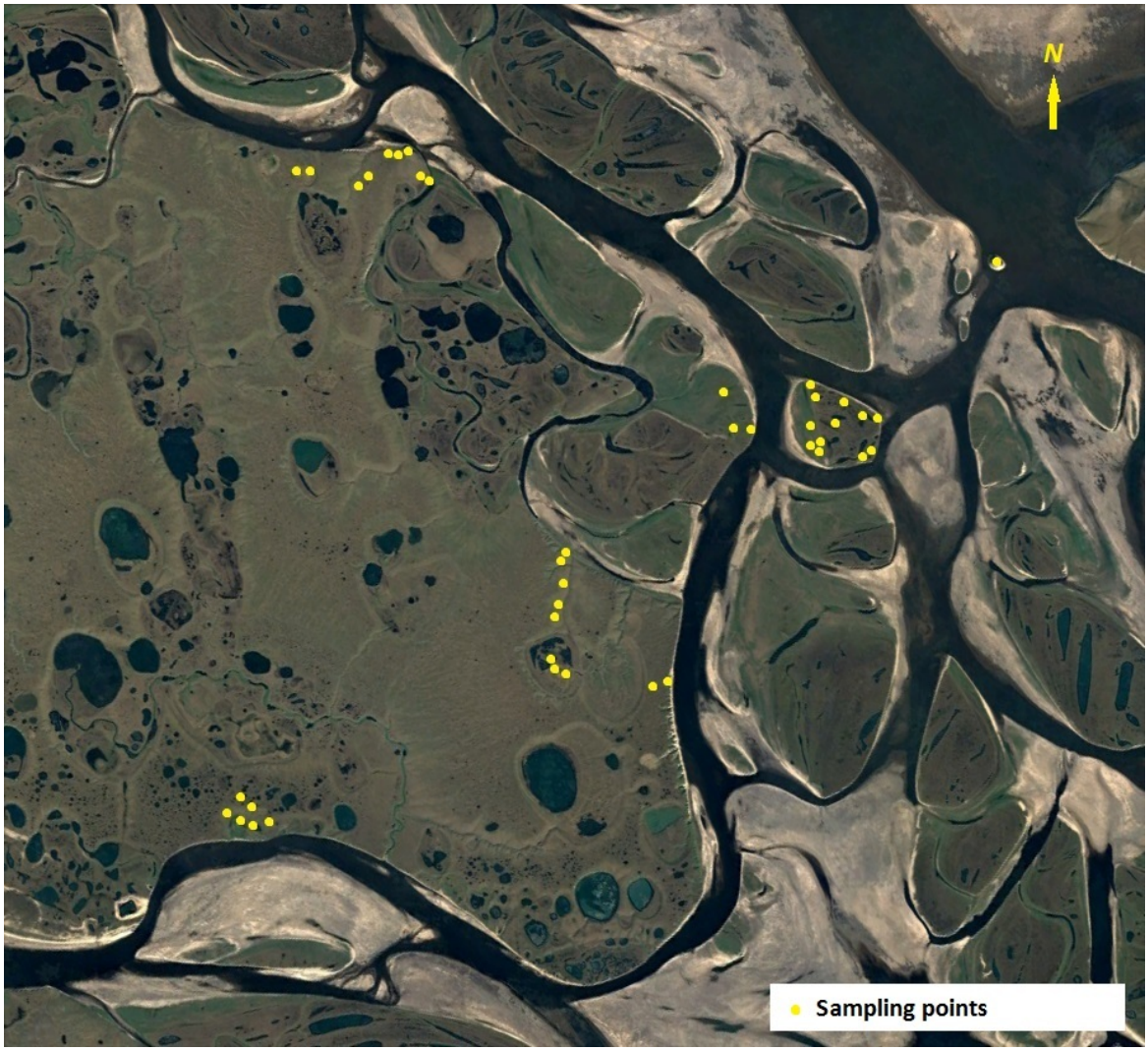

Figure 2.15.-1: Sampling points

Table 2.15.-1: Overview of soil samples for SOC and soil cover heterogeneity.

Analysis	pH	SOC	Granulometric composition	Radiocarbon dating
Number of samples	176	176	176	50

Figure 2.15.-2: Permafrost-affected soil profile excavated in the northeastern part of Kurungnakh Island

References

Abramova, E.N. (1996) Copepoda (Crustacea, Copepoda) of the Lena Delta Reserve. Hydrobiological Investigations in Natural Reserve, Moscow, 8: 5-16 (in Russian)

Abramova, E., and Tuschling, K. (2005) A 12-year study of the seasonal and interannual dynamics of mesozooplankton in the Laptev Sea: Significance of salinity regime and life cycle patterns. Global and Planetary Change 481(3): 141-164

Akroume, E., Zeller, B., Buée, M., Santenoise, P., and Saint-André L. (2016) Improving the design of long-term monitoring experiments in forests: a new method for the assessment of local soil variability by combining infrared spectroscopy and dendrometric data // Annals of Forest Science. DOI 10.1007/s13595-016-0572-3

Alekseev, V.R., and Souissi, A. (2011) A new species within the Eurytemora affinis complex (Copepoda: Calanoida) from the Atlantic Coast of USA, with observations on eight morphologically different European populations, Zootaxa, 2767: 41–56

Bailey, A., Noone, D., Berkelhammer, M., Steen-Larsen, H. C., and Sato, P. (2015) The stability and calibration of water vapor isotope ratio measurements during long-term deployments, Atmos. Meas. Tech., 8, 4521-4538, doi:10.5194/amt-8-4521-2015

Biasi, C., Jokinen, S., Marushchak, M., Hämäläinen, K., Trubnikova, T., Oinonen, M., and Martikainen, P. (2014) Microbial Respiration in Arctic Upland and Peat Soils as a Source of Atmospheric Carbon Dioxide. Ecosystems 17, 112-126

Boike, J., Georgi, C., Kirilin, G., Muster, S., Abramova, K., Fedorova, I, Chetverova, A., Grigoriev, M., Bornemann, N., and Langer, M. (2015) Thermal processes of thermokarst lakes in the continuous permafrost zone of northern Siberia – observations and modeling (Lena River Delta, Siberia), Biogeosciences, 12 (20), pp. 5941-5965, doi:10.5194/bg-12-5941-2015.

Boike, J., Kattenstroth, B., Abramova, K., Bornemann, N., Chetverova, A., Fedorova, I., Froeb, K., Grigoriev, M.,Grueber, M., Kutzbach, L., Langer, M., Minke, M., Muster, S.,Piel, K., Pfeiffer, E.-M., Stoof, G., Westermann, S., Wischnewski, K., Wille, C., and Hubberten, H.-W. (2012) Baseline characteristics of climate, permafrost, and land cover from a new permafrost observatory in the Lena River Delta, Siberia (1998–2011), Biogeosciences, 10, 2105–2128

Boike, J., Kattenstroth, B., Abramova, K., Bornemann, N., Chetverova, A., Fedorova, I., Fröb, K., Grigoriev, M., Grüber, M., Kutzbach, L., Langer, M., Minke, M., Muster, S., Piel, K., Pfeiffer, E.-M., Stoof, G., Westermann, S., Wischnewski, K., Wille, C., and Hubberten, H.-W. (2013) Baseline characteristics of climate, permafrost and land cover from a new permafrost observatory in the Lena River Delta, Siberia (1998–2011). Biogeosciences, 10, 2105-2128, doi:10.5194/bg-10-2105-2013.

Bornemann, L.C. (2011) Soil organic carbon pools and their spatial patterns – rapid assessment using mid-infrared spectroscopy. Dissertation. Rheinischen Friedrich-Wilhelms-Universität, Bonn. 135 p.

Butler, R.F. (1998) Paleomagnetism: Magnetic Domains to Geologic Terranes (electronic ed.). Department of Geosciences, Tucson, Arizona. 238 pp.

Dunlop, D.J. (2002) Theory and application of the Day plot ðMrs=Ms versus Hcr=Hc) 1. Theoretical curves and tests using titanomagnetite data, J. Geophys. Res. 107(B3), 10.1029/2001JB0004

McGuire A. D., Christensen T.R., Hayes D., Heroult A., Euskirchen E., Kimball J.S., Koven C., Lafleur P., Miller P.A., Oechel W., Peylin P., Williams M., and Yi, Y (2012) An assessment of the carbon balance of Arctic tundra: comparisons among observations, process models, and atmospheric inversions. Biogeosciences, 9, 3185–3204.

Hardie, S.M.L., Garnett, M.H., Fallick, A.E., Rowland, A.P., and Ostle, N.J. (2005) Carbon dioxide capture using a zeolite molecular sieve sampling system for isotopic studies (^{13}C and ^{14}C) of respiration. Radiocarbon 47, 441-451.

Hicks Pries, C.E., Schuur, E.A.G., and Crummer, K.G. (2013) Thawing permafrost increases old soil and autotrophic respiration in tundra: Partitioning ecosystem respiration using $\delta^{13}C$ and $\Delta^{14}C$. Global Change Biology 19, 649-661.

Hicks Pries, C.E., Schuur, E.A.G., Natali, S.M., and Crummer, K.G. (2015) Old soil carbon losses increase with ecosystem respiration in experimentally thawed tundra. Nature Climate Change 6, 214-218.

Hodgetts L., Dawson P., and Eastaugh E. (2011) Archaeological magnetometry in an Arctic setting: a case study from Maguse Lake, Nunavut. Journal of Archaeological Sciences 38: 1754–1762.

Höfle, S., Rethemeyer, J., Mueller, C.W., and John, S. (2013) Organic matter composition and stabilization in a polygonal tundra soil of the Lena Delta. Biogeosciences 10, 3145-3158.

Höfle, S.T., Kusch, S., Talbot, H.M., Mollenhauer, G., Zubrzycki, S., Burghardt, S., and Rethemeyer, J. (2015) Characterisation of bacterial populations in Arctic permafrost soils using bacteriohopanepolyols. Organic Geochemistry 88, 1-16.

Hugelius G., Bockheim J.G., Camill P., Elberling B., Grosse G., Harden J.W., Johnson K., Jorgenson T., Koven C.D., Kuhry P., Michaelson G., Mishra U., Palmtag J., Ping C.-L., O'Donnell J., Schirrmeister L., Schuur E.A.G., Sheng Y., Smith L. C., Strauss J., and Yu Z., (2013) A new data set for estimating organic carbon storage to 3m depth in soils of the northern circumpolar permafrost region. Earth Syst. Sci. Data, 5, 393–402.

Hugelius, G., Strauss, J., Zubrzycki, S., Harden, J.W., Schuur, E.A.G., Ping, C.-L., Schirrmeister, L., Grosse, G., Michaelson, G.J., Koven, C.D., O'Donnell, J.A., Elberling, B.U., Mishra, Camill, P., Yu, Z., Palmtag, J., and Kuhry P. (2014). Estimated stocks of circumpolar permafrost carbon with quantified uncertainty ranges and identified data gaps. Biogeosciences, 11, 6573–6593.

Jones M.C., Grosse G., Jones B.M., and Walter Anthony K.M. (2012): Peat accumulation in a thermokarst-affected landscape in continuous ice-rich permafrost, Seward Peninsula, Alaska. Journal of Geophysical Research, 117, G00M07.

Kirschbaum M.F. (2004) Soil respiration under prolonged soil warming rate: are rate reductins caused by acclimation or substrate loss? Global Change Biology 10, 1870-1877.

Lee, C.E. (2000) Global phylogeography of a cryptic copepod species complex and reproductive isolation between genetically proximate 'populations'. Evolution 54: 2014–2027.

Melillo J.M., Steudler P.A., Aber J.D., Newkirk K., Lux H., Bowles F.P., Catricala C., Magill A., Ahrens T., and Morrisseau S. (2002) Soil warming and carbon-cycle feedbacks to the climate system. Science 298, 2173.

Morgenstern, A. (2012) Thermokarst and thermal erosion: Degradation of Siberian ice-rich permafrost. PhD thesis, University of Potsdam.

Morgenstern, A., Grosse, G., Arcos, D. R., Günther, F., Overduin, P. P., and Schirrmeister, L. (in prep. a): Thermo-erosional landforms in Siberian ice-rich permafrost.

Morgenstern, A., Polakowski, L., Chetverova, A., Fedorova, I., Skorospekhova, T., Bobrova, O., Eulenburg, A., Heim, B., Boike, J., and Overduin, P. (in prep. b): Contribution of permafrost degradation landforms to summer export of DOC from Yedoma-type Ice Complex to rivers, Lena Delta, Siberia.

Novichkova, A., Chertoprud, E., and G'islason, G.M. (2014) Freshwater Crustacea (Cladocera, Copepoda) of Iceland: taxonomy, ecology, and biogeography. Polar Biology 37:1755–1767 DOI 10.1007/s00300-014-1559-x

Peterjohn W.T., Melillo J.M., Bowles F.P., and Steudler P.A. (1993). Soil warming and trace gas fluxes: experimental design and preliminary flux results. Oecologia 93, 18-24.

Polakowski, L. (2015): Summer surface water chemistry dynamics in different landscape units from Yedoma Ice Complex to the Lena River. Master thesis, University of Potsdam.

Regmi P., Grosse G., Jones M.C., Jones B.M., Walter Anthony K.M. (2012): Characterizing Post-Drainage Succession in Thermokarst Lake Basins on the Seward Peninsula, Alaska with TerraSAR-X Backscatter and Landsat-based NDVI Data. Remote Sensing, 4(12): 3741-3765. doi: 10.3390/rs4123741.

Schirrmeister, L., Grosse, G., Schnelle, M., Fuchs, M., Krbetschek, M., Ulrich, M., Kunitsky, V., Grigoriev, M., Andreev, A., Kienast, F., Meyer, H., Babiy, O., Klimova, I., Bobrov, A., Wetterich, S., and Schwamborn, G. (2011) Late Quaternary paleoenvironmental records from the western Lena Delta, Arctic Siberia. Palaeogeography, Palaeoclimatology, Palaeoecology 299, 175-196.

Siewert, C. (2002) Method for determining the qualitative composition of the or-ganic soil substance of mineral soils. App. No.: 09/601,256; PCT Filed: Jan. 30, 1998; PCT Pub. No.: WO99/39180, Aug. 5, 1999; Patent No.: US 6,382,830 B1

Siewert, C. (2004) Rapid Screening of Soil Properties using Thermogravimetry Soil Sci. Soc. Am. J. 68:1656–1661 (2004).

Siewert, M.B., and Hugelius, G. (2015) Landscape controls of soils and soil organic carbon storage in the Lena River Delta (Manuscript).

Steen-Larsen, H.C., Sveinbjörnsdottir, A.E., Peters, A.J., Masson-Delmotte, V., Guishard, M.P., Hsiao, G., Jouzel, J., Noone, D., Warren, J.K., and White, J.W.C. (2014) Climatic controls on water vapor deuterium excess in the marine boundary layer of the North Atlantic based on 500 days of in situ, continuous measurements, Atmos. Chem. Phys., 14, 7741-7756, doi:10.5194/acp-14-7741-2014

Walter Anthony, K.M., Zimov, S.A., Grosse, G., Jones, M.C., Anthony, P.M., Chapin III, F.S., Finlay, J.C., Mack, M.C., Davydov, S., Frenzel, P., and Frolking, S. (2014): A shift of thermokarst lakes from carbon sources to sinks during the Holocene epoch. Nature. doi: 10.1038/nature13560

Wetterich, S., S. Kuzmina, A.A. Andreev, F. Kienast, H. Meyer, L. Schirrmeister, T. Kuznetsova, and M. Sierralta (2008) Palaeoenvironmental dynamics inferred from late Quaternary permafrost deposits on Kurungnakh Island, Lena Delta, northeast Siberia, Russia, Quat. Sci. Rev., 27, 1523–1540.

Zubrzycki S., Kutzbach L., Grosse G., Desyatkin A., and Pfeiffer E.-M. (2013) Organic carbon and total nitrogen stocks in soils of the Lena River Delta. Biogeosciences, 10, 3507–3524.

3. DELTA REGION

3.1. Coastal and Offshore Permafrost in the Lena Delta and Laptev Sea

Bennet Juhls [1], Matthias Winkel [2], Trond Ryberg [2], Paul Overduin [1], Mikhail Grigoriev [3]

[1] Alfred Wegener Institute Helmholtz Center for Polar and Marine Research, Potsdam, Germany

[2] Helmholtz Centre Potsdam - GFZ German Research Centre for Geosciences

[3] Mel'nikov Permafrost Institute, Siberian Branch, Russian Academy of Sciences, Yakutsk, Russia

Fieldwork period August 21-September 16, 2016

Itinerary:
August 23, 2016 – Tiksi, Sakha Republic, Russia
August 24, 2016 – Musotakh Island, Buor Khaya Bay
August 25-September 1, 2016 – Lena Delta and Samoylov Station
September 2-5, 2016 – western Laptev Sea
September 6-8, 2016 – return through the Lena Delta
September 9-11. 2016 – Buor Khaya Bay
September 12-14, 2016 – Tiksi, Sakha Republic, Russia

Objectives

This expedition grew out of a need to conduct research in the western Laptev Sea region and the opportunity presented by a new vessel operating out of Tiksi, the Nicole. The western Laptev Sea is a seldom studied continental shelf region bordered to the south by small river deltas and estuaries, as well as open coastline along most of which ice-rich Pleistocene deposits are currently undergoing rapid thermo-erosion. This region of shelf is broad (over 500 km at points) and very shallow, so that permafrost is thought to exist beneath most of its seabed. This permafrost was inundated by rising sea levels following the Last Glacial Maximum and has probably been degrading since its transgression. Measurements of sediment temperature or state, however, are practically non-existent. The degree to which rivers and thermokarst basins degraded permafrost before its transgression is an open question. Answering that question is key to assessing Arctic methane emissions in the offshore environment and the impact of continued climate warming on Arctic Ocean continental shelves.

Permafrost warms and thaws most rapidly immediately after it is inundated by sea water, which means that work close to the coast can tell us much about how it degrades and with what consequences. The shallow waters of the Laptev Sea restrict marine work to vessels with shallow draught, to work from the shoreline or the sea ice. There are few ships operating in central or eastern Siberian. This year Arctic Geo Center Tiksi (AGC.Tiksi, formerly Polus) began operating a 15 m yacht, the Nicole, from Tiksi. This ship made it possible to navigate in water as shallow as three meters and to cover large distances relatively rapidly. Coincident development of a novel technique for detecting the depth of permafrost below the seabed (Overduin et al., 2015) made such a research platform ideal for testing out the newest prototype, MOBSI (Mobile Ocean Bottom Seismic Instrument). The ship also provided an economic means of reaching an instrumented borehole in need of maintenance at Cape Mamontov Klyk ("mammoth tusk") in the western Laptev Sea. This borehole is the landward end of a series of submarine permafrost boreholes drilled in 2005 (Overduin et al., COAST exp. report).

Submarine permafrost is currently of interest due to its functions as a repository for organic carbon and a cap on gas migration. As long as it remains frozen, permafrost can preserve organic carbon (plant and animal remains) from decay. Such decay produces greenhouse gases, such as methane (CH_4) and carbon dioxide (CO_2). Other sources of greenhouse gases exist, such as hydrocarbon reservoirs. As long as it remains frozen, permafrost has a very low permeability for gas and can trap it and so prevent its release. Particularly beneath the seabed, permafrost may not necessarily be frozen. It can persist as cryotic sediment (temperature below 0°C) without any ice. In this case, both of its functions, as repository and barrier, are compromised. Recently observations of more rapid erosion (Günther et al. 2015) and the long-term record of observations from Samoylov Station in the Lena Delta (Boike et al. 2015) suggest that an intensification of processes affecting permafrost in the region is underway.

Methane release due to permafrost thaw, in particular, has been the subject of much recent contention. One of the goals of this expedition is therefore to investigate methane concentrations in the Laptev Sea and to focus on the microbes that mitigate its release. Another important aspect is the oxidation of methane in anoxic environments, which has been investigated only recently. First results points towards an important microbial filter at the permafrost thaw front and in cryotic sediments where permafrost degrade. Not much is known about anaerobic oxidation of methane (AOM) in cold environments and the microbes involved in this process. Understanding of the microbial community composition and enrichment of key microbes is the essential goal to understand methane dynamics in submarine permafrost regions.

The goals of this expedition are to better understand submarine permafrost dynamics and their effect on and interaction with methane emissions in the Laptev Sea and Lena Delta region. To this end, our objectives are: 1. to carry out experimental tests of the prototype passive seismic measurement method and device, MOBSI, in a variety of subaqueous permafrost settings (including lacustrine, fluvial, and marine) that offer some form of validation (boreholes, historical records, temperature measurements, etc.); 2. to study late summer thaw dynamics in a rapidly changing coastal setting (Muostakh Island's northern end) using an array of passive seismic instruments; 3. download borehole data from the Cape Mamontov Klyk borehole and perform basic maintenance; 4. measure coastal erosion rates at key coastal monitoring sites; 5. measure methane concentrations in the

seabed, water column and atmosphere; 6. measure methane concentrations and study microbial methane oxidation in the active layer and at the permafrost in a marine setting; and 7. collect sample material from remote locations for colleagues (see following section).

Supplementary goals

The utility of our research vessel, the Nicole, attracted interest from a number of other researchers who expressed interest in sample material. In the interest of completeness, we list them here and include these samples in the results of our expedition (Table A 3.1.-1 to Table A 3.1.-34 in the Appendix).

1. Plankton samples – Katja Abramova, Head Scientist, Lena Delta Nature Reserve, Tiksi, Sakha Republic, Russia
2. Hydrological samples – Irina Federova, Otto-Schmidt Laboratory, Arctic and Antarctic Research Institute (AARI), St. Petersburg, Russia
3. Biomarker dating samples – Gesine Mollenhauer, Alfred Wegener Institute Helmholtz Center for Polar and Marine Research, Bremerhaven, Germany
4. Water column methane concentrations – Ingeborg Bussmann Alfred Wegener Institute Helmholtz Center for Polar and Marine Research, Helgoland, Germany
5. Soil samples for microbial cultures – Prof. Dr. Dirk Wagner, German Research Centre for Geoscience (GFZ) Helmholtz Center, Potsdam, Germany
6. Soil samples for microbial plasmid extractions – Dr. Fabian Horn, German Research Centre for Geoscience (GFZ) Helmholtz Center, Potsdam, Germany, in cooperation with the University of Warsaw

The research vessel

Research sites for this expedition were reached on board the yacht Nicole (Fig. 3.1.-1), chartered through the company Arctic Geo Science-Tiksi (AGC-Tiksi), led by Pavel Geryukov. The yacht Nicole is a Raffaelli ouragan power boat outfitted with two Detroit 550 HP diesel engines, a generator with a power reserve of up to 15 days, a 2400 l fuel tank and an 800 l freshwater tank. It has a width of 4.7 m, a length of 15.7 m and a draught of 1.2 m. The boat can carry a load of up to one ton, depending on load distribution. The boat can accommodate up to six expedition members in addition to the crew. It has three cabins with double berths, three WCs, two with shower, and a galley with gas stove, refrigerator and microwave. The crew on this expedition consisted of the captain (“sturmmann”) Viktor Nikolayevich Pudovkin and the mechanic Sergey Vitalyevich Pugakov.

Figure 3.1.-1: The RV Nicole of the company Arctic Geo Science Tiksi

The expedition

The cruise aboard the Nicole began from Tiksi (Fig. 3.1.-2 and 3.1.-3). With stops at Muostakh Island (Fig. 3.1.-3 and 3.1.-4) and the eastern coast of the Bykovsky Peninsula (Fig. 3.1.-5), the trip continued into Lena delta via the Bykovskaya Channel. Measurements and sampling was carried out at and around the Samoylov Research Station on Samoylov Island (Fig. 3.1.-6 to 3.1.-8), before the westward trip continued via the Olenyokskaya Channel. Further westward, the trip to Cape Mamontov Klyk in the western Laptev Sea (Fig. 3.1.-9) by weather-dependent delays in the bay south of Terpai Tumus. The return trip mirrored the westward trip, with an additional stop at Ivashkina Lagoon on the Bykovsky Peninsula (Fig. 3.1.-5).

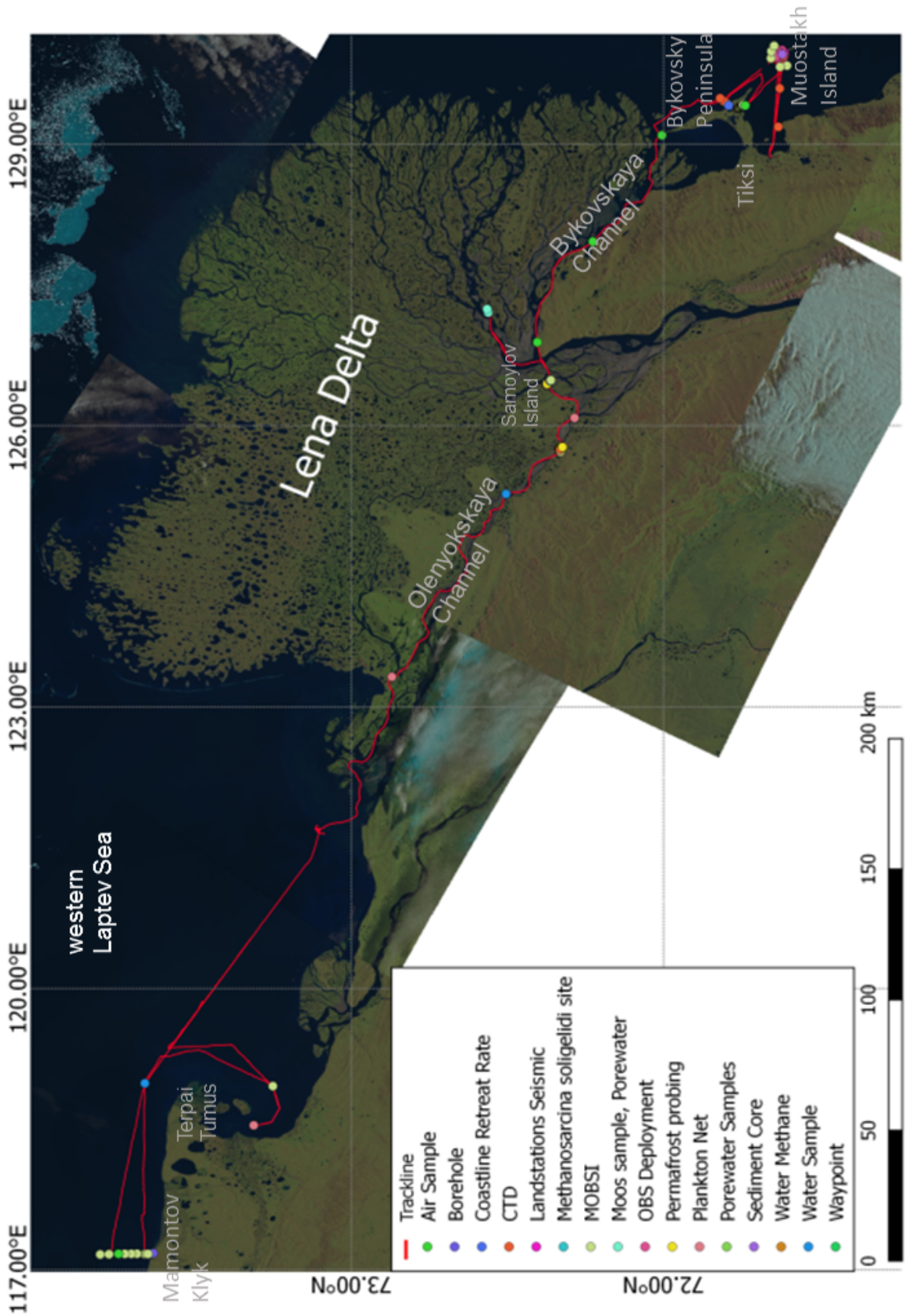

Figure 3.1.-2: Overview map with the expedition route and all sample locations

Methods & results

Subsea permafrost dynamics

We conducted two passive seismic studies in the Lena Delta and adjacent Laptev Sea. During our 2013 seismic field measurement at Muostakh Island, we recorded some 10 local seismic events within ~40 days of station deployment. The design of the seismic network did not allow for precise locating of those events. During the recent field campaign, we reinstalled a seismic network consisting of 15 land and 17 Ocean Bottom Stations (OBS) at and around Muostakh Island, recording continously the seismic activity for two weeks. The design of the network was optimized for locating seismic events (small earth or ice-quakes). First data inspection yielded a large number (up to 20 events per days) of small quakes which might be associated with dynamic processes in the submarine permafrost layer and/or active erosional events (rock or ice falls).

The second study focused at the determination of the thickness of thawed sediment above a submarine/subaquatic permafrost layer by passive seismic measurements. Ambient seismic noise recorded sufficiently long can be analyzed and the thickness of the unfrozen layer above the permafrost can be derived (Overduin et al., 2015). Based on our experience with OBS during the 2013 campaign at Muostakh Island, an ambient seismic noise of several minutes per location appeared to be sufficient to derive the depth of the submarine permafrost table. At GFZ we developed a seismic broad-band sensor, (water proof casing with cabled communication to a hand-held PC unit) which was first tested in the Lena Delta/Laptev Sea. Special data processing software was developed to enable in-field/real-time data quality assessment. All components showed their resistance to the occurring harsh environmental conditions and generally worked very well, in-field data evaluation of the collected data looked very promising. We conducted these measurements at 94 locations, i.e. along profiles crossing branches of the Lena, across the Ivashkina Lagoon and Banya Lake (Samoylov), around Muostakh Island and at Mamontovy Khayata.

Validation data for the thickness of thawed sediment (or the depth of the permafrost table below the surface or sea floor) were measured with a permafrost probe. A 10-m long permafrost probe was used but found impracticable for permafrost table depths much beyond 2 m. Historical data will be used from drilling and probing projects at Muostakh Island (Kunitsky 1998, Slagoda 2004), Mamontovy Khayata (Grigoriev, 2008), Cape Mamontov Klyk (Schirrmeister 2007) and Ivashkina Lagoon (unpublished data).

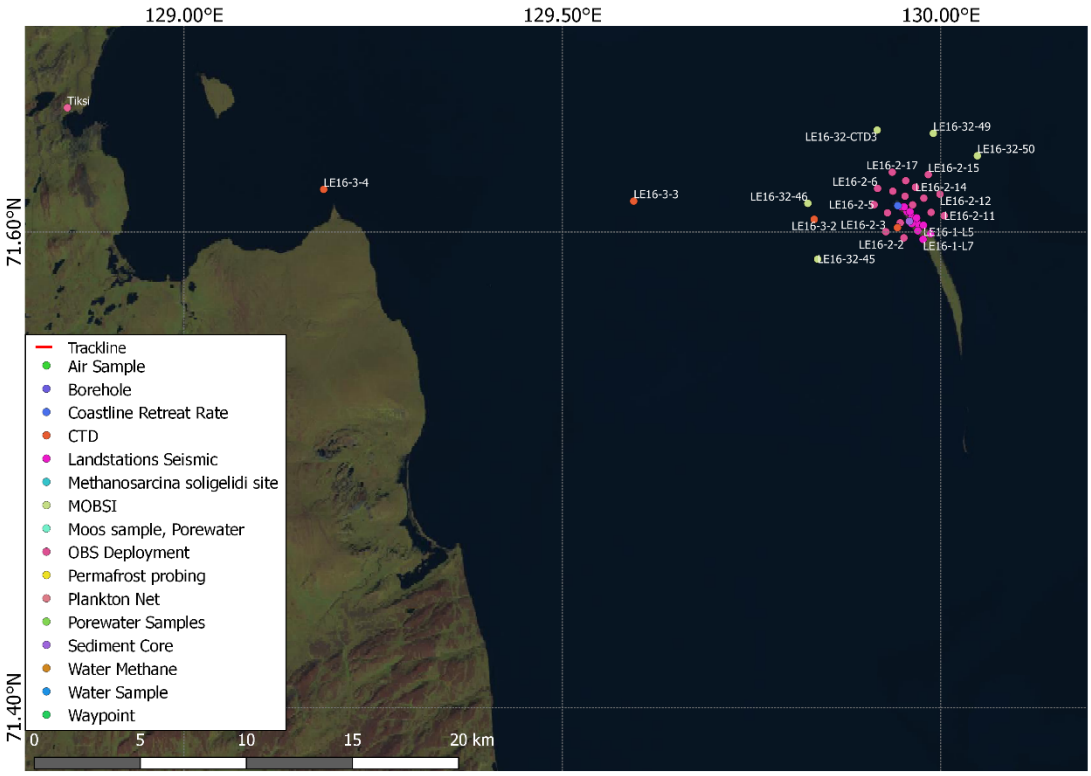

Figure 3.1.-3: Map Tiksi - Muostakh sample locations

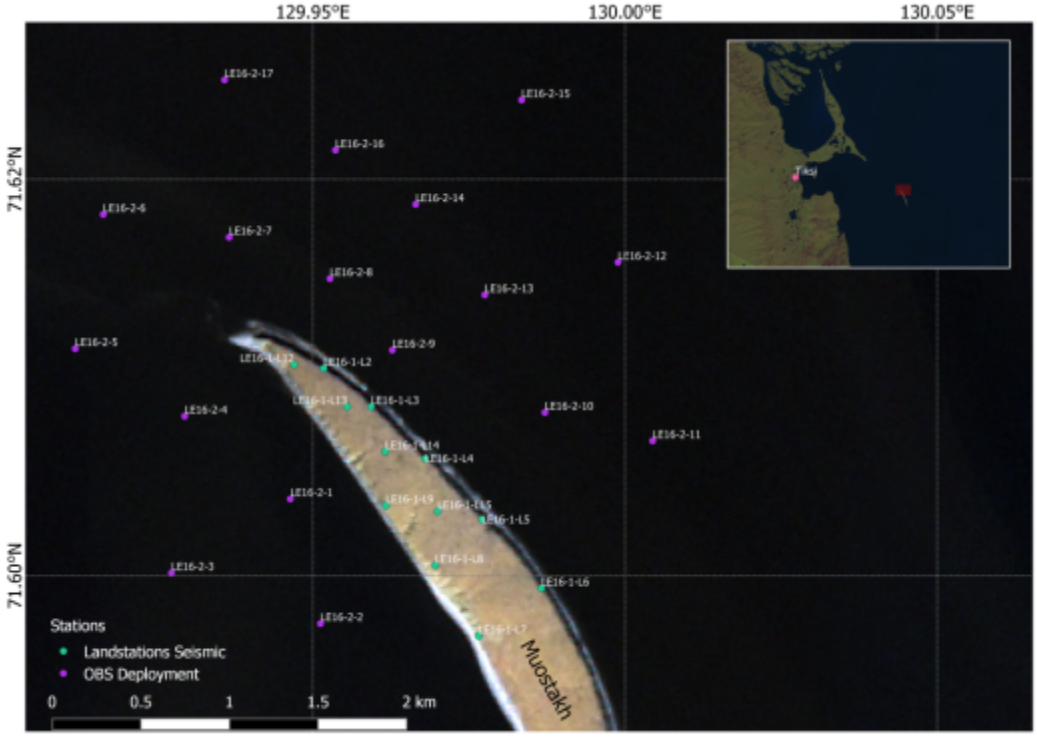

Figure 3.1.-4: Muostakh Island seismic locations

Figure 3.1.-5: Bykovsky- Ivashkina lagoon sample locations

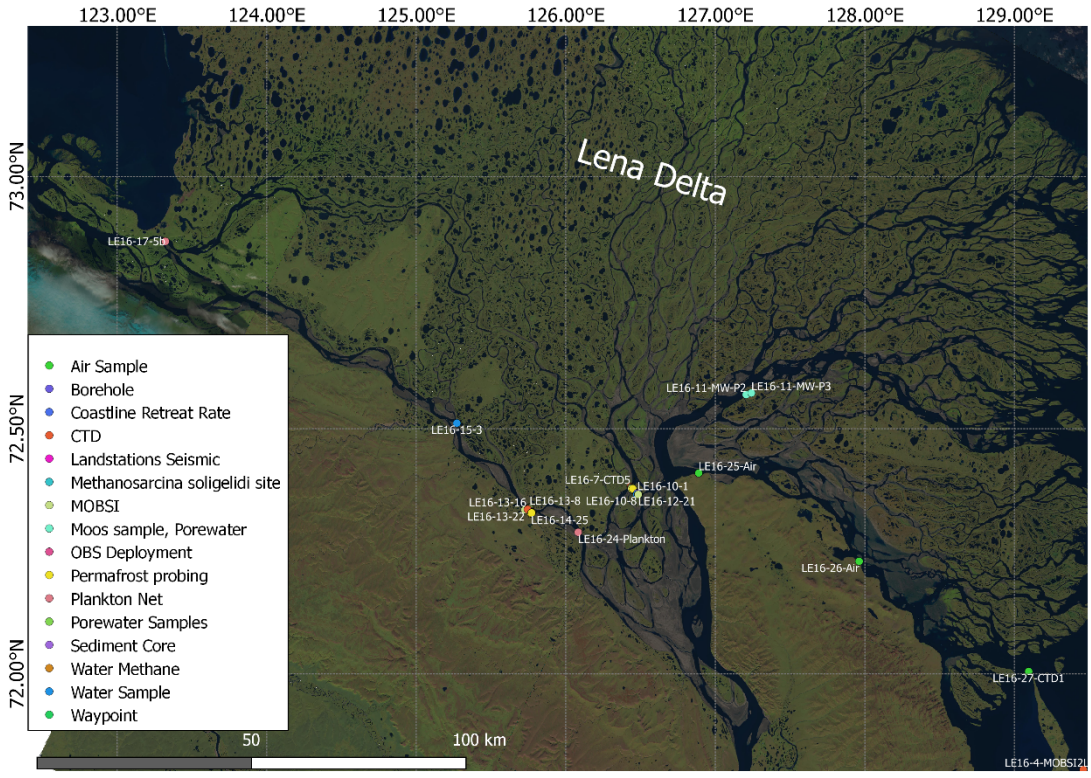

Figure 3.1.-6: Inner Lena Delta sample locations

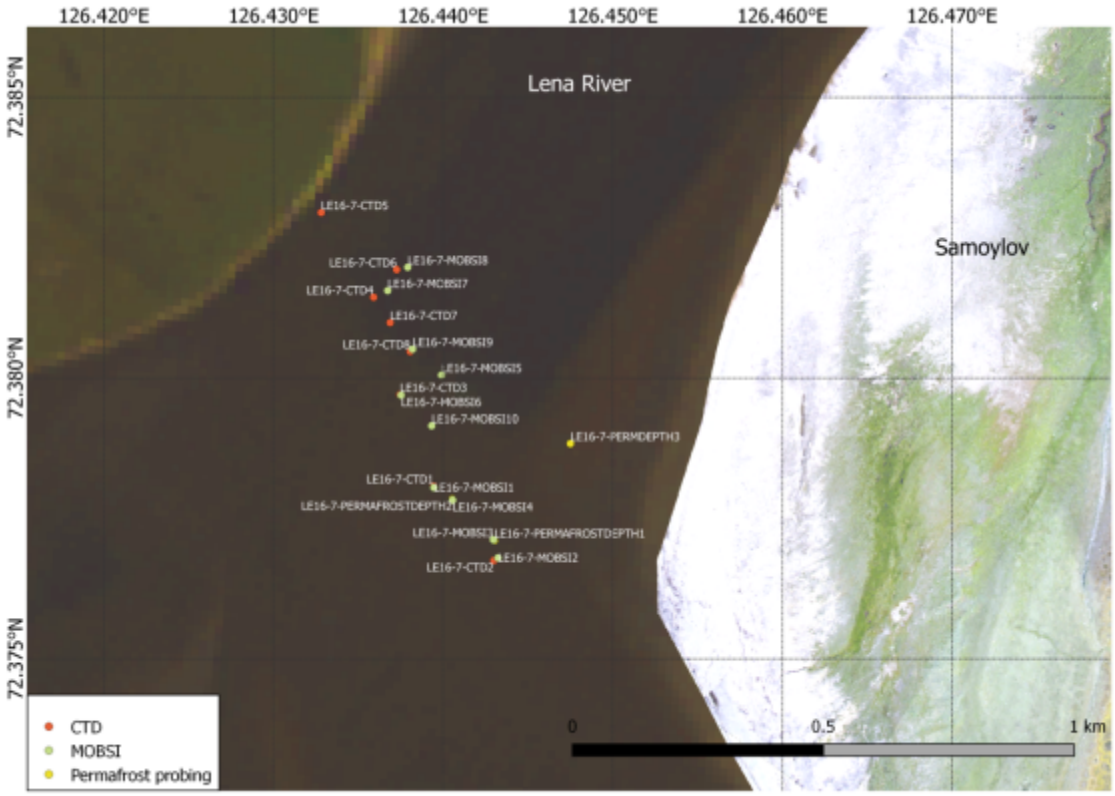

Figure 3.1.-7: Lena River Channel - Samoylov sample locations

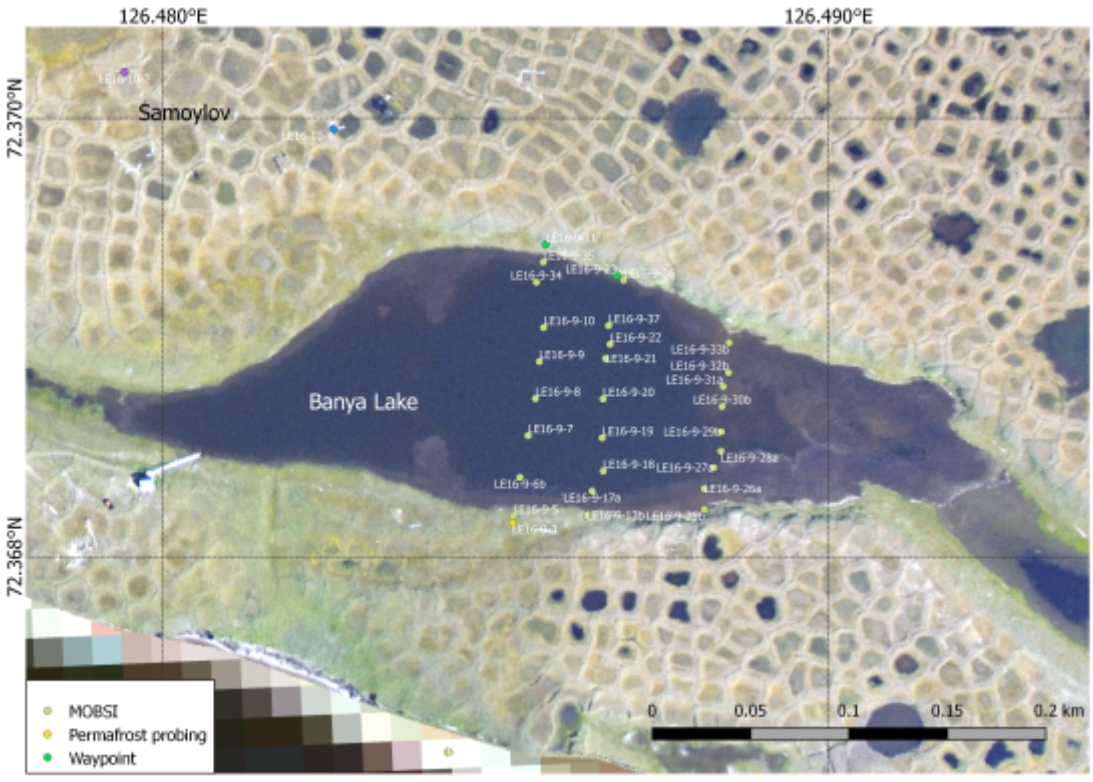

Figure 3.1.-8: Banya Lake (Samoylov Island) sample locations

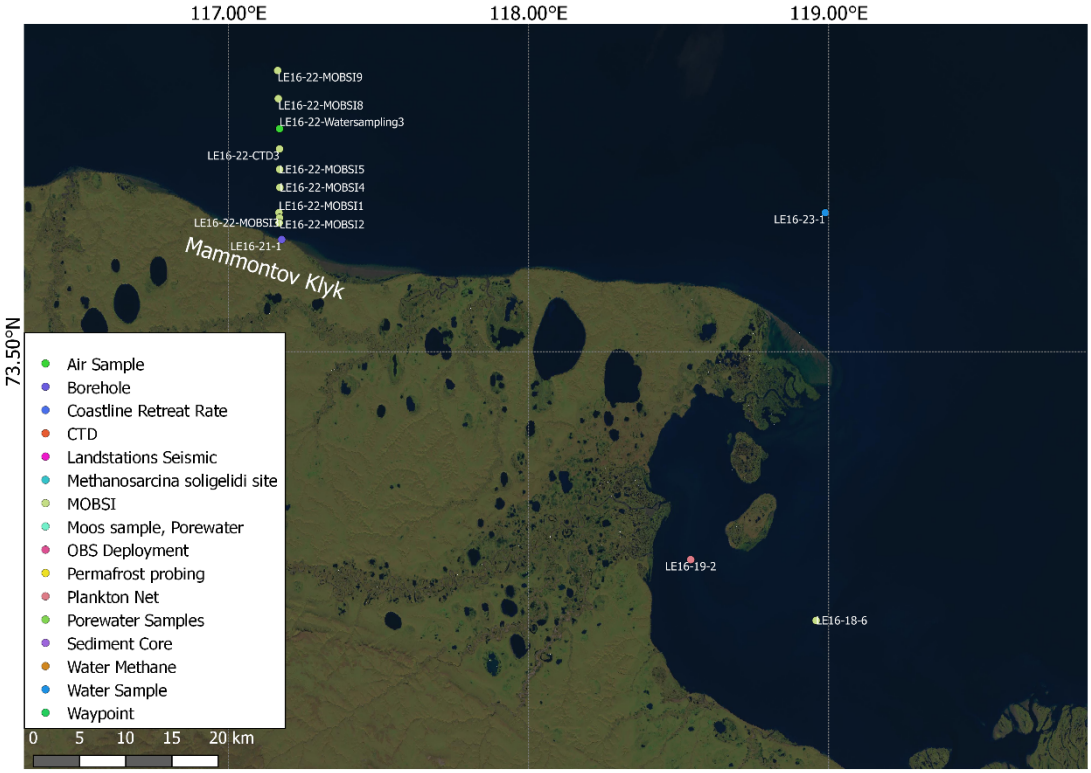

Figure 3.1.-9: Laptev Sea - Mammontov Klyk sample locations

Permafrost temperature (COAST C1 borehole)

Station LE16-21 (Table A 3.1.-22 in the Appendix) was the recovery of data from the COAST project C1 borehole thermistor string (Schirrmeister Fahrtbericht 2007). The borehole was last visited in 2011. Details on the borehole, datalogger and thermistor string are available in Günther (Fahrtbericht 2013). The borehole was visited on September 4th in the evening. The batteries were exhausted and replaced, whereafter contact was established with the datalogger (Manufacturer: RBR; Model: XR420) using the original RBR software. The original programming from 2011 until 2017 was still operating. By effecting a “100% data retrieval”, all data for the time period were recovered, although there was a problem with the time signature. The data for each sensor were constant at high negative values for almost the entire period of record, with the exception of the first measurements. Based on consultation with RBR, this is consistent with a severed thermistor chain. The presence of an ice plug in the borehole at the base of the active layer made maintenance difficult. The RBR thermistor chain is probably also iced in at a variety of greater depths as a result of sublimation, freezing, thawing and re-freezing within the borehole over the annual cycle (Günther et al., 2013). Additionally, the borehole visit was curtailed, first by approaching darkness, and secondly, by the imminence of poor weather. For these reasons, it was not practical to attempt to remove or replace the thermistor string. The recommendations for borehole maintenance and improvement made in 2011 remain in effect. The borehole remains as it was, the logger has been re-programmed to make measurements every 4 hours, but the thermistor string is severed - in principle, the borehole has been abandoned. The datalogger could in principle be

retrieved and possibly fitted with a new thermistor chain, although the model is no longer supported. In any case, the thermistor string should probably be reinforced with a steel cable.

The depth to permafrost outside of the casing was 45 cm (measured multiple times around the casing). The casing extended 80 to 83 cm above the ground surface with the lid on. The ice plug inside the casing was located at 146 cm below the upper edge of the casing (without the lid on).

Coastline position change rate (erosion)

At specific key sites, measurements of the position of the upper edge of the coastal exposure relative to some benchmark were made. For most key sites, these measurements are made at irregular intervals, up to annually (e.g. Muostakh Island). By comparing distances from one measurement to the next, it is possible to determine a mean coastline position change rate. Table A 3.1.-1 in the Appendix presents key site names, positions, and measurements dates.

Water column

Water column conductivity and temperature were determined with a Sontek CastAway CTD sensor, which measured electrical conductivity with a 6-electrode flow through cell, temperature with a thermistor and water pressure. Locations were automatically saved using onboard GPS, ideally prior to and following each cast. Electrical conductivity and pH were additionally measured using a laboratory instrument (WTW), usually within an hour of sampling. A graph comparing “specific conductance” (as designated by the manufacturer; in fact, this value is temperature-corrected conductivity) from the CastAway to the laboratory-determined, temperature corrected conductivities is presented in Fig. 3.1.-10.

Water samples were collected for pH & electrical conductivity, stable isotope ratios, major ion concentrations, coloured dissolved organic matter (cDOM), turbidity and methane concentration (see above). Water column samples were sampled with an UWITEC water sampler. Bottom water was recovered either from the UWITEC gravity corer or with the water sampler, depending on whether or not sediment was sampled. Ion samples were filtered with 0.45 µm effective pore-size (cellulose acetate) or 0.22 µm PES (polyethylsulfonate) and frozen for transport. Isotope, cDOM and turbidity were kept cool until during transport and shipping. pH and electrical conductivity were measured on board after sampling using a laboratory WTW instrument.

Turbidity, sediment subsamples and cDOM samples were sent to the Otto-Schmidt Laboratory at the Arctic and Antarctic Research Institute for analysis. Ion concentrations and stable isotopes were sent to AWI Potsdam.

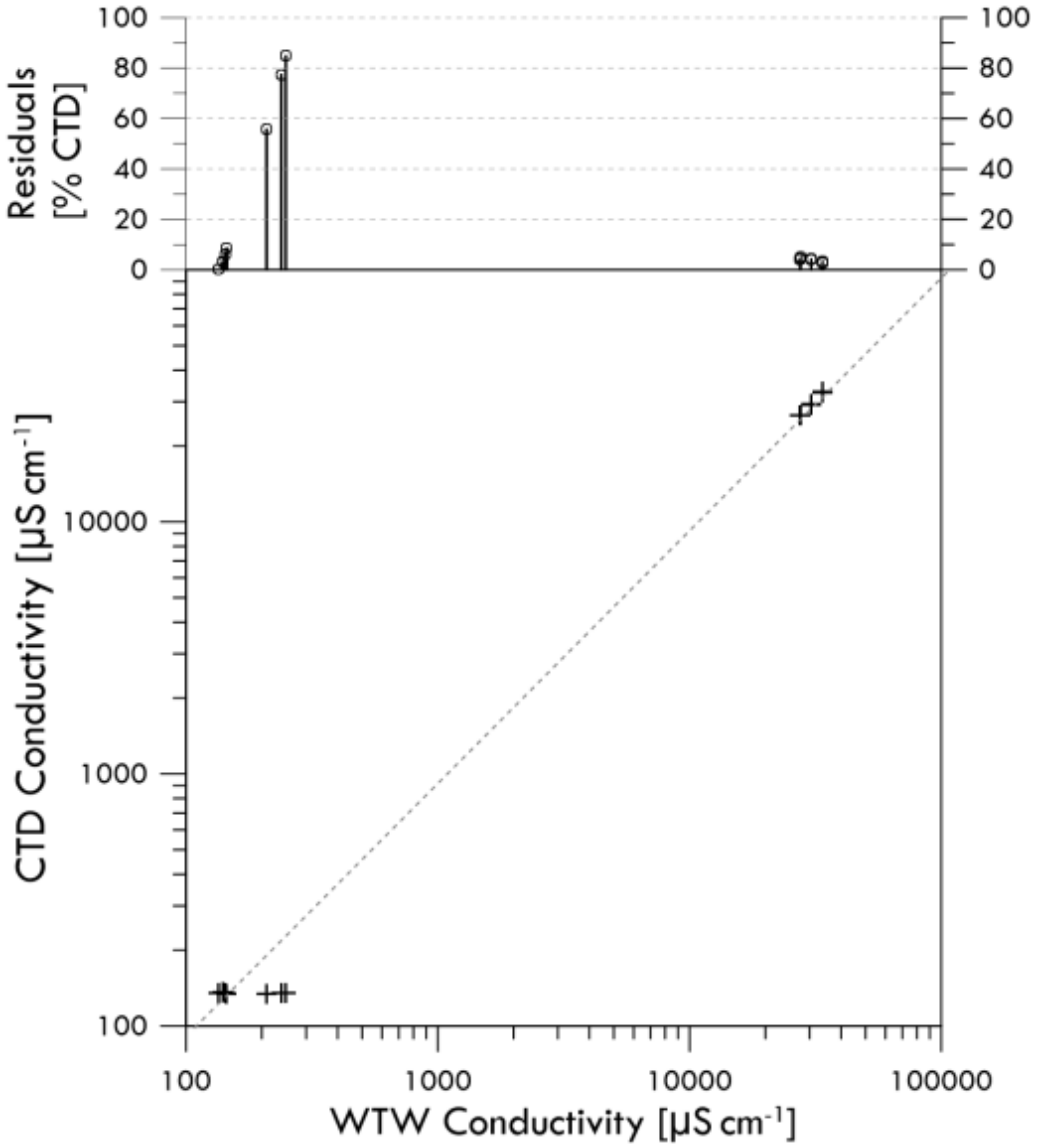

Fig. 3.1.-10: Comparison of electrical conductivities measured with the Sontek CastAway CTD and the WTW benchtop pH-Conductivity-Dissolved Oxygen instrument. The upper graph shows the differences in measures values as percentage of the CTD value.

Sediment

Surface sediment was sampled using a hand-deployed Uwitec gravity corer outfitted with 2 additional weights. Recovery in soft silty sediments (e.g. the gulf south of Terpai Tumus) was typically between 15 and 25 cm, while recovery in sandy sediments (e.g. offshore Cape Mamontov Klyk) was either not successful or restricted to only a few cm. Sediment samples were taken for methane concentration, organic carbon dating and sediment composition (see station lists for details on which samples were collected at which site).

Methane concentration

- subsampling of 3 cm³ sediment preserved in a high molar NaCl solution to detect headspace gas measurements by gas chromatography

- subsampling of water column to measure methane by stopping microbial processes with 2.5 M H_2SO_4 to detect headspace gas measurements by gas chromatography
- air samples for methane measurements by gas chromatography

Microbial sampling

- preservation of DNA and cells through freezing and RNAlater conservation
- biogeochemical measurements of potential ions, hydrocarbons and minerals involved in the AOM process
- preservation of material by freezing for inoculation of media to enrich microbes involved in AOM
- preservation of material by freezing for inoculation of rate measurements
- preservation of material by freezing for extraction of core lipids

Plankton

The plankton net was deployed from on board the yacht. It was rinsed with an open stopcock, lowered to the seabed with the stopcock closed and pulled up through the complete water column. The position (GPS or CTD onboard GPS) and the angle of inclination (± 5°) from the vertical were recorded in order to compensate for increased path length due to non-vertical deployment. In principle, the angle of inclination of the path was never 0°, due to drift or current, but ranged between 10 and 60°. The sample trapped in the net's receptacle was then collected in a specimen bottle and treated with 5 mL 40% formol.

3.2. Lena Delta as a result of interactions between the river and the sea

Dmitriy Bolshiyanov [1], Sergey Pravkin [2]

[1] St. Petersburg State University, St. Petersburg, Russia

[2] Arctic and Antarctic Research Institute, Russian Federal Service for Hydrometeorology and Environmental Monitoring, St. Petersburg, Russia

Fieldwork period June 28 to August 2, 2016 (banks of the Lena River from Yakutsk to delta, Samoylov Island)

Objectives

Our research focussed on the geomorphological and geological structure of the Lena River Valley and its paleogeographic reconstruction. An attempt is made to define the role of the main part of the Lena Valley in the formation of the Lena Delta.

Methods

1. ^{14}C Dating
2. OSL Dating
3. Spore and pollen analyses
4. Diatom analyses
5. Mapping

Preliminary results

The Lena River is the longest and full-flowing river in the East Siberia. During the 19th annual Russian-German expedition to the shores of the Laptev Sea in 1998, the structure of the delta itself and of the coastline were investigated for the first time in the context of this ongoing cooperative research. During the ensuing years, the main target of research remained the Lena River Delta and its structure and the development. We posit that the delta is the result of interactions between the river and sea. Although marine factors have been widely investigated and research results have been published (Bolshiyanov et al., 2013), there is little understanding of interaction between sea and river during different stages of delta evolution.

In 2014 ship-based studies were carried in the lower part of the river from the delta to the village Kyusyur. Over a period of a few days, river terraces were observed, measured, and dated. Unexpected results were obtained, especially from the Chekurovka area. As a result, two participants of the 2016 expedition traveled by rubber boat from Yakutsk to the mouth of the Viluy River (400 km) in July 2016 aboard the *Merzlotoved* ship of the Mel'nikov Permafrost Institute, Yakutsk. The 2014 route was extended downstream to Samoylov Island, a distance of 1150 km (Fig. 3.2.-1). Terraces and sediments during the first stage of the route were accessed from the ship by boat, allowing sampling of a rich variety of exposed sections and outcrops. In addition, ship-board descriptions of the river bank and island morphology were made and some landings at outcrops were possible.

A variety of river channel processes and morphologies could be identified and described for different sections of the river along the route. One of the most significant factors defining and differentiating these sections of the Lena River and the changes to its valley is the inflow of the Aldan River. Prior to its confluence, the Lena River has many arms channel and is characterized by a tranquil flow. Downstream from the confluence, the width of which is 4.5 km, driftwood appears in large quantities, covering the slopes of terraces and the floodplain. It lies at an altitude of up to 5 m downstream of the Aldan River inflow, increasing further downstream to up to 8 m. Upstream of the confluence, what driftwood can be observed lies at a height of 2-3 m above the low-water channel.

The main influence of the Aldan River on bed formation is that its waters carry ten times as much suspended sediments as the waters of the Lena at the inflow. This feature is due to the influx of water of the Aldan, well expressed in the structure of terraces and floodplains. All accumulative terraces below the Aldan inflow are composed of bedded gray silty sediments. Upstream from the mouth of the Aldan River, terraces have a yellow color and are mostly composed of bedded sands. An example of the latter is the extensive Bestyakh terrace that extends along the right bank from the Lena Pillars almost to the Aldan River. But 50-70 km upstream from the mouth of the Aldan, the first river terrace on the right bank of the Lena consists of Aldan sediments, indicating that the Aldan River confluence with Lena River lay upstream from its modern position a few thousand years ago. Between Cape Xenia-Hayata and the village of Batamay on the right bank of the Lena, terraces with heights of 30-35, 20-25 and 8-10 m were observed that are composed of Aldan alluvium. Downstream from this section, and in particular downstream from Sangar, high terraces are compound and denudated.

The Viluy River confluence with the Lena River has a smaller influence on the Lena River valley than the Aldan River confluence. The floodplain and the first terrace of the Viluy River at its mouth are composed of sands. At the mouth of the Viluy River there are three Cretaceous outcrops with heights of 120 to 150 m that were included in its alluvial plain. Alluvial accumulation terraces with heights of 25 to 30 meters and denudation terraces at 60 and 120 m were observed on the slopes of the Ust-Viluyskiy ridge. Downstream from the mouth of the Viluy River bed-formation factor develops as type many arms channels.

In the region of Zhigansk erosion escarpments on the left bank of the river expose Cretaceous and Quaternary sediments. Downstream the bed of the Lena River valley is contracted by Cretaceous cliffs to a width of 8.5 km width with a channel width of only 3 km. Near the village of Kystatyam, the flood plain expands again up to 36 km width. Cliffs up to 150 m high form the river bank for many kilometers along the river. They are composed of nearly horizontal layers of Cretaceous sands and sandstone. Accumulative low terraces (at 7-10 and 12-15 m) and higher denudation terraces developed in Cretaceous sediments can be observed at the mouths of tributaries and on the slopes of the valleys of the tributaries.

The village of Siktyah is located on 15-20 and 35-45-m high denudation terraces in the lower reach of the river. Here, the Lena River flow initially to the west and then to the east and forms a latitudinal segment before turning north to flow through the "Lena pipe". Upstream of the "Lena pipe", on the right bank, the first observation can be made of a 10

m terrace outcrop of organic and mineral deposits which is called “sloyenka”. Such sloyenka deposits are widely distributed in the Lena Delta and mark stages of high sea level in the past.

Terraces are visible at different levels along the “Lena pipe”. For example, the following levels could be observed at the mouth of the Tigie River on the left bank of the Lena River: floodplain (3-4 m), the first terrace (15-20 m), and terraces at heights of 80, 100 and 120 meters. The right slope of the Lena River valley is terraced here too. There are extended terraces height of 20, 80, 120-140, 180-200 m. The Kyusyur is located on the first 20-meter terrace. The river flows out of the "Lena pipe" at the islands of Tas-Ary and Tit-Ary where denudation terraces have formed at heights of 20, 40-60 and 100 m on the slopes of the valley.

The Bestyakh terrace near Yakutsk has been dated using optically stimulated luminescence (OSL). It was formed 18-25 thousand years ago during the coldest stage of the upper Neopleistocene. The Bestyakh terrace is composed of alluvial sediments, as is the sand and aleurite terrace downstream from the Aldan Mouth. Our research contradicts previously published geological data, according to which the most recent map of the Quaternary deposits of Russia (1:2 500 000 scale) was composed. This map identifies this terraces as having an Aeolian origin.

We dated sands of terraces on the left bank of the Lena near Yakutsk (Bolshiyanov et al., 2016). Their age was between 182 to 234 thousand years. The age of alluvium from the 54-62 m terrace at the mouth of the Ebetem River near Kyusyur was 164 thousand years.

We obtained the most unexpected dates for alluvium dating on samples from the slopes of the Lena Valley near Chekurovka. Samples from a height of 50 m above the river were 1300-2000 years old. These dates are consistent with the dating of the first terrace of the Lena Delta. However, due to the large height difference and small lateral separation, (95 km between of the Chekurovka and the Lena Delta), it is difficult to understand how the deposits could have formed at the same time.

Dates obtained as a result of our research suggest that processes forming the Lena River valley have not been fully understood. In some areas, we were able to identify accurately the height, quantity and composition of deposits of terraces, in others areas only to approximate. Our results underscore the necessity of further research of the Lena River using all available methods.

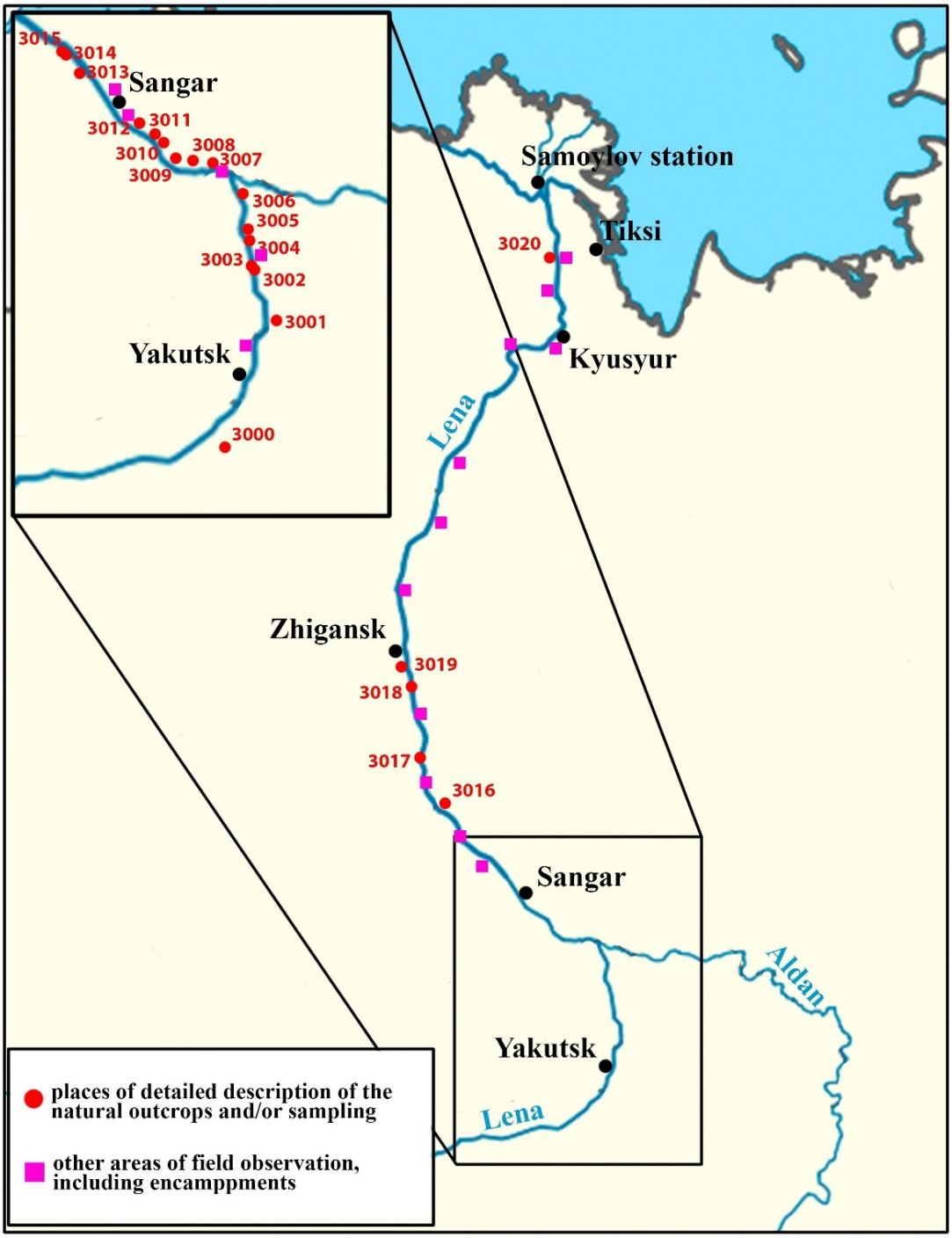

Figure 3.2.-1: Map of sampling and observation points

3.3. Seismicity of the Laptev Sea Rift

Wolfram H. Geissler [1], Sergey Shibaev [2], Christian Haberland[1], Sergey Petrunin [2], Frank Krueger [4], Dmitri Peresypkin [2], Daniel Vollmer [4], Stepan Gukov [5], Rustam Tuktarov [2], Boris Baranov [6]

[1] Alfred Wegener Institute Helmholtz Center for Polar and Marine Research, Bremerhaven, Germany

[2] Yakutsk Branch Geophysical Survey Russian Academy of Sciences, Yakutsk, Russia

[3] Helmholtz Centre Potsdam - GFZ German Research Centre for Geosciences

[4] Institute of Earth and Environmental Science, Potsdam University, Potsdam, Germany

[5] Yakutsk Branch Geophysical Survey Russian Academy of Sciences, Tiksi, Russia

[6] P. P. Shirshov Institute of Oceanology, Russian Academy of Sciences, Moscow, Russia

Fieldwork period July 22 to August 05, 2016 (Lena Delta, Tiksi)

Objectives

Extensional tectonics is one of the key players in shaping the Earth's landscape. We want to study one of only very few examples of transition between oceanic and continental rifting. Generally, rifting processes are associated with earthquake and also magmatic activity. In principle, these processes hold risk potential, for instance, earthquakes or fluid escape close to the continental slope of the Laptev Sea might cause major submarine landslides and expulsion of the great amounts of methane influencing on climate change.

The Laptev Sea region is one these very few places on Earth where mid-ocean spreading centres continue into continental rift zones. The Gakkel Ridge, the active spreading centre in the Eurasia Basin of the Arctic Ocean, is characterized by well-defined seismicity close to its axial graben. In contrast below the Laptev Sea Shelf, which consists of a series of sediment filled grabens (500 km wide, 700 km long), only more diffuse seismic activity is observed. The pre-rift basement in the Laptev Sea is most probably formed by Late-Paleozoic and Late-Mesozoic fold belts (Drachev et al., 2010). The Laptev Rift Basin is filled with Upper Cretaceous and Cenozoic sediments of variable thickness (1.5 to 14 km). The westernmost limit of seismicity is located close to edge of thick lithosphere of the Siberian Shield (Sloan et al., 2011), which indicates some structural control on the recent tectonic activity. Focal depths are mainly <25 km (continent) and <10 km (ocean) (Franke et al., 2000; Fujita et al., 2009). Sparse observations of upper mantle earthquakes (Avetisov, 1999; Kovachev et al., 1994) are under debate. The pole of rotation is very close to the study area, most probably to the south of the Lena Delta (e.g. Gaina et al., 2002). Existing data indicate changes between compressional and extensional tectonic phases over short distances. This might be a consequence of the fact that the pole of rotation is close to our study area. The Khatanga-Lomonosov Shear Zone marks the border between the Gakkel Ridge and Laptev Sea Rift System, but its nature and extent is debated (e.g., Jokat et al., 2013; Laverov et al., 2013).

According to Franke et al. (2000), crustal extension is concentrated in the eastern Laptev Sea area. Fault plane solutions are sparse and mostly not well determined to describe the movements in greater detail. Thus, with this project we intend to investigate details on tectonic movements in the Laptev Sea to better describe this amagmatic rifting and its consequences in an Arctic and global context. In general, we intend to increase the number of seismological stations for monitoring local earthquakes in the Laptev Sea/Lena Delta to fulfil the following objectives

(1) Location of microseismicity and its relationship with active faults. We want to identify seismologically active faults zones. In a first step, we like to deploy instruments in earthquake areas, which are already identified by the global seismological network, though with low spatial resolution.

(2) Focal mechanisms. What is the present geodynamic setting, where is extension and where is compression in the Laptev Sea and in the Lena delta region, where is the exact pole of rotation? What is the relation of the recent seismicity to pre-existing crustal and lithosphere structures (e.g. western Verkhoyansk Fold-and-Thrust Belt/Olenek Zone or South Anyui Suture)?

(3) Lithosphere structure. It is interesting to note that despite the Cenozoic continental rifting in the Laptev Sea little volcanism is known. Thus, we like to compare the deep crustal and upper mantle structure with other continental rift systems (e.g. Afar) to enhance our understanding on the driving forces.

Methods

In a first step, we want to study the local and regional seismicity and lithospheric structure by means of a network of seismological stations and a seismological array. During the 2016 fieldwork, we installed 12 seismological stations in the Lena delta to study the local seismicity along the southern part of the Olenek Fault Zone (Fig. 3.3.-1; Table 3.3.-1) and 13 stations in an array SE of Tiksi to study the regional seismicity of the Laptev Sea (Table 3.3.-2). Instrumentation of the stations includes Cube data loggers and Mark-1 Hz Seismometers. The stations run autonomously with batteries. This first installation is dedicated to test the station configuration under the extremely harsh environmental conditions in northern Siberia and to gain a first set of data. The Mel'nikov Permafrost Institute, Yakutsk and the Samoylov Station logistically supported the fieldwork.

Preliminary results

The installation of stations went well. The array SE of Tiksi was installed in the period 23.-30.7.2016. An all-terrain vehicle was used to reach the station sites. Two stations in the mountain range SW of the Lena delta were installed on 25.7.2016 with the help of a helicopter. All stations in the SW Lena delta and along the Lena river were installed with the help of the vessel *Merslotoved* of the Mel'nikov Permafrost Institute and a boat transfer from Samoylov station to Amerika Khaja.

No test data was retrieved from the network stations, but it was possible to get first data from the seismological array. These data show its location capability. Seven earthquakes could be located, one within the delta and six along the coast of or within the Buor Khaja bay which is located to the east of the array (Table 3.3.-3). The location was done with a fixed $V_P = 6\ \frac{km}{s}$ and $V_S = \frac{6}{\sqrt{3}}\ \frac{km}{s}$. The measured slownesses of P and S waves indicate an

increased $\frac{V_P}{V_S}$ ratio of 1.9. Additionally, there are more than 100 small events, which most probably stem from the coastal area close to the array.

Table 3.3.-1: Station list Lena Delta

Name	Locality	Latitude °N	Longitude °E	Elevation (m)	date	s\n seismo-meter	s\n record-er
LD004	DeLong-Chalta	72,654	124,347	12	2707 2016	1006	DC-620
LD007	Mountains	72,184	124,889	264	2507 2016	1007	DC-621
LD008	Tchaika	72,442	125,313	12	2507 2016	1009	DC-622
LD010	Tchai-Tumus	72,326	125,760	34	2607 2016	1015	DC-623
LD011	Amerika-Chaja	72,476	126,275	73	3107 2016	1170	DC-624
LD012	Pik Stalin	72,174	126,107	30	2707 2016	1178	DC-625
LD014	Mountains	71,888	126,036	241	2507 2016	1190	DC-626
LD015 (B)	GeoCamp	72,117	126,982	54	3007 2016	1331a	DC-627
LD016 (C)	By Stolb	72,400	127,147	71	0108 2016	1335	DC-628
LD018	White Mountains	71,929	127,313	23	2807 2016	1336	DC-629
LD019 (D)	Nordenshiel d	72,075	128,325	35	0308 2016	1342a	DC-630
LD021	Lena Castle/Tigie	71,399	127,247	111	2907 2016	1348a	DC-631

Table 3.3.-2: Station list Tiksi array

Name	Latitude [°N]	Longitude [°E]	Elevation [m]	date hour	s\n seismometer	s\n recorder
TIK01	71,574	129,073	135	23072016 1500	1831	DC-632
TIK02	71,576	129,068	139	23072016 1800	1889	DC-633
TIK03	71,576	129,078	131	24072016 1200	1895	DC-634
TIK04	71,574	129,081	136	24072016 1500	2828	DC-636
TIK05	71,572	129,078	140	26072016 1300	2829	DC-637
TIK06	71,572	129,069	121	26072016 1600	2860	DC-638
TIK07	71,574	129,065	119	26072016 1800	4191	DC-640
TIK08	71,584	129,069	85	27072016 1300	4192	DC-641
TIK09	71,579	129,099	98	27072016 1600	2830	DC-301
TIK10	71,569	129,097	120	28072016 1200	2858	DC-302

TIK11	71,563	129,075	146	28072016 1700	2859	DC-303
TIK12	71,572	129,043	50	29072016 1200	3045	DC-304
TIK13	71,582	129,049	109	29072016 1600	3052	DC-305

Table 3.3.-3: List of located earthquakes

Origin time		Latitude [°N]	Longitude [°E]	Depth [km]
23.07.2016	14:08:17.6	71,377	129,414	18
26.07.2016	12:21:40.3	71,813	130,445	28
26.07.2016	12:23:27.5	71,817	130,403	28
26.07.2016	12:25:09.9	71,827	130,361	33
26.07.2016	18:15:21.4	72,660	125,358	? (Pn)
28.07.2016	02:57:17.3	71,610	130,122	14
28.07.2016	10:37:19.1	71,394	129,420	24

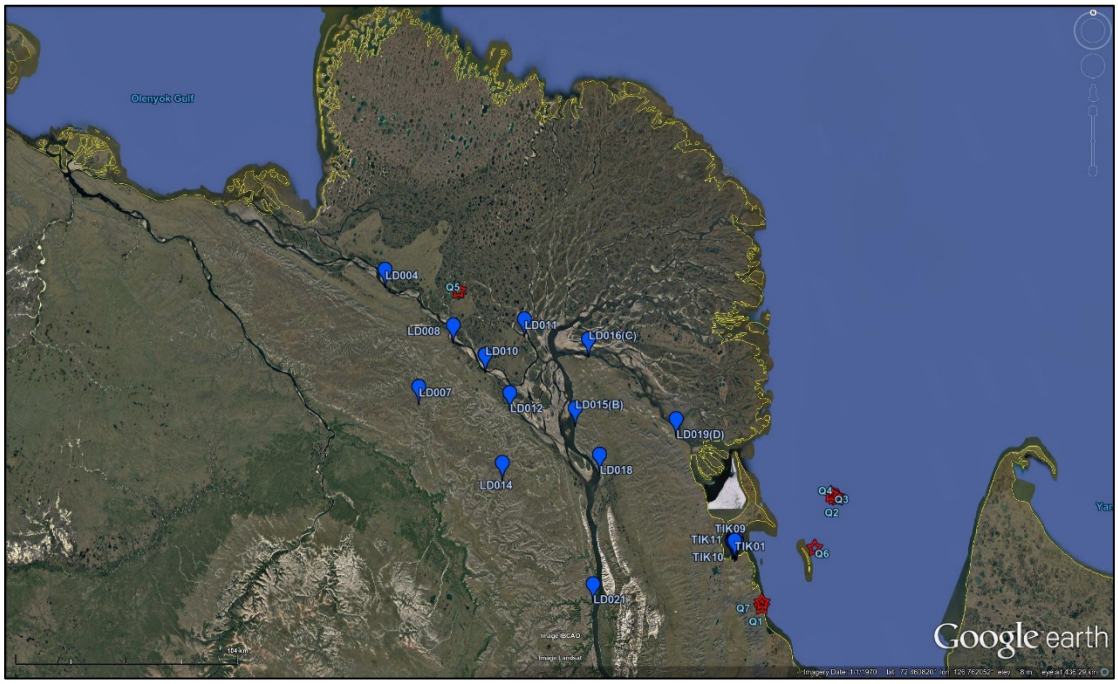

Figure 3.3.-1: Map of the study area showing the station distribution (blue marks). Red stars mark locations of earthquakes located within the first couple of days of operation of the seismological array SE of Tiksi.

Acknowledgements

We are grateful to our Russian and German colleagues who helped to start the experiment. Instruments were provided by Geophysical Instrument Pool Potsdam (GIPP). We appreciate also the support of the Mel'nikov Permafrost Institute, Yakutsk, which made their vessel available to us. We thank the captain and crew of the vessel *Merslotoved* as well as all people of the Samoylov Island research station.

References

Avetisov, G.P. (1999) Geodynamics of the zone of continental continuation of Mid-Arctic earthquakes belt (Laptev Sea), Phys. Earth Planet. Inter.,114, 59–70.

Bolshiyanov D.Yu., Makarov A.S., Schneider W., and Stoof G. (2013) Origin and development of the Lena River Delta. SPb: AARI. 267 p.

Bolshiyanov D.Yu., Thiede J., Savelyeva L.A., Fedorov G.B., Zhirov A.I., Pravkin S.A. et al. (2016) By studying the stages of development of the Lena River Valley // Geology and Mineral Resources of the North-East of Russia: Materials of the All-Russian scientific-practical conference. Editor Polufuntikova L.I. - Yakutsk: NEFU Publishing House, pp. 469-472.

Drachev, S.S., Malyshev, N.A., and Nikishin, A.M. (2010) Tectonic history and petroleum geology of the Russian Arctic Shelves: an overview, Petroleum Geology Conference series, 7, 591-619, doi: 10.1144/0070591.

Franke, D., Krüger, F., and Klinge, K. (2000) Tectonics of the Laptev Sea – Moma 'Rift' Region: Investigation with Seismologic Broadband Data, J. Seismology,4, 99–116.

Fujita, K., B. M. Kozmin, B.M., Mackey, K.G., Riegel, S.A., McLean, M.S., and Imaev, V.S. (2009) Seismotectonics of the Chersky Seismic Belt, eastern Sakha Republic (Yakutia) and Magadan District, Russia, Stephan Mueller Spec. Publ. Ser.,4, 117–145.

Gaina, C., Roest, W.R., and Müller, R.D. (2002) Late Cretaceous-Cenozoic deformation of northeast Asia, Earth Planet. Sci. Lett.,197, 273-286.

Grigoriev, M. N. (2008) Kriomorfogenez i litodinamika pribrezhnoshelfovoi zony morei Vostochnoi Sibiri (Cryomorhogenesis and lithodynamics of the East Siberian near-shore shelf zone), Habilitation thesis, Melnikov Permafrost Institute, Russian Academy of Sciences, Siberian Branch, Yakutsk, 291 pp.

Günther, F., Overduin, P.P., Makarov, A.S. and Grigoriev, M.N. (2013), Russian-German Cooperation SYSTEM LAPTEV SEA: The Expeditions Laptev Sea - Mamontov Klyk 2011 & Buor Khaya 2012. Berichte zur Polar- und Meeresforschung, Vol. 664, ISSN 1866-3192.

Jokat, W., Ickrath, M., and O'Connor, J., (2013) Seismic transect across the Lomonosov and Mendeleev Ridges: Constraints on the geological evolution of the Amerasia Basin, Arctic Ocean, Geophysical Research Letters, 40(19), 5047-5051.

Kovachev, S.A., Kuzin, I.P., and Soloviev, S.L. (1994) (engl. 1995) Short-term study of microseismicity in the GubaBuorkhaya, Laptev Sea, using ocean bottom Seismographs, Physics of the Solid Earth,30(7/8), 647-658.

Kunitsky, V. V. (1998), Kriolitologiya Nizovya Leny (Cryolithology of the Lower Lena), Melnikov Permafrost Institute, Russian Academy of Sciences, Siberian Branch, Yakutsk.

Laverov, N. P., Lobkovsky, L. I., Kononov, M. V., Dobretsov, N. L., Vernikovsky, V. A., Sokolov, S. D., and Shipilov, E. V. (2013) A geodynamic model of the evolution of the Arctic basin and adjacent territories in the Mesozoic and Cenozoic and the outer limit of the Russian Continental Shelf, Geotectonics, 47(1), 1-30.

Overduin, P.P., Haberland C., Ryberg T., Kneier F., Jacobi T., Grigoriev M.N., and Ohrnberger M. (2015), Submarine permafrost depth from ambient seismic noise, Geophys. Res. Lett., 42, 7581 – 7588, doi:10.1002/2015GL065409.

Slagoda, E.A. (2004) Kriolitogennye otlozheniya primorskoi ravniny morya Laptevykh: litologiya i mikromorfologiya (poluostrov Bykovskiy i ostrov Muostakh), Cryolitogenic sediments of the Laptev Sea coastal lowland: lithology and micromorphology (Bykovsky Peninsula and Muostakh Island), Ekspress, Tyumen

Schirrmeister, L. (2007) Expeditions in Siberia in 2005, Berichte zur Polar- und Meeresforschung (Reports on Polar and Marine Research), Bremerhaven, Alfred Wegener Institute for Polar and Marine Research, Vol. 550, 289 p

4. BEENCHIME

4.1. Reconnaissance study at Beenchime Salaatinsky Crater

Georg Schwamborn [1], Lutz Schirrmeister [1], Christoph Manthey [1], Ulli Raschke [2], Anatoly Zhuravlev [3], Nikolai Oparin [3], Maria Oshchepkova [3], Andrei Prokopiev [3]

[1] Alfred Wegener Institute Helmholtz Center for Polar and Marine Research, Potsdam, Germany

[2] Museum für Naturkunde, Leibniz Institute for Evolution and Biodiversity Science, Berlin, Germany

[3] Laboratory of Geodynamics and Regional Geology, Diamond and Precious Metal Geology Institute, Siberian Branch Russian Academy of Sciences, Yakutsk, Russia

Fieldwork period July 12 to 26, 2016

Introduction

Beenchime Salaatinsky Crater (BSC) is located west of the Olenek River at N 121°40', E 71°00' in Northern Yakutia (Fig. 4.1.-1). The area belongs to the north-eastern slope of the Olenek uplift framing the Siberian craton from the east. The name giving Beenchime Salaata River runs along the southern edge of the basin. The crater is virtually unknown in terms of its age and origin. Based on a first geomorphological appraisal the basin is thought to be the result of a Mesozoic volcanic explosion such as the kimberlitic pipes as occurring several times in the northern Siberia craton (Pinchuk et al., 1971; Khain, 1985). Alternatively, there is the interpretation of a meteor impact that created the basin, because suevitic breccia has been identified in the area (Mikhailov et al., 1979, Masaitis, 1999). Associated astrobleme age estimates are not based on physical data, but are linked to the geomorphologically downworn crater rim; the BSC is listed as 65 Ma old (Moon et al., 2001), <65 Ma old (Grieve, 1987), or 40±20 Ma old (data from the Earth Impact Database, 2016). In contrast, geological mapping and drilling in the late 1980ies revealed that the crater is formed in Cambrian sediment rocks and has been covered by Permian dolomites, which have not been affected by any impact or volcanic event (Aerogeology, 1990).

Objectives

Scientific key interests are (i) to identify geologic material for crater age determination, (ii) to elucidate Late Quaternary environmental and climate history based on sediment archives from a prominent lake in the BSC's centre and unconsolidated frozen deposits, (iii) to identify key questions for potential future work including a scientific strategy.

The field campaign was devoted (i) to collect sediment samples from the unnamed lake in the BSC's centre (listed in Table A 4.1.1.-1 in the Appendix), (ii) to collect samples from

permafrost within the crater, (iii) to collect fluvial sediments from rivers surrounding or draining BSC, (iv) to collect bedrock samples from the crater rim (Fig. 4.1.-2).

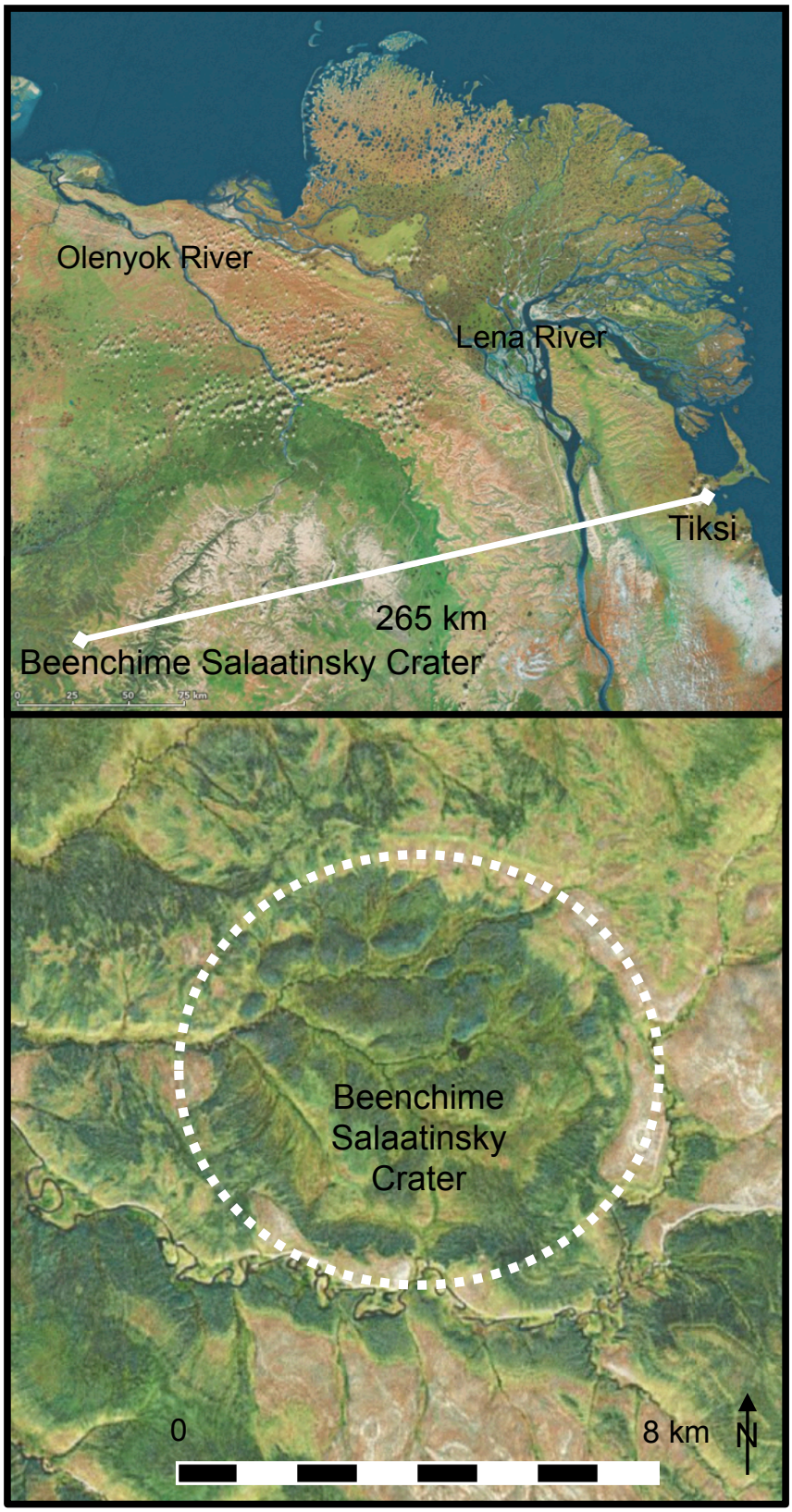

Figure 4.1.-1: WorldView-2 imagery (2013) of the study site Beenchime Salaatinsky Crater (BSC) in northern Yakutia. The crater is 265 km SW from Tiksi, the next airstrip (inset). The crater has 8 km in diameter, is placed in Palaeozoic rock. Note the lake close to the centre of the crater.

Logistics

The Alfred Wegener Institute, Potsdam and the Diamond and Precious Metal Geology Institute (IDPMG) of the Siberian Branch Russian Academy of Sciences, Yakutsk jointly organized and conducted the field study. Permission procedures were kindly arranged by the Arctic and Antarctic Research Insititute, St. Petersburg (AARI) and local transport, helicopter transfer and Tiksi-based housing were organized by the Roshydromet Hydrobase in Tiksi. The scientific group had four German participants from three institutions and three Russian participants from one institution. The campaign lasted three weeks with two weeks in the field (Table 4.1.-1) in the Olenek River uplands. Scientists established a campground in the forested tundra (Fig. 4.1.-3).

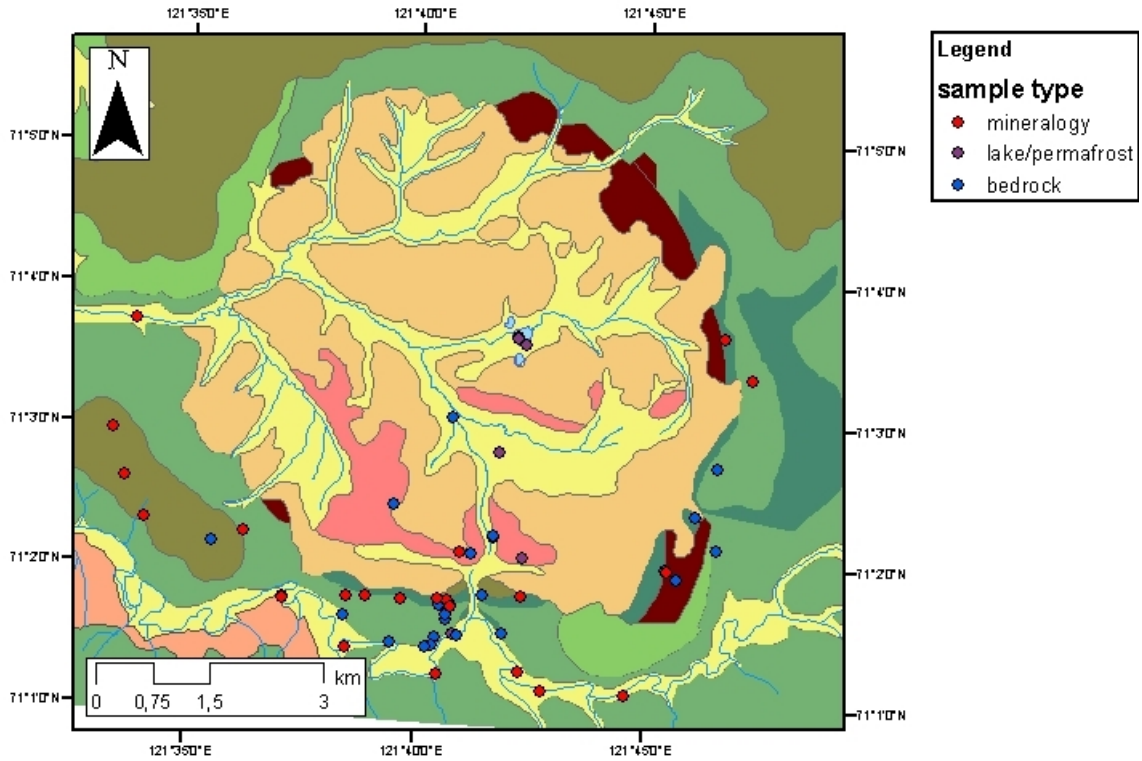

Figure 4.1.-2: Distribution of sample sites across the southern part of BSC; for geological legend see Fig. 4.2.-2

Table 4.1.-1: Itinerary of the campaign

Date	Activity
10.07.2016	Departure from Potsdam / Berlin via Moscow, Yakutsk to Tiksi
11.07.2016	Tiksi, field preparation
12.07.2016	Departure by helicopter to BSC, camp at Beenchime Salaata River, southern rim of BSC (total distance Tiksi-BSC: 265 km, flight time: 90 min)
13.07.2016	Start fieldwork
26.07.2016	End fieldwork
27.09.2016	Tiksi, packaging
29.09.2016	Return via Yakutsk, Moscow to Berlin
30.07.2016	Arrival to Berlin / Potsdam

Figure 4.1.-3: (Left) Camp ground in forested tundra, (right) field party photograph

4.2. Palaeoclimate and palaeoenvironmental reconstruction from permafrost and lake deposits at Beenchime Salaatinsky Crater

Christoph Manthey [1], Lutz Schirrmeister [1], Georg Schwamborn [1]

[1] Alfred Wegener Institute Helmholtz Center for Polar and Marine Research, Potsdam, Germany

Objectives

Beenchime Salaatinsky Crater (BSC) is a circular structure lying in northern Yakutia close to the rivers Beenchime in the south and Salaata in the west, which give the crater its name (Fig. 4.2.-1). The structure was part of the non-glaciated portion of northern Siberia during the LGM (Hubberten et al., 2004). Referring to works done by Pinchuk (1971) and Mikhailov et al. (1979) the inner part is filled with Quaternary sediments. This study aims to evaluate the potential of the crater deposits as environmental archives for Late Quaternary palaeoclimate and palaeoenvironmental reconstruction. To this end, the uppermost sediments of a lake (300 m in diameter, up to 4.5 m deep, Fig. 4.2.-2) close to the center of the crater and unconsolidated permafrost deposits in the valley floors were sampled for sedimentary and ground ice analysis.

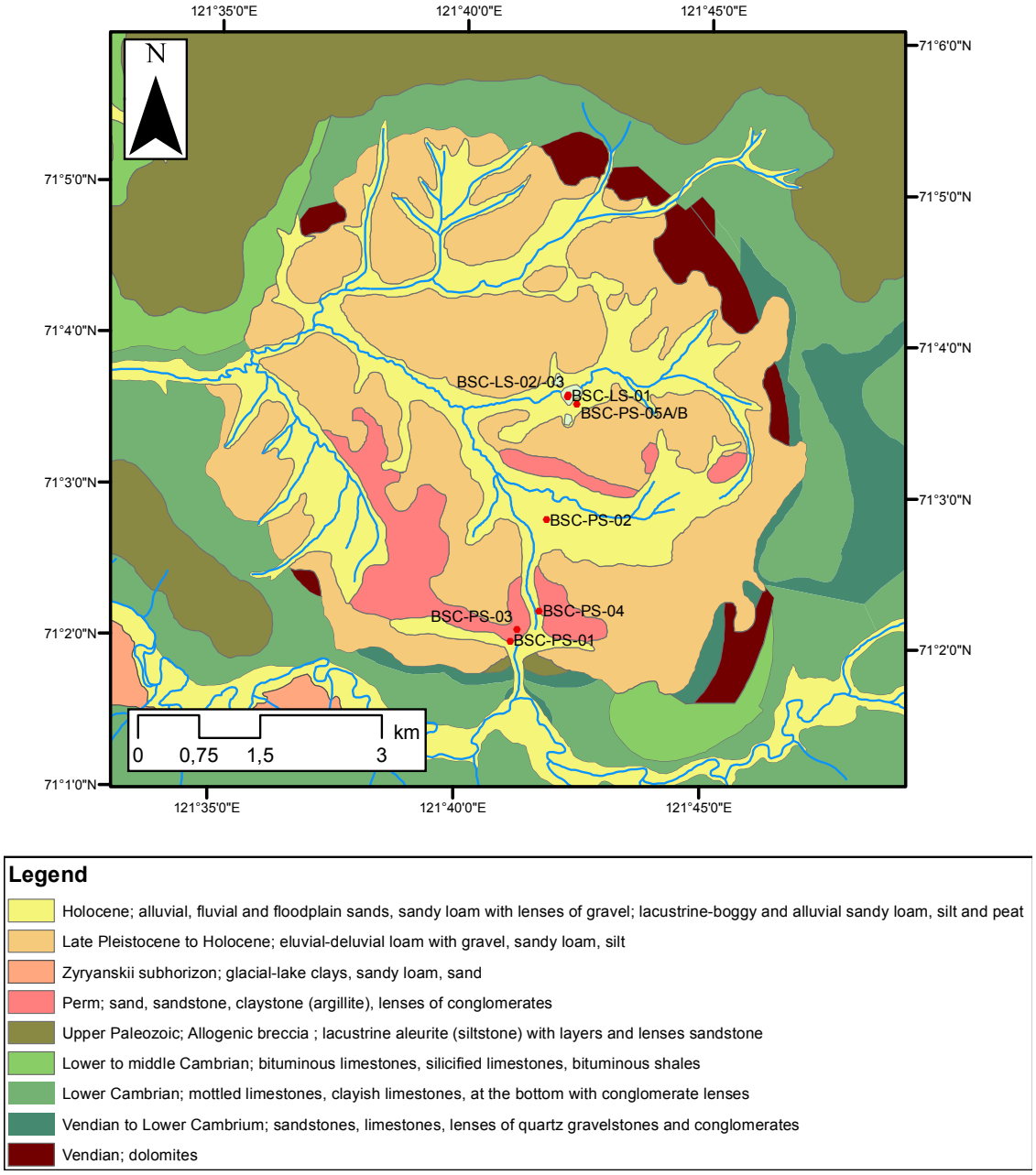

Figure 4.2.-1: Geological map of BSC and locations of lake and permafrost samples

Study Site

BSC is 8 km in diameter with a fairly gentle topographic relief and a difference of about 60 m from the highest (208 m a.s.l.) to the lowest point (140 m a.s.l.). The area is part of the forested tundra zone characterized by areas covered mainly with shrubs or grass and areas dominated by larix stands (Fig. 4.2.-2). The basin fill of the crater can be divided into three geomorphic levels (Fig. 4.2.-3); the low level (140-150 m a.s.l.) has polygonal frozen ground, partly boggy and waterlogged, and a drainage pattern with seasonal or periodically active streams. The intermediate level (150-165 m a.s.l.) has slopes and erosional remnants of ancient fluvial terraces. The high level (165-208 m a.s.l.) consists of bedrock building the crater rim.

Figure 4.2.-2: (Left) The outside of the southern crater rim, (middle) high center polygons that are widespread in the valley floors, (right) the studied lake in the center part of the crater (300 m in diameter, view from east to west)

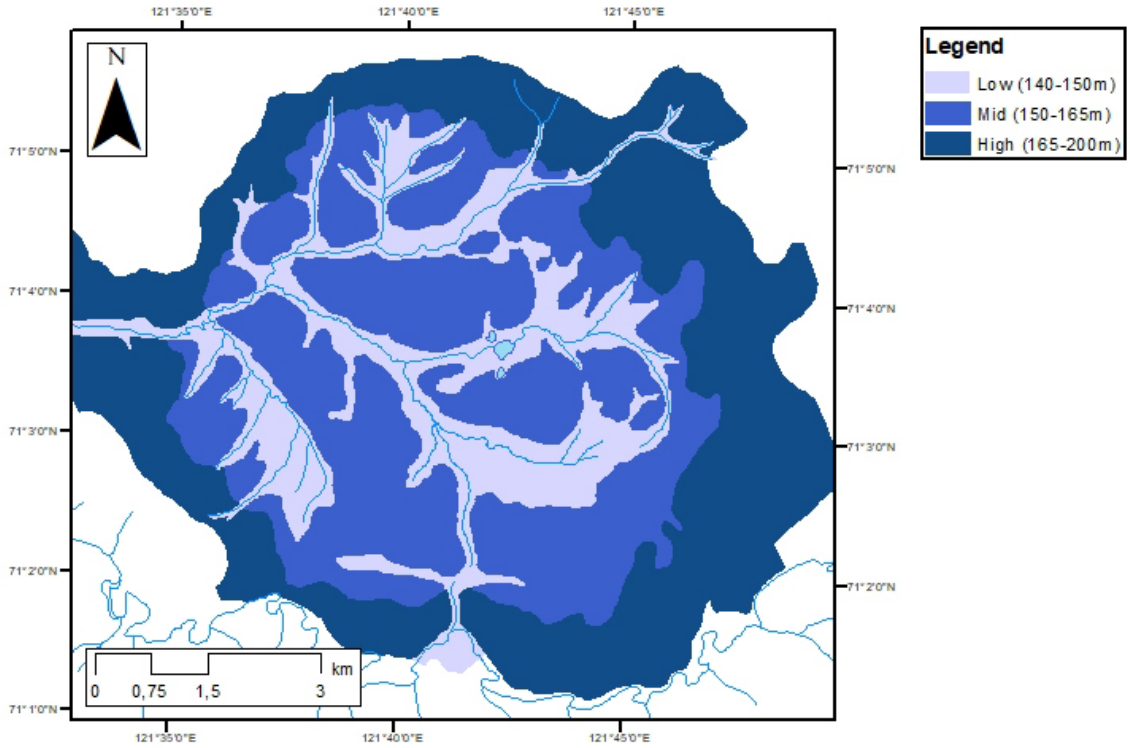

Figure 4.2.-3: Map showing the main geomorphic levels of BSC

During two weeks of fieldwork several techniques were applied for gathering field data and samples. For lake sediment sampling a gravity corer was used to extract three short cores from the central lake, four pits were dug to sample the active layer in the valley floor, and four short cores were drilled from permafrost using a 2-stroke engine to extract more samples from the frozen ground below (Fig. 4.2.-4). For information on bathymetry and sediment geometry in the lake we acquired ground-penetrating radar profiles (50 MHz and 200 MHz antennas), in addition. Lake water samples from different depths were taken for hydrochemical analyses. For comparison, also samples from the nearby Beenchime River and from bedload sediment were collected. Water and ground ice samples were measured for pH and electric conductivity already in the field.

Figure 4.2.-4: (Left) Field images from permafrost coring, (middle) digging pits in the active layer, (right) ground penetrating radar profiling in the lake

Preliminary results

Short lake cores

The upper sedimentary fill of the central lake was sampled three times from the deeper part of the lake (Fig. 4.2.-5). Two cores had a length of 0.22 m (BSC-LS-01 and -02, for location see Fig. 4.2.-1) and one with a length of 0.54 m (BSC-LS-03). BSC-LS-01 was already subsampled in the field into 10 sequent samples for later Pb/Cs dating. All cores have an organic-rich upper layer with low clastic grain content overlying a more compact layer with higher mineral portion of sandy silt. At the bottom of core BSC-LS-03 additionally a third lighter layer with increased sand content was observed.

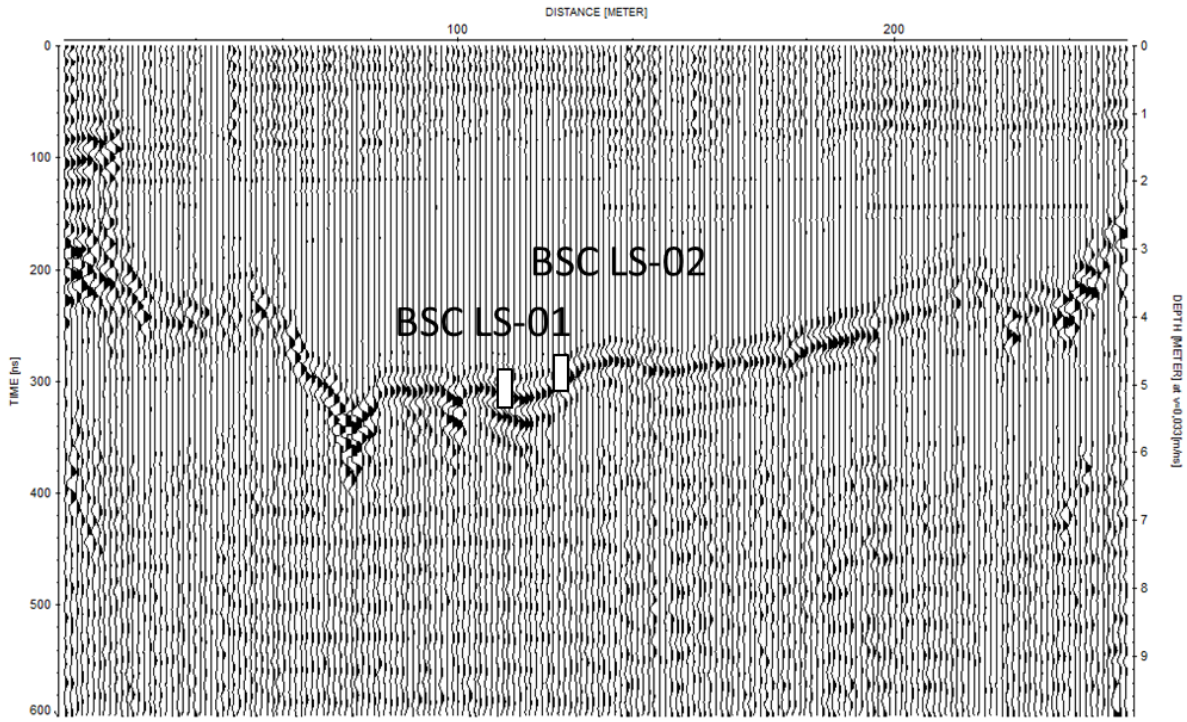

Figure 4.2.-5: A 50 MHz profile from W to E across the unnamed lake in the crater center. Approximate lake coring positions are given. Left axis is for travel time (ns), right axis denotes for depth (m) using a GPR velocity of 0.033 m/ns in water. GPR data has been filtered using a standard processing scheme (i.e. static correction, bandpass, background removal, gain function).

BSC-PS-01

The first pit into unfrozen deposits and coring of upper permafrost was done at the lower end of a sediment terrace of the mid-level (Fig. 4.2.-1). The active layer depth was 1.0 m and the borehole reached a total depth of 1.65 m below surface. The substrate is dominated by reddish fine sand in the upper 0.45 m while the lower part consists of greyish fine sand. At 1.3 to 1.4 m a clay layer appeared. The cryostructure is dominated by pore ice in the fine sand layers on top and massive (structure less) at the bottom of the record (Fig. 4.2.-6). The ground ice portion appears to increase downward.

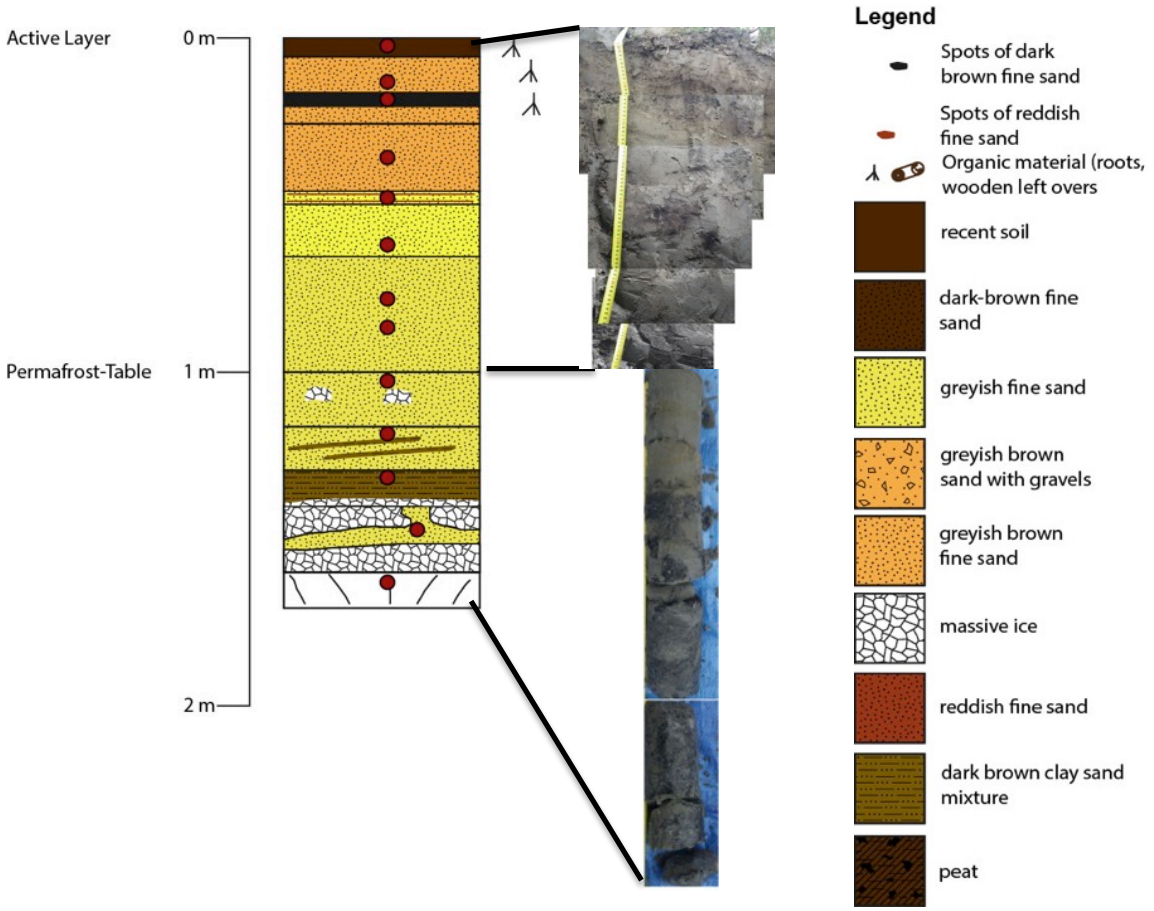

Figure 4.2.-6: Stratigraphic column of BSC-PS-01, red dots indicate spots where samples were taken

BSC-PS-02

The second column was extracted from a high-center polygon located in the central crater area (Fig. 4.2.-1). The active layer was 0.3 m thick and coring reached a total depth of 1.85 m below surface. The stratigraphy is dominated by peat containing centimeter scale organic remnants (i.e. twigs, roots). The ground ice fabric consists of pore ice with scattered ice crusts around organic macro remains. To the lower end of the record few ice lenses in the centimeter scale appear. At the bottom of the record pure ice was hit. Vertically aligned mm-scale air bubbles suggest that the ground ice belongs to the upper portion of an ice wedge (Fig. 4.2.-7).

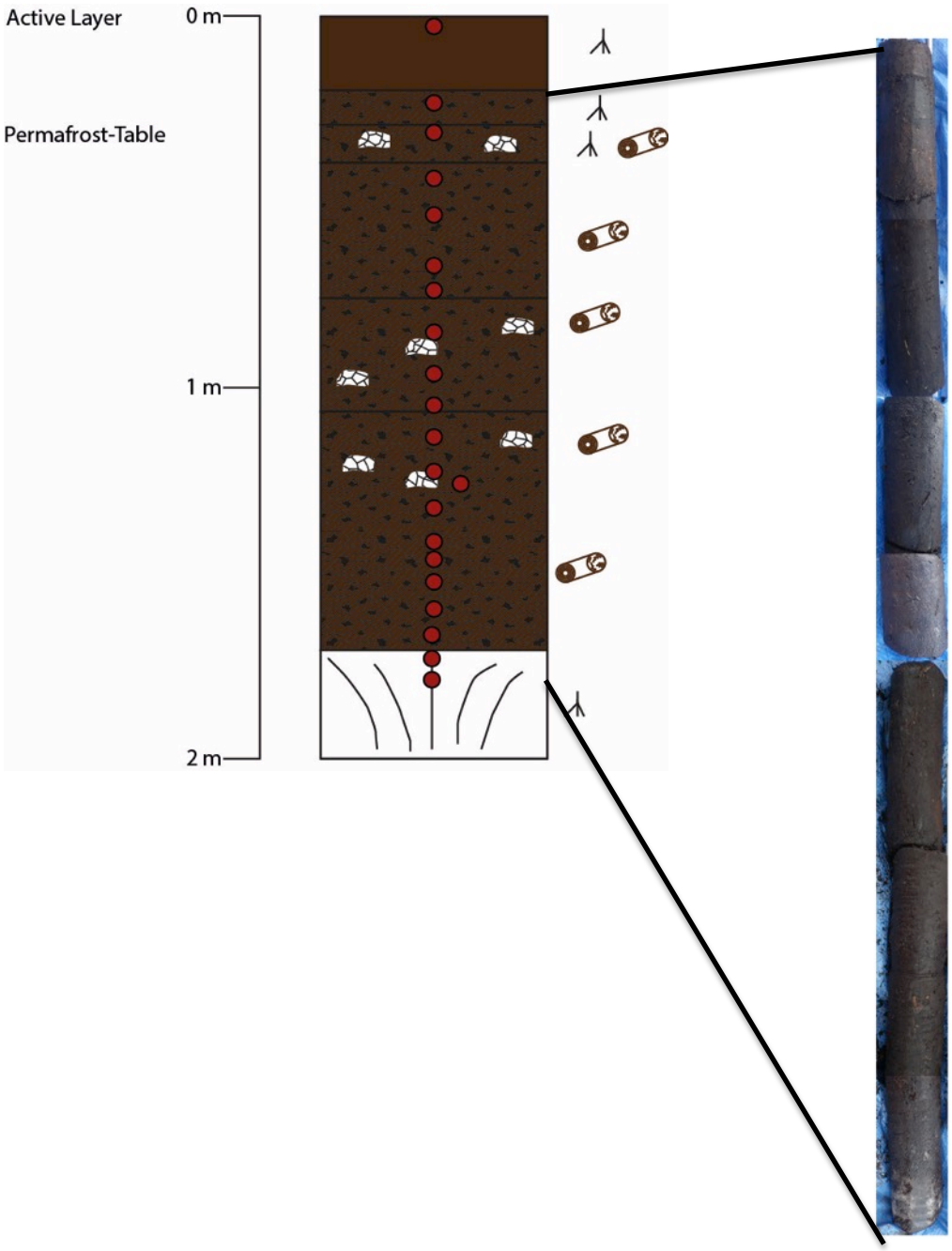

Figure 4.2.-7: Stratigraphic column of BSC-PS-02, red dots indicate spots where samples were taken (legend see Fig. 4.2.-6)

BSC-PS-03

The third column was extracted close to the first one. A pit was dug to the permafrost table at 1.1 m depth. The upper part down to 0.3 m is characterized by reddish fine sand on top of greyish sand containing pebbles and black organic rich layers. Below 0.5 m depth the material exhibits various iron oxide spots (Fig. 4.2.-8).

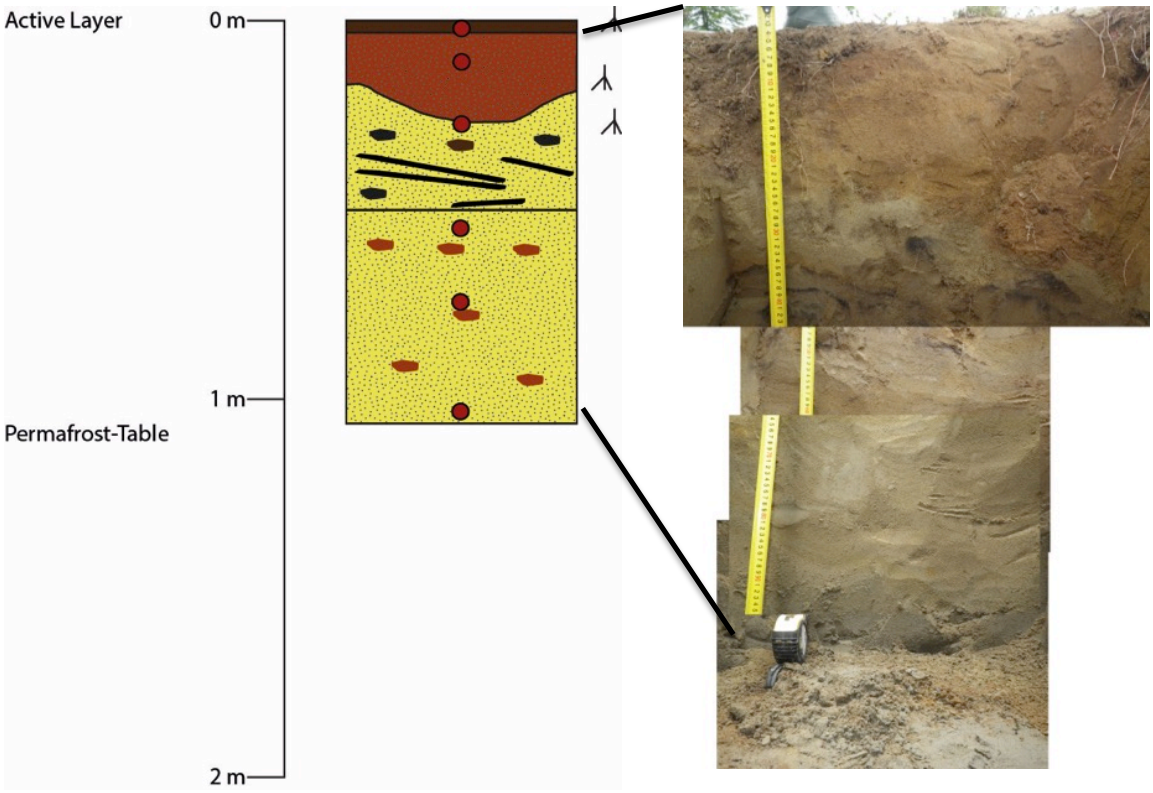

Figure 4.2.-8: Stratigraphic column of BSC-PS-03, red dots indicate spots where samples were taken (legend see Fig. 4.2.-6)

BSC-PS-04

Sample site BSC-PS-04 is located east of BSC-PS-03 in a distance of 350 m on the other side of the central boggy valley (Fig. 4.2.-1). The valley floor is covered by polygonal patterned ground. The pit was dug to 1.2 m depth to the permafrost table. The column is dominated by fine sand with some pebbles in the upper part and degraded rootlets. A tilted boundary is seen down to 0.8 m depth, where a sediment layer made of dark fine sand and containing detrital organics is separated from a reddish fine sandy layer at 1.0 to 1.2 m depth (Fig. 4.2.-9).

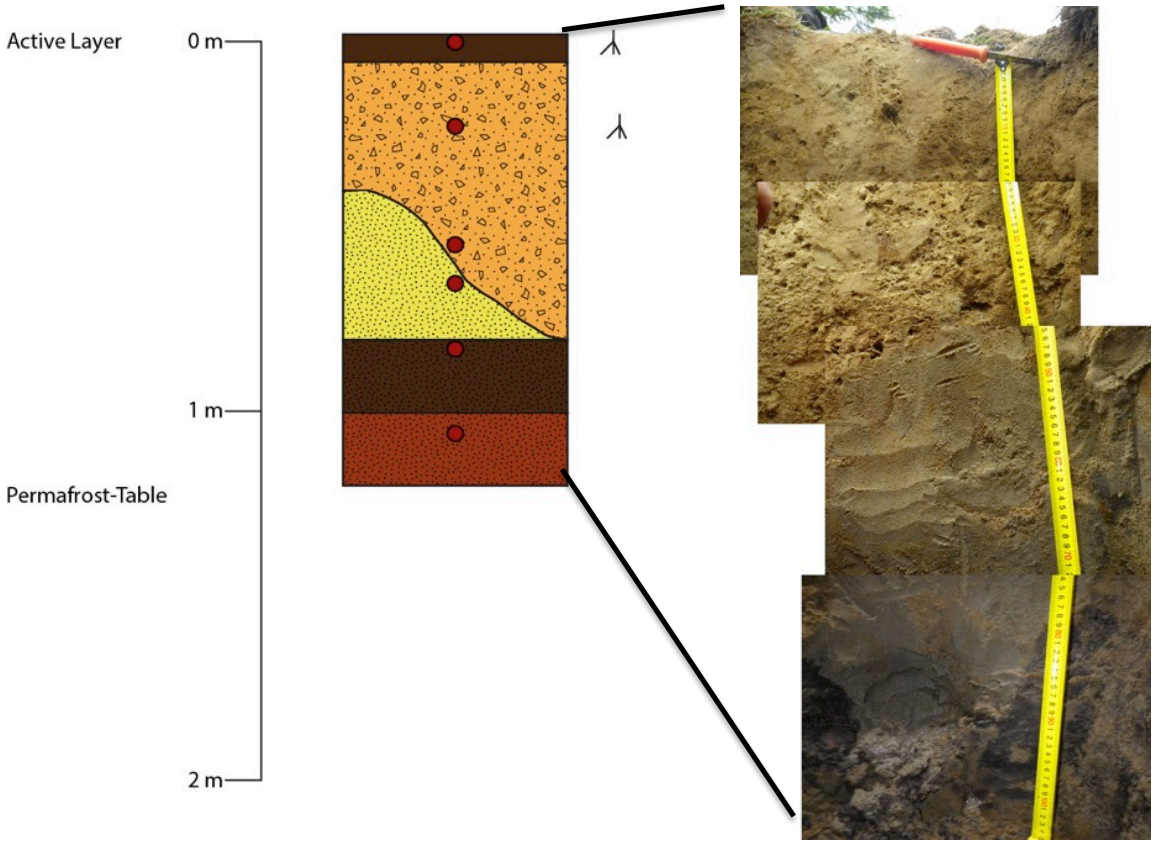

Figure 4.2.-9: Stratigraphic column of BSC-PS-04, red dots indicate spots where samples were taken (legend see Fig. 4.2.-6)

BSC-PS-05A

BSC-PS-05A was cored from the rim of a low centre polygon in a distance of 100 m south of the central lake (Fig. 4.2.-1). The total depth is 1.05 m. The active layer was 0.2 m thick. The column consists of peat, which contains lenticular ice lenses and a low sand content. Few cm-sized wooden remains are scattered in the record. Between 0.9 to 1.05 m depth massive ice presumably belonging to an ice wedge was encountered (Fig. 4.2.-10).

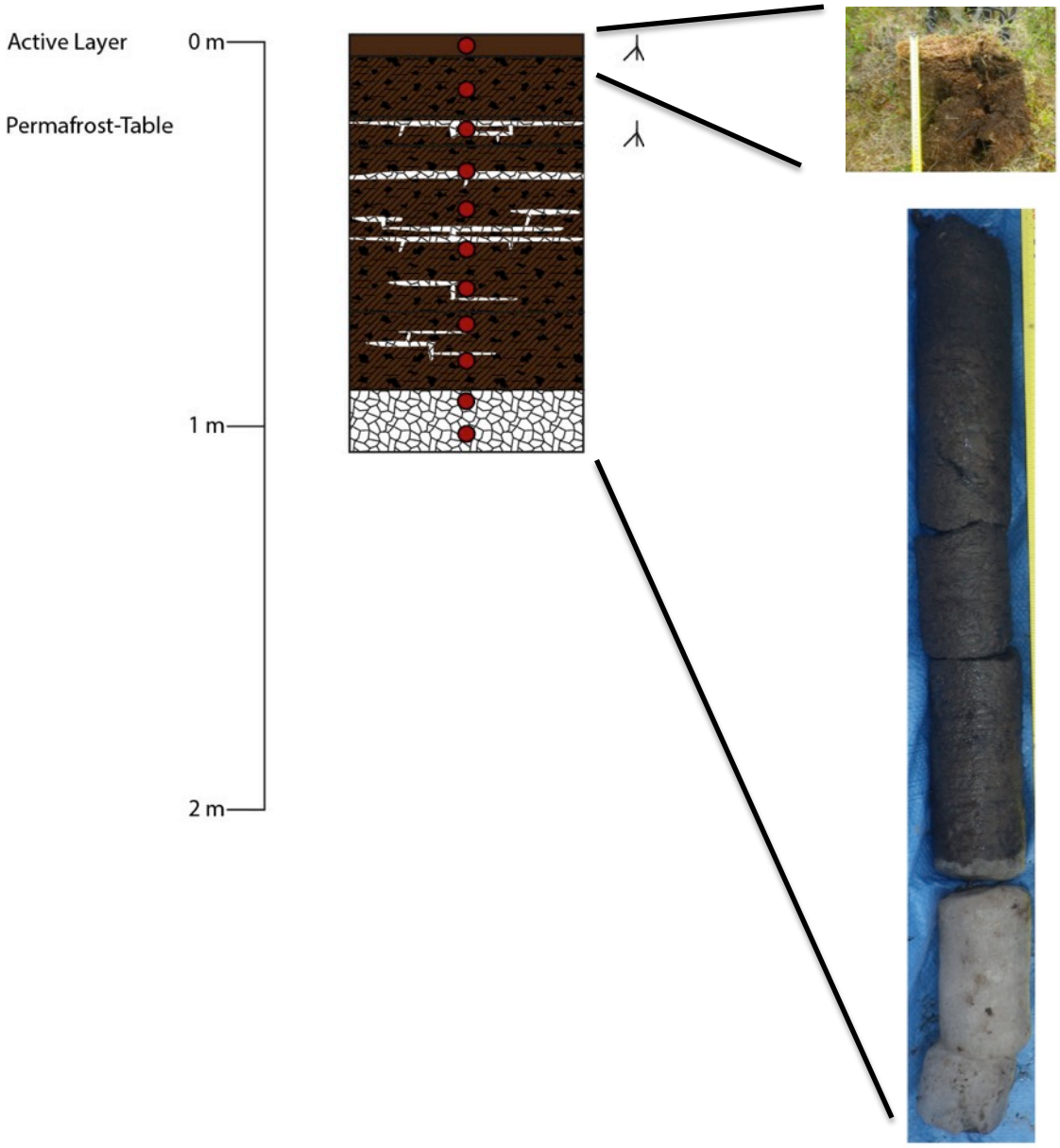

Figure 4.2.-10: Stratigraphic column of BSC-PS-05A, red dots indicate spots where samples were taken

BSC-PS-05B

BSC-PS-05B is a 0.8 m long record cored in a distance of 5 m west of BSC-PS-05A in a more central part of the low center polygon. The active layer was 0.4 m thick and is dominated by peat with low sediment content. In permafrost the peaty substrate has a

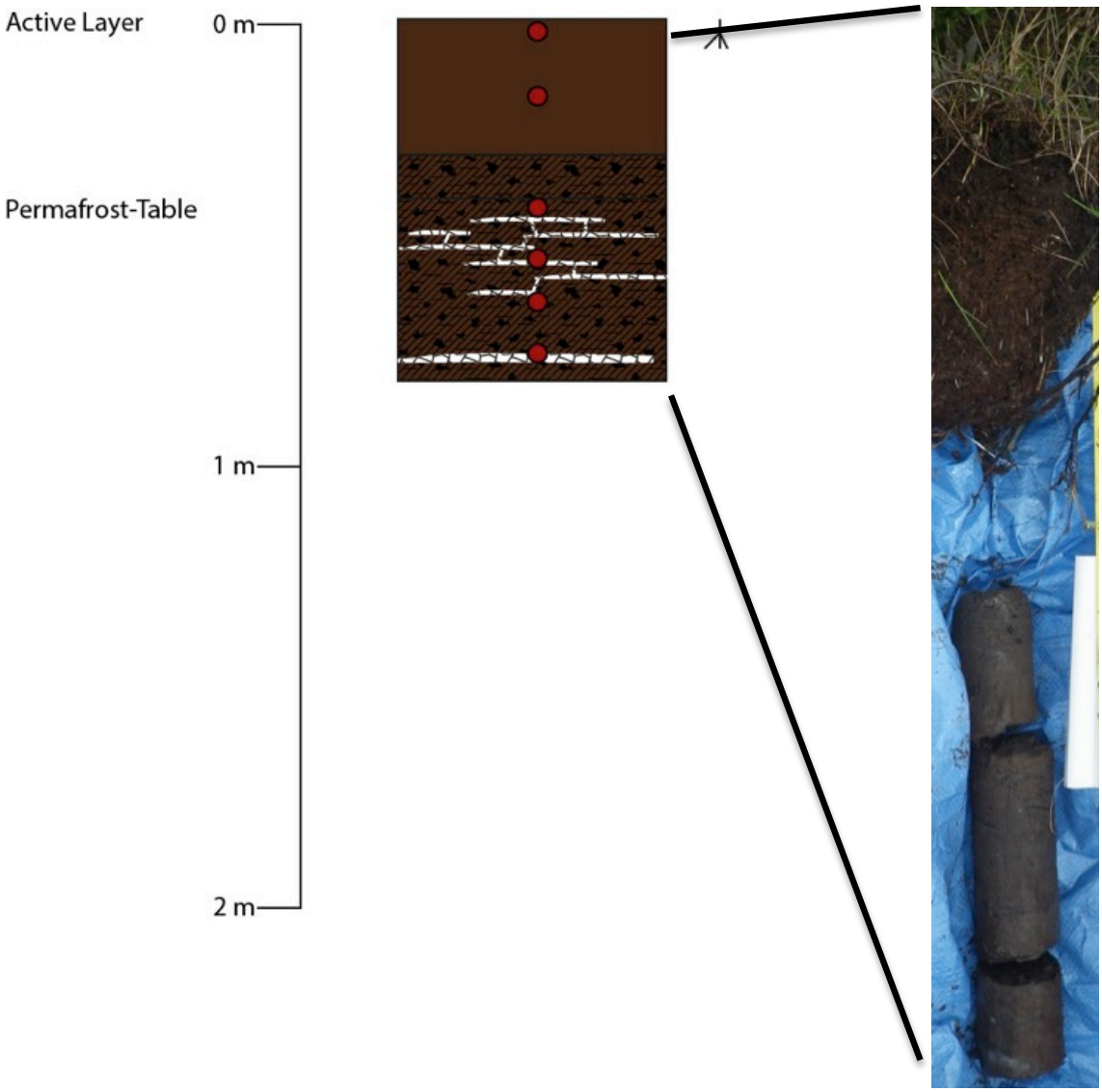

ground ice fabric characterized by pore ice and lenticular ice lenses (Fig. 4.2.-11).

Figure 4.2.-11: Stratigraphic column of BSC-PS-05B, red dots indicate spots where samples were taken

Water samples

Water samples of the central lake (BSC-W-01 to -03) and the Beenchime River (BSC-W-04) nearby were taken for hydrochemical analysis. Electrical conductivity and pH-values were measured in the field. Table 4.2.-1 lists that all samples have a slightly basic pH ranging between 7.2 and 7.9. The electrical conductivity of the river water is higher by a factor of two compared with the lake water.

Table 4.2.-1: Electrical conductivity and pH values of lake and river water from BSC.

Sample	depth_top [m]	depth_bottom [m]	elect. conductivity [µS/cm]	pH
BSC-W-01	4.2	3.5	161	7.17
BSC-W-02	2.3	3	159	7.38
BSC-W-03	0.3	1	159	7.41
BSC-W-04			325	7.85

Further work

Sediment analysis will include ^{14}C AMS and Pb/Cs dating, $\delta^{13}C$, TC (total carbon), TOC (total organic carbon), TN (total nitrogen), grain size determination, and magnetic susceptibility measurements. The ground ice will be measured for water stable isotope composition (D/H, $^{18}O/^{16}O$) (Table 4.2.-2). A list of water and sediment samples is included in the Appendix (Table A 4.2.-1).

Table 4.2.-2: Amount of samples and planned analyses

Sample type	Samples	Number of Subsamples	Planned Analyses
Sediment	92	BSC-PS, BSC-LS, BSC-EG, BSC-FS	Grain size analyzis, ^{14}C AMS and Pb/Cs dating, TC, TOC, TN, $\delta^{13}C$, magnetic susceptibility
Water	27	BSC-W	δD, $\delta^{18}O$

4.3. Placer studies using precious metals and heavy mineral assemblages in Beenchime Salaatinsky Crater

Anatoly Zhuravlev [1], Nikolai Oparin [1], Maria Oshchepkova [1], Andrei Prokopiev [1]

[1] Laboratory of Geodynamics and Regional Geology, Diamond and Precious Metal Geology Institute, Siberian Branch Russian Academy of Sciences, Yakutsk, Russia

Background information

In geological terms the BSC depression is located in the field of Cambrian rocks (Fig. 4.3.-1). The most ancient geologic formations in the area are sediments of the Kessyusinsky (siltstones, sandstones, dolomites, conglomerates) and Erkeketsky (argillaceous limestone) formations of the lower Cambrian. In the watershed area variegated bituminous, silicified limestones and shales of the Kuonamskoy formation are exposed. Cambrian layers to the north and west of the structure are covered with poorly lithified Permian sandstone, which is interbedded with siltstones and conglomerates lenses.

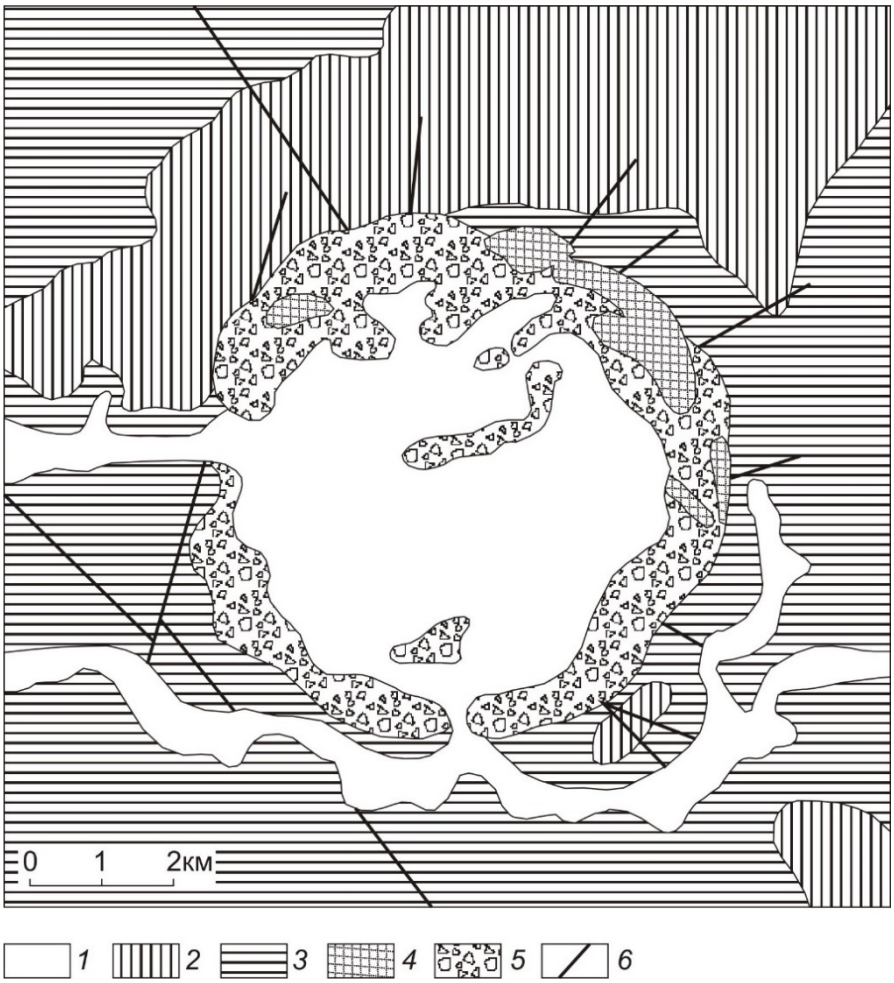

Figure 4.3.-1: Geological map of Beenchime-Salaatinsky depression. 1 – alluvial Quaternary sediments, 2 – bituminous limestones, silicified limestones, shales, 3 - argillaceous limestones Erkeketsky formation, 4 - siltstones, sandstones, dolomites, conglomerates of the Kessyusinsky formation, 5 – breccias, 6 – faults (Mikhailov et al., 1979, modified)

For the first time Pinchuk (1971) discovered the BSC depression as an independent structure using airborne photogeomorphological analysis data. A tectonomagmatic (kimberlite) nature of the depression was suggested similar to kimberlite pipes, which are found further south in Central Yakutia. In contrast, the material collected by Mikhailov et al. (1979), indicates that the structure is an astrobleme. Some limestone specimens were interpreted to show shatter-cone surfaces, the only distinctive shock-deformation feature that can be seen macroscopically. Between 1985 and 1990 «Aerogeology» (1990) carried out a series of studies in this depression, which included mapping, multiple exposure sampling and various bedrock drill cores (<65 m length at maximum). The results suggested a Late Paleozoic age of the structure; the bedrock stratigraphy consists of Cambrian formations whereas the basin filling has prominent Permian formations that are not related to the crater structure. However, high-pressured phases of silica (coesite and stishovite) and melting traces of minerals, which would be the most reliable evidence of an impact origin of the depression, were not detected. Therefore, the data obtained by PGE «Aerogeology» are not sufficient to define this structure as astrobleme.

Methods

For an improved genetic interpretation of the BSC structure based on mineral analysis we took samples from nearby river sediments and bedrock outcrops. This may allow detecting high-pressure minerals showing the impact origin of the depression. A total of 10 sediment samples and 54 rock specimens have been collected (Table A 4.2.-1 in the Appendix).

We sampled fluvial sediments (i) from the Beenchime-Salaata River tangentially flowing south of the basin, (ii) from the tributary flowing into Beenchime-Salaata River southeast of the basin and, (iii) and from the outlet exiting BSC to the west (Fig. 4.1.-2).

Samples have been obtained by sieving the fluvial bedload down to grain sizes of <2 mm. Subsequently the heavy mineral fraction has been separated using a wooden cradle, where the heavy fraction accumulated in the central furrow after repeated manual washing (Fig. 4.3.-2). A typical heavy fraction sample had a weight of 0.5 kg. For laboratory studies, we look at several fractions <2 mm. We will divide all material with sieves down to size fractions of 2-1 mm; 1-0.5 mm; -0.5-0.25 mm; 0.25-0.16 mm; and <0.16 mm. Based on experience we will focus on the fractions 1-0.5 mm; 0.5-0.25 mm; and 0.25-0.16 mm. Other fractions we will examine too, but commonly they rarely contain prominent heavy minerals.

Rock samples have been collected from outcrops forming the crater rim in the south and southwest to west. Petrographic analysis of the mineral composition will be based on thin section microscopy and microprobe analyses. In the laboratory, it is planned to include a diagnostic survey of minerals using (i) Raman spectroscopy and (ii) X-ray studies of rock samples in order to determine their mineral composition.

Figure 4.3.-2: Sieving and enriching the heavy mineral fraction from river sediment

4.4. Bedrock studies in Beenchime Salaatinskaya Crater

Ulli Raschke [1]

[1] Museum für Naturkunde, Leibniz Institute for Evolution and Biodiversity Science, Berlin, Germany

Objectives

- Investigation of the possible impact origin of this crater structure.
- Age determination of the crater.
- Should an impact origin be confirmed, the attempt of reconstructing the emplacement of impact rocks and crater modification will be made.

Methods

In the field:

- Sampling of possible impact breccia (melt-bearing or suevite-like) within the crater and of country rocks along the crater rim and in its vicinity as well as at any exposure within the central part of the structure.
- Search for possible shatter cones at the SE crater rim (according to Mikhailov et al., 1979).
- Mapping of geological structures (faults, bedding, etc.) in the field.

Post-expedition at the Museum für Naturkunde:

- Petrographic description of all samples.
- Petrographic investigation for possible shock metamorphic effects.
- Geochemical study of selected samples by XRF analysis.
- Development of a structural model of the basin and interpretation of its tectonic implications.

Preliminary results

Our work focused on exposure studies in the southern, south-western and eastern crater rim. The distribution of bedrock samples is given in Fig. 4.1.-2 their locations are listed in the Appendix (Table A 4.4.-1).

The lithological classification and study of shock metamorphosed effects is based on 15 samples with a mass of <1 kg. The samples belong mainly to Cambrian or Precambrian limestone from the southern and eastern crater rim (Fig. 4.4.-1). Furthermore, mixed layers of sandstone and limestone or sandstone containing a calcareous matrix were studied at the inner part of the southern crater rim (Fig. 4.4.-2). In addition, Precambrian dolomites were found at the south-eastern crater rim breccia of carbonate and sandstone at the eastern rim (Fig. 4.4.-3). So far polarized light microscopy has not shown any clear indication for impact produced shock metamorphism. Nevertheless, the breccia consists of a fine-grained groundmass (possible recrystallized melt) and phenocrysts or clasts of

limestone, sandstone, and dolomite. In one case immiscibility melt mixture - probably silica melt - with drops or inclusions of carbonate was found.

Figure 4.4.-1: Carbonates cliffs outcropping at Beenchime Salaata River, southern crater rim (crater outside)

Figure 4.4.-2: Brecciated calcareous sandstone southern crater wall (crater inside)

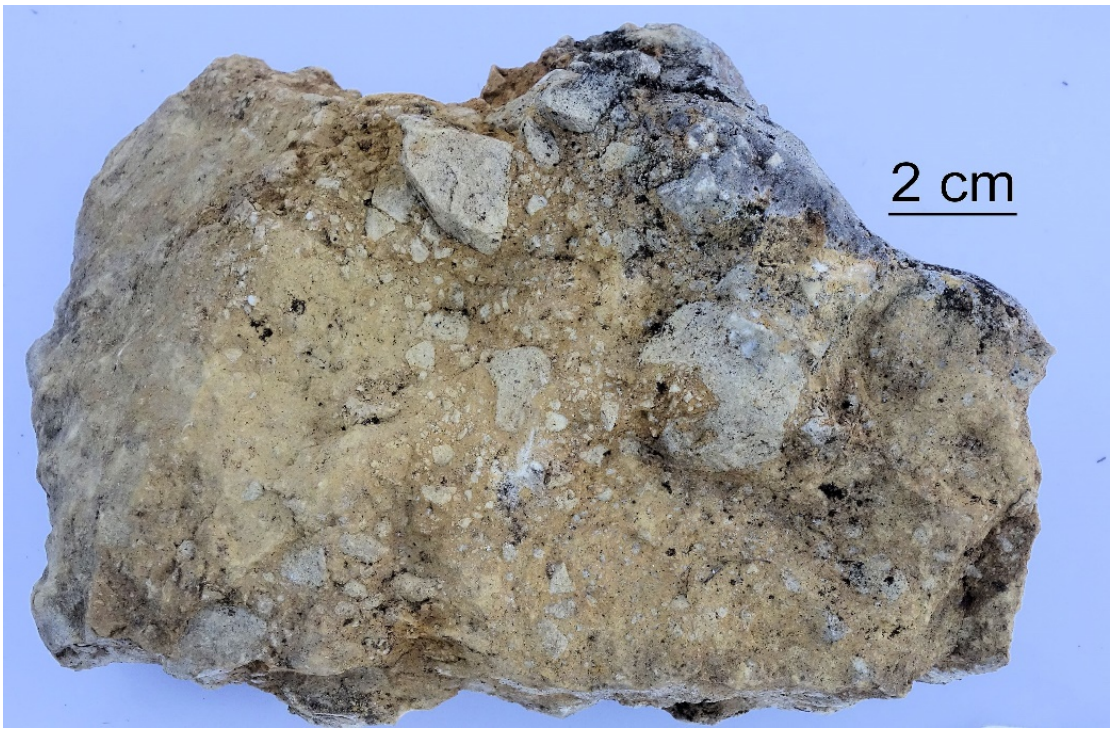

Figure 4.4.-3: Polymict breccia with clasts of limestone and sandstone

Outlook

Selected individual rock samples could be analyzed already concerning rock types and evidences of possible impact origin. This pilot study will be accomplished when all rock and sediment samples are analyzed. The investigation of shock diagnostic features has to be completed. Especially, the samples of the autogenic breccia have a potential for containing shock metamorphosed minerals and lithic clasts. Additional studies of the different kinds of matrix (obviously melt) is mandatory. A further step is the creation of a modern, digital geological map, including DEM (Digital Elevation Model). Another question is the age of the crater. Here we plan to determine the $^{40}Ar/^{39}Ar$ ratio or a U/Pb ratio.

References

Aerogeology, Ministry of Geology USSR united production geology (ed.) (1990) Cosmic-air-geological expedition #3: Geological map of area „Astroproblem“. Geological interpretation of air photography and cosmic photography materials with additional inspection works for searching meaningfully interpreted structures and draw, geological-mineralogical map w/ scale 1:200.000 in area between river Bur and Olenek. Attachment 26, 1:30800. Cosmic-air-geological expedition #3; Ostashkin, I.M. (head), Kareva, E.V., Marchenko, N.K.

Earth Impact Database (2016) http://www.passc.net/EarthImpactDatabase/AsiaRussia. html (March 2016).

Grieve, R.A. (1987) Terrestrial impact structures, Annual Review of Earth and Planetary Sciences, 15, 245-270.

Hubberten, H.-W., Andreev, A.A., Astakhov, V.I., Demidov, I., Dowdeswell, J.A., Henriksen, M., Hjort, C., Houmark-Nielsen, M., Jakobsson, M., Kuzmina, S., Larsen, E., Lunkka, J.P., Lysa, A., Mangerud, J., Möller, P., Saarnisto, M., Schirrmeister, L., Sher, A.V, Siegert, C., Siegert, M.J., and Svendsen, J.I. (2004) The periglacial climate and environment in northern Eurasia during the Last Glaciation. Quaternary Science Reviews 23, 1333-1357. doi:10.1016/j.quascirev.2003.12.012.

Masaitis, L.V. (1999) Impact structures of northeastern Eurasia: The territories of Russia and adjacent countries. Meteoritics & Planetary Science 34, 691-711, doi: 10.1111/j.1945-5100.1999.tb01381.x

Mikhailov, M.V., Shurygin, A.G., and Khar'yuzov, L.S. (1979) The Beyenchime Salaata meteorite crater, Doklady Akademii Nauk SSSR, 245, 76-78 [in Russian].

Moon, H.K., Min, B.H., Fletcher, A.B., Kim, B.G., Han, W., Chun, M.Y., and Lee, W.B. (2001) Terrestrial impact cratering chronology: a preliminary analysis, Journal of Astronomy and Space Sciences 18,191-208.

Pinchuk, L.Y. (1971) Morphology and genesis of Beenchime Salaatinsky depression // Kimberlite volcanism and prospects of primary diamond content of the north-eastern Siberian platform, Proceedings Arctic Geology Research Institute, Leningrad, 123-126 [in Russian].

5. KEPERVEEM

5.1. Past and present vegetation dynamics at the most eastern extension of the Siberian boreal treeline

Stefan Kruse [1], Kathleen Stoof-Leichsenring [1]

[1] Alfred Wegener Institute Helmholtz Center for Polar and Marine Research, Potsdam, Germany

Participants

Russian: Nikolai Kirillin, Ivan Kochesgin, Luidmila Pestryakova (expedition leader), Alekesey Pestryakov, Stepan Timnenkov, Lena Uschnitskaja and Evgeni Zakharov

German: Esther Hemmens, Ulrike Herzschuh (expedition leader), Stefan Kruse, Kathleen Stoof-Leichsenring, Ellen Schnabel, Julius Schröder and Daronja Trense

Fieldwork period

June 28 to July 26, 2016, Keperveem, Chukotka, Russia

Objectives

Temperatures in the Arctic are warming (ACIA, 2005), which in consequence releases tree growth from the limiting warmth deficit at the arctic treeline. MacDonald et al. (2008) pointed out that the mean temperature of July and the length of the growing season are the most important factors determining the position of the treeline. The current increase in temperatures is most probably promoting tree growth and will lead to northward shifts in forest distribution (ACIA, 2005). This is accompanied by the decline of vast tundra areas, and can putatively reduce albedo effects, leading to a positive feedback between vegetation and climate (Bonan, 2008). The tundra-taiga ecotone in Siberia is formed mono-dominantly by stands of *Larix* (larch), with the species *Larix gmelinii* (Rupr.) Kuzen. distributed in Central Siberia and east of Lena L. cajanderi Mayr. (Abaimov, 2010; Kajimoto et al., 2007). The projected climate changes will strongly affect the distribution and population dynamics of larch tree.

Temporal and spatial tree stand dynamics, using methods of dendrochronology and forest ecology are analyzed to understand how tree stands responded towards past climate changes and to optimize projections of future changes. A genetic assessment of treeline populations will be used to analyze the reproductive success and assumed patterns of past and current treeline movements.

Documented changes in vegetation across the Siberian treeline ecotone can be considered as a proxy for related changing variables, such as temperature and lake-water chemistry (Herzschuh et al. 2013), which in turn can affect microbial aquatic vegetation (like algae) in the embedded lakes.

In order to reconstruct past dynamics in terrestrial and aquatic vegetation we sampled sediment cores (short and long cores) from glacial and thermo karst lakes across the treeline ecotone. We will utilize pollen and sedimentary ancient DNA (sedaDNA) analyses for taxonomic identification of past vegetational communities and its changes across Holocene time scales. The reconstruction of terrestrial vegetation with pollen analyses will recover regional changes in plant communities, whereas as local signals of vegetation change will be investigated using sedaDNA. Reconstructions of aquatic communities will contribute to the understanding of lake environmental changes and related evolutionary imprints on environmentally sensitive algae, like diatoms.

Generally, this expedition complements a west–east transect across the Siberian tundra-taiga ecotone, in which similar regions has been sampled in previous expeditions in 2011 & 2013 (below Taimyr Peninsula), 2012 (along the Kolyma river), 2014 (at Buor Khaya Peninsula).

Methods

In the vicinity of four locations with the field names 16-KP-01 to 16-KP-04, sampling of lakes and vegetation were performed (Fig. 5.1.-1).

1. Vegetation analyses

In total 58 locations for vegetation surveys were visited (Table A 5.1.-1 in the Appendix). We placed them into areas with different larch tree cover: from treeless tundra locations (V08, Fig. 5.1.-4) to open larch forests at slopes (V04, Fig. 5.1.-3) and in lowlands (V12, Fig. 5.1.-5) covering different tree densities on various slopes and aspects. Beforehand the locations were chosen to range different trends in an initial LANDSAT trend analysis 2000-2015 (data not shown). Visited points were between 100 to 900 above sea level with a slope of 0 to 14 m over 10 m and roughly twice as many had an aspect towards south (Fig. 5.1.-2).

At all locations, we recorded vegetation cover at five 2x2 m plots, one at the centre and one 7.5 m apart from the centre in each of the four cardinal points. All major plants groups, lichen and moss cover, deadwood and open soil were considered. At each of these plots a soil profile was dug at the centre and a surface sample from the topsoil was sampled standardized with a hand sampling cylinder of 50 cm^2. Additionally, the thaw depth of the active layer above the permafrost table was probed with a metal rod device.

Vegetation plots

At 52 locations (Table A 5.1.-1 in the Appendix, "plot") we estimated the larch tree stem density by counting trees >40 cm and recording the heights of each tree within a radius of 15 m from the centre. Additionally to *Larix* Mill. trees, the four occurring shrubby plant groups *Pinus* L., *Alnus* Mill. and *Salix* L. were estimated in their cover and their maximum height as well (Table A 5.1. in the Appendix). At two additional points (Table A 5.1. in the Appendix, "grid") were trees recently recruited heavily after a fire we had to adjust our sampling protocol and we recorded every tree at two 5x5 m plots.

From each of these visited plots we surveyed 10 trees more intensively (see protocol below), five >2 m and five <2 m if possible, or else the closest individuals to the plot and we searched for larch seedlings (<40 cm) at each vegetation cover survey area and recorded their individual properties and took genetic samples of up to ten individuals per 2x2 m area.

Larch tree stands

At four locations (Table A 5.1.-1 in the Appendix, "intensive grid") we laid out a grid over at least 20x20 m of a tree stand with 2 m sub-grids. We extended the area in 2 m rings to ensure we have at least 50 individuals >2 m in each plot thus we had to increase the area to maximum 36x36 m (Table A 5.1.-1 in the Appendix). Inside this grid, we surveyed every tree >40 cm (see protocol below) and additionally individuals <40 cm were recorded only at the centre 12x12 m.

Larch tree sampling

For each surveyed tree we recorded the position (with a GPS device at the plots or the exact position in the laid out grid) and individual properties of every tree exceeding 40 cm: height, basal diameter and diameter at breast height (i.e. at a height of 130 cm), crown diameter (in two directions), start of crown, number of cones (binned to three categories: this years', old and degraded ones) and we assessed the vitality state of each tree in 5 categories ('--' highly damaged, less than 10% living branches to '++' very dense crown structure and vital).
For dendrochronological analyses we took from each plot tree cores or discs at basal and breast height of a maximum of 10 trees >2 m which were surveyed at plots and additionally 10 between 0.4 and 2 m, and further 10 <0.4 m, where the latter individuals were taken as a whole. Cones of the same individuals and, if available, 10 of each separated cone class were sampled for a more detailed seed analysis in the lab. Finally, for genetic analyses we took 4-5 short shoots of needles of the same trees and dried them in the field on silica gel.

2. Lake analyses

In the vicinity of each of the four visited field sites 22 lakes were sampled (Table A 5.1.-2 in the Appendix) for lake water, surface sediment and lake sediment cores. We sampled three glacial lakes (Fig. 5.1.-6) and additional 19 thermo karst lakes (Fig. 5.1.-7). Basic physical and chemical water measurements (like water depth, Secchi depth, pH, conductivity, temperature) were performed at the lake. Further, water samples were sub-sampled and prepared at the camp for subsequent laboratory analyses at AWI. Surface sediments from glacial lakes were sampled in a transect across the lake, whereas small thermo karst lakes were sampled once at the maximum water depth. All surface samples were taken with a sediment grabber. Similarly, several short sediment cores and long cores were taken in the glacial lakes, whereas only two cores at the same position were taken in the thermo karst lakes. Sediment core sampling was performed with a UWITEC gravity coring system. Sediment cores for chronology surveys were sub-sampled in the field in 0.5 cm slices and stored in plastic bags. The other cores were stored dark and cold and will be sampled at AWI laboratories later on. In total, 27 m of cored material was sampled.

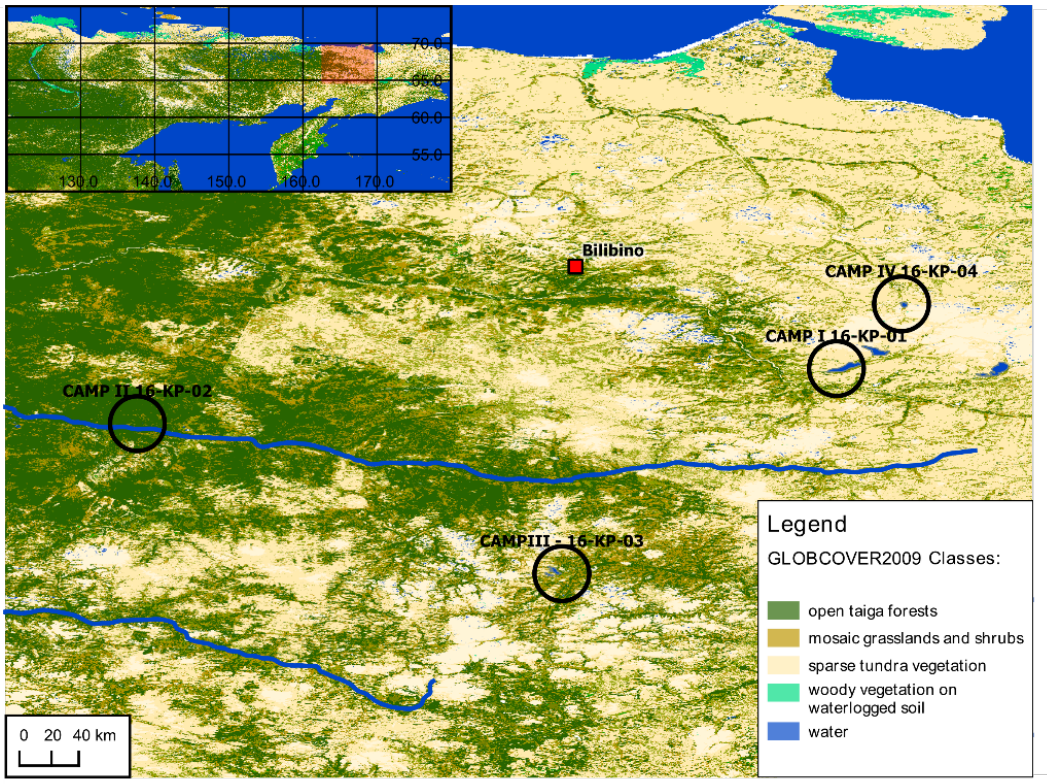

Figure 5.1.-1: Overview map of the expedition sites in Chukotka, north-east Siberia; GLOBCOVER2009 data from Bontemps et al. (2011)

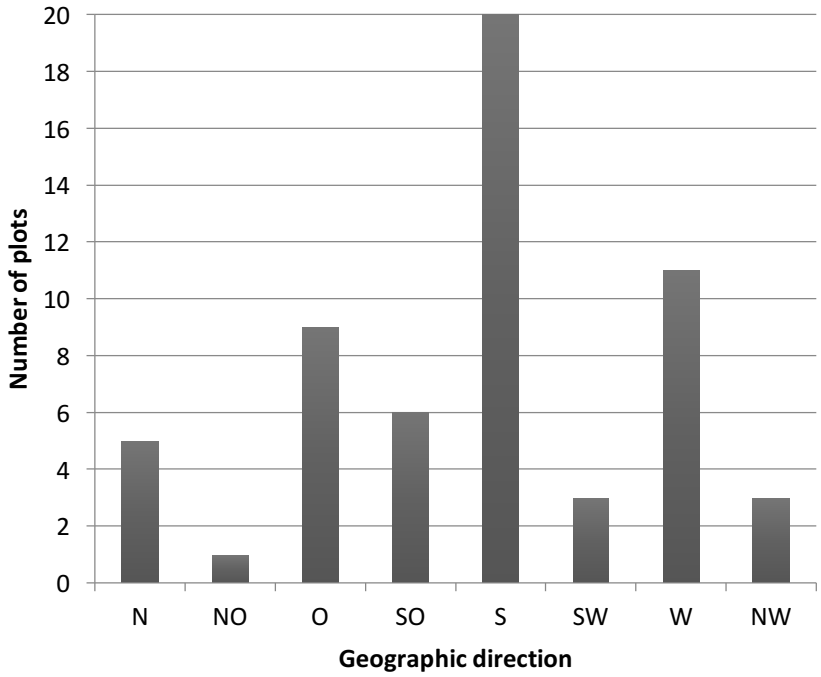

Figure 5.1.-2: Geographic directions of slopes of 58 visited field locations for vegetation analyses

Figure 5.1.-3: 5.7.2016 V04 360°x180° Picture taken from plot centre. The shadow in the lower left part belongs to the tripod used to take the pictures. Picture taken by S. Kruse.

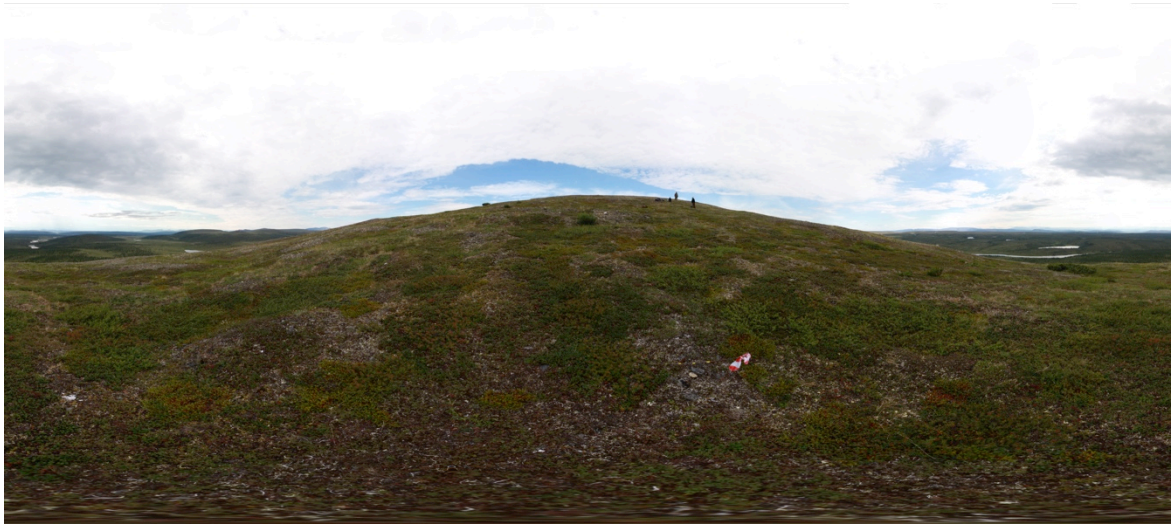

Figure 5.1.-4: 6.7.2016 V08 360°x180° Picture taken from plot centre; picture taken by S. Kruse

Figure 5.1.-5: 7.7.2016 V12 360°x180° Picture taken from plot centre; picture taken by S. Kruse

Figure 5.1.-6: Typical mountainous thermo karst ponds; picture taken by K. Stoof-Leichsenring

Figure 5.1.-7: Glacial lake Nutenvut (Camp 3); picture taken by K. Stoof-Leichsenring

References

Abaimov, A. P. (2010) Geographical Distribution and Genetics of Siberian Larch Species. In Osawa, A., Zyryanova, O. A., Matsuura, Y., Kajimoto, T., and Wein, R. W. (Eds.). (2010) Permafrost ecosystems: Siberian larch forests (Vol. 209). Springer Science & Business Media.

ACIA (2005) Arctic Climate Impact Assessment. Cambridge University Press, Cambridge, United Kingdom and New York, NY, USA. http://www.acia.uaf.edu.

Bonan, G.B. (2008) Forests and Climate Change: Forcings, Feedbacks, and the Climate Benefits of Forests. Science 320 (5882) (Juni 13): 1444–1449. doi:10.1126/science.1155121.

Bontemps, S., Defourny, P., Bogaert, E.V., Arino, O., Kalogirou, V., and Perez, J.R. (2011) GLOBCOVER 2009-Products description and validation report.

Herzschuh, U. et al. (2013) Siberian larch forests and the ion content of thaw lakes form a geochemically functional entity. Nature Communications 4, 2408.

Kajimoto T., Osawa, O., Matsuura, Y., Abaimov A.P., Zyryanova, O.A., Kondo, K., Tokuchi, N., and Hirobe M. (2007) Individual-based measurement and analysis of root system development: case studies for Larix gmelinii trees growing on the permafrost region in Siberia. Journal of Forest Research CN - 0000 12 (2) (Mai 14): 103–112. doi:10.1007/s10310-006-0259-y.

6. CENTRAL YAKUTIA

6.1. Short term climate variability in extreme continental environments of northeastern Siberia - Expedition Yakutia 2016

Boris K. Biskaborn [1], Yurii Kublitskii [2], Sarah Mosser [1], Liudmila Syrykh [2], Eugeniy Zakharov [3], Lena Ushnietskaya [3], Bernhard Diekmann [1]

[1] Alfred Wegener Institute Helmholtz Center for Polar and Marine Research, Potsdam, Germany

[2] Herzen State Pedagogical University, St. Petersburg, Russia

[3] North-Eastern Federal University, Yakutsk, Russia

Fieldwork period August 27 to September 9 2016, Yakutsk - Vilyusky District (Lake Satagay and surroundings) - Yakutsk

Introduction and Objectives

AWI Expeditions in the SibLake Programme at the AWI to Northeastern Siberia, outside of the Lena Delta, are based on long-term cooperations with Russian partners, i.e. the Northeastern Federal University Yakutsk (NEFU) and the Herzen State Pedagogical University in St. Petersburg. This initiative is related to the scientific programme of the AWI in PACES II, Topic 3.1: Circumpolar climate variability and global teleconnections at seasonal to orbital time scales. Given the high spatial variability of environmental features over time, it is necessary to collect data from multiple representative study areas, especially in the vast Russian permafrost regions, where only few data exist available to the community in earth and environmental science.

Hence, scientists in the AWI Periglacial Dynamics Section conducted numerous field trips over the last years to create a set of samples and data that enables new insights into ecological (Herzschuh et al., 2013) and climatic dynamics (e.g. Biskaborn et al., 2012, 2013, 2016) in “unexplored” areas of the Russian Arctic. The overall aim is to pinpoint connections of Arctic to sub-Arctic palaeoenvironmental changes between the periglacial and highly continental landmasses of Yakutia and the maritime-influenced setting of Kamchatka.

The expedition “Yakutia 2016” aimed to gain further insights in the Siberian environmental history. Therefor we returned to Lake Satagay in Central Yakutia whose sediments have been analysed before in a pilot study by Popp (2007). The sediments show a high variability of the environmental proxies over the last 7.000 years with short term fluctuations, which seem to indicate a cyclicity associated to sun-spot activity. Since the core material of the first expedition was not sufficient enough to perform a more precise

age-depth model, more material was needed to identify and understand the short-term climate fluctuations during the Holocene. Furthermore, we aimed to investigate the trophic interactions of different lakes in the closer surroundings by sampling the biological compartments and to analyse the modern ecological state of macrozoobenthos. As a side project, we aim to extend the data set on ecological monitoring of small mammals in the North-east Siberia.

Methods

With the help of our Russian partners at the North-East Federal University in Yakutsk it is possible to cope with very demanding logistical challenges coming along with conducting German-Russian expeditions in the Siberian Arctic. Therefore, the field trip was planned and conducted very carefully as unique opportunity, assuming that it is very unlikely to return to the study site.

We used a Kamaz (truck) to reach the lake sites from Yakutsk (Fig. 6.1.-1). Our field work comprised palaeolimnological and limnological methods forming a comprehensive approach that was conducted in a similar way at each site. We performed simple bathymetry (water depth) measurements from a small rubber-platform on water. We performed measurements of the thickness of the Holocene infill. The Holocene is underlain by sandy clay deposits and hence the higher resistivity against penetration with a steel rod from the Russian peat corer (without cutterhead) served as indicator for the Pleistocene Holocene boundary.

Surface sediments were sampled in transects across the lake with a sediment grabber. We retrieved sediment cores at multiple sites using a Russian peat corer and an UWITEC gravity corer. Sediment cores were stored in PVC plastic tubes in dark and cold using thermoboxes. Short cores have been subsampled in 0.5 cm slices a few hours after retrieval and stored in plastic bags to avoid mixing of Pb and Cs in the sediment column that will be used for dating in addition to radiocarbon dating.

We collected water samples, which were analysed for pH, temperature, and conductivity in the field, and will be analysed for anions and cations in laboratories of AWI in Potsdam. We sampled algae, zooplankton and benthic organisms in the lakes and, where possible, narrow-headed voles (*Microtus gregalis*) in the adjacent forested catchments and analysed them in the camp.

Preliminary results

The study area is located in Central Yakutia, Vilyusky District, in the Republic of Sakha, within a marshy plain that is dissedted by a system of river valleys and underlain by continuous permafrost. Thermokarst lakes and alasses (flat thaw depressions) and bulgunykhi, dome-shaped cryogenic highlands, are common landscape features.

In September 2016, we collected 48 m of sediment core material and sediment surface samples at 25 sample locations in three lakes from the Satagay region (Table A 6.1.-1 in the Appendix). Lake Liunkju showed similar geomorphology as compared to crater lakes in the proximity to Lake Satagay that can also provide information on short term climate fluctuations and will serve as comparative case study in addition to Lake Satagay. Limnological and climatic parameters of the studied lakes are shown in Table A 6.1.-2 in

the Appendix. We measured water depth in 275 points on Liunkju Lake, 194 points on Satagay Lake and 12 points on Bety Lake. We took water samples from surface and bottom water of Satagay and Bety lakes that are currently analysed for anion and cation concentrations.

Lake Satagay sediments revealed a significant variability of the penetration depth of steel rods. Fig. 6.1.-2 illustrates the water depth of Lake Satagay and estimated thickness of the Holocene infill, indicating that sedimentation rates were highest in the central part of the basin over the last decade. We assume that subsidence due to thermokarst activity in the Early Holocene started at this point and subsequently developed in western direction, which therefore very likely contains the most continuous sedimentation record.

During field work in summer 2016 we could retrieve the uppermost 1.7 m of sediments, which could not be sampled by Russian peat corer in the previous expedition, because of strong disturbance. PG2362 represents the longest extracted sediment core from that location (Fig. 6.1.-1 and 6.1.-2) and will be used for high resolution X-ray fluorescense analysis and radiocarbon dating.

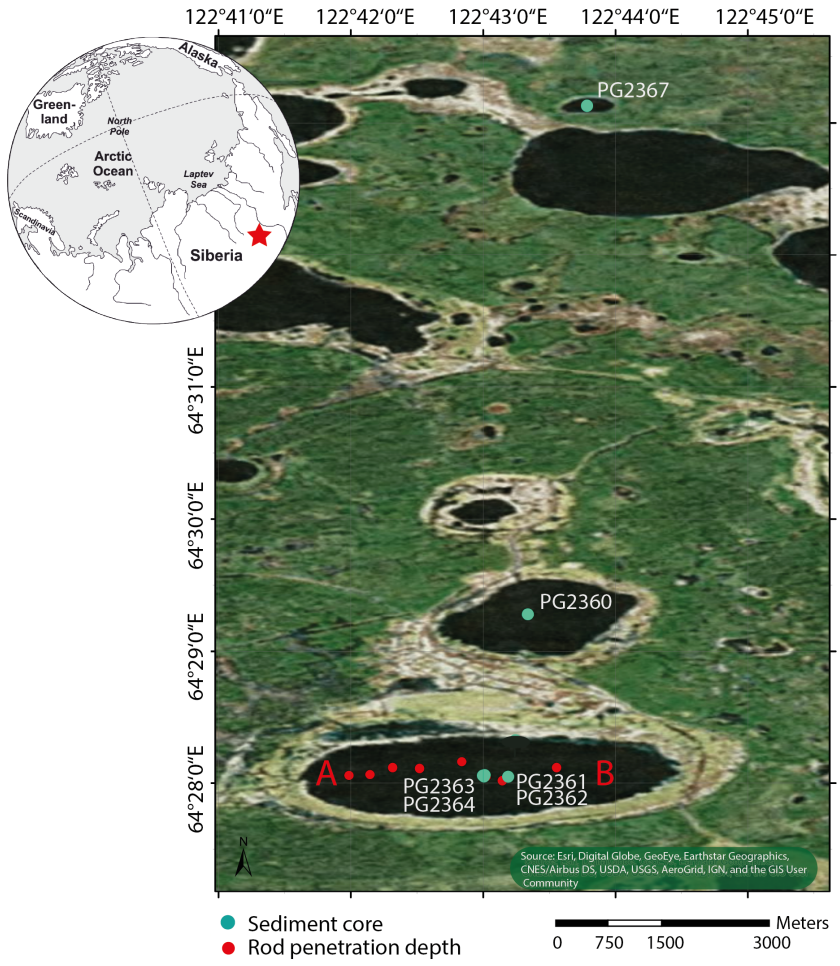

Figure 6.1.-1: Expedition Yakutia 2016 - map of the study area and sample site locations

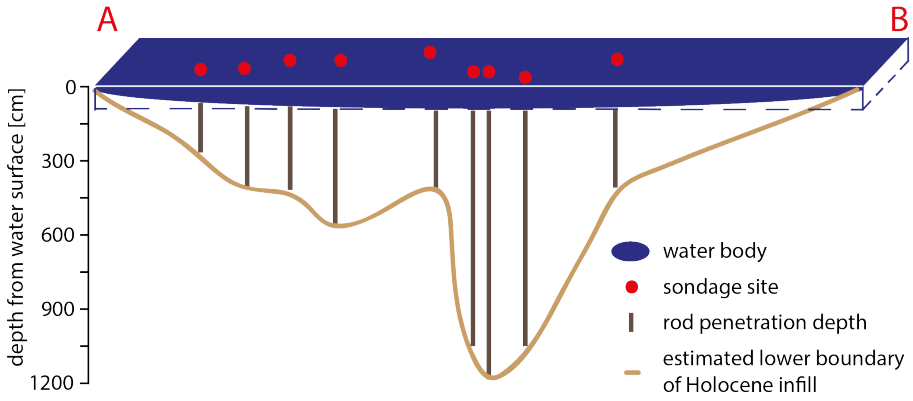

Figure 6.1.-2: Profile across Lake Satagay with measured rod penetration depth that indicates thickness of the Holocene sediment infill, underlain by sandy clay

References

Biskaborn, B.K., Herzschuh, U., Bolshiyanov, D., Savelieva, L., and Diekmann, B. (2012) Environmental variability in northeastern Siberia during the last similar to 13,300 yr inferred from lake diatoms and sediment-geochemical parameters. Palaeogeography Palaeoclimatology Palaeoecology 329, 22-36.

Biskaborn, B., Herzschuh, U., Bolshiyanov, D., Savelieva, L., Zibulski, R., and Diekmann, B. (2013) Late Holocene thermokarst variability inferred from diatoms in a lake sediment record from the Lena Delta, Siberian Arctic. Journal of Paleolimnology 49, 155-170.

Biskaborn, B.K., Subetto, D.A., Savelieva, L.A., Vakhrameeva, P.S., Hansche, A., Herzschuh, U., Klemm, J., Heinecke, L., Pestryakova, L.A., Meyer, H., Kuhn, G., and Diekmann, B. (2016) Late Quaternary vegetation and lake system dynamics in north-eastern Siberia: Implications for seasonal climate variability. Quaternary Science Reviews 147, 406-421.

Herzschuh, U., Pestryakova, L.A., Savelieva, L.A., Heinecke, L., Böhmer, T., Biskaborn, B., Andreev, A., Ramisch, A., Shinneman, A.L.C., and Birks, H.J.B. (2013) Siberian larch forests and the ion content of thaw lakes form a geochemically functional entity. Nature Communications 4.

Popp, S., (2007) Late Quaternary Environment of Central Yakutia (NE Siberia): Signals in Frozen Ground and Terrestrial Sediments, Dissertation, Alfred Wegener Institute for Polar and Marine Research. University Potsdam, pp. 85.

APPENDIX

Table A 2.1.-1: Changes in snow cover depth during the period of investigation

meter	location		depth of snow (cm)		
		07.04.2016 (SP-1)	15.04.2016 (SP-2)	22.04.2016 (SP-3)	26.04.2016 (SP-5)
0	next polygon	44	45.5	47	-
1	rim	47	48	51	48
2	rim	41	50	49	53
3	rim	31	35	34	34
4	rim	25	31	32	33.5
5	polygonal pond	54	59	58	59
6	polygonal pond	54	54	58	57
7	polygonal pond	43	54	53	50
8	polygonal pond	32	49	46	44.5
9	polygonal pond	35	44	42	41
10	polygonal pond	39	38	39	39
11	polygonal pond	40	38	39	38
12	polygonal pond	32	36	34	34.5
13	polygonal pond	32	39	35	35
14	polygonal pond	32	38	37	35
15	polygonal pond	37	45	43	41.5
16	polygonal pond	38	50	47	47
17	polygonal pond	36	43	44	-
18	polygonal pond	36	41	41	40.5
19	polygonal pond	39	42	41	39.5
20	polygonal pond	31	40.5	32	27
21	rim	18.5	29	19	18
22	rim	11	15	10	9
23	rim	44	50	40	29.5

meter	location		depth of snow (cm)		
24	next polygon	22	27	25	-
25	next polygon	21	30	29	-

Table A 2.1.-2: List of samples for isotope analyses

Nr	Sample	Date	Type	Use	depth from	depth to	Remarks
1	LD16-SP-1-1-I1	08.04.16	snow	isotopes	1	5	
2	LD16-SP-1-1-I2	08.04.16	snow	isotopes	6	10	
3	LD16-SP-1-1-I3	08.04.16	snow	isotopes	11	15	
4	LD16-SP-1-1-I4	08.04.16	snow	isotopes	16	20	
5	LD16-SP-1-1-I5	08.04.16	snow	isotopes	21	25	
6	LD16-SP-1-1-I6	08.04.16	snow	isotopes	24	28	
7	LD16-SP-1-1-I7	08.04.16	snow	isotopes	28,5	32,5	depth hoar crust
8	LD16-SP-1-1-I8	08.04.16	snow	isotopes	32,5	36,5	depth hoar
9	LD16-SP-1-1-I9	08.04.16	snow	isotopes	40	44	depth hoar
10	LD16-SP-1-1-I10	08.04.16	snow	isotopes	0	3	top crust
11	LD16-SP-1-2-I1	08.04.16	snow	isotopes	3	7	
12	LD16-SP-1-2-I2	08.04.16	snow	isotopes	8	12	
13	LD16-SP-1-2-I3	08.04.16	snow	isotopes	13	15	
14	LD16-SP-1-2-I4	08.04.16	snow	isotopes	16	20	above DH
15	LD16-SP-1-2-I5	08.04.16	snow	isotopes	21	25	DH crust
16	LD16-SP-1-2-I6	08.04.16	snow	isotopes	26	30	DH
17	LD16-SP-1-2-I7	08.04.16	snow	isotopes	35	40	DH
18	LD16-SP-1-2-I8	08.04.16	snow	isotopes	21	26	5-6 cm of crust above DH from frost crack
19	LD16-SP-1-4-I1	08.04.16	snow	isotopes	2	6	
20	LD16-SP-1-4-I2	08.04.16	snow	isotopes	8	12	
21	LD16-SP-1-4-I3	08.04.16	snow	isotopes	14	18	
22	LD16-SP-1-4-I4	08.04.16	snow	isotopes	19	23	
23	LD16-SP-1-4-I5	08.04.16	snow	isotopes	1	6	top crust
24	LD16-SP-1-6-I1	09.04.16	snow	isotopes	0	1	

Nr	Sample	Date	Type	Use	depth from	depth to	Remarks
25	LD16-SP-1-6-I2	09.04.16	snow	isotopes	1	5	top crust
26	LD16-SP-1-6-I3	09.04.16	snow	isotopes	6	10	
27	LD16-SP-1-6-I4	09.04.16	snow	isotopes	11	15	
28	LD16-SP-1-6-I5	09.04.16	snow	isotopes	16	20	
29	LD16-SP-1-6-I6	09.04.16	snow	isotopes	21	25	compact
30	LD16-SP-1-6-I7	09.04.16	snow	isotopes	26	30	
31	LD16-SP-1-6-I8	09.04.16	snow	isotopes	31	35	crust
32	LD16-SP-1-6-I9	09.04.16	snow	isotopes	36	40	DH
33	LD16-SP-1-6-I10	09.04.16	snow	isotopes	42	46	DH
34	LD16-SP-1-6-I11	09.04.16	snow	isotopes	47	51	DH, surface
35	LD16-SP-1-8-I1	09.04.16	snow	isotopes	0	1	loose snow
36	LD16-SP-1-8-I2	09.04.16	snow	isotopes	1	5	
37	LD16-SP-1-8-I3	09.04.16	snow	isotopes	6	10	
38	LD16-SP-1-8-I4	09.04.16	snow	isotopes	11	15	
39	LD16-SP-1-8-I5	09.04.16	snow	isotopes	16	20	
40	LD16-SP-1-8-I6	09.04.16	snow	isotopes	21	25	
41	LD16-SP-1-8-I7	09.04.16	snow	isotopes	26	30	
42	LD16-SP-1-8-I8	09.04.16	snow	isotopes	32	34	DH
43	LD16-SP-1-12-I1	09.04.16	snow	isotopes	0	0,5	loose snow
44	LD16-SP-1-12-I2	09.04.16	snow	isotopes	1	5	uniform snow pack
45	LD16-SP-1-12-I3	09.04.16	snow	isotopes	6	10	uniform snow pack
46	LD16-SP-1-12-I4	09.04.16	snow	isotopes	11	15	uniform snow pack
47	LD16-SP-1-12-I5	09.04.16	snow	isotopes	16	20	uniform snow pack
48	LD16-SP-1-12-	09.04.16	snow	isotopes	21	25	DH?

Nr	Sample	Date	Type	Use	depth from	depth to	Remarks
	I6						
49	LD16-SP-1-12-I7	09.04.16	snow	isotopes	26	30	DH
50	LD16-SP-1-16-I1	09.04.16	snow	isotopes	0	1	loose snow
51	LD16-SP-1-16-I2	09.04.16	snow	isotopes	1	5	snow
52	LD16-SP-1-16-I3	09.04.16	snow	isotopes	6	10	
53	LD16-SP-1-16-I4	09.04.16	snow	isotopes	11	15	
54	LD16-SP-1-16-I5	09.04.16	snow	isotopes	16	20	
55	LD16-SP-1-16-I6	09.04.16	snow	isotopes	21	25	dense crust
56	LD16-SP-1-16-I7	09.04.16	snow	isotopes	26	30	dense crust
57	LD16-SP-1-16-I8	09.04.16	snow	isotopes	31	35	DH
58	LD16-SP-1-16-I9	09.04.16	snow	isotopes	34	38	DH
59	LD16-SP-1-18-I1	09.04.16	snow	isotopes	0	0,5	loose snow
60	LD16-SP-1-18-I2	09.04.16	snow	isotopes	1	5	snow
61	LD16-SP-1-18-I3	09.04.16	snow	isotopes	6	10	snow
62	LD16-SP-1-18-I4	09.04.16	snow	isotopes	11	15	ice crust
63	LD16-SP-1-18-I5	09.04.16	snow	isotopes	16	20	DH crust
64	LD16-SP-1-18-I6	09.04.16	snow	isotopes	21	25	DH crust
65	LD16-SP-1-18-I7	09.04.16	snow	isotopes	25	35	DH

Nr	Sample	Date	Type	Use	depth from	depth to	Remarks
66	LD16-SP-1-20-I1	09.04.16	snow	isotopes	0	1	snow cover
67	LD16-SP-1-20-I2	09.04.16	snow	isotopes	1	5	
68	LD16-SP-1-20-I3	09.04.16	snow	isotopes	6	10	ice crust
69	LD16-SP-1-20-I4	09.04.16	snow	isotopes	11	15	DH
70	LD16-SP-1-20-I5	09.04.16	snow	isotopes	16	20	DH
71	LD16-SP-1-20-I6	09.04.16	snow	isotopes	20		DH near vegetation cover
72	LD16-SP-1-22-I1	09.04.16	snow	isotopes	0	1	snow cover
73	LD16-SP-1-22-I2	09.04.16	snow	isotopes	1	5	
74	LD16-SP-1-22-I3	09.04.16	snow	isotopes	6	10	DH
75	LD16-SP-1-23-I1	09.04.16	snow	isotopes	0	1	snow cover
76	LD16-SP-1-23-I2	09.04.16	snow	isotopes	1	5	
77	LD16-SP-1-23-I3	09.04.16	snow	isotopes	6	10	
78	LD16-SP-1-23-I4	09.04.16	snow	isotopes	11	15	
79	LD16-SP-1-23-I5	09.04.16	snow	isotopes	16	20	
80	LD16-SP-1-23-I6	09.04.16	snow	isotopes	21	25	
81	LD16-SP-1-23-I7	09.04.16	snow	isotopes	26	30	
82	LD16-SP-1-23-I8	09.04.16	snow	isotopes	31	35	

Nr	Sample	Date	Type	Use	depth from	depth to	Remarks
83	LD16-SP-1-23-I9	09.04.16	snow	isotopes	35	43	DH near vegetation cover
84	LD16-SP-1-1	09.04.16	snow	isotopes	0	46	bottle; tube sampling
85	LD16-SP-1-2	09.04.16	snow	isotopes	0	59	bottle; tube sampling
86	LD16-SP-1-4	09.04.16	snow	isotopes	0	37	bottle; tube sampling
87	LD16-SP-1-6	09.04.16	snow	isotopes	0	51	bottle; tube sampling
88	LD16-SP-1-8	09.04.16	snow	isotopes	0	48	bottle; tube sampling
89	LD16-SP-1-10	09.04.16	snow	isotopes	0	40	bottle; tube sampling
90	LD16-SP-1-12	09.04.16	snow	isotopes	0	35	bottle; tube sampling
91	LD16-SP-1-14	09.04.16	snow	isotopes	0	38	bottle; tube sampling
92	LD16-SP-1-16	09.04.16	snow	isotopes	0	49	bottle; tube sampling
93	LD16-SP-1-18	09.04.16	snow	isotopes	0	41,5	bottle; tube sampling
94	LD16-SP-1-20	09.04.16	snow	isotopes	0	39,5	bottle; tube sampling
95	LD16-SP-1-22	09.04.16	snow	isotopes	0	13	bottle; tube sampling
96	LD16-SP-1-23	09.04.16	snow	isotopes	0	47	bottle; tube sampling
97	LD16-BH-1A	12.04.16	pond ice	isotopes	0	-37	borehole; polygon pond
98	LD16-BH-1B	12.04.16	pond ice	isotopes	0	-103	borehole pond + AL
99	LD16-BH-2	13.04.16	sediment	isotopes	0	-66	core; polygon wall

Nr	Sample	Date	Type	Use	depth from	depth to	Remarks
100	LD16-BH-3-1	13.04.16	sediment	isotopes	0		core pieces; polygon wall
101	LD16-BH-3-2	13.04.16	sediment	isotopes	0		core pieces; polygon wall
102	LD16-BH-3-3	13.04.16	sediment	isotopes	0		core pieces; polygon wall
103	LD16-BH-3-4	13.04.16	sediment	isotopes	0		core pieces; polygon wall
104	LD16-BH-3-5	13.04.16	sediment	isotopes	0		core pieces; polygon wall
105	LD16-BH-3-6	13.04.16	sediment	isotopes	0		core pieces; polygon wall
106	LD16-BH-3-7	13.04.16	sediment	isotopes	0		core pieces; polygon wall
106	LD16-BH-3-7	13.04.16	sediment	isotopes	0		core pieces; polygon wall
107	LD16-BH-3-8	13.04.16	sediment	isotopes	0		core pieces; polygon wall
108	LD16-BH-3-9	13.04.16	sediment	isotopes	0		core pieces; polygon wall
109	LD16-BH-3-10	13.04.16	sediment	isotopes	0		core pieces; polygon wall
110	LD16-FCS-1	14.04.16	snow	isotopes			bottle, snow
111	LD16-FCS-2	14.04.16	snow	isotopes			bottle, depth hoar
112	LD16-FCS-3	14.04.16	snow	isotopes			bottle, snow
113	LD16-FCS-4	14.04.16	snow	isotopes			bottle, depth hoar
114	LD16-FCS-5	14.04.16	snow	isotopes			bottle, snow
115	LD16-FCS-6	14.04.16	snow	isotopes			bottle, depth hoar
116	LD16-FCS-7	14.04.16	snow	isotopes			bottle, snow
117	LD16-FCS-8	14.04.16	snow	isotopes			bottle, depth hoar

Nr	Sample	Date	Type	Use	depth from	depth to	Remarks
118	LD16-FCS-9	14.04.16	snow	isotopes			bottle, snow
119	LD16-FCS-10	14.04.16	snow	isotopes			bottle, depth hoar
120	LD16-FCS-11	14.04.16	snow	isotopes			bottle, snow
121	LD16-FCS-12	14.04.16	snow	isotopes			bottle, depth hoar
122	LD16-FCS-13	14.04.16	snow	isotopes			bottle, snow
123	LD16-FCS-14	14.04.16	snow	isotopes			bottle, depth hoar
124	LD16-FCS-15	14.04.16	snow	isotopes			bottle, snow
125	LD16-FCS-16	14.04.16	snow	isotopes			bottle, depth hoar
126	LD16-SP-2-1-I1	15.04.16	snow	isotopes	1	5	
127	LD16-SP-2-1-I2	15.04.16	snow	isotopes	6	10	
128	LD16-SP-2-1-I3	15.04.16	snow	isotopes	11	15	
129	LD16-SP-2-1-I4	15.04.16	snow	isotopes	16	20	
130	LD16-SP-2-1-I5	15.04.16	snow	isotopes	21	25	
131	LD16-SP-2-1-I6	15.04.16	snow	isotopes	26	30	
132	LD16-SP-2-1-I7	15.04.16	snow	isotopes	31	35	
133	LD16-SP-2-1-I8	15.04.16	snow	isotopes	36	40	
134	LD16-SP-2-1-I9	15.04.16	snow	isotopes	41	48	
135	LD16-SP-2-2-I1	15.04.16	snow	isotopes	0	1	fresh snow
136	LD16-SP-2-2-I2	15.04.16	snow	isotopes	1	5	
137	LD16-SP-2-2-I3	15.04.16	snow	isotopes	6	10	
138	LD16-SP-2-2-I4	15.04.16	snow	isotopes	11	15	
139	LD16-SP-2-2-I5	15.04.16	snow	isotopes	16	20	
140	LD16-SP-2-2-I6	15.04.16	snow	isotopes	21	25	
141	LD16-SP-2-2-I7	15.04.16	snow	isotopes	26	30	DH crust
142	LD16-SP-2-2-I8	15.04.16	snow	isotopes	31	35	DH

Nr	Sample	Date	Type	Use	depth from	depth to	Remarks
143	LD16-SP-2-2-I9	15.04.16	snow	isotopes	36	40	DH
144	LD16-SP-2-2-I10	15.04.16	snow	isotopes	44	48	DH
145	LD16-SP-2-4-I1	15.04.16	snow	isotopes	0	1	fresh snow
146	LD16-SP-2-4-I2	15.04.16	snow	isotopes	1	5	
147	LD16-SP-2-4-I3	15.04.16	snow	isotopes	6	10	
148	LD16-SP-2-4-I4	15.04.16	snow	isotopes	11	15	
149	LD16-SP-2-4-I5	15.04.16	snow	isotopes	16	20	DH crust
150	LD16-SP-2-4-I6	15.04.16	snow	isotopes	21	25	DH
151	LD16-SP-2-4-I7	15.04.16	snow	isotopes	27	31	DH
152	LD16-SP-2-6-I1	15.04.16	snow	isotopes	0	1	fresh snow
153	LD16-SP-2-6-I2	15.04.16	snow	isotopes	1	5	
154	LD16-SP-2-6-I3	15.04.16	snow	isotopes	6	10	
155	LD16-SP-2-6-I4	15.04.16	snow	isotopes	11	15	
156	LD16-SP-2-6-I5	15.04.16	snow	isotopes	16	20	
157	LD16-SP-2-6-I6	15.04.16	snow	isotopes	21	25	
158	LD16-SP-2-6-I7	15.04.16	snow	isotopes	26	30	
159	LD16-SP-2-6-I8	15.04.16	snow	isotopes	31	35	DH crust
160	LD16-SP-2-6-I9	15.04.16	snow	isotopes	36	40	DH crust
161	LD16-SP-2-6-I10	15.04.16	snow	isotopes	41	45	DH
162	LD16-SP-2-6-I11	15.04.16	snow	isotopes	46	50	DH
163	LD16-SP-2-6-I12	15.04.16	snow	isotopes	53	57	DH
164	LD16-SP-2-8-I1	15.04.16	snow	isotopes	0	1	fresh snow
165	LD16-SP-2-8-I2	15.04.16	snow	isotopes	1	5	
166	LD16-SP-2-8-I3	15.04.16	snow	isotopes	6	10	
167	LD16-SP-2-8-I4	15.04.16	snow	isotopes	11	15	

Nr	Sample	Date	Type	Use	depth from	depth to	Remarks
168	LD16-SP-2-8-I5	15.04.16	snow	isotopes	16	20	
169	LD16-SP-2-8-I6	15.04.16	snow	isotopes	21	25	
170	LD16-SP-2-8-I7	15.04.16	snow	isotopes	26	30	
171	LD16-SP-2-8-I8	15.04.16	snow	isotopes	31	35	DH crust
172	LD16-SP-2-8-I9	15.04.16	snow	isotopes	36	40	DH crust
173	LD16-SP-2-8-I10	15.04.16	snow	isotopes	40	46	
174	LD16-SP-2-12-I1	15.04.16	snow	isotopes	0	1	fresh snow
175	LD16-SP-2-12-I2	15.04.16	snow	isotopes	1	5	
176	LD16-SP-2-12-I3	15.04.16	snow	isotopes	6	10	
177	LD16-SP-2-12-I4	15.04.16	snow	isotopes	11	15	
178	LD16-SP-2-12-I5	15.04.16	snow	isotopes	16	20	
179	LD16-SP-2-12-I6	15.04.16	snow	isotopes	21	25	DH
180	LD16-SP-2-12-I7	15.04.16	snow	isotopes	26	34	DH
181	LD16-SP-2-16-I1	15.04.16	snow	isotopes	0	1	fresh snow
182	LD16-SP-2-16-I2	15.04.16	snow	isotopes	1	5	
183	LD16-SP-2-16-I3	15.04.16	snow	isotopes	6	10	
184	LD16-SP-2-16-I4	15.04.16	snow	isotopes	11	15	
185	LD16-SP-2-16-I5	15.04.16	snow	isotopes	16	20	
186	LD16-SP-2-16-I6	15.04.16	snow	isotopes	21	25	
187	LD16-SP-2-16-	15.04.16	snow	isotopes	26	30	

Nr	Sample	Date	Type	Use	depth from	depth to	Remarks
	I7						
188	LD16-SP-2-16-I8	15.04.16	snow	isotopes	31	35	DH crust
189	LD16-SP-2-16-I9	15.04.16	snow	isotopes	36	40	DH crust
190	LD16-SP-2-16-I10	15.04.16	snow	isotopes	41	45	DH
191	LD16-SP-2-16-I11	15.04.16	snow	isotopes	45	49	DH
192	LD16-SP-2-18-I1	15.04.16	snow	isotopes	0	1	
193	LD16-SP-2-18-I2	15.04.16	snow	isotopes	1	5	
194	LD16-SP-2-18-I3	15.04.16	snow	isotopes	6	10	
195	LD16-SP-2-18-I4	15.04.16	snow	isotopes	11	15	DH crust
196	LD16-SP-2-18-I5	15.04.16	snow	isotopes	16	20	DH crust
197	LD16-SP-2-18-I6	15.04.16	snow	isotopes	21	25	DH
198	LD16-SP-2-18-I7	15.04.16	snow	isotopes	26	30	DH
199	LD16-SP-2-18-I8	15.04.16	snow	isotopes	31	35	DH
200	LD16-SP-2-18-I9	15.04.16	snow	isotopes	36	41	DH
201	LD16-SP-2-20-I1	15.04.16	snow	isotopes	0	1	fresh snow
202	LD16-SP-2-20-I2	15.04.16	snow	isotopes	1	5	
203	LD16-SP-2-20-I3	15.04.16	snow	isotopes	6	10	DH crust
204	LD16-SP-2-20-I4	15.04.16	snow	isotopes	11	15	DH crust

Nr	Sample	Date	Type	Use	depth from	depth to	Remarks
205	LD16-SP-2-20-I5	15.04.16	snow	isotopes	16	20	DH
206	LD16-SP-2-20-I6	15.04.16	snow	isotopes	21	25	DH
207	LD16-SP-2-22-I1	15.04.16	snow	isotopes	0	1	fresh snow
208	LD16-SP-2-22-I2	15.04.16	snow	isotopes	1	5	
209	LD16-SP-2-22-I3	15.04.16	snow	isotopes	6	10	DH
210	LD16-SP-2-23-I1	15.04.16	snow	isotopes	0	1	fresh snow
211	LD16-SP-2-23-I2	15.04.16	snow	isotopes	1	5	
212	LD16-SP-2-23-I3	15.04.16	snow	isotopes	6	10	
213	LD16-SP-2-23-I4	15.04.16	snow	isotopes	11	15	DH crust
214	LD16-SP-2-23-I5	15.04.16	snow	isotopes	16	20	DH
215	LD16-SP-2-23-I6	15.04.16	snow	isotopes	21	25	DH
216	LD16-SP-2-23-I7	15.04.16	snow	isotopes	26	30	DH
217	LD16-SP-2-23-I8	15.04.16	snow	isotopes	30	43	DH
218	LD16-P4-1	16.04.16	sediment	isotopes	0	77	
219	LD16-P4-2	16.04.16	sediment	isotopes	77	140	
220	LD16-P4-3	16.04.16	sediment	isotopes	140	189	
221	LD16-P5	16.04.16	sediment	isotopes	0	197	sampled and described by Lars, 6 Segments
222	LD16-PW-1	17.04.16	snow	isotopes			for Thomas, polygon wall

Nr	Sample	Date	Type	Use	depth from	depth to	Remarks
223	LD16-PC-1	17.04.16	snow	isotopes			for Thomas, polygon center
224	LD16-IC-1	17.04.16	ice	isotopes			bottle; sublimation crystals, butterfly wings
225	LD16-SP-4-1	17.04.16	snow	isotopes	0	73	snow/firn core near station
226	LD16-SP-4-2	17.04.16	snow	isotopes	73	160	
227	LD16-SP-4-3	17.04.16	snow	isotopes	160	235	
228	LD16-BH-5-1	19.04.16	lake ice	isotopes			bottle; topmost 2 cm
229	LD16-BH-5-2	19.04.16	lake ice	isotopes			bottle; middle section
230	LD16-BH-5-3	19.04.16	lake ice	isotopes			bottle; bottommost 2 cm
231	LD16-BH-5-4	19.04.16	texture ice	isotopes			bottle; pore water from thawed sediment below lake ice
232	LD16-BH-6-1	19.04.16	lake ice	isotopes	0	33	
233	LD16-BH-6-2	19.04.16	lake ice	isotopes	33	62	
234	LD16-BH-6-3	19.04.16	lake ice	isotopes	62	112	
235	LD16-BH-6-4	19.04.16	lake ice	isotopes	112	129	
236	LD16-BH-6-5	19.04.16	lake ice	isotopes	129	161	
237	LD16-BH-6-6	19.04.16	lake ice	isotopes	161	202	
238	LD16-BH-6-7	19.04.16	lake ice	isotopes	202	233,5	from frozen core barrel, refrozen lake water?

Nr	Sample	Date	Type	Use	depth from	depth to	Remarks
239	LD16-SW-1	19.04.16	lake water	isotopes			bottle
240	LD16-SW-2	19.04.16	lake water	isotopes			bottle
241	LD16-IC-2	19.04.16	ice crystals	isotopes			bottle; butterfly wings
242	LD16-RI-1	19.04.16	regelation ice	isotopes			bottle; sosulki = Eiszapfen
243	LD16-PW-1	21.04.16	snow	isotopes			for Thomas
244	LD16-PC-1	21.04.16	snow	isotopes			for Thomas
245	LD16-SP-3-1	22.04.16	snow	isotopes	0	51	bottle; tube sampling
246	LD16-SP-3-2	22.04.16	snow	isotopes	0	49	bottle; tube sampling
247	LD16-SP-3-4	22.04.16	snow	isotopes	0	32	bottle; tube sampling
248	LD16-SP-3-6	22.04.16	snow	isotopes	0	58	bottle; tube sampling
249	LD16-SP-3-8	22.04.16	snow	isotopes	0	46	bottle; tube sampling
250	LD16-SP-3-10	22.04.16	snow	isotopes	0	39	bottle; tube sampling
251	LD16-SP-3-12	22.04.16	snow	isotopes	0	34	bottle; tube sampling
252	LD16-SP-3-14	22.04.16	snow	isotopes	0	37	bottle; tube sampling
253	LD16-SP-3-16	22.04.16	snow	isotopes	0	47	bottle; tube sampling
254	LD16-SP-3-18	22.04.16	snow	isotopes	0	41	bottle; tube sampling
255	LD16-SP-3-20	22.04.16	snow	isotopes	0	32	bottle; tube sampling
256	LD16-SP-3-22	22.04.16	snow	isotopes	0	10	bottle; tube sampling
257	LD16-SP-3-23	22.04.16	snow	isotopes	0	40	bottle; tube

Nr	Sample	Date	Type	Use	depth from	depth to	Remarks
							sampling
258	LD16-SP-3-1-I1	23.04.16	snow	isotopes	0	1	fresh snow
259	LD16-SP-3-1-I2	23.04.16	snow	isotopes	1	5	
260	LD16-SP-3-1-I3	23.04.16	snow	isotopes	6	10	
261	LD16-SP-3-1-I4	23.04.16	snow	isotopes	11	15	
262	LD16-SP-3-1-I5	23.04.16	snow	isotopes	16	20	
263	LD16-SP-3-1-I6	23.04.16	snow	isotopes	21	25	
264	LD16-SP-3-1-I7	23.04.16	snow	isotopes	26	30	
265	LD16-SP-3-1-I8	23.04.16	snow	isotopes	31	35	DH crust
266	LD16-SP-3-1-I9	23.04.16	snow	isotopes	36	40	DH
267	LD16-SP-3-1-I10	23.04.16	snow	isotopes	41	47	DH
268	LD16-SP-3-2-I1	23.04.16	snow	isotopes	0	1	fresh snow
269	LD16-SP-3-2-I2	23.04.16	snow	isotopes	1	5	
270	LD16-SP-3-2-I3	23.04.16	snow	isotopes	6	10	
271	LD16-SP-3-2-I4	23.04.16	snow	isotopes	11	15	
272	LD16-SP-3-2-I5	23.04.16	snow	isotopes	16	20	
273	LD16-SP-3-2-I6	23.04.16	snow	isotopes	21	25	
274	LD16-SP-3-2-I7	23.04.16	snow	isotopes	26	30	
275	LD16-SP-3-2-I8	23.04.16	snow	isotopes	31	35	DH crust
276	LD16-SP-3-2-I9	23.04.16	snow	isotopes	36	40	DH crust
277	LD16-SP-3-2-I10	23.04.16	snow	isotopes	41	51	DH
278	LD16-SP-3-4-I1	23.04.16	snow	isotopes	0	1	fresh snow
279	LD16-SP-3-4-I2	23.04.16	snow	isotopes	1	5	
280	LD16-SP-3-4-I3	23.04.16	snow	isotopes	6	10	
281	LD16-SP-3-4-I4	23.04.16	snow	isotopes	11	15	
282	LD16-SP-3-4-I5	23.04.16	snow	isotopes	16	20	

Nr	Sample	Date	Type	Use	depth from	depth to	Remarks
283	LD16-SP-3-4-I6	23.04.16	snow	isotopes	21	25	DH crust
284	LD16-SP-3-4-I7	23.04.16	snow	isotopes	26	32	DH
285	LD16-SP-3-6-I1	23.04.16	snow	isotopes	0	1	fresh snow
286	LD16-SP-3-6-I2	23.04.16	snow	isotopes	1	5	
287	LD16-SP-3-6-I3	23.04.16	snow	isotopes	6	10	
288	LD16-SP-3-6-I4	23.04.16	snow	isotopes	11	15	
289	LD16-SP-3-6-I5	23.04.16	snow	isotopes	16	20	
290	LD16-SP-3-6-I6	23.04.16	snow	isotopes	21	25	
291	LD16-SP-3-6-I7	23.04.16	snow	isotopes	26	30	
292	LD16-SP-3-6-I8	23.04.16	snow	isotopes	31	35	
293	LD16-SP-3-6-I9	23.04.16	snow	isotopes	36	40	DH crust
294	LD16-SP-3-6-I10	23.04.16	snow	isotopes	41	45	DH
295	LD16-SP-3-6-I11	23.04.16	snow	isotopes	46	50	DH
296	LD16-SP-3-6-I12	23.04.16	snow	isotopes	51	56	DH
297	LD16-SP-3-8-I1	23.04.16	snow	isotopes	0	1	fresh snow
298	LD16-SP-3-8-I2	23.04.16	snow	isotopes	1	5	
299	LD16-SP-3-8-I3	23.04.16	snow	isotopes	6	10	
300	LD16-SP-3-8-I4	23.04.16	snow	isotopes	11	15	
301	LD16-SP-3-8-I5	23.04.16	snow	isotopes	16	20	
302	LD16-SP-3-8-I6	23.04.16	snow	isotopes	21	25	
303	LD16-SP-3-8-I7	23.04.16	snow	isotopes	26	30	
304	LD16-SP-3-8-I8	23.04.16	snow	isotopes	31	35	
305	LD16-SP-3-8-I9	23.04.16	snow	isotopes	36	40	DH crust
306	LD16-SP-3-8-I10	23.04.16	snow	isotopes	41	45	DH
307	LD16-SP-3-12-I1	23.04.16	snow	isotopes	0	1	fresh snow

Nr	Sample	Date	Type	Use	depth from	depth to	Remarks
308	LD16-SP-3-12-I2	23.04.16	snow	isotopes	1	5	
309	LD16-SP-3-12-I3	23.04.16	snow	isotopes	6	10	
310	LD16-SP-3-12-I4	23.04.16	snow	isotopes	11	15	
311	LD16-SP-3-12-I5	23.04.16	snow	isotopes	16	20	
312	LD16-SP-3-12-I6	23.04.16	snow	isotopes	21	25	
313	LD16-SP-3-12-I7	23.04.16	snow	isotopes	26	30	
314	LD16-SP-3-12-I8	23.04.16	snow	isotopes	30	34	
315	LD16-SP-3-16-I1	23.04.16	snow	isotopes	0	1	fresh snow
316	LD16-SP-3-16-I2	23.04.16	snow	isotopes	1	5	
317	LD16-SP-3-16-I3	23.04.16	snow	isotopes	6	10	
318	LD16-SP-3-16-I4	23.04.16	snow	isotopes	11	15	
319	LD16-SP-3-16-I5	23.04.16	snow	isotopes	16	20	
320	LD16-SP-3-16-I6	23.04.16	snow	isotopes	21	25	DH crust
321	LD16-SP-3-16-I7	23.04.16	snow	isotopes	26	30	DH crust
322	LD16-SP-3-16-I8	23.04.16	snow	isotopes	31	35	DH crust
323	LD16-SP-3-16-I9	23.04.16	snow	isotopes	36	40	DH crust
324	LD16-SP-3-16-I10	23.04.16	snow	isotopes	40	47	DH
325	LD16-SP-3-18-	23.04.16	snow	isotopes	0	1	fresh snow

Nr	Sample	Date	Type	Use	depth from	depth to	Remarks
	I1						
326	LD16-SP-3-18-I2	23.04.16	snow	isotopes	1	5	
327	LD16-SP-3-18-I3	23.04.16	snow	isotopes	6	10	
328	LD16-SP-3-18-I4	23.04.16	snow	isotopes	11	15	
329	LD16-SP-3-18-I5	23.04.16	snow	isotopes	16	20	DH crust
330	LD16-SP-3-18-I6	23.04.16	snow	isotopes	21	25	DH
331	LD16-SP-3-18-I7	23.04.16	snow	isotopes	26	30	DH
332	LD16-SP-3-18-I8	23.04.16	snow	isotopes	31	35	DH
333	LD16-SP-3-20-I1	23.04.16	snow	isotopes	0	1	fresh snow
334	LD16-SP-3-20-I2	23.04.16	snow	isotopes	1	5	
335	LD16-SP-3-20-I3	23.04.16	snow	isotopes	6	10	DH crust
336	LD16-SP-3-20-I4	23.04.16	snow	isotopes	11	15	DH crust
337	LD16-SP-3-20-I5	23.04.16	snow	isotopes	16	20	DH
338	LD16-SP-3-22-I1	23.04.16	snow	isotopes	0	1	fresh snow
339	LD16-SP-3-22-I2	23.04.16	snow	isotopes	1	5	
340	LD16-SP-3-22-I3	23.04.16	snow	isotopes	6	11	DH
341	LD16-SP-3-23-I1	23.04.16	snow	isotopes	0	1	fresh snow
342	LD16-SP-3-23-I2	23.04.16	snow	isotopes	1	5	

Nr	Sample	Date	Type	Use	depth from	depth to	Remarks
343	LD16-SP-3-23-I3	23.04.16	snow	isotopes	6	10	
344	LD16-SP-3-23-I4	23.04.16	snow	isotopes	11	15	
345	LD16-SP-3-23-I5	23.04.16	snow	isotopes	16	20	DH
346	LD16-SP-3-23-I6	23.04.16	snow	isotopes	21	36	DH
347	LD16-SP-5-2-I1	26.04.16	snow	isotopes	1	5	
348	LD16-SP-5-2-I2	26.04.16	snow	isotopes	6	10	
349	LD16-SP-5-2-I3	26.04.16	snow	isotopes	11	15	
350	LD16-SP-5-2-I4	26.04.16	snow	isotopes	16	20	
351	LD16-SP-5-2-I5	26.04.16	snow	isotopes	21	25	
352	LD16-SP-5-2-I6	26.04.16	snow	isotopes	26	30	
353	LD16-SP-5-2-I7	26.04.16	snow	isotopes	31	35	
354	LD16-SP-5-2-I8	26.04.16	snow	isotopes	36	40	DH crust
355	LD16-SP-5-2-I9	26.04.16	snow	isotopes	41	45	DH
356	LD16-SP-5-2-I10	26.04.16	snow	isotopes	46	53	DH
357	LD16-SP-5-4-I1	26.04.16	snow	isotopes	1	5	
358	LD16-SP-5-4-I2	26.04.16	snow	isotopes	6	10	
359	LD16-SP-5-4-I3	26.04.16	snow	isotopes	11	15	
360	LD16-SP-5-4-I4	26.04.16	snow	isotopes	16	20	
361	LD16-SP-5-4-I5	26.04.16	snow	isotopes	21	25	
362	LD16-SP-5-4-I6	26.04.16	snow	isotopes	26	33,5	
363	LD16-SP-5-12-I1	26.04.16	snow	isotopes	1	5	
364	LD16-SP-5-12-I2	26.04.16	snow	isotopes	6	10	

Table A 2.9.-1: Sample locations, depths, and types. A detailed list will be available on www.pangaea.de

sample location	coordinates		water depth [m]	description	sampled depths	sample types
LR-mid	N 72°23´59.3''	E 126°42´22.0''	25-28	Lena main channel-middle	2, 12, 24	DOC, POC, DIC
LR-east	N 72°23´59.2''	E 126°43´36.0''	9-10	Lena main channel-east shore	1, 4, 8	DOC, POC
LR-west	N 72°23´44.2''	E 126°40´43.2''	11-12	Lena main channel-west shore	1, 4, 8	DOC, POC
LL-1	N 72°17´55.4''	E 126°10´30.5''	4	Lucky Lake-center	surface, 2, 3.7	DOC, POC, DIC
LL-2	N 72°17´46.4''	E 126°09´39.8''	3.5	Lucky Lake, 50 to 70 m before outflow	surface, 2, 3.3	DOC, POC, DIC
LL-inflow	N 72°17´31.3''	E 126°11´39.2''	surface sample	Lucky Lake-inflow		DOC, POC, DIC
LL-outflow	N 72°17´40.0''	E 126°09´17.9''	surface sample	Lucky Lake-outflow		DOC, POC, DIC
OL-1	N 72°17´41.7''	E 126°12´10.1''	5	Oval Lake-center	surface, 2.5, 4.5	DOC, POC, DIC
NL-1	N 72°23´04.1''	E 126°29´20.4''	4	North Lake-center	surface, 3.7	DOC, POC, DIC
NL-outflow	N 72°23´05.8''	E 126°28´58.4''	surface sample	North Lake-outflow		DOC, POC, DIC
NL Polygon-1	N 72°23´02.2''	E 126°29´09.0''	surface sample	North Lake-northernmost polygon		DOC, POC, DIC
NL Polygon-2	N 72°23´01.4''	E 126°29´07.7''	surface sample	North lake-polygon		DOC, POC
NL Polygon-3	N 72°23´00.8''	E 126°29´08.2''	surface sample	North Lake-southernmost polygon		DOC, POC
FP-outflow	N 72°23´20.1''	E 126°28´58.3''	surface sample	Floodplain-outflow		DOC, POC
Trofimovskaya	N72°26'56.1"	E126°40'18.0"	14	n.a.	2.8, 11.2	DOC, POC
Bykowskaya	N72°24'15.5"	E126°46'58.2"	9	n.a.	surface, 5.4	DOC, POC
Olenyokskaya-1	N72°39'40.6"	E124°21'04.3"	6.2	n.a.	3.7	DOC, POC
Olenyokskaya-2	N72°21'32.3"	E125°40'37.2"	9.4	n.a.	10.7	DOC, POC
Olenyokskaya-3	N72°30'28.4"	E125°16'38.7"	17.8	n.a.	5.6	DOC, POC
Olenyokskaya-4	N72°17'46.1"	E126°05'40.0"	10	n.a.	6	DOC, POC
Tumatskaya	N72°25'00.1"	E126°27'24.8"	14.8	n.a.	8.9	DOC, POC
L16-t-1	N 62°09´42.2''	E 129°54´17.6''	n.a.	n.a.	surface	unfiltered water
L16-t-2	N 62°36´32.1''	E 129°48´25.1''	n.a.	n.a.	surface	unfiltered water

sample location	coordinates		water depth [m]	description	sampled depths	sample types
L16-t-3	N 63°21´14.2''	E 129°28´11.5''	n.a.	n.a.	surface	unfiltered water
L16-t-4	N 63°31´01.0''	E 128°51´37.4''	n.a.	n.a.	surface	unfiltered water
L16-t-5	N 63°53´07.6''	E 127°29´07.3''	n.a.	n.a.	surface	unfiltered water
L16-t-6	N 64°20´59.2''	E 126°33´24.3''	n.a.	n.a.	surface	unfiltered water
L16-t-7	N 64°28´05.1''	E 126°04´08.9''	n.a.	n.a.	surface	unfiltered water
L16-t-8	N 65°03´01.1''	E 124°48´26.4''	n.a.	n.a.	surface	unfiltered water
L16-t-9	N 65°28´07.6''	E 124°20´34.4''	n.a.	n.a.	surface	unfiltered water
L16-t-10	N 66°15´08.7''	E 123°56´58.8''	n.a.	n.a.	surface	unfiltered water
L16-t-11	N 66°48´15.1''	E 123°23´42.7''	n.a.	n.a.	surface	unfiltered water
L16-t-12	N 67°35´12.3''	E 123°00´51.9''	n.a.	n.a.	surface	unfiltered water
L16-t-13	N 68°00´19.0''	E 123°15´31.5''	n.a.	n.a.	surface	unfiltered water
L16-t-14	N 68°43´29.3''	E 123°59´28.3''	n.a.	n.a.	surface	unfiltered water
L16-t-15	N 69°23´38.1''	E 124°45´29.7''	n.a.	n.a.	surface	unfiltered water
L16-t-16	N 70°05´35.0''	E 125°51´15.4''	n.a.	n.a.	surface	unfiltered water
L16-t-17	N 70°29´53.4''	E 126°45´44.2''	n.a.	n.a.	surface	unfiltered water
L16-t-18	N 71°04´05.2''	E 127°32´40.3''	n.a.	n.a.	surface	unfiltered water
L16-t-19	N 71°26´35.2''	E 127°19´27.4''	n.a.	n.a.	surface	unfiltered water
L16-t-20	N 72°03´00.9''	E 126°57´52.1''	n.a.	n.a.	surface	unfiltered water

Table A 2.11.-1: Soil pit and core samples from DTLB on Kurungnakh Island.

Site	Method	Lat [°]	Long [°]	Date	Sample	Depth [cm]	Planned analyses
KUR16-DTLB-1	Soil pit	72,34154	126,25545	21.07.2016	KUR16-DTLB-1-1	0-11	lithology, geochemistry
	Core tube				KUR16-DTLB-1-2	11-21	lithology, geochemistry
					KUR16-DTLB-1-3	21-31	lithology, geochemistry
					KUR16-DTLB-1-4	31-38	lithology, geochemistry
					KUR16-DTLB-1-5	38-40	lithology, geochemistry, ^{14}C
					KUR16-DTLB-1-6	40-50	lithology, geochemistry
					KUR16-DTLB-1-7	50-59	lithology, geochemistry
					KUR16-DTLB-1-8	59-69	lithology, geochemistry
					KUR16-DTLB-1-9	69-69.5	lithology, geochemistry, ^{14}C
					KUR16-DTLB-1-10	69.5-75	lithology, geochemistry
					KUR16-DTLB-1-11	75-75.5	lithology, geochemistry, ^{14}C
					KUR16-DTLB-1-12	75.5-79.5	lithology, geochemistry
KUR16-DTLB-17	Soil pit	72,31934	126,05557	22.07.2016	KUR16-DTLB-17-1	0-9	lithology, geochemistry
	SIPRE				KUR16-DTLB-17-2	9-19	lithology, geochemistry
					KUR16-DTLB-17-3	19-20	lithology, geochemistry, ^{14}C
					KUR16-DTLB-17-4	20-30	lithology, geochemistry
					KUR16-DTLB-17-5	30-40	lithology, geochemistry
					KUR16-DTLB-17-6	40-50	lithology, geochemistry
					KUR16-DTLB-17-7	50-60	lithology, geochemistry
					KUR16-DTLB-17-8	60-70	lithology, geochemistry
					KUR16-DTLB-17-9	70-80	lithology, geochemistry
					KUR16-DTLB-17-10	80-89	lithology, geochemistry
					KUR16-DTLB-17-11	89-90	lithology, geochemistry, ^{14}C
					KUR16-DTLB-17-12	90-100	lithology, geochemistry
					KUR16-DTLB-17-13	100-110	lithology, geochemistry
					KUR16-DTLB-17-14	113-114	lithology, geochemistry, ^{14}C
					KUR16-DTLB-17-15	120-130	lithology, geochemistry
					KUR16-DTLB-17-16	140-150	lithology, geochemistry

Site	Method	Lat [°]	Long [°]	Date	Sample	Depth [cm]	Planned analyses
KUR16-DTLB-16	Soil pit	72,31554	126,07531	22.07.2016	KUR16-DTLB-16-1	0-8	lithology, geochemistry
	SIPRE				KUR16-DTLB-16-2	9-13	lithology, geochemistry
					KUR16-DTLB-16-3	13-14	lithology, geochemistry, ^{14}C
					KUR16-DTLB-16-4	14-20	lithology, geochemistry
					KUR16-DTLB-16-5	20-30	lithology, geochemistry
					KUR16-DTLB-16-6	30-40	lithology, geochemistry
					KUR16-DTLB-16-7	40-50	lithology, geochemistry
					KUR16-DTLB-16-8	50-60	lithology, geochemistry
					KUR16-DTLB-16-9	60-70	lithology, geochemistry
					KUR16-DTLB-16-10	70-80	lithology, geochemistry
					KUR16-DTLB-16-11	80-90	lithology, geochemistry
					KUR16-DTLB-16-12	90-100	lithology, geochemistry
					KUR16-DTLB-16-13	110-120	lithology, geochemistry
					KUR16-DTLB-16-14	130-140	lithology, geochemistry
KUR16-DTLB-10	Soil pit	72,29070	126,18488	23.07.2016	KUR16-DTLB-10-1	0-10	lithology, geochemistry
	Soil pit				KUR16-DTLB-10-2	10-20	lithology, geochemistry
	SIPRE				KUR16-DTLB-10-3	20-30	lithology, geochemistry
					KUR16-DTLB-10-4	30-31	lithology, geochemistry, ^{14}C
					KUR16-DTLB-10-5	31-40	lithology, geochemistry
					KUR16-DTLB-10-6	40-50	lithology, geochemistry
					KUR16-DTLB-10-7	50-60	lithology, geochemistry
					KUR16-DTLB-10-8	60-70	lithology, geochemistry
					KUR16-DTLB-10-9	70-72	lithology, geochemistry
					KUR16-DTLB-10-10	72-73	lithology, geochemistry, ^{14}C
					KUR16-DTLB-10-11	73-80	lithology, geochemistry
					KUR16-DTLB-10-12	80-92	lithology, geochemistry
					KUR16-DTLB-10-13	92-105	lithology, geochemistry
					KUR16-DTLB-10-14	105-122	lithology, geochemistry
KU	Soil pit	72	126	23	KUR16-DTLB-	0-4	lithology, geochemistry

Site	Method	Lat [°]	Long [°]	Date	Sample	Depth [cm]	Planned analyses
					9-1		
	Soil pit				KUR16-DTLB-9-2	4-13	lithology, geochemistry
	Soil pit				KUR16-DTLB-9-3	13-22	lithology, geochemistry
	SIPRE				KUR16-DTLB-9-4	22-27	lithology, geochemistry
					KUR16-DTLB-9-5	27-28	lithology, geochemistry, ^{14}C
					KUR16-DTLB-9-6	28-41	lithology, geochemistry
					KUR16-DTLB-9-7	41-50	lithology, geochemistry
					KUR16-DTLB-9-8	50-60	lithology, geochemistry
					KUR16-DTLB-9-9	60-70	lithology, geochemistry
					KUR16-DTLB-9-10	70-83	lithology, geochemistry
					KUR16-DTLB-9-11	83-96	lithology, geochemistry
					KUR16-DTLB-9-12	96-104	lithology, geochemistry
					KUR16-DTLB-9-13	104-114	lithology, geochemistry
KUR16-DTLB-21	Soil pit	72,28780	126,19218	23.07.2016	KUR16-DTLB-21-1	0-4	lithology, geochemistry
	Soil pit				KUR16-DTLB-21-2	4-9	lithology, geochemistry
	SIPRE				KUR16-DTLB-21-3	9-13	lithology, geochemistry
					KUR16-DTLB-21-4	24-29	lithology, geochemistry
					KUR16-DTLB-21-5	43-53	lithology, geochemistry
					KUR16-DTLB-21-6	65-70	lithology, geochemistry
					KUR16-DTLB-21-7	82-86	lithology, geochemistry
					KUR16-DTLB-21-8	92-97	lithology, geochemistry
					KUR16-DTLB-21-9	106-111	lithology, geochemistry

Table A 2.11.-2: Soil pit and core samples for TEV on Kurungnakh Island.

Site	Method	N	E	Date	Sample	Depth	Planned analyses
KUR16-TEV1-1.1	Pit	72.21169	126.17499	26.07.2016	KUR16_TEV1-1.1-1	0-9	Lithology, geochemistry, $d^{13}C$
	SIPRE				KUR16_TEV1-1.1-2	9-20	Lithology, geochemistry, $d^{13}C$
					KUR16_TEV1-1.1-3	20-30	Lithology, geochemistry, $d^{13}C$
					KUR16_TEV1-1.1-4	30-40	Lithology, geochemistry, $d^{13}C$
					KUR16_TEV1-1.1-5	40-50	Lithology, geochemistry, $d^{13}C$
					KUR16_TEV1-1.1-6	50-63	Lithology, geochemistry, $d^{13}C$
					KUR16_TEV1-1.1-7	63-76	Lithology, geochemistry, $d^{13}C$
					KUR16_TEV1-1.1-8	76-90	Lithology, geochemistry, $d^{13}C$
					KUR16_TEV1-1.1-9	90-106	Lithology, geochemistry, $d^{13}C$
					KUR16_TEV1-1.1-10	106-120	Lithology, geochemistry, $d^{13}C$
KUR16-TEV1-1.2	Pit	72.21179	126.17487	26.07.2016	KUR16-TEV1-1.2-1	0-9	Lithology, geochemistry, $d^{13}C$
	SIPRE				KUR16-TEV1-1.2-2	9-19	Lithology, geochemistry, $d^{13}C$
					KUR16-TEV1-1.2-3	19-30	Lithology, geochemistry, $d^{13}C$
					KUR16-TEV1-1.2-4	30-40	Lithology, geochemistry, $d^{13}C$
					KUR16-TEV1-1.2-5	40-50	Lithology, geochemistry, $d^{13}C$
					KUR16-TEV1-1.2-6	50-60	Lithology, geochemistry, $d^{13}C$
					KUR16-TEV1-1.2-7	60-70	Lithology, geochemistry, $d^{13}C$
					KUR16-TEV1-1.2-8	70-80	Lithology, geochemistry, $d^{13}C$
					KUR16-TEV1-1.2-9	80-86	Lithology, geochemistry, $d^{13}C$
					KUR16-TEV1-1.2-10	86-100	Lithology, geochemistry, $d^{13}C$
KUR16-TEV1-1.3	Pit	72.21192	126.17482	26.07.2016	KUR16-TEV1-1.3-1	0-9	Lithology, geochemistry, $d^{13}C$
	SIPRE				KUR16-TEV1-1.3-2	9-20	Lithology, geochemistry, $d^{13}C$
					KUR16-TEV1-1.3-3	20-30	Lithology, geochemistry, $d^{13}C$
					KUR16-TEV1-1.3-4	30-36	Lithology, geochemistry, $d^{13}C$
					KUR16-TEV1-1.3-5	36-50	Lithology, geochemistry, $d^{13}C$
					KUR16-TEV1-1.3-6	50-61	Lithology, geochemistry, $d^{13}C$
					KUR16-TEV1-1.3-7	61-70	Lithology, geochemistry, $d^{13}C$
					KUR16-TEV1-1.3-8	70-76	Lithology, geochemistry, $d^{13}C$

Site	Method	N	E	Date	Sample	Depth	Planned analyses
					KUR16-TEV1-1.3-9	76-130	Lithology, geochemistry, $d^{13}C$
KUR16-TEV1-2.1	Pit	72.35629	126.30618	27.07.2016	KUR16-TEV1-2.1-1	0-10	Lithology, geochemistry, $d^{13}C$
	Pit				KUR16-TEV1-2.1-2	10-13	Lithology, geochemistry, $d^{13}C$
	SIPRE				KUR16-TEV1-2.1-3	13-20	Lithology, geochemistry, $d^{13}C$
					KUR16-TEV1-2.1-4	20-30	Lithology, geochemistry, $d^{13}C$
					KUR16-TEV1-2.1-5	30-40	Lithology, geochemistry, $d^{13}C$
					KUR16-TEV1-2.1-6	40-51	Lithology, geochemistry, $d^{13}C$
					KUR16-TEV1-2.1-7	51-61	Lithology, geochemistry, $d^{13}C$
					KUR16-TEV1-2.1-8	61-84	Lithology, geochemistry, $d^{13}C$
KUR16-TEV1-2.2	Pit	72.35635	126.30457	27.07.2016	KUR16-TEV1-2.2-1	0-8	Lithology, geochemistry, $d^{13}C$
	Pit				KUR16-TEV1-2.2-2	8-13	Lithology, geochemistry, $d^{13}C$
	SIPRE				KUR16-TEV1-2.2-3	9-20	Lithology, geochemistry, $d^{13}C$
					KUR16-TEV1-2.2-4	20-30	Lithology, geochemistry, $d^{13}C$
					KUR16-TEV1-2.2-5	30-40	Lithology, geochemistry, $d^{13}C$
					KUR16-TEV1-2.2-6	40-50	Lithology, geochemistry, $d^{13}C$
					KUR16-TEV1-2.2-7	50-60	Lithology, geochemistry, $d^{13}C$
					KUR16-TEV1-2.2-8	60-70	Lithology, geochemistry, $d^{13}C$
					KUR16-TEV1-2.2-9	70-84	Lithology, geochemistry, $d^{13}C$
					KUR16-TEV1-2.2-10	84-101	Lithology, geochemistry, $d^{13}C$
KUR16-TEV1-2.3	Pit	72.35628	126.30355	27.07.2016	KUR16-TEV1-2.3-1	0-5	Lithology, geochemistry, $d^{13}C$
	Pit				KUR16-TEV1-2.3-2	5-13	Lithology, geochemistry, $d^{13}C$
	Pit				KUR16-TEV1-2.3-3	13-22	Lithology, geochemistry, $d^{13}C$
	SIPRE				KUR16-TEV1-2.3-4	22-30	Lithology, geochemistry, $d^{13}C$
					KUR16-TEV1-2.3-5	30-40	Lithology, geochemistry, $d^{13}C$
					KUR16-TEV1-2.3-6	40-50	Lithology, geochemistry, $d^{13}C$
					KUR16-TEV1-2.3-7	50-65	Lithology, geochemistry, $d^{13}C$
					KUR16-TEV1-2.3-8	65-80	Lithology, geochemistry, $d^{13}C$
					KUR16-TEV1-2.3-9	80-98	Lithology, geochemistry, $d^{13}C$
KUR16-	Pit	72.	12	27. 07. 20	KUR16-	0-12	Lithology, geochemistry,

Site	Method	N	E	Date	Sample	Depth	Planned analyses
					TEV1-2.4-1		$d^{13}C$
	Pit				KUR16-TEV1-2.4-2	12-22	Lithology, geochemistry, $d^{13}C$
	SIPRE				KUR16-TEV1-2.4-3	22-37	Lithology, geochemistry, $d^{13}C$
					KUR16-TEV1-2.4-4	37-50	Lithology, geochemistry, $d^{13}C$
					KUR16-TEV1-2.4-5	50-62	Lithology, geochemistry, $d^{13}C$
					KUR16-TEV1-2.4-6	62-76	Lithology, geochemistry, $d^{13}C$
KUR16-TEV1-2.5	Pit	72.2123	126.18039	26.07.2016	KUR16-TEV1-2.5-0	0-3	Lithology, geochemistry, $d^{13}C$
	Pit				KUR16-TEV1-2.5-1	3-28 FV 4	Lithology, geochemistry, $d^{13}C$
	Pit				KUR16-TEV1-2.5-2	3-28 FV 17	Lithology, geochemistry, $d^{13}C$
	SIPRE				KUR16-TEV1-2.5-3	28-40	Lithology, geochemistry, $d^{13}C$
					KUR16-TEV1-2.5-4	40-50	Lithology, geochemistry, $d^{13}C$
					KUR16-TEV1-2.5-5	50-60	Lithology, geochemistry, $d^{13}C$
					KUR16-TEV1-2.5-6	60-70	Lithology, geochemistry, $d^{13}C$
					KUR16-TEV1-2.5-7	70-77	Lithology, geochemistry, $d^{13}C$
					KUR16-TEV1-2.5-8	77-90	Lithology, geochemistry, $d^{13}C$
					KUR16-TEV1-2.5-9	90-100	Lithology, geochemistry, $d^{13}C$
					KUR16-TEV1-2.5-10	100-118	Lithology, geochemistry, $d^{13}C$
KUR16-TEV1-3.1	Pit	72.35756	126.3071	27.07.2016	KUR16-TEV1-3.1-1	0-4	Lithology, geochemistry, $d^{13}C$
	Pit				KUR16-TEV1-3.1-2	4-14 FV	Lithology, geochemistry, $d^{13}C$
	Pit				KUR16-TEV1-3.1-3	14-24 FV	Lithology, geochemistry, $d^{13}C$
	SIPRE				KUR16-TEV1-3.1-4	24-34	Lithology, geochemistry, $d^{13}C$
					KUR16-TEV1-3.1-5	34-44	Lithology, geochemistry, $d^{13}C$
					KUR16-TEV1-3.1-6	44-52	Lithology, geochemistry, $d^{13}C$
					KUR16-TEV1-3.1-7	52-60	Lithology, geochemistry, $d^{13}C$
					KUR16-TEV1-3.1-8	60-80	Lithology, geochemistry, $d^{13}C$
					KUR16-TEV1-3.1-9	80-100	Lithology, geochemistry, $d^{13}C$
KUR16-TEV1-3.2	Pit	72.35776	126.30626	27.07.2016	KUR16-TEV1-3.2-1	0-15	Lithology, geochemistry, $d^{13}C$
	Pit				KUR16-TEV1-3.2-2	15-18	Lithology, geochemistry, $d^{13}C$
	SIPRE				KUR16-TEV1-3.2-3	18-30	Lithology, geochemistry, $d^{13}C$

Site	Method	N	E	Date	Sample	Depth	Planned analyses
					KUR16-TEV1-3.2-4	30-40	Lithology, geochemistry, $d^{13}C$
					KUR16-TEV1-3.2-5	40-50	Lithology, geochemistry, $d^{13}C$
					KUR16-TEV1-3.2-6	50-62	Lithology, geochemistry, $d^{13}C$
					KUR16-TEV1-3.2-7	62-72	Lithology, geochemistry, $d^{13}C$
					KUR16-TEV1-3.2-8	72-84	Lithology, geochemistry, $d^{13}C$
					KUR16-TEV1-3.2-9	84-90	Lithology, geochemistry, $d^{13}C$
					KUR16-TEV1-3.2-10	90-100	Lithology, geochemistry, $d^{13}C$
KUR16-TEV1-3.3	Pit	72.35794	126.3055	27.07.2016	KUR16-TEV1-3.3-1	0-6	Lithology, geochemistry, $d^{13}C$
	Pit				KUR16-TEV1-3.3-2	6-21 FV	Lithology, geochemistry, $d^{13}C$
	SIPRE				KUR16-TEV1-3.3-3	21-27	Lithology, geochemistry, $d^{13}C$
					KUR16-TEV1-3.3-4	27-40	Lithology, geochemistry, $d^{13}C$
					KUR16-TEV1-3.3-5	40-50	Lithology, geochemistry, $d^{13}C$
					KUR16-TEV1-3.3-6	50-58	Lithology, geochemistry, $d^{13}C$
					KUR16-TEV1-3.3-7	58-70	Lithology, geochemistry, $d^{13}C$
					KUR16-TEV1-3.3-8	70-80	Lithology, geochemistry, $d^{13}C$
					KUR16-TEV1-3.3-9	80-90	Lithology, geochemistry, $d^{13}C$
					KUR16-TEV1-3.3-10	90-100	Lithology, geochemistry, $d^{13}C$

Table A 2.11.-3: Active layer depths measured on Kurungnakh Island.

Site	Day	Active Layer Depth [cm]
KUR16-DTLB-1	21.07.2016	11
KUR16-DTLB-17	22.07.2016	9
KUR16-DTLB-16	22.07.2016	9
KUR16-DTLB-10	23.07.2016	20
KUR16-DTLB-9	23.07.2016	22
KUR16-DTLB-21	23.07-2016	9
KUR16-TEV-1-1.1	26.07.2016	9
KUR16-TEV-1-1.2	26.07.2016	9
KUR16-TEV-1-1.3	26.07.2016	9
KUR16-TEV-1-2.1	27.07.2016	13
KUR16-TEV-1-2.2	27.07.2016	5-13
KUR16-TEV-1-2.3	27.07.2016	22
KUR16-TEV-1-2.4	27.07.2016	22
KUR16-TEV-1-2.5	26.07.2016	28
KUR16-TEV-1-3.1	27.07.2016	14
KUR16-TEV-1-3.2	27.07.2016	10-18
KUR16-TEV-1-3.3	27.07.2016	17-20

Table A 2.11.-4: Samples of surface water, snow, and ground ice on Kurungnakh Island.

Site	Day	Lat [°]	Lon [°]	Sample type	Planned analyses				
					Ani-ons	Cati-ons	DOC	cDOM	Iso-topes
KUR16_W_01	20.07.2016	72,36207	126,29531	surface water	-	-	x	-	x
KUR16_W_02	20.07.2016	72,36151	126,29288	snow	-	-	-	-	x
KUR16_W_03	20.07.2016	72,33199	126,25028	surface water	-	-	x	-	x
KUR16_W_04	20.07.2016	72,33071	126,24233	surface water	-	-	x	-	x
KUR16_W_05	20.07.2016	72,33224	126,25787	surface water	-	-	x	-	x
KUR16_W_06	21.07.2016	72,33361	126,27378	surface water	-	-	x	-	x
KUR16_W_07	21.07.2016	72,33358	126,27412	surface water	-	-	x	-	x
KUR16_W_08	21.07.2016	72,33298	126,27448	surface water	-	-	x	-	x
KUR16_W_09	21.07.2016	72,33259	126,28515	surface water	-	-	x	-	x
KUR16_W_10	22.07.2016	72,31956	126,05505	surface water	-	-	x	-	x
KUR16_W_11	22.07.2016	72,31556	126,07423	surface water	-	-	x	-	x
KUR16_W_12	23.07.2016	72,2907	126,18488	ground water	-	-	x	-	x
KUR16_W_13	23.07.2016	72,29152	126,18272	surface water	-	-	x	-	x
KUR16_W_14	23.07.2016	72,29384	126,18037	surface water	x	x	x	x	x
KUR16_W_15	23.07.2016	72,29326	126,18143	surface water	-	-	x	-	x
KUR16_W_16	23.07.2016	72,2931	126,20975	surface water	x	x	x	x	x
KUR16_W_17	23.07.2016	72,2924	126,21093	ground water	-	-	x	-	x
KUR16_W_18	23.07.2016	72,28691	126,19661	surface water	x	x	x	x	x
KUR16_W_19	23.07.2016	72,28534	126,20061	surface water	x	x	x	x	x
KUR16_W_20	23.07.2016	72,28166	126,19286	surface water	-	-	x	-	x
KUR16_W_21	26.07.2016	72,35397	126,32758	surface water	-	-	x	x	x
KUR16_W_22	27.07.2016	72,35819	126,3068	surface water	-	-	x	-	x
KUR16_W_23	28.07.2016	72,29406	126,15216	surface water	x	x	x	x	x
KUR16_W_24	28.07.2016	72,29102	126,16923	surface water	x	x	x	x	x
KUR16_W_25	28.07.2016	72,33374	126,28323	surface water	-	-	x	-	x
KUR16_W_26	28.07.2016	72,3336	126,27684	surface water	-	-	x	-	x
KUR16_W_27	28.07.	72,33	126,27	surface	-	-	x	-	x

Site	Day	Lat [°]	Lon [°]	Sample type	Planned analyses				
					Ani-ons	Cati-ons	DOC	cDOM	Iso-topes
	2016	305089	90484	water					
KUR16_W_28	28.07.2016	72,33247	126,29331	surface water	-	-	x	x	x
KUR16_W_50	05.08.2016	72,33936	126,29383	surface water	-	-	x	-	x
KUR16_W_51	05.08.2016	72,3336	126,27684	surface water	-	-	x	-	x
KUR16_W_52	05.08.2016	72,333083	126,274556	surface water	-	-	x	-	x
KUR16_W_53	05.08.2016	72,32487	126,26608	surface water	-	-	x	-	x
SAR16_W_01	24.07.2016	72,57224	127,23244	surface water	x	x	x	x	x
KUR16-TEV-2 ICE-1	21.07.2016	72,33328	126,27485	ice	-	-	-	-	x
KUR16-TEV-2 ICE-2	21.07.2016	72,33328	126,27485	ice	-	-	-	-	x
KUR16-TEV-2 ICE-3	21.07.2016	72,33328	126,27485	ice	-	-	-	-	x
KUR16-Ice-1	20.07.2016	72,33078	126,24286	ice	-	-	-	-	x
KUR16_TEV2_SN	28.07.2016	72,33332	126,27763	snow	-	-	-	-	x
KUR16_TEV1_1.1-2	26.07.2016	72,21169	126,17499	pore water	-	-	x	-	x
KUR16_TEV1_1.1-3	26.07.2016	72,21169	126,17499	pore water	-	-	x	-	x
KUR16_TEV1_1.1-4	26.07.2016	72,21169	126,17499	pore water	-	-	x	-	x
KUR16_TEV1_1.1-5	26.07.2016	72,21169	126,17499	pore water	-	-	x	-	x
KUR16_TEV1_1.1-6	26.07.2016	72,21169	126,17499	pore water	-	-	x	-	x
KUR16_TEV1_1.1-7	26.07.2016	72,21169	126,17499	pore water	-	-	x	-	x
KUR16_TEV1_1.1-8	26.07.2016	72,21169	126,17499	pore water	-	-	x	-	x
KUR16_TEV1_1.1-9	26.07.2016	72,21169	126,17499	pore water	-	-	x	-	-
KUR16_TEV1_1.1-10	26.07.2016	72,21169	126,17499	ice wedge ice	-	-	x	-	x
KUR16_TEV1_1.2-11	26.07.2016	72,21179	126,17487	ice wedge ice	-	-	-	-	x
KUR16_TEV1_1.3-9	26.07.2016	72,21192	126,17482	ice wedge ice	-	-	-	-	x
KUR16_TEV1_2.1-8	27.07.2016	72,35629	126,30618	ice wedge ice	-	-	-	-	x
KUR16_TEV1_2.4-6	27.07.2016	72,35636	126,30259	ice wedge ice	-	-	-	-	x

Table A 2.12.-1: Temperature measuring sites

Label	Coordinates	Start time	Comments
c1	N 72,28911 E 126,18870	2016.07.24 16:00	outside of alas
c2	N 72,28974 E 126,1868	2016.07.24 20:00	alas slope (k6 sampling point)
c3	N 72,29131 E 126,1864	2016.07.25 16:00	alas bottom (k9 sampling point)
c4	N 72,33978 E 126,292	2016.07.27 16:00	25 m from the cliff (e3 sampling point)
c5	N 72,34017 E 126,2901	2016.07.27 16:00	100 m from the cliff (e4 sampling point)

Table A 2.12.-2: List of samples

Site	Sample	Coordinates [N°; E°]	Date	Method (active layer, cm)	Depth [cm]	Moisture/Ice content, vol% (±10%)	Bulk density [g cm-3] *	Analyses
Samoylov Island	t1	72,37605	12.07.2016	Soil pit (12)	0-12	-	-	C, N, pH, CEC, EC, LOI
		126,47936		Core tube	13-20	59	1,3	C, N, ST, pH, CEC, EC, LOI, k
					20-30	55	1,2	C, N, ST, pH, CEC, EC, LOI, k
					30-40	49	1,4	C, N, ST, pH, CEC, EC, LOI, k
					40-49	51	1,4	C, N, ST, pH, CEC, EC, LOI, k
					49-60	49	1,2	C, N, ST, pH, LOI, k
					60-70	53	1,6	C, N, ST, pH, LOI, k
					70-80	56	1,1	C, N, ST, pH, LOI, k
					80-90	50	1,2	C, N, ST, pH, LOI, k
					90-100	57	1,3	C, N, ST, pH, LOI
	t2	72,37603	12.07.2016	Soil pit (42)	2-6	31	1,0	C, N, pH, CEC, EC, LOI, k
		126,47867			6-10	26	1,7	C, N, ST, pH, CEC, EC, LOI, k
					13-22(24)	29	1,9	C, N, ST, pH, CEC, EC, LOI, k
					22(24)-28	37	2,0	C, N, ST, pH, CEC, EC, LOI, k
					28-42	23	1,9	C, N, ST, pH, CEC, EC, LOI, k
				Core tube	40-70	22	0,9	C, N, ST, pH, LOI
					70-80	36	1,7	C, N, ST, pH, LOI
					80-100	52	1,4	C, N, ST, pH, LOI
	t3	72,36703	17.07.2016	Soil pit (40)	0-5	15	0,9	C, N, pH, CEC, EC, LOI, k
		126,48639			5-9	28	0,8	C, N, ST, pH, CEC, EC, LOI, k
					9-17(18)	37	1,4	C, N, ST, pH, CEC, EC, LOI, k
					17(18)-20	28	0,8	C, N, ST, pH, CEC, EC, LOI, k
					35-40	-	-	C, N, ST, pH, CEC, EC, LOI
			20.07.20	Core tube	40-50	38	0,7	C, N, ST, pH, CEC, EC, LOI, k

Site	Sample	Coordinates [N°; E°]	Date	Method (active layer, cm)	Depth [cm]	Moisture/Ice content, vol% (±10%)	Bulk density [g cm-3] *	Analyses
			16		50-55	62	0,8	C, N, ST, pH, LOI, k
					55-70	54	0,8	C, N, ST, pH, LOI, k
					70-80	70	0,8	C, N, ST, pH, LOI, k
					80-90	66	1,0	C, N, ST, pH, LOI, k
					90-100	75	1,0	C, N, ST, pH, LOI, k
	t4	72,36681	19.07.2016	Soil pit (35)	0-4(6)	-	-	C, N, pH, CEC, EC, LOI
		126,48886			4(6)-6(8)	28	1,1	C, N, ST, pH, CEC, EC, LOI, k
					6(8)-13(16)	31	0,8	C, N, ST, pH, CEC, EC, LOI, k
					16(18)-27	22	0,7	C, N, ST, pH, CEC, EC, LOI, k
					27-35	21	0,7	C, N, ST, pH, CEC, EC, LOI, k
			20.07.2016	Core tube	35-50	72	0,7	C, N, ST, pH, CEC, EC, LOI, k
					50-60	77	0,7	C, N, ST, pH, LOI, k
					60-70	83	0,8	C, N, ST, pH, LOI, k
					70-80	86	0,8	C, N, ST, pH, LOI, k
					80-92	89	0,9	C, N, ST, pH, LOI, k
					92-100	91	0,5	C, N, ST, pH, LOI, k
	t5	72,37222	20.07.2016	Soil pit (21)	2(3)-6(7)	34	1,0	C, N, ST, pH, CEC, EC, LOI, k
		126,48608			6(7)-13	46	1,5	C, N, ST, pH, CEC, EC, LOI, k
					13-21	61	2,3	C, N, ST, pH, CEC, EC, LOI, k
				Core tube	21-30	48	0,9	C, N, ST, pH, CEC, EC, LOI, k
					30-40	54	1,0	C, N, ST, pH, CEC, EC, LOI, k
					40-49	67	1,0	C, N, ST, pH, CEC, EC, LOI, k
					49-60	68	0,9	C, N, ST, pH, LOI, k
					60-70	104	1,0	C, N, ST, pH, LOI, k
					70-80	92	0,7	C, N, ST, pH, LOI, k

Site	Sample	Coordinates [N°; E°]	Date	Method (active layer, cm)	Depth [cm]	Moisture/Ice content, vol% (±10%)	Bulk density [g cm-3] *	Analyses
					80-90	99	0,7	C, N, ST, pH, LOI, k
					90-100	110	0,8	C, N, ST, pH, LOI, k
	t6	72,37222	20.07.2016	Core tube (30)	30-45	68	0,8	C, N, ST, pH, CEC, EC, LOI, k
		126,48608			45-60	81	0,9	C, N, ST, pH, CEC, EC, LOI, k
					60-76	78	0,9	C, N, ST, pH, CEC, EC, LOI
					76-87	78	0,7	C, N, ST, pH, LOI
					87-100	59	0,9	C, N, ST, pH, LOI
	t7	72,37604	26.07.2016	Soil pit (20)	0-10	-	-	C, N, pH, CEC, EC, LOI
		126,47934			10-12	-	0,7	C, N, ST, pH, CEC, EC, LOI
					12-20	47	1,7	C, N, ST, pH, CEC, EC, LOI
				Core tube	20-30	33	1,0	C, N, ST, pH, CEC, EC, LOI, k
					30-40	56	1,5	C, N, ST, pH, CEC, EC, LOI, k
					40-50	58	1,3	C, N, ST, pH, CEC, EC, LOI, k
					50-60	79	1,1	C, N, ST, pH, LOI, k
					60-70	75	0,9	C, N, ST, pH, LOI, k
					70-80	56	1,0	C, N, ST, pH, LOI, k
					80-90	70	1,1	C, N, ST, pH, LOI, k
					90-100	104	0,7	C, N, ST, pH, LOI, k
	t8	72,37603	26.07.2016	Core tube (12)	12-20	45	1,5	C, N, ST, pH, CEC, EC, LOI, k
		126,47914			20-30	37	1,4	C, N, ST, pH, CEC, EC, LOI, k
					30-40	40	1,1	C, N, ST, pH, CEC, EC, LOI, k
					40-50	47	1,4	C, N, ST, pH, CEC, EC, LOI, k
					50-60	52	1,3	C, N, ST, pH, LOI, k
					60-70	38	1,3	C, N, ST, pH, LOI, k
					70-80	66	-	C, N, ST, pH, LOI, k

Site	Sample	Coordinates [N°; E°]	Date	Method (active layer, cm)	Depth [cm]	Moisture/Ice content, vol% (±10%)	Bulk density [g cm-3] *	Analyses
					80-90	48	1,3	C, N, ST, pH, LOI, k
					90-100	54	1,1	C, N, ST, pH, LOI, k
	t9	72,37601	26.07.2016	Soil pit (12)	10-12	-	-	C, N, ST, pH, CEC, EC, LOI
		126,47898		Core tube	12-20	35	1,4	C, N, ST, pH, CEC, EC, LOI, k
					20-30	26	0,9	C, N, ST, pH, CEC, EC, LOI, k
					30-40	43	1,5	C, N, ST, pH, CEC, EC, LOI, k
					40-50	39	1,3	C, N, ST, pH, CEC, EC, LOI, k
					50-60	47	1,3	C, N, ST, pH, LOI, k
					60-70	57	1,4	C, N, ST, pH, LOI, k
					70-80	46	1,4	C, N, ST, pH, LOI, k
					80-90	52	1,3	C, N, ST, pH, LOI, k
					90-100	49	1,4	C, N, ST, pH, LOI, k
Kurungnakh Island	k1	72,28917	18.07.2016	Soil pit (20)	0-4(6)	-	-	C, N, pH, CEC, EC, Tm, LOI
		126,18683			4(6)-7(10)	42	1,2	C, N, ST, pH, CEC, EC, Tm, LOI, k
					7(10)-20	41	1,4	C, N, ST, pH, CEC, EC, Tm, LOI, k
			25.07.2016	Core tube	20-30	20	1,0	C, N, ST, pH, CEC, EC, Tm, LOI, k
					30-40	24	1,0	C, N, ST, pH, CEC, EC, Tm, LOI, k
					40-50	51	1,1	C, N, ST, pH, CEC, EC, Tm, LOI, k
					50-60	72	1,2	C, N, ST, pH, Tm, LOI, k
					60-70	43	0,9	C, N, ST, pH, Tm, LOI, k
					70-80	58	1,2	C, N, ST, pH, Tm, LOI, k
					80-90	47	0,8	C, N, ST, pH, Tm, LOI, k
					90-100	69	1,0	C, N, ST, pH,

Site	Sample	Coordinates [N°; E°]	Date	Method (active layer, cm)	Depth [cm]	Moisture/Ice content, vol% (±10%)	Bulk density [g cm-3] *	Analyses
								Tm, LOI, k
	k 2	72,28922	18.07.2016	Soil pit (13)	0-8(9)	16	-	C, N, pH, CEC, Tm, EC, Tm, LOI, k
		126,18697			8(9)-11(13)	41	1,1	C, N, ST, pH, CEC, EC, Tm, LOI, k
	k 3	72,28939	18.07.2016	Soil pit (17)	0-6(10)	56	1,3	C, N, pH, CEC, EC, Tm, LOI, k
		126,18683			6(10)-16	31	1,5	C, N, ST, pH, CEC, EC, Tm, LOI, k
	k 4	72,28947	23.07.2016	Soil pit (22)	0-7(8)	8	-	C, N, pH, CEC, EC, Tm, LOI, k, MS
		126,18717			7(8)-11	69	1,7	C, N, ST, pH, CEC, EC, Tm, LOI, k, MS
					11-15	33	1,1	C, N, ST, pH, CEC, EC, Tm, LOI, k, MS
					15-22	37	1,7	C, N, ST, pH, CEC, EC, Tm, LOI, k, MS
				Core tube	22-30	35	1,1	C, N, ST, pH, CEC, EC, Tm, LOI, k, MS
					30-40	21	0,9	C, N, ST, pH, CEC, EC, Tm, LOI, k, MS
					40-50	54	1,3	C, N, ST, pH, CEC, EC, Tm, LOI, k, MS
					50-60	65	1,2	C, N, ST, pH, CEC, EC, Tm, LOI, k, MS
					60-73	65	1,2	C, N, ST, pH, CEC, EC, Tm, LOI, k, MS
					73-80	43	0,9	C, N, ST, pH, CEC, EC, Tm, LOI, k, MS
					80-90	54	1,0	C, N, ST, pH, CEC, EC, Tm, LOI, k, MS
					90-100	58	1,2	C, N, ST, pH, CEC, EC, Tm, LOI, k, MS
	k 5	72,28951	23.07.20	Core tube (10)	10-14	-	-	C, N, ST, pH, CEC, EC, Tm,

Site	Sample	Coordinates [N°; E°]	Date	Method (active layer, cm)	Depth [cm]	Moisture/Ice content, vol% (±10%)	Bulk density [g cm-3] *	Analyses
			16					LOI, k
		126,18735			14-20	67	-	C, N, ST, pH, CEC, EC, Tm, LOI, k
					20-30	12	-	C, N, ST, pH, CEC, EC, Tm, LOI, k
					30-40	59	1,2	C, N, ST, pH, CEC, EC, Tm, LOI, k
					40-50	58	1,2	C, N, ST, pH, CEC, EC, Tm, LOI, k
					50-60	74	1,4	C, N, ST, pH, Tm, LOI, k
					60-70	65	0,8	C, N, ST, pH, Tm, LOI, k
					70-80	92	1,1	C, N, ST, pH, Tm, LOI, k
					80-90	63	0,8	C, N, ST, pH, Tm, LOI, k
					90-100	71	1,0	C, N, ST, pH, Tm, LOI, k
	k 6	72,28967	23.07.2016	Soil pit (40)	0-5(8)	13	-	C, N, pH, CEC, EC, Tm, LOI, k, MS
		126,18669			5(8)-12	47	1,3	C, N, ST, pH, CEC, EC, Tm, LOI, k, MS
					12-18(20)	60	2,0	C, N, ST, pH, CEC, EC, Tm, LOI, k, MS
					18(20)-30	59	2,4	C, N, ST, pH, CEC, EC, Tm, LOI, k, MS
					30-40	31	1,0	C, N, ST, pH, CEC, EC, Tm, LOI, k, MS
				Core tube	40-50	47	1,1	C, N, ST, pH, CEC, EC, Tm, LOI, k, MS
					50-60	47	1,4	C, N, ST, pH, Tm, LOI, k, MS
					60-70	49	1,4	C, N, ST, pH, Tm, LOI, k, MS
					70-80	47	1,2	C, N, ST, pH, Tm, LOI, k, MS
					80-90	64	1,6	C, N, ST, pH, Tm, LOI, k, MS

Site	Sample	Coordinates [N°; E°]	Date	Method (active layer, cm)	Depth [cm]	Moisture/Ice content, vol% (±10%)	Bulk density [g cm-3] *	Analyses
					90-100	44	1,3	C, N, ST, pH, Tm, LOI, k, MS
	k 7	72,28981	25.07.2016	Soil pit (10)	0-10	-	-	C, N, pH, CEC, EC, Tm, LOI, MS
		126,18669		Core tube	10-20	46	0,8	C, N, ST, pH, CEC, EC, Tm, LOI, k, MS
					20-30	57	1,0	C, N, ST, pH, CEC, EC, Tm, LOI, k, MS
					30-40	49	1,1	C, N, ST, pH, CEC, EC, Tm, LOI, k, MS
					40-50	41	0,9	C, N, ST, pH, CEC, EC, Tm, LOI, k, MS
					50-60	44	1,2	C, N, ST, pH, Tm, LOI, k, MS
					60-70	52	1,3	C, N, ST, pH, Tm, LOI, k, MS
					70-80	51	1,4	C, N, ST, pH, Tm, LOI, k, MS
					80-90	30	0,9	C, N, ST, pH, Tm, LOI, k, MS
					90-100	51	1,6	C, N, ST, pH, Tm, LOI, k, MS
					100-110	42	1,2	C, N, ST, pH, Tm, LOI, k, MS
	k 8	72,28989	25.07.2016	Soil pit (10)	0-10	-	-	C, N, pH, CEC, EC, Tm, LOI
		126,18658		Core tube	10-20	43	0,8	C, N, ST, pH, CEC, EC, Tm, LOI, k
					20-30	55	1,0	C, N, ST, pH, CEC, EC, Tm, LOI, k
					30-40	50	0,9	C, N, ST, pH, CEC, EC, Tm, LOI, k
					40-50	62	1,3	C, N, ST, pH, CEC, EC, Tm, LOI, k
					50-60	47	1,0	C, N, ST, pH, Tm, LOI, k
					60-70	41	1,2	C, N, ST, pH, Tm, LOI, k
					70-80	37	1,3	C, N, ST, pH, Tm, LOI, k

Site	Sample	Coordinates [N°; E°]	Date	Method (active layer, cm)	Depth [cm]	Moisture/Ice content, vol% (±10%)	Bulk density [g cm-3] *	Analyses
					80-90	43	1,3	C, N, ST, pH, Tm, LOI, k
					90-100	24	-	C, N, ST, pH, Tm, LOI, k
	k 9	72,2913	25.07.2016	Soil pit (18)	0-7	-	-	C, N, ST, pH, CEC, EC, Tm, LOI
		126,18639			7-15	-	0,6	C, N, ST, pH, CEC, EC, Tm, LOI
					15-17	-	1,9	C, N, ST, pH, CEC, EC, Tm, LOI
					15(17)-20	31	1,7	C, N, ST, pH, CEC, EC, Tm, LOI
				Core tube	20-30	48	1,1	C, N, ST, pH, CEC, EC, Tm, LOI, k
					30-40	36	1,1	C, N, ST, pH, CEC, EC, Tm, LOI, k
					40-50	35	0,9	C, N, ST, pH, CEC, EC, Tm, LOI, k
					50-60	50	-	C, N, ST, pH, Tm, LOI, k
					60-70	66	1,0	C, N, ST, pH, Tm, LOI, k
					70-80	62	1,0	C, N, ST, pH, Tm, LOI, k
					80-90	57	1,0	C, N, ST, pH, Tm, LOI, k
					90-100	76	1,0	C, N, ST, pH, Tm, LOI, k
	e 3	72,33978	27.07.2016	Core tube	10-20	+	+	C, N, ST, pH, CEC, EC, LOI, k
		126,29197			20-30	+	+	C, N, ST, pH, CEC, EC, LOI, k
					30-40	+	+	C, N, ST, pH, CEC, EC, LOI, k
					40-50	+	+	C, N, ST, pH, CEC, EC, LOI, k
					50-60	+	+	C, N, ST, pH, CEC, EC, LOI, k
					70-100	+	+	C, N, ST, pH, LOI, k
	e 4	72,34017	27.07.2016	Soil pit	0-12	+	+	C, N, ST, pH, CEC, EC, LOI, k
		126,2901				Moisture		

Site	Sample	Coordinates [N°; E°]	Date	Method (active layer, cm)	Depth [cm]	Moisture/Ice content, vol% (±10%)	Bulk density [g cm-3] *	Analyses
						/Ice content, vol% (±10%)		

* bulk density of undisturbed soil samples with natural soil water content (in its natural state)

C – total carbon

N – total nitrogen

ST – soil texture

pH – soil acidity

CEC – cation exchange capacity

LOI – loss of ignition

EC - electrical conductivity

Tm – Thermogravimetry

k – magnetic susceptibility (measured in the field)

MS – magnetic studies: magnetic properties analysis at the established procedure (Butler, 1998) (including magnetic mineral composition, susceptibility, Day plot (Dunlop, 2002))

NIRS-MIRS – mid–near-infrared spectroscopic analysis - all samples will be analyzed

Table A 2.13.-1: List of zooplankton samples obtained during April-May 2016 on Samoylov Island

Banya-I lake								
№	Date	T_{water}, ° C	Depth, m	S, µS/cm	pH	O_2, mg/l	O_2, %	Ice, m
1.	18.04.	0,0	4	277	6,86	6,24		2,00
2.	13.04.	0,0	4	272	6,96	6,15	45,8	
3.	17.04.	0,0	4	291	6,91	6,08	49,9	
4.	02.04.	0,0	4	286	6,97	7,03	55,7	
5.	27.04.	0,0	4	284	6,92	6,57	49,6	
6.	04.05.	0,0	4	288	6,93	8,06	71,8	
Banya-II lake								
1.	08.04.	0,0	10	138	6,97	10,90		2,06
2.	13.04.	0,0	12	132	6,99	12,02	89,9	
3.	17.04.	0,0	12	137	7,12	9,48	93,1	
4.	22.04.	0,0	12	134	7,04	9,69	82,4	
5.	27.04.	0,0	10	134	7,00	9,26	76,9	
6.	04.05.	0,0	11	136	6,95	9,92	80,7	
Banya-III lake								
1.	18.04.	0,0	6,5	236	7,26	9,52	73,1	2,10
2.	23.04.	0,0	6	238	7,27			
3.	28.04.	0,0	6	229	7,26	9,74	73,8	
4.	02.05.	0,0	6	224		8,37	66,9	
5.	07.05.	0,0	6	232	7,12	10,16	78,1	
Fish lake								
1.	09.04.	0,0	6	160	7,25	10,26	91,1	1,92
2.	14.04.	0,0	6	158	7,05	10,10	71,4	
3.	18.04.	0,0	6	155	7,08	10,34	78,1	

4.	23.04.	0,0	5	149	7,00				
5.	28.04.	0,0	5	145	7,07	8,94	71,3		
6.	02.05.	0,0	5	150	6,99	9,34	70,8		
7.	07.05.	0,0	5	145		9,37	76,4		
South lake									
1.	23.04.	0,0	3,5	436	6,95			2,13	
Olenyokskaya channel									
1.	04.05.	0,0	5	504	7,33	8,43	60,3	1,48	

Table A 2.13.-2: Species composition and distribution of zooplankton in the lakes in April-May 2016

Rotifera	Banya- 1	Banya-II	Banya-III	South	Fish
Keratella cochlearis (Gosse)	×	×	×		×
K. quadrata reticulata Carlin	×				
K. quadrata quadrata (Müller)			×		
Kellicottia longispina (Kellicott)	×	×	×	×	×
Notholca squamula (Müller)	×				
Polyarthra dolychoptera Idelson	×		×		
P. Longiremis Carlin	×				
Asplanchna sp.		×			
Filinia sp.	×		×		×
Rotatoria sp.	×	×	×	×	×
Copepoda					
Eudiaptomus graciloides (Lilljeborg)	×	×	×		×
Limnocalanus johanseni (Marsh)		×			×
Calanoida juv.			×		
Cyclops vicinus Uljanin	×				
C. kikuchii Smirnov					×
C. kolensis Lilljeborg		×	×	×	
C. abyssorum Sars			×		
Cyclops sp.	×			×	
Diacyclops bicuspidatus (Claus)	×				
D. bisetosus Rehberg			×		
Eucyclops c.f. Serrulatus Fischer			×		
Cyclopoida juv.	×	×	×		×
Harpacticoida juv.	×				
Nauplii Copepoda	×	×	×		×
Caldocera					
Chydorus sphaericus s.l. (Müller)	×		×		
Daphnia longiremis Sars			×		
Daphnia sp. juv.					×
Ostracoda	×	×	×		×

Table A 2.14.-1: List of zooplankton samples and additional data collected in July-August 2016

Qualitative analyses							
Lakes	**date**	**depth, m**	**T_{water}**	**O2, mg/l**	**O2, %**	**pH**	**C,mS/cm**
Samoylov Island							
South							
1.	12.07.	3,5	6,4				
2.	18.07.	3,5	10,1			7,66	109
3.	25.07.	3,5	10,8			7,79	101
4.	02.08.	3,5	10,6				
5.	08.08.	3,5	9,8				
6.	14.08.	3,5	9,8	7,70	79,6	7,65	113
7.	23.08.	3,5	8,2	7,16	70,5	7,87	115
Banya-I							
8.	10.07.	4,0	7,1				
9.	18.07.	3,5	7,4				
10.	21.07.	4,5	9,5			7,79	84
11.	27.07.	4,0	10,8			7,60	96
12.	03.08.	4,0	10,9	7,32	72,2	7,62	122
13.	10.08.	4,5	10,3	7,73	72,1	7,74	92
14.	18.08.	4,0	9,8	7,50	70,0	7,75	94
15.	25.08.	4,0	7,9	7,77	78,0	7,85	94
Banya-II							
16.	12.07.	10,0	5,7				
17.	18.07.	12,0	8,7			7,50	81
18.	25.07.	12,0	9,8			8,00	74
19.	02.08.	11,0	10,6				
20.	08.08.	12,0	10,1				
21.	14.08.	12,0	10,1	7,70	77,9	7,63	85
22.	23.08.	12,0	9,0	6,92	67,3	7,75	84
Banya-III							
23.	12.07.	7,5	6,5				
24.	18.07.	7,5	11,8			7,55	97
25.	25.07.	7,5	10,2			7,66	93
26.	02.08.	7,0	10,6				
27.	08.08.	7,5	10,2				
28.	14.08.	7,5	10,3	6,71	71,9	7,65	112
29.	23.08.	7,0	9,0	6,88	68,7	7,72	110
Fish							
30.	16.07.	6,0	7,6				
31.	21.07.	6,0	9,0			7,67	86

32.	27.07.	6,0	10,4			7,66	88
33.	03.08.	6,0	10,9	6,82	67,7	7,76	107
34.	10.08.	6,0	10,3	8,75	89,2	7,70	88
35.	18.08.	6,0	10,0	7,23	66,8	7,63	85
36.	25.08.	6,0	8,7	7,16	72,1	7,78	86
Polygon pond							
37.	25.07.	100l	10,6				
38.	18.08.	100l	9,2	7,34	70,5	7,08	118
39.	25.08.	100l	6,5				
Tundra marsh							
40.	25.08.	50l	6,4	9,10	82,7	7,91	250
Amerika-Khaya Island							
41. Small channel	16.08.	Qual.	11,6			7,37	128
42. Small lake	16.08.	Qual.	8,8			6,84	60
Tit-Ary Island							
43. Oxbow lake	17.08.	Qual.	10,8			7,47	61
44. Thermokarst lake	17.08.	Qual.	10,8			7,61	80
45. Polygon pond	17.08.	Qual.	10,2				
Sagastyr Island	N 73 21 655	E 126 34 188					
46. Sagastyr lake	21.08.	Qual.	7,5				
47. Polygon pond	21.08.	Qual.	7,8				
48. Tumat. channel	21.08.	Qual.	8,2				
Khardyrgastakh Island	N73 23 036	E126 44 037					
49. Polygon pond	21.08.	Qual.	7,5				
50. Marsh	21.08.	Qual.	7,8				

Table A 2.14.-2: List of zooplankton samples obtained in marine expedition in August

station	location	sample date [yymmdd]	sample time [UTC]	latitude N	longitude E	depth [cm]	temperature [°]	container	comment
LE16-13	Chay Tumus	160831	06:49	72.33682	125.74561	0-600	9,2	transparent plastic tube	40° angle
LE16-17	Nagym	160902	02:44	72.87309	123.32154	0-522	9,15	transparent plastic tube	40° angle
LE16-18	Terpai Tumus	160903	05:14	73.2427	118.9583	0-634	4,98	transparent plastic tube	20° angle
LE16-19	Terpai Tums	160904	00:36	73.3013	118.5404	0-432	6,6	transparent plastic tube	10° angle
LE16-22	Mamontov Klyk	160905	04:14	73.71058	117.17025	0-616	4,82	transparent plastic tube	40° angle, less plankton
LE16-23	Transect MK to LD	160905	11:47	73.6316	118.9889	0-922	4,96	transparent plastic tube	60° angle
LE16-24	Olenyokskaya channel	160906	10:50	72.29042	126.08268	0-840	10,45	brown plastic bottle	20° angle
LE16-27	Bykovsky Mys	160908	23:57 (160907)	72.00485	129.09566	0-832	8,5	brown plastic bottle	15° angle
LE16-31	Ivashkina Lagoon	160909	10:35	71.72868	129.41249	0-368	6,9	brown plastic bottle	0° angle

Table A 3.1.-1: List of key sites visited during the expedition at which coastal erosion was monitored through determination of coastline position.

Key site name	Station number	Date
Muostakh Island North Cape	LE16-1-CR1 to LE16-1-CR6	24.08.2016
Mamontovy Khayata, Bykovsky Peninsula	LE16-5-1-CR	25.08.2016
Old Station, Samoylov Island	LE16-6-CR1	26.08.2016
Cape Mamontov Klyk, western Laptev See	LE16-20-CR1	04.09.2016

Sample list

Table A 3.1.-2: List of sediment, water and air samples collected during the 2016 cruise of the Nicole.

Station	Location	Sample ID	Sample type	Analysis	Sample date [yymmdd]	Latitude N	Longitude E	Depth [cm]		
								Water	Sedi-ment	Perma-frost (b.s.b.)
LE16-1	Muostakh island	LD16-MI-05	sediment	DNA	160824	71.61104	129.94315	600	0-5	
LE16-1	Muostakh island	LD16-MI-15	sediment	DNA	160824	71.61104	129.94315	634	0-2	-
LE16-1	Muostakh island	LD16-MI-25-30	sediment	DNA	160824	71.61104	129.94315	634	2-4	-
LE16-1	Muostakh island	LD16-MI-35-40	sediment	DNA	160824	71.61104	129.94315	634	4-6	-
LE16-1	Muostakh island	LD16-MI-45-50	sediment	DNA	160824	71.61104	129.94315	432	0-5	-
LE16-1	Muostakh island	LD16-MI-55	sediment	DNA	160824	71.61104	129.94315	120	-	-
LE16-1	Muostakh island	LD16-MI-60	sediment	DNA	160824	71.61104	129.94315	480	-	-
LE16-1	Muostakh island	LD16-MI-65	sediment	DNA	160824	71.61104	129.94315	256	-	-
LE16-1	Muostakh island	LD16-MI-05	sediment	methane	160824	71.61104	129.94315	1024	-	-
LE16-1	Muostakh island	LD16-MI-15	sediment	methane	160824	71.61104	129.94315	100	-	-
LE16-1	Muostakh island	LD16-MI-25-30	sediment	methane	160824	71.61104	129.94315	400	-	-
LE16-1	Muostakh island	LD16-MI-35-40	sediment	methane	160824	71.61104	129.94315	53	-	-
LE16-1	Muostakh island	LD16-MI-45-50	sediment	methane	160824	71.61104	129.94315	125	-	-
LE16-1	Muostakh island	LD16-MI-55	sediment	methane	160824	71.61104	129.94315	500	-	-
LE16-1	Muostakh island	LD16-MI-60	sediment	methane	160824	71.61104	129.94315	634	-	-
LE16-1	Muostakh island	LD16-MI-65	sediment	methane	160824	71.61104	129.94315	53	-	-
LE16-1	Muostakh island	LD16-MI-10	water	Fe2+	160824	71.61104	129.94315	90	-	-
LE16-1	Muostakh island	LD16-MI-35	water	Fe2+	160824	71.61104	129.94315	340	-	-
LE16-1	Muostakh island	LD16-MI-55	water	Fe2+	160824	71.61104	129.94315	432	-	-
LE16-1	Muostakh island	LD16-MI-60	water	Fe2+	160824	71.61104	129.94315	53	-	-

Station	Location	Sample ID	Sample type	Analysis	Sample date [yymmdd]	Latitude N	Longitude E	Depth		[cm]
								Water	Sedi-ment	Perma-frost (b.s.b.)
LE16-1	Muostakh island	LD16-MI-10	water	ions (anions)	160824	71.61104	129.94315	140	-	-
LE16-1	Muostakh island	LD16-MI-35	water	ions (anions)	160824	71.61104	129.94315	500	-	-
LE16-1	Muostakh island	LD16-MI-55	water	ions (anions)	160824	71.61104	129.94315	616	-	-
LE16-1	Muostakh island	LD16-MI-60	water	ions (anions)	160824	71.61104	129.94315	53	-	-
LE16-1	Muostakh island	LD16-MI-10	water	ions (cations)	160824	71.61104	129.94315	170	-	-
LE16-1	Muostakh island	LD16-MI-35	water	ions (cations)	160824	71.61104	129.94315	700	-	-
LE16-1	Muostakh island	LD16-MI-55	water	ions (cations)	160824	71.61104	129.94315	840	-	-
LE16-1	Muostakh island	LD16-MI-60	water	ions (cations)	160824	71.61104	129.94315	-	5	-
LE16-1	Muostakh island	LD16-MI-10	water	ions (cations)	160824	71.61104	129.94315	-	15	65
LE16-1	Muostakh island	LD16-MI-35	water	ions (cations)	160824	71.61104	129.94315	-	20-30	65
LE16-1	Muostakh island	LD16-MI-55	water	ions (cations)	160824	71.61104	129.94315	-	30-40	65
LE16-1	Muostakh island	LD16-MI-60	water	ions (cations)	160824	71.61104	129.94315	-	40-50	65
LE16-1	Muostakh island	LD16-MI-10	water	volatile fatty acids	160824	71.61104	129.94315	-	50-55	65
LE16-1	Muostakh island	LD16-MI-35	water	volatile fatty acids	160824	71.61104	129.94315	-	55-60	65

Station	Location	Sample ID	Sample type	Analysis	Sample date [yymmdd]	Latitude N	Longitude E		Depth	[cm]
								Water	Sedi-ment	Perma-frost (b.s.b.)
LE16-1	Muostakh island	LD16-MI-55	water	volatile fatty acids	160824	71.61104	129.94315	-	60-65	65
LE16-1	Muostakh island	LD16-MI-60	water	volatile fatty acids	160824	71.61104	129.94315	1	-	65
LE16-10	Samoylov Island	AK_S9 CP 0-10 cm	dead plant material+ sediment	DNA, enrichment	160828	72.37021	126.47942	1	-	50
LE16-10	Samoylov Island	AK_S9 CP 0-10 cm	dead plant material+ sediment	DNA, enrichment	160828	72.37021	126.47942	1	-	50
LE16-10	Samoylov Island	AK_S9 CP 10-20 cm	dead plant material+ sediment	DNA, enrichment	160828	72.37021	126.47942	1	-	50
LE16-10	Samoylov Island	AK_S9 CP 10-20 cm	dead plant material+ sediment	DNA, enrichment	160828	72.37021	126.47942	-	0-10	-
LE16-10	Samoylov Island	AK_S9 CP 20-30 cm	dead plant material+ sediment	DNA, enrichment	160828	72.37021	126.47942	-	10-20	77-78
LE16-10	Samoylov Island	AK_S9 CP 20-30 cm	dead plant material+ sediment	DNA, enrichment	160828	72.37021	126.47942	-	20-30	77-78
LE16-10	Samoylov Island	AK_S9 CP 30-39 cm	dead plant material+ sediment	DNA, enrichment	160828	72.37021	126.47942	-	30-40	77-78
LE16-10	Samoylov Island	AK_S9 CP 30-39 cm	dead plant material+ sediment	DNA, enrichment	160828	72.37021	126.47942	-	40-50	77-78

Station	Location	Sample ID	Sample type	Analysis	Sample date [yymmdd]	Latitude N	Longitude E		Depth	[cm]
								Water	Sedi-ment	Perma-frost (b.s.b.)
LE16-10	Samoylov Island	AK_S0 CP 0-10 cm	dead plant material+ sediment	DNA, enrichment	160828	72.36995	126.48256	-	50-60	77-78
LE16-10	Samoylov Island	AK_S0 CP 0-10 cm	dead plant material+ sediment	DNA, enrichment	160828	72.36995	126.48256	-	70-60	77-78
LE16-10	Samoylov Island	AK_S0 CP 10-20 cm	dead plant material+ sediment	DNA, enrichment	160828	72.36995	126.48256	-	70-75	77-78
LE16-10	Samoylov Island	AK_S0 CP 10-20 cm	dead plant material+ sediment	DNA, enrichment	160828	72.36995	126.48256	-	0-15	77-78
LE16-10	Samoylov Island	AK_S0 CP 20-30 cm	dead plant material+ sediment	DNA, enrichment	160828	72.36995	126.48256	-	15-35	100
LE16-10	Samoylov Island	AK_S0 CP 20-30 cm	dead plant material+ sediment	DNA, enrichment	160828	72.36995	126.48256	-	35-45	100
LE16-10	Samoylov Island	AK_S0 CP 30-40 cm	dead plant material+ sediment	DNA, enrichment	160828	72.36995	126.48256	-	45-55	100
LE16-10	Samoylov Island	AK_S0 CP 30-40 cm	dead plant material+ sediment	DNA, enrichment	160828	72.36995	126.48256	-	60-70	100
LE16-10	Samoylov Island	AK_S0 CP 40-50 cm	dead plant material+ sediment	DNA, enrichment	160828	72.36995	126.48256	-	70-80	100
LE16-10	Samoylov Island	AK_S11 CP 0-10 cm	dead plant material+ sediment	DNA, enrichment	160828	72.36983	126.47791	-	80-90	100

Station	Location	Sample ID	Sample type	Analysis	Sample date [yymmdd]	Latitude N	Longitude E	Depth		[cm]
								Water	Sedi-ment	Perma-frost (b.s.b.)
LE16-10	Samoylov Island	AK_S11 CP 0-10 cm	dead plant material+ sediment	DNA, enrichment	160828	72.36983	126.47791	-	0-10	100
LE16-10	Samoylov Island	AK_S11 CP 10-20 cm	dead plant material+ sediment	DNA, enrichment	160828	72.36983	126.47791	-	10-20	-
LE16-10	Samoylov Island	AK_S11 CP 10-20 cm	dead plant material+ sediment	DNA, enrichment	160828	72.36983	126.47791	-	20-30	-
LE16-10	Samoylov Island	AK_S11 CP 20-30 cm	dead plant material+ sediment	DNA, enrichment	160828	72.36983	126.47791	-	30-35	-
LE16-10	Samoylov Island	AK_S11 CP 20-30 cm	dead plant material+ sediment	DNA, enrichment	160828	72.36983	126.47791	-	35-40	-
LE16-10	Samoylov Island	AK_S11 CP 30-40 cm	dead plant material+ sediment	DNA, enrichment	160828	72.36983	126.47791	-	40-45	-
LE16-10	Samoylov Island	AK_S11 CP 30-40 cm	dead plant material+ sediment	DNA, enrichment	160828	72.36983	126.47791	-	45-50	-
LE16-10	Samoylov Island	AK_S11 CP 40-45 cm	dead plant material+ sediment	DNA, enrichment	160828	72.36983	126.47791	-	50-55	-
LE16-10	Samoylov Island	AK_S0 open water	filtered water	DNA	160828	72.36995	126.48256	-	55-60	-
LE16-10	Samoylov Island	AK_S0 open water	filtered water	DNA	160828	72.36995	126.48256	-	60-65	-
LE16-10	Samoylov Island	AK_S0 open water	filtered water	DNA	160828	72.36995	126.48256	-	65-70	-

Station	Location	Sample ID	Sample type	Analysis	Sample date [yymmdd]	Latitude N	Longitude E	Depth		[cm]
								Water	Sedi-ment	Perma-frost (b.s.b.)
LE16-10	Samoylov island	Lena River Reference	filtered water	DNA	160830	72.36757	126.4753	-	70-76	-
LE16-10	Samoylov Island	AK_S9 Rim 5 cm	sediment	DNA, enrichment	160827	72.37021	126.47942	-	5	-
LE16-10	Samoylov Island	AK_S9 Rim 10 cm	sediment	DNA, enrichment	160827	72.37021	126.47942	-	10	77
LE16-10	Samoylov Island	AK_S9 Rim 15 cm	sediment	DNA, enrichment	160827	72.37021	126.47942	-	15	77
LE16-10	Samoylov Island	AK_S9 Rim 17-18 cm	sediment	DNA, enrichment	160827	72.37021	126.47942	-	20	77
LE16-10	Samoylov Island	AK_S9 Rim 19-20 cm	sediment	DNA, enrichment	160827	72.37021	126.47942	-	25	77
LE16-10	Samoylov Island	AK_S9 Rim 22-23 cm	sediment	DNA, enrichment	160827	72.37021	126.47942	-	30	77
LE16-10	Samoylov Island	AK_S9 Rim 24-25 cm	sediment	DNA, enrichment	160827	72.37021	126.47942	-	5	77
LE16-10	Samoylov Island	AK_S9 Rim 27-28 cm	sediment	DNA, enrichment	160827	72.37021	126.47942	-	10	57.5
LE16-10	Samoylov Island	AK_S9 Rim 29-30 cm	sediment	DNA, enrichment	160827	72.37021	126.47942	-	15	57.5
LE16-10	Samoylov Island	AK_S9 Rim 32-33 cm	sediment	DNA, enrichment	160827	72.37021	126.47942	-	17-18	57.5

Station	Location	Sample ID	Sample type	Analysis	Sample date [yymmdd]	Latitude N	Longitude E		Depth	[cm]
								Water	Sedi-ment	Perma-frost (b.s.b.)
				nt						
LE16-10	Samoylov Island	AK_S0 Rim 0-5 cm	sediment	DNA, enrichment	160828	72.36995	126.48256	-	19-20	57.5
LE16-10	Samoylov Island	AK_S0 Rim 5-10 cm	sediment	DNA, enrichment	160828	72.36995	126.48256	-	22-23	57.5
LE16-10	Samoylov Island	AK_S0 Rim 5-10 cm	sediment	DNA, enrichment	160828	72.36995	126.48256	-	24-25	57.5
LE16-10	Samoylov Island	AK_S0 Rim 10-15 cm	sediment	DNA, enrichment	160828	72.36995	126.48256	-	27-28	57.5
LE16-10	Samoylov Island	AK_S0 Rim 10-15 cm	sediment	DNA, enrichment	160828	72.36995	126.48256	-	29-30	57.5
LE16-10	Samoylov Island	AK_S0 Rim 15-20 cm	sediment	DNA, enrichment	160828	72.36995	126.48256	-	32-33	57.5
LE16-10	Samoylov Island	AK_S0 Rim 15-20 cm	sediment	DNA, enrichment	160828	72.36995	126.48256	-	0-10	57.5
LE16-10	Samoylov Island	AK_S0 Rim 20-25 cm	sediment	DNA, enrichment	160828	72.36995	126.48256	-	0-10	39
LE16-10	Samoylov Island	AK_S0 Rim 20-25 cm	sediment	DNA, enrichment	160828	72.36995	126.48256	-	10-20	39
LE16-10	Samoylov Island	AK_S0 Rim 25-30 cm	sediment	DNA, enrichme	160828	72.36995	126.48256	-	10-20	39

Station	Location	Sample ID	Sample type	Analysis	Sample date [yymmdd]	Latitude N	Longitude E		Depth	[cm]
								Water	Sedi-ment	Perma-frost (b.s.b.)
				nt						
LE16-10	Samoylov Island	AK_S0 Rim 25-30 cm	sediment	DNA, enrichment	160828	72.36995	126.48256	-	20-30	39
LE16-10	Samoylov Island	AK_S0 Rim 30-35 cm	sediment	DNA, enrichment	160828	72.36995	126.48256	-	20-30	39
LE16-10	Samoylov Island	AK_S0 Rim 30-35 cm	sediment	DNA, enrichment	160828	72.36995	126.48256	-	30-39	39
LE16-10	Samoylov Island	AK_S11 Rim 0-5 cm	sediment	DNA, enrichment	160828	72.36983	126.47791	-	30-39	39
LE16-10	Samoylov Island	AK_S11 Rim 5-15 cm	sediment	DNA, enrichment	160828	72.36983	126.47791	-	0-10	39
LE16-10	Samoylov Island	AK_S11 Rim 5-15 cm	sediment	DNA, enrichment	160828	72.36983	126.47791	-	0-10	50
LE16-10	Samoylov Island	AK_S11 Rim 15-25 cm	sediment	DNA, enrichment	160828	72.36983	126.47791	-	10-20	50
LE16-10	Samoylov Island	AK_S11 Rim 15-25 cm	sediment	DNA, enrichment	160828	72.36983	126.47791	-	10-20	50
LE16-10	Samoylov Island	AK_S11 Rim 25-35 cm	sediment	DNA, enrichment	160828	72.36983	126.47791	-	20-30	50
LE16-10	Samoylov Island	AK_S11 Rim 25-35 cm	sediment	DNA, enrichme	160828	72.36983	126.47791	-	20-30	50

Station	Location	Sample ID	Sample type	Analysis	Sample date [yymmdd]	Latitude N	Longitude E		Depth	[cm]
								Water	Sedi-ment	Perma-frost (b.s.b.)
				nt						
LE16-10	Samoylov Island	AK_S11 Rim 35-40 cm	sediment	DNA, enrichment	160828	72.36983	126.47791	-	30-40	50
LE16-10	Samoylov Island	AK_S9 Rim	sediment	methane	160827	72.37021	126.47942	-	30-40	50
LE16-10	Samoylov Island	AK_S9 Rim	sediment	methane	160827	72.37021	126.47942	-	40-50	50
LE16-10	Samoylov Island	AK_S9 Rim	sediment	methane	160827	72.37021	126.47942	-	0-5	50
LE16-10	Samoylov Island	AK_S9 Rim	sediment	methane	160827	72.37021	126.47942	-	5-10	48
LE16-10	Samoylov Island	AK_S9 Rim	sediment	methane	160827	72.37021	126.47942	-	5-10	48
LE16-10	Samoylov Island	AK_S9 Rim	sediment	methane	160827	72.37021	126.47942	-	10-15	48
LE16-10	Samoylov Island	AK_S9 Rim	sediment	methane	160827	72.37021	126.47942	-	10-15	48
LE16-10	Samoylov Island	AK_S9 CP	sediment	methane	160828	72.37021	126.47942	-	15-20	48
LE16-10	Samoylov Island	AK_S9 CP	sediment	methane	160828	72.37021	126.47942	-	15-20	48
LE16-10	Samoylov Island	AK_S9 CP	sediment	methane	160828	72.37021	126.47942	-	20-25	48
LE16-10	Samoylov Island	AK_S9 CP	sediment	methane	160828	72.37021	126.47942	-	20-25	48
LE16-10	Samoylov Island	AK_S9 CP	sediment	methane	160828	72.37021	126.47942	-	25-30	48
LE16-10	Samoylov Island	AK_S0 CP	sediment	methane	160828	72.36995	126.48256	-	25-30	48
LE16-10	Samoylov Island	AK_S0 CP	sediment	methane	160828	72.36995	126.48256	-	30-35	48
LE16-10	Samoylov Island	AK_S0 CP	sediment	methane	160828	72.36995	126.48256	-	30-35	48
LE16-10	Samoylov Island	AK_S0 CP	sediment	methane	160828	72.36995	126.48256	1	-	48
LE16-10	Samoylov Island	AK_S0 CP	sediment	methane	160828	72.36995	126.48256	1	-	-
LE16-10	Samoylov Island	AK_S0 Rim	sediment	methane	160828	72.36995	126.48256	1	-	-
LE16-10	Samoylov Island	AK_S0 Rim	sediment	methane	160828	72.36995	126.48256	-	0-10	-
LE16-10	Samoylov Island	AK_S0 Rim	sediment	methane	160828	72.36995	126.48256	-	0-10	45

Station	Location	Sample ID	Sample type	Analysis	Sample date [yymmdd]	Latitude N	Longitude E	Depth [cm]		
								Water	Sedi-ment	Perma-frost (b.s.b.)
LE16-10	Samoylov Island	AK_S0 Rim	sediment	methane	160828	72.36995	126.48256	-	10-20	45
LE16-10	Samoylov Island	AK_S11 CP	sediment	methane	160828	72.36983	126.47791	-	10-20	45
LE16-10	Samoylov Island	AK_S11 CP	sediment	methane	160828	72.36983	126.47791	-	20-30	45
LE16-10	Samoylov Island	AK_S11 CP	sediment	methane	160828	72.36983	126.47791	-	20-30	45
LE16-10	Samoylov Island	AK_S11 CP	sediment	methane	160828	72.36983	126.47791	-	30-40	45
LE16-10	Samoylov Island	AK_S11 CP	sediment	methane	160828	72.36983	126.47791	-	30-40	45
LE16-10	Samoylov Island	AK_S11 Rim	sediment	methane	160828	72.36983	126.47791	-	40-45	45
LE16-10	Samoylov Island	AK_S11 Rim	sediment	methane	160828	72.36983	126.47791	-	0-5	45
LE16-10	Samoylov Island	AK_S11 Rim	sediment	methane	160828	72.36983	126.47791	-	5-15	50
LE16-10	Samoylov Island	AK_S11 Rim	sediment	methane	160828	72.36983	126.47791	-	5-15	50
LE16-10	Samoylov Island	AK_S11 Rim	sediment	methane	160828	72.36983	126.47791	-	15-25	50
LE16-10	Samoylov Island	AK_S11 Rim	sediment	methane	160828	72.36983	126.47791	-	15-25	50
LE16-10	Samoylov Island	AK_S0 open water	water	DNA, enrichment	160829	72.36995	126.48256	-	25-35	50
LE16-10	Samoylov Island	AK_S0 open water	water	DNA, enrichment	160830	72.36995	126.48256	-	25-35	50
LE16-10	Samoylov Island	AK_S0 open water	water	DNA, enrichment	160831	72.36995	126.48256	-	35-40	50
LE16-10	Samoylov island	Lena River Reference	water	DNA, enrichment	160830	72.36757	126.4753	-	-	50
LE16-10	Samoylov island	Lena River Reference	water	DNA, enrichment	160830	72.36757	126.4753	-	-	-

Station	Location	Sample ID	Sample type	Analysis	Sample date [yymmdd]	Latitude N	Longitude E	Depth [cm]		
								Water	Sedi-ment	Perma-frost (b.s.b.)
LE16-10	Samoylov island	Lena River Reference	water	DNA, enrichment	160830	72.36757	126.4753	-	-	-
LE16-10	Samoylov island	AK_S9 Rim 23 cm	water	Fe2+	160827	72.37021	126.47942	-	-	-
LE16-10	Samoylov island	AK_S9 Rim 34,5 cm	water	Fe2+	160827	72.37021	126.47942	0-3	-	-
LE16-10	Samoylov island	AK_S9 Rim 46 cm	water	Fe2+	160827	72.37021	126.47942	-	-	-
LE16-10	Samoylov island	AK_S9 Rim 57 cm	water	Fe2+	160827	72.37021	126.47942	-	-	-
LE16-10	Samoylov island	AK_S9 CP 7 cm	water	Fe2+	160827	72.37021	126.47942	-	-	-
LE16-10	Samoylov island	AK_S9 CP 12 cm	water	Fe2+	160827	72.37021	126.47942	-	-	-
LE16-10	Samoylov island	AK_S9 CP 23 cm	water	Fe2+	160827	72.37021	126.47942	-	-	-
LE16-10	Samoylov island	AK_S9 CP 34,5 cm	water	Fe2+	160827	72.37021	126.47942	-	-	-
LE16-10	Samoylov island	AK_S9 CP 37,5 cm	water	Fe2+	160827	72.37021	126.47942	-	-	-
LE16-10	Samoylov island	AK_S0 CP 7 cm	water	Fe2+	160828	72.36995	126.48256	634	0-2	-
LE16-10	Samoylov island	AK_S0 CP 12 cm	water	Fe2+	160828	72.36995	126.48256	634	2-4	-
LE16-10	Samoylov island	AK_S0 CP 23 cm	water	Fe2+	160828	72.36995	126.48256	634	4-6	-
LE16-10	Samoylov island	AK_S0 CP 34,5 cm	water	Fe2+	160828	72.36995	126.48256	634	6-8	-
LE16-10	Samoylov island	AK_S0 CP 46 cm	water	Fe2+	160828	72.36995	126.48256	634	8-10	-

Station	Location	Sample ID	Sample type	Analysis	Sample date [yymmdd]	Latitude N	Longitude E	Depth [cm]		
								Water	Sedi-ment	Perma-frost (b.s.b.)
LE16-10	Samoylov island	AK_S0 CP 50 cm	water	Fe2+	160828	72.36995	126.48256	634	10-12	-
LE16-10	Samoylov island	AK_S0 Rim 17 cm	water	Fe2+	160828	72.36995	126.48256	634	12-14	-
LE16-10	Samoylov island	AK_S0 Rim 23	water	Fe2+	160828	72.36995	126.48256	634	14-16	-
LE16-10	Samoylov island	AK_S0 Rim 34,5 cm	water	Fe2+	160828	72.36995	126.48256	432	0-2	-
LE16-10	Samoylov island	AK_S0 Rim 46 cm	water	Fe2+	160828	72.36995	126.48256	432	2-4	-
LE16-10	Samoylov island	AK_S0 Rim 48 cm	water	Fe2+	160828	72.36995	126.48256	432	4-6	-
LE16-10	Samoylov island	AK_S0 open water	water	Fe2+	160828	72.36995	126.48256	432	6-8	-
LE16-10	Samoylov island	AK_S11 CP 7 cm	water	Fe2+	160828	72.36983	126.47791	432	8-10	-
LE16-10	Samoylov island	AK_S11 CP 12 cm	water	Fe2+	160828	72.36983	126.47791	432	10-12	-
LE16-10	Samoylov island	AK_S11 CP 23 cm	water	Fe2+	160828	72.36983	126.47791	432	12-14	-
LE16-10	Samoylov island	AK_S11 CP 34,5 cm	water	Fe2+	160828	72.36983	126.47791	432	14-18	-
LE16-10	Samoylov island	AK_S11 CP 45 cm	water	Fe2+	160828	72.36983	126.47791	-	0-10	-
LE16-10	Samoylov island	AK_S11 Rim 12 cm	water	Fe2+	160828	72.36983	126.47791	-	10-20	77-78
LE16-10	Samoylov island	AK_S11 Rim 17 cm	water	Fe2+	160828	72.36983	126.47791	-	20-30	77-78
LE16-10	Samoylov island	AK_S11 Rim 23 cm	water	Fe2+	160828	72.36983	126.47791	-	30-40	77-78
LE16-10	Samoylov island	AK_S11 Rim	water	Fe2+	160828	72.36983	126.47791	-	40-50	77-78

Station	Location	Sample ID	Sample type	Analysis	Sample date [yymmdd]	Latitude N	Longitude E	Depth [cm]		
								Water	Sedi-ment	Perma-frost (b.s.b.)
		34,5 cm								
LE16-10	Samoylov island	AK_S11 Rim 46 cm	water	Fe2+	160828	72.36983	126.47791	-	50-60	77-78
LE16-10	Samoylov island	AK_S11 Rim 50 cm	water	Fe2+	160828	72.36983	126.47791	-	60-70	77-78
LE16-10	Samoylov Island	Lena River Reference	water	Fe2+	160830	72.36757	126.4753	-	70-75	77-78
LE16-10	Samoylov Island	Lena River Reference	water	Fe2+	160830	72.36757	126.4753	-	0-15	77-78
LE16-10	Samoylov Island	AK_S9 Rim 23 cm	water	ions (anions)	160827	72.37021	126.47942	-	15-35	100
LE16-10	Samoylov Island	AK_S9 Rim 34,5 cm	water	ions (anions)	160827	72.37021	126.47942	-	35-45	100
LE16-10	Samoylov Island	AK_S9 Rim 46 cm	water	ions (anions)	160827	72.37021	126.47942	-	45-55	100
LE16-10	Samoylov Island	AK_S9 Rim 57 cm	water	ions (anions)	160827	72.37021	126.47942	-	55-60	100
LE16-10	Samoylov Island	AK_S9 CP 7 cm	water	ions (anions)	160827	72.37021	126.47942	-	60-65	100
LE16-10	Samoylov Island	AK_S9 CP 12 cm	water	ions (anions)	160827	72.37021	126.47942	-	65-70	100
LE16-10	Samoylov Island	AK_S9 CP 23 cm	water	ions (anions)	160827	72.37021	126.47942	-	70-80	100
LE16-10	Samoylov Island	AK_S9 CP 34,5 cm	water	ions (anions)	160827	72.37021	126.47942	-	80-90	100
LE16-10	Samoylov Island	AK_S9 CP 37,5 cm	water	ions (anions)	160827	72.37021	126.47942	-	0-10	100
LE16-10	Samoylov Island	AK_S0 CP 7 cm	water	ions (anions)	160828	72.36995	126.48256	-	10-20	76
LE16-10	Samoylov Island	AK_S0 CP 12	water	ions	160828	72.36995	126.48256	-	20-30	76

Station	Location	Sample ID	Sample type	Analysis	Sample date [yymmdd]	Latitude N	Longitude E	Depth [cm]		
								Water	Sedi-ment	Perma-frost (b.s.b.)
		cm		(anions)						
LE16-10	Samoylov Island	AK_S0 CP 23 cm	water	ions (anions)	160828	72.36995	126.48256	-	30-35	76
LE16-10	Samoylov Island	AK_S0 CP 34,5 cm	water	ions (anions)	160828	72.36995	126.48256	-	35-40	76
LE16-10	Samoylov Island	AK_S0 CP 46 cm	water	ions (anions)	160828	72.36995	126.48256	-	40-45	76
LE16-10	Samoylov Island	AK_S0 CP 50 cm	water	ions (anions)	160828	72.36995	126.48256	-	45-50	76
LE16-10	Samoylov Island	AK_S0 Rim 17 cm	water	ions (anions)	160828	72.36995	126.48256	-	50-55	76
LE16-10	Samoylov Island	AK_S0 Rim 23	water	ions (anions)	160828	72.36995	126.48256	-	55-60	76
LE16-10	Samoylov Island	AK_S0 Rim 34,5 cm	water	ions (anions)	160828	72.36995	126.48256	-	60-65	76
LE16-10	Samoylov Island	AK_S0 Rim 46 cm	water	ions (anions)	160828	72.36995	126.48256	-	65-70	76
LE16-10	Samoylov Island	AK_S0 Rim 48 cm	water	ions (anions)	160828	72.36995	126.48256	-	70-76	76
LE16-10	Samoylov Island	AK_S0 open water	water	ions (anions)	160828	72.36995	126.48256	-	10	76
LE16-10	Samoylov Island	AK_S11 CP 7 cm	water	ions (anions)	160828	72.36983	126.47791	-	30	65
LE16-10	Samoylov Island	AK_S11 CP 12 cm	water	ions (anions)	160828	72.36983	126.47791	-	50	65
LE16-10	Samoylov Island	AK_S11 CP 23 cm	water	ions (anions)	160828	72.36983	126.47791	-	55	65
LE16-10	Samoylov Island	AK_S11 CP 34,5 cm	water	ions (anions)	160828	72.36983	126.47791	-	23	65
LE16-10	Samoylov Island	AK_S11 CP 45	water	ions	160828	72.36983	126.47791	-	34.5	57.5

Station	Location	Sample ID	Sample type	Analysis	Sample date [yymmdd]	Latitude N	Longitude E	Depth [cm]		
								Water	Sedi-ment	Perma-frost (b.s.b.)
		cm		(anions)						
LE16-10	Samoylov Island	AK_S11 Rim 12 cm	water	ions (anions)	160828	72.36983	126.47791	-	46	57.5
LE16-10	Samoylov Island	AK_S11 Rim 17 cm	water	ions (anions)	160828	72.36983	126.47791	-	57	57.5
LE16-10	Samoylov Island	AK_S11 Rim 23 cm	water	ions (anions)	160828	72.36983	126.47791	-	7	57.5
LE16-10	Samoylov Island	AK_S11 Rim 34,5 cm	water	ions (anions)	160828	72.36983	126.47791	-	12	39
LE16-10	Samoylov Island	AK_S11 Rim 46 cm	water	ions (anions)	160828	72.36983	126.47791	-	23	39
LE16-10	Samoylov Island	AK_S11 Rim 50 cm	water	ions (anions)	160828	72.36983	126.47791	-	34.5	39
LE16-10	Samoylov Island	Lena River Reference	water	ions (anions)	160830	72.36757	126.4753	-	37.5	39
LE16-10	Samoylov Island	Lena River Reference	water	ions (anions)	160830	72.36757	126.4753	-	7	39
LE16-10	Samoylov Island	AK_S9 Rim 23 cm	water	ions (cations)	160827	72.37021	126.47942	-	12	50
LE16-10	Samoylov Island	AK_S9 Rim 34,5 cm	water	ions (cations)	160827	72.37021	126.47942	-	23	50
LE16-10	Samoylov Island	AK_S9 Rim 46 cm	water	ions (cations)	160827	72.37021	126.47942	-	34.5	50
LE16-10	Samoylov Island	AK_S9 Rim 57 cm	water	ions (cations)	160827	72.37021	126.47942	-	46	50
LE16-10	Samoylov Island	AK_S9 CP 7 cm	water	ions (cations)	160827	72.37021	126.47942	-	50	50
LE16-10	Samoylov Island	AK_S9 CP 12 cm	water	ions (cations)	160827	72.37021	126.47942	-	17	50
LE16-10	Samoylov Island	AK_S9 CP 23	water	ions	160827	72.37021	126.47942	-	23	48

Station	Location	Sample ID	Sample type	Analysis	Sample date [yymmdd]	Latitude N	Longitude E	Depth [cm]		
								Water	Sedi-ment	Perma-frost (b.s.b.)
		cm		(cations)						
LE16-10	Samoylov Island	AK_S9 CP 34,5 cm	water	ions (cations)	160827	72.37021	126.47942	-	34.5	48
LE16-10	Samoylov Island	AK_S9 CP 37,5 cm	water	ions (cations)	160827	72.37021	126.47942	-	46	48
LE16-10	Samoylov Island	AK_S9 Rim 23 cm	water	ions (cations)	160827	72.37021	126.47942	-	48	48
LE16-10	Samoylov Island	AK_S9 Rim 34,5 cm	water	ions (cations)	160827	72.37021	126.47942	1	-	48
LE16-10	Samoylov Island	AK_S9 Rim 46 cm	water	ions (cations)	160827	72.37021	126.47942	-	7	50
LE16-10	Samoylov Island	AK_S9 Rim 57 cm	water	ions (cations)	160827	72.37021	126.47942	-	12	45
LE16-10	Samoylov Island	AK_S9 CP 7 cm	water	ions (cations)	160827	72.37021	126.47942	-	23	45
LE16-10	Samoylov Island	AK_S9 CP 12 cm	water	ions (cations)	160827	72.37021	126.47942	-	34.5	45
LE16-10	Samoylov Island	AK_S9 CP 23 cm	water	ions (cations)	160827	72.37021	126.47942	-	45	45
LE16-10	Samoylov Island	AK_S9 CP 34,5 cm	water	ions (cations)	160827	72.37021	126.47942	-	12	45
LE16-10	Samoylov Island	AK_S9 CP 37,5 cm	water	ions (cations)	160827	72.37021	126.47942	-	17	50
LE16-10	Samoylov Island	AK_S0 CP 7 cm	water	ions (cations)	160828	72.36995	126.48256	-	23	50
LE16-10	Samoylov Island	AK_S0 CP 12 cm	water	ions (cations)	160828	72.36995	126.48256	-	34.5	50
LE16-10	Samoylov Island	AK_S0 CP 23 cm	water	ions (cations)	160828	72.36995	126.48256	-	46	50
LE16-10	Samoylov Island	AK_S0 CP 34,5	water	ions	160828	72.36995	126.48256	-	50	50

Station	Location	Sample ID	Sample type	Analysis	Sample date [yymmdd]	Latitude N	Longitude E	Depth [cm]		
								Water	Sedi-ment	Perma-frost (b.s.b.)
		cm		(cations)						
LE16-10	Samoylov Island	AK_S0 CP 46 cm	water	ions (cations)	160828	72.36995	126.48256	1	-	50
LE16-10	Samoylov Island	AK_S0 CP 50 cm	water	ions (cations)	160828	72.36995	126.48256	1	-	-
LE16-10	Samoylov Island	AK_S0 Rim 17 cm	water	ions (cations)	160828	72.36995	126.48256	-	-	-
LE16-10	Samoylov Island	AK_S0 Rim 23	water	ions (cations)	160828	72.36995	126.48256	-	-	-
LE16-10	Samoylov Island	AK_S0 Rim 34,5 cm	water	ions (cations)	160828	72.36995	126.48256	-	12	-
LE16-10	Samoylov Island	AK_S0 Rim 46 cm	water	ions (cations)	160828	72.36995	126.48256	-	17	77-78
LE16-10	Samoylov Island	AK_S0 Rim 48 cm	water	ions (cations)	160828	72.36995	126.48256	-	23	77-79
LE16-10	Samoylov Island	AK_S0 open water	water	ions (cations)	160828	72.36995	126.48256	-	34.5	77-80
LE16-10	Samoylov Island	AK_S0 CP 7 cm	water	ions (cations)	160828	72.36995	126.48256	-	46	77-81
LE16-10	Samoylov Island	AK_S0 CP 12 cm	water	ions (cations)	160828	72.36995	126.48256	-	57	77-82
LE16-10	Samoylov Island	AK_S0 CP 23 cm	water	ions (cations)	160828	72.36995	126.48256	-	67	77-83
LE16-10	Samoylov Island	AK_S0 CP 34,5 cm	water	ions (cations)	160828	72.36995	126.48256	-	77	77-84
LE16-10	Samoylov Island	AK_S0 CP 46 cm	water	ions (cations)	160828	72.36995	126.48256	-	7	77-85
LE16-10	Samoylov Island	AK_S0 CP 50 cm	water	ions (cations)	160828	72.36995	126.48256	-	12	100
LE16-10	Samoylov Island	AK_S0 Rim 17	water	ions	160828	72.36995	126.48256	-	17	100

Station	Location	Sample ID	Sample type	Analysis	Sample date [yymmdd]	Latitude N	Longitude E	Depth		[cm]
								Water	Sedi-ment	Perma-frost (b.s.b.)
		cm		(cations)						
LE16-10	Samoylov Island	AK_S0 Rim 23	water	ions (cations)	160828	72.36995	126.48256	-	23	100
LE16-10	Samoylov Island	AK_S0 Rim 34,5 cm	water	ions (cations)	160828	72.36995	126.48256	-	34.5	100
LE16-10	Samoylov Island	AK_S0 Rim 46 cm	water	ions (cations)	160828	72.36995	126.48256	-	46	100
LE16-10	Samoylov Island	AK_S0 Rim 48 cm	water	ions (cations)	160828	72.36995	126.48256	-	56	100
LE16-10	Samoylov Island	AK_S0 open water	water	ions (cations)	160828	72.36995	126.48256	-	66	100
LE16-10	Samoylov Island	AK_S11 CP 7 cm	water	ions (cations)	160828	72.36983	126.47791	-	76	100
LE16-10	Samoylov Island	AK_S11 CP 12 cm	water	ions (cations)	160828	72.36983	126.47791	-	86	100
LE16-10	Samoylov Island	AK_S11 CP 23 cm	water	ions (cations)	160828	72.36983	126.47791	-	98	100
LE16-10	Samoylov Island	AK_S11 CP 34,5 cm	water	ions (cations)	160828	72.36983	126.47791	-	10-20	100
LE16-10	Samoylov Island	AK_S11 CP 45 cm	water	ions (cations)	160828	72.36983	126.47791	-	20-30	76
LE16-10	Samoylov Island	AK_S11 Rim 12 cm	water	ions (cations)	160828	72.36983	126.47791	-	30-40	76
LE16-10	Samoylov Island	AK_S11 Rim 17 cm	water	ions (cations)	160828	72.36983	126.47791	-	40-50	76
LE16-10	Samoylov Island	AK_S11 Rim 23 cm	water	ions (cations)	160828	72.36983	126.47791	-	50-60	76
LE16-10	Samoylov Island	AK_S11 Rim 34,5 cm	water	ions (cations)	160828	72.36983	126.47791	-	60-70	76
LE16-10	Samoylov Island	AK_S11 Rim 46	water	ions	160828	72.36983	126.47791	120	-	76

Station	Location	Sample ID	Sample type	Analysis	Sample date [yymmdd]	Latitude N	Longitude E	Depth [cm]		
								Water	Sedi-ment	Perma-frost (b.s.b.)
		cm		(cations)						
LE16-10	Samoylov Island	AK_S11 Rim 50 cm	water	ions (cations)	160828	72.36983	126.47791	480	-	-
LE16-10	Samoylov Island	AK_S11 CP 7 cm	water	ions (cations)	160828	72.36983	126.47791	256	-	-
LE16-10	Samoylov Island	AK_S11 CP 12 cm	water	ions (cations)	160828	72.36983	126.47791	1024	-	-
LE16-10	Samoylov Island	AK_S11 CP 23 cm	water	ions (cations)	160828	72.36983	126.47791	100	-	-
LE16-10	Samoylov Island	AK_S11 CP 34,5 cm	water	ions (cations)	160828	72.36983	126.47791	400	-	-
LE16-10	Samoylov Island	AK_S11 CP 45 cm	water	ions (cations)	160828	72.36983	126.47791	53	-	-
LE16-10	Samoylov Island	AK_S11 Rim 12 cm	water	ions (cations)	160828	72.36983	126.47791	125	-	-
LE16-10	Samoylov Island	AK_S11 Rim 17 cm	water	ions (cations)	160828	72.36983	126.47791	500	-	-
LE16-10	Samoylov Island	AK_S11 Rim 23 cm	water	ions (cations)	160828	72.36983	126.47791	634	-	-
LE16-10	Samoylov Island	AK_S11 Rim 34,5 cm	water	ions (cations)	160828	72.36983	126.47791	53	-	-
LE16-10	Samoylov Island	AK_S11 Rim 46 cm	water	ions (cations)	160828	72.36983	126.47791	90	-	-
LE16-10	Samoylov Island	AK_S11 Rim 50 cm	water	ions (cations)	160828	72.36983	126.47791	340	-	-
LE16-10	Samoylov Island	Lena River Reference	water	ions (cations)	160830	72.36757	126.4753	432	-	-
LE16-10	Samoylov Island	Lena River Reference	water	ions (cations)	160830	72.36757	126.4753	432	-	-
LE16-10	Samoylov Island	Lena River	water	ions	160830	72.36757	126.4753	53	-	-

Station	Location	Sample ID	Sample type	Analysis	Sample date [yymmdd]	Latitude N	Longitude E	Depth [cm]		
								Water	Sedi-ment	Perma-frost (b.s.b.)
		Reference		(cations)						
LE16-10	Samoylov Island	Lena River Reference	water	ions (cations)	160830	72.36757	126.4753	53	-	-
LE16-10	Samoylov island	AK_S9 Rim 23 cm	water	volatile fatty acids	160827	72.37021	126.47942	140	-	-
LE16-10	Samoylov island	AK_S9 Rim 34,5 cm	water	volatile fatty acids	160827	72.37021	126.47942	140	-	-
LE16-10	Samoylov island	AK_S9 Rim 46 cm	water	volatile fatty acids	160827	72.37021	126.47942	500	-	-
LE16-10	Samoylov island	AK_S9 Rim 57 cm	water	volatile fatty acids	160827	72.37021	126.47942	500	-	-
LE16-10	Samoylov island	AK_S9 CP 7 cm	water	volatile fatty acids	160827	72.37021	126.47942	616	-	-
LE16-10	Samoylov island	AK_S9 CP 12 cm	water	volatile fatty acids	160827	72.37021	126.47942	616	-	-
LE16-10	Samoylov island	AK_S9 CP 23 cm	water	volatile fatty acids	160827	72.37021	126.47942	53	-	-
LE16-10	Samoylov island	AK_S9 CP 34,5 cm	water	volatile fatty acids	160827	72.37021	126.47942	53	-	-
LE16-10	Samoylov island	AK_S9 CP 37,5 cm	water	volatile fatty acids	160827	72.37021	126.47942	170	-	-

Station	Location	Sample ID	Sample type	Analysis	Sample date [yymmdd]	Latitude N	Longitude E	Depth Water	Depth Sediment	[cm] Permafrost (b.s.b.)
LE16-10	Samoylov island	AK_S0 CP 7 cm	water	volatile fatty acids	160828	72.36995	126.48256	170	-	-
LE16-10	Samoylov island	AK_S0 CP 12 cm	water	volatile fatty acids	160828	72.36995	126.48256	700	-	-
LE16-10	Samoylov island	AK_S0 CP 23 cm	water	volatile fatty acids	160828	72.36995	126.48256	700	-	-
LE16-10	Samoylov island	AK_S0 CP 34,5 cm	water	volatile fatty acids	160828	72.36995	126.48256	840	-	-
LE16-10	Samoylov island	AK_S0 CP 46 cm	water	volatile fatty acids	160828	72.36995	126.48256	840	-	-
LE16-10	Samoylov island	AK_S0 CP 50 cm	water	volatile fatty acids	160828	72.36995	126.48256	53	-	-
LE16-10	Samoylov island	AK_S0 Rim 17 cm	water	volatile fatty acids	160828	72.36995	126.48256	53	-	-
LE16-10	Samoylov island	AK_S0 Rim 23	water	volatile fatty acids	160828	72.36995	126.48256	200	-	-
LE16-10	Samoylov island	AK_S0 Rim 34,5 cm	water	volatile fatty acids	160828	72.36995	126.48256	200	-	-
LE16-10	Samoylov island	AK_S0 Rim 46 cm	water	volatile fatty acids	160828	72.36995	126.48256	840	-	-

Station	Location	Sample ID	Sample type	Analysis	Sample date [yymmdd]	Latitude N	Longitude E	Depth [cm]		
								Water	Sedi-ment	Perma-frost (b.s.b.)
LE16-10	Samoylov island	AK_S0 Rim 48 cm	water	volatile fatty acids	160828	72.36995	126.48256	840	-	-
LE16-10	Samoylov island	AK_S0 open water	water	volatile fatty acids	160828	72.36995	126.48256	935	-	-
LE16-10	Samoylov island	AK_S11 CP 7 cm	water	volatile fatty acids	160828	72.36983	126.47791	935	-	-
LE16-10	Samoylov island	AK_S11 CP 12 cm	water	volatile fatty acids	160828	72.36983	126.47791	53	-	-
LE16-10	Samoylov island	AK_S11 CP 23 cm	water	volatile fatty acids	160828	72.36983	126.47791	53	-	-
LE16-10	Samoylov island	AK_S11 CP 34,5 cm	water	volatile fatty acids	160828	72.36983	126.47791	250	-	-
LE16-10	Samoylov island	AK_S11 CP 45 cm	water	volatile fatty acids	160828	72.36983	126.47791	250	-	-
LE16-10	Samoylov island	AK_S11 Rim 12 cm	water	volatile fatty acids	160828	72.36983	126.47791	1000	-	-
LE16-10	Samoylov island	AK_S11 Rim 17 cm	water	volatile fatty acids	160828	72.36983	126.47791	1000	-	-
LE16-10	Samoylov island	AK_S11 Rim 23 cm	water	volatile fatty acids	160828	72.36983	126.47791	53	-	-

Station	Location	Sample ID	Sample type	Analysis	Sample date [yymmdd]	Latitude N	Longitude E	Depth [cm]		
								Water	Sedi-ment	Perma-frost (b.s.b.)
LE16-10	Samoylov island	AK_S11 Rim 34,5 cm	water	volatile fatty acids	160828	72.36983	126.47791	53	-	-
LE16-10	Samoylov island	AK_S11 Rim 46 cm	water	volatile fatty acids	160828	72.36983	126.47791	165	-	-
LE16-10	Samoylov island	AK_S11 Rim 50 cm	water	volatile fatty acids	160828	72.36983	126.47791	165	-	-
LE16-10	Samoylov Island	Lena River Reference	water	volatile fatty acids	160830	72.36757	126.4753	640	-	-
LE16-10	Samoylov Island	Lena River Reference	water	volatile fatty acids	160830	72.36757	126.4753	640	-	-
LE16-10	Samoylov Island	AK_S9 Rim 23 cm	water	water (pore) back up	160827	72.37021	126.47942	832	-	-
LE16-10	Samoylov Island	AK_S9 Rim 34,5 cm	water	water (pore) back up	160827	72.37021	126.47942	832	-	-
LE16-10	Samoylov Island	AK_S9 Rim 46 cm	water	water (pore) back up	160827	72.37021	126.47942	53	-	-
LE16-10	Samoylov Island	AK_S9 Rim 57 cm	water	water (pore) back up	160827	72.37021	126.47942	53	-	-
LE16-10	Samoylov Island	AK_S9 CP 7 cm	water	water (pore) back up	160827	72.37021	126.47942	368	-	-

Station	Location	Sample ID	Sample type	Analysis	Sample date [yymmdd]	Latitude N	Longitude E	Depth [cm]		
								Water	Sedi-ment	Perma-frost (b.s.b.)
LE16-10	Samoylov Island	AK_S9 CP 12 cm	water	water (pore) back up	160827	72.37021	126.47942	368	-	-
LE16-10	Samoylov Island	AK_S9 CP 23 cm	water	water (pore) back up	160827	72.37021	126.47942	-	10	-
LE16-10	Samoylov Island	AK_S9 CP 34,5 cm	water	water (pore) back up	160827	72.37021	126.47942	-	30	65
LE16-10	Samoylov Island	AK_S9 CP 37,5 cm	water	water (pore) back up	160827	72.37021	126.47942	-	50	65
LE16-10	Samoylov island	AK_S0 CP 7 cm	water	water (pore) back up	160828	72.36995	126.48256	-	55	65
LE16-10	Samoylov island	AK_S0 CP 12 cm	water	water (pore) back up	160828	72.36995	126.48256	-	23	65
LE16-10	Samoylov island	AK_S0 CP 23 cm	water	water (pore) back up	160828	72.36995	126.48256	-	34.5	57.5
LE16-10	Samoylov island	AK_S0 CP 34,5 cm	water	water (pore) back up	160828	72.36995	126.48256	-	46	57.5
LE16-10	Samoylov island	AK_S0 CP 46 cm	water	water (pore) back up	160828	72.36995	126.48256	-	57	57.5
LE16-10	Samoylov island	AK_S0 CP 50 cm	water	water (pore) back up	160828	72.36995	126.48256	-	7	57.5

Station	Location	Sample ID	Sample type	Analysis	Sample date [yymmdd]	Latitude N	Longitude E	Depth [cm]		
								Water	Sedi-ment	Perma-frost (b.s.b.)
LE16-10	Samoylov island	AK_S0 Rim 17 cm	water	water (pore) back up	160828	72.36995	126.48256	-	12	39
LE16-10	Samoylov island	AK_S0 Rim 23	water	water (pore) back up	160828	72.36995	126.48256	-	23	39
LE16-10	Samoylov island	AK_S0 Rim 34,5 cm	water	water (pore) back up	160828	72.36995	126.48256	-	34.5	39
LE16-10	Samoylov island	AK_S0 Rim 46 cm	water	water (pore) back up	160828	72.36995	126.48256	-	37.5	39
LE16-10	Samoylov island	AK_S0 Rim 48 cm	water	water (pore) back up	160828	72.36995	126.48256	-	7	39
LE16-10	Samoylov island	AK_S11 CP 7 cm	water	water (pore) back up	160828	72.36983	126.47791	-	12	50
LE16-10	Samoylov island	AK_S11 CP 12 cm	water	water (pore) back up	160828	72.36983	126.47791	-	23	50
LE16-10	Samoylov island	AK_S11 CP 23 cm	water	water (pore) back up	160828	72.36983	126.47791	-	34.5	50
LE16-10	Samoylov island	AK_S11 CP 34,5 cm	water	water (pore) back up	160828	72.36983	126.47791	-	46	50
LE16-10	Samoylov island	AK_S11 CP 45 cm	water	water (pore) back up	160828	72.36983	126.47791	-	50	50

Station	Location	Sample ID	Sample type	Analysis	Sample date [yymmdd]	Latitude N	Longitude E	Depth [cm]		
								Water	Sedi-ment	Perma-frost (b.s.b.)
LE16-10	Samoylov island	AK_S11 Rim 12 cm	water	water (pore) back up	160828	72.36983	126.47791	-	17	50
LE16-10	Samoylov island	AK_S11 Rim 17 cm	water	water (pore) back up	160828	72.36983	126.47791	-	23	48
LE16-10	Samoylov island	AK_S11 Rim 23 cm	water	water (pore) back up	160828	72.36983	126.47791	-	34.5	48
LE16-10	Samoylov island	AK_S11 Rim 34,5 cm	water	water (pore) back up	160828	72.36983	126.47791	-	46	48
LE16-10	Samoylov island	AK_S11 Rim 46 cm	water	water (pore) back up	160828	72.36983	126.47791	-	48	48
LE16-10	Samoylov island	AK_S11 Rim 50 cm	water	water (pore) back up	160828	72.36983	126.47791	1	-	48
LE16-10	Samoylov island	AK_S0 open water	water	water back up	160828	72.36995	126.48256	-	7	50
LE16-10	Samoylov island	Lena River Reference	water	water back up	160830	72.36757	126.4753	-	12	45
LE16-11	Sardakh Island	MW_P2 Unknown moss emers	moss	DNA, enrichment	160829	72.56838	127.20632	-	23	45
LE16-11	Sardakh Island	MW_P2 unknown moss submers	moss	DNA, enrichment	160829	72.56838	127.20632	-	34.5	45
LE16-11	Sardakh Island	MW_P2 Scorpidium emers	moss	DNA, enrichment	160829	72.56838	127.20632	-	45	45

Station	Location	Sample ID	Sample type	Analysis	Sample date [yymmdd]	Latitude N	Longitude E		Depth	[cm]
								Water	Sedi-ment	Perma-frost (b.s.b.)
LE16-11	Sardakh Island	Sphagnum next to lake	moss	DNA, enrichment	160829	-	-	-	12	45
LE16-11	Sardakh Island	MW_P3 Scorpidium emers site of pond	moss	DNA, enrichment	160829	72.57157	127.24133	-	17	50
LE16-11	Sardakh Island	MW_P3 Scorpidium emers next to Sphagnum	moss	DNA, enrichment	160829	72.57157	127.24133	-	23	50
LE16-11	Sardakh Island	MW_P3 Sphagnum emers	moss	DNA, enrichment	160829	72.57157	127.24133	-	34.5	50
LE16-11	Sardakh Island	MW_P2 Reference plant (Carex?) emers	plant	DNA, enrichment	160829	72.56838	127.20632	-	46	50
LE16-11	Sardakh Island	MW_P3 Reference plant grass	plant	DNA, enrichment	160829	72.57157	127.24133	-	50	50
LE16-11	Sardakh Island	MW_P2 Pond 1	water	Fe2+	160829	72.56838	127.20632	1	-	50
LE16-11	Sardakh Island	MW_P3 Pond 2	water	Fe2+	160829	72,57157	127.24133	1	-	-
LE16-11	Sardakh Island	MW_P2 Pond 1	water	ions (anions)	160829	72.56838	127.20632	-	-	-
LE16-11	Sardakh Island	MW_P3 Pond 2	water	ions (anions)	160829	72,57157	127.24133	-	-	-
LE16-11	Sardakh Island	MW_P2 Pond 1	water	ions (cations)	160829	72.56838	127.20632	-	12	-
LE16-11	Sardakh Island	MW_P3 Pond 2	water	ions (cations)	160829	72,57157	127.24133	-	17	77-78

Station	Location	Sample ID	Sample type	Analysis	Sample date [yymmdd]	Latitude N	Longitude E	Depth [cm]		
								Water	Sedi-ment	Perma-frost (b.s.b.)
LE16-11	Sardakh Island	MW_P2 Pond 1	water	ions (cations)	160829	72.56838	127.20632	-	23	77-78
LE16-11	Sardakh Island	MW_P3 Pond 2	water	ions (cations)	160829	72,57157	127.24133	-	34.5	77-78
LE16-11	Sardakh Island	MW_P2 Pond 1	water	volatile fatty acids	160829	72.56838	127.20632	-	46	77-78
LE16-11	Sardakh Island	MW_P3 Pond 2	water	volatile fatty acids	160829	72,57157	127.24133	-	57	77-78
LE16-11	Sardakh Island	MW_P2 Pond 1	water	water back up	160829	72.56838	127.20632	-	67	77-78
LE16-11	Sardakh Island	MW_P3 Pond 2	water	water back up	160829	72,57157	127.24133	-	77	77-78
LE16-13	Chay Tumus	air sample	air	methane	160831	72.33682	125.74561	-	7	77-78
LE16-13	Chay Tumus	?	sediment	14C	160831	72.33682	125.74561	-	12	100
LE16-13	Chay Tumus	bottom sediment 0-2 cm	sediment	methane	160831	72.33682	125.74561	-	17	100
LE16-13	Chay Tumus	bottom sediment 0-2 cm	sediment	methane	160831	72.33682	125.74561	-	23	100
LE16-13	Chay Tumus	1081	water	methane	160831	72.33682	125.74561	-	34.5	100
LE16-13	Chay Tumus	1082	water	methane	160831	72.33682	125.74561	-	46	100
LE16-13	Chay Tumus	1083	water	methane	160831	72.33682	125.74561	-	56	100
LE16-13	Chay Tumus	1084	water	methane	160831	72.33682	125.74561	-	66	100
LE16-13	Chay Tumus	1085	water	methane	160831	72.33682	125.74561	-	76	100
LE16-13	Chay Tumus	1086	water	methane	160831	72.33682	125.74561	-	86	100
LE16-13	Chay Tumus	1087	water	methane	160831	72.33682	125.74561	-	98	100

Station	Location	Sample ID	Sample type	Analysis	Sample date [yymmdd]	Latitude N	Longitude E	Depth [cm]		
								Water	Sedi-ment	Perma-frost (b.s.b.)
LE16-13	Chay Tumus	1088	water	methane	160831	72.33682	125.74561	-	10-20	100
LE16-13	Chay Tumus	?	water	plankton	160831	72.33682	125.74561	-	20-30	-
LE16-13	Chay Tumus	bottom sediment	sediment	pore size	160831	72.33682	125.74561	-	30-40	-
LE16-13	Chay Tumus	6 "cDOM"	water	cDOM	160831	72.33682	125.74561	-	40-50	-
LE16-13	Chay Tumus	5 "cDOM"	water	cDOM	160831	72.33682	125.74561	-	50-60	-
LE16-13	Chay Tumus	6 "ions filtered"	water	ions	160831	72.33682	125.74561	-	60-70	-
LE16-13	Chay Tumus	5 "ions filtered"	water	ions	160831	72.33682	125.74561	-	10	-
LE16-13	Chay Tumus	6 "isotopes"	water	isotopes analysis	160831	72.33682	125.74561	-	30	65
LE16-13	Chay Tumus	5 "isotopes"	water	isotopes analysis	160831	72.33682	125.74561	-	50	65
LE16-13	Chay Tumus	bottle 6 turbiditiy	water	turbidity	160831	72.33682	125.74561	-	55	65
LE16-13	Chay Tumus	bottle 7 turbidity	water	turbidity	160831	72.33682	125.74561	-	10	65
LE16-13	Chay Tumus	bottle 5 turbidity	water	turbidity	160831	72.33682	125.74561	-	30	65
LE16-13	Chay Tumus	bottle 8 turbidity	water	turbidity	160831	72.33682	125.74561	-	50	65
LE16-15		9 "ions filtered"	water	ions	160901	72.5112	125.2713	-	55	65
LE16-15		10 "ions filtered"	water	ions	160901	72.5112	125.2713	-	23	65
LE-16-15		9 "cDOM"	water	cDOM	160901	72.5112	125.2713	-	34.5	57.5
LE-16-15		10 "cDOM"	water	cDOM	160901	72.5112	125.2713	-	46	57.5
LE-16-15		9 "isotopes"	water	isotopes analysis	160901	72.5112	125.2713	-	57	57.5
LE-16-15		10 "isotopes"	water	isotopes analysis	160901	72.5112	125.2713	-	7	57.5
LE-16-		bottle 1 turbiditiy	water	turbidity	160901	72.5112	125.2713	-	12	39

Station	Location	Sample ID	Sample type	Analysis	Sample date [yymmdd]	Latitude N	Longitude E	Depth [cm]		
								Water	Sedi-ment	Perma-frost (b.s.b.)
15										
LE-16-15		bottle 4 turbidity	water	turbidity	160901	72.5112	125.2713	-	23	39
LE-16-15		bottle 2 turbidity	water	turbidity	160901	72.5112	125.2713	-	34.5	39
LE-16-15		bottle 3 turbidity	water	turbidity	160901	72.5112	125.2713	-	37.5	39
LE16-17	Nagym	air sample	air	methane	160902	72.87309	123.32154	-	23	39
LE16-17	Nagym	bottom sediment 0-2 cm	sediment	methane	160902	72.87309	123.32154	-	34.5	57.5
LE16-17	Nagym	bottom sediment 0-2 cm	sediment	methane	160902	72.87309	123.32154	-	46	57.5
LE16-17	Nagym	bottom sediment	sediment	pore size	160902	72.87309	123.32154	-	57	57.5
LE16-17	Nagym	17 "cDOM"	water	cDOM	160902	72.87309	123.32154	-	7	57.5
LE16-17	Nagym	14 "cDOM"	water	cDOM	160902	72.87309	123.32154	-	12	39
LE16-17	Nagym	17 "ions filtered"	water	ions	160902	72.87309	123.32154	-	23	39
LE16-17	Nagym	14 "ions filtered"	water	ions	160902	72.87309	123.32154	-	34.5	39
LE16-17	Nagym	17 "isotopes"	water	isotopes analysis	160902	72.87309	123.32154	-	37.5	39
LE16-17	Nagym	14 "isotopes"	water	isotopes analysis	160902	72.87309	123.32154	-	7	39
LE16-17	Nagym	1089	water	methane	160902	72.87309	123.32154	-	12	50
LE16-17	Nagym	1090	water	methane	160902	72.87309	123.32154	-	23	50
LE16-17	Nagym	1091	water	methane	160902	72.87309	123.32154	-	34.5	50
LE16-17	Nagym	1092	water	methane	160902	72.87309	123.32154	-	46	50
LE16-17	Nagym	1093	water	methane	160902	72.87309	123.32154	-	50	50

Station	Location	Sample ID	Sample type	Analysis	Sample date [yymmdd]	Latitude N	Longitude E	Depth [cm]		
								Water	Sedi-ment	Perma-frost (b.s.b.)
LE16-17	Nagym	1094	water	methane	160902	72.87309	123.32154	-	17	50
LE16-17	Nagym	1095	water	methane	160902	72.87309	123.32154	-	23	48
LE16-17	Nagym	1096	water	methane	160902	72.87309	123.32154	-	34.5	48
LE16-17	Nagym	bottle 17 turbiditiy	water	turbidity	160902	72.87309	123.32154	-	46	48
LE16-17	Nagym	bottle 11 turbidity	water	turbidity	160902	72.87309	123.32154	-	48	48
LE16-17	Nagym	bottle13 turbidity	water	turbidity	160902	72.87309	123.32154	1	-	48
LE16-17	Nagym	bottle 14 turbidity	water	turbidity	160902	72.87309	123.32154	-	7	50
LE16-17	Nagym	?	water	plankton	160902	72.87309	123.32154	-	12	50
LE16-18	Terpai Tumus	?	sediment	14C	160903	73.2427	118.9583	-	23	50
LE16-18	Terpai Tumus	?	sediment	14C	160903	73.2427	118.9583	-	34.5	50
LE16-18	Terpai Tumus	?	sediment	14C	160903	73.2427	118.9583	-	46	50
LE16-18	Terpai Tumus	bottom sediment 0-2 cm	sediment	DNA, enrichment	160903	73.2427	118.9583	-	50	50
LE16-18	Terpai Tumus	deep sediment 2-4 cm	sediment	DNA, enrichment	160903	73.2427	118.9583	-	17	50
LE16-18	Terpai Tumus	deep sediment 4-6 cm	sediment	DNA, enrichment	160903	73.2427	118.9583	-	23	48
LE16-18	Terpai Tumus	deep sediment 6-8 cm	sediment	DNA, enrichment	160903	73.2427	118.9583	-	34.5	48
LE16-18	Terpai Tumus	deep sediment 8-10 cm	sediment	DNA, enrichme	160903	73.2427	118.9583	-	46	48

Station	Location	Sample ID	Sample type	Analysis	Sample date [yymmdd]	Latitude N	Longitude E	Depth		[cm]
								Water	Sedi-ment	Perma-frost (b.s.b.)
				nt						
LE16-18	Terpai Tumus	deep sediment 10-12 cm	sediment	DNA, enrichment	160903	73.2427	118.9583	-	48	48
LE16-18	Terpai Tumus	deep sediment 12-14 cm	sediment	DNA, enrichment	160903	73.2427	118.9583	1	-	48
LE16-18	Terpai Tumus	deep sediment 14-16 cm	sediment	DNA, enrichment	160903	73.2427	118.9583	-	7	50
LE16-18	Terpai Tumus	bottom sediment 0-2 cm	sediment	methane	160903	73.2427	118.9583	-	12	45
LE16-18	Terpai Tumus	bottom sediment 0-2 cm	sediment	methane	160903	73.2427	118.9583	-	23	45
LE16-18	Terpai Tumus	deep sediment 14-16 cm	sediment	methane	160903	73.2427	118.9583	-	34.5	45
LE16-18	Terpai Tumus	deep sediment 14-16 cm	sediment	methane	160903	73.2427	118.9583	-	45	45
LE16-18	Terpai Tumus	cDOM	water	cDOM	160903	73.2427	118.9583	-	12	45
LE16-18	Terpai Tumus	cDOM	water	cDOM	160903	73.2427	118.9583	-	17	50
LE16-18	Terpai Tumus	cDOM	water	cDOM	160903	73.2427	118.9583	-	23	50
LE16-18	Terpai Tumus	cDOM	water	cDOM	160903	73.2427	118.9583	-	34.5	50
LE16-18	Terpai Tumus	ions	water	ions	160903	73.2427	118.9583	-	46	50
LE16-18	Terpai Tumus	ions	water	ions	160903	73.2427	118.9583	-	50	50
LE16-18	Terpai Tumus	ions	water	ions	160903	73.2427	118.9583	-	7	50
LE16-18	Terpai Tumus	ions	water	ions	160903	73.2427	118.9583	-	12	45
LE16-18	Terpai Tumus	isotopes	water	isotopes analysis	160903	73.2427	118.9583	-	23	45

Station	Location	Sample ID	Sample type	Analysis	Sample date [yymmdd]	Latitude N	Longitude E	Depth [cm]		
								Water	Sedi-ment	Perma-frost (b.s.b.)
LE16-18	Terpai Tumus	isotopes	water	isotopes analysis	160903	73.2427	118.9583	-	34.5	45
LE16-18	Terpai Tumus	isotopes	water	isotopes analysis	160903	73.2427	118.9583	-	45	45
LE16-18	Terpai Tumus	isotopes	water	isotopes analysis	160903	73.2427	118.9583	-	12	45
LE16-18	Terpai Tumus	1097	water	methane	160903	73.2427	118.9583	-	17	50
LE16-18	Terpai Tumus	1098	water	methane	160903	73.2427	118.9583	-	23	50
LE16-18	Terpai Tumus	1099	water	methane	160903	73.2427	118.9583	-	34,5	50
LE16-18	Terpai Tumus	1100	water	methane	160903	73.2427	118.9583	-	46	50
LE16-18	Terpai Tumus	1101	water	methane	160903	73.2427	118.9583	-	50	50
LE16-18	Terpai Tumus	1102	water	methane	160903	73.2427	118.9583	1	-	50
LE16-18	Terpai Tumus	1103	water	methane	160903	73.2427	118.9583	1	-	-
LE16-18	Terpai Tumus	1104	water	methane	160903	73.2427	118.9583	1	-	-
LE16-18	Terpai Tumus	?	water	plankton	160903	73.2427	118.9583	1	-	-
LE-16-18	Terpai Tumus	bottom sediment	sediment	pore size	160903	73.2427	118.9583	-	-	-
LE16-19	Terpai Tumus	air sample	air	methane	160904	73.3013	118.5404	-	-	-
LE16-19	Terpai Tumus	?	sediment	14C	160904	73.3013	118.5404	-	-	-
LE16-19	Terpai Tumus	bottom sediment 0-2 cm	sediment	DNA, enrichment	160904	73.3013	118.5404	-	-	-
LE16-19	Terpai Tumus	deep sediment 2-4 cm	sediment	DNA, enrichment	160904	73.3013	118.5404	-	12	-
LE16-19	Terpai Tumus	deep sediment 4-6 cm	sediment	DNA, enrichme	160904	73.3013	118.5404	-	17	77-78

Station	Location	Sample ID	Sample type	Analysis	Sample date [yymmdd]	Latitude N	Longitude E	Depth [cm]		
								Water	Sedi-ment	Perma-frost (b.s.b.)
				nt						
LE16-19	Terpai Tumus	deep sediment 6-8 cm	sediment	DNA, enrichment	160904	73.3013	118.5404	-	23	77-78
LE16-19	Terpai Tumus	deep sediment 8-10 cm	sediment	DNA, enrichment	160904	73.3013	118.5404	-	34.5	77-78
LE16-19	Terpai Tumus	deep sediment 10-12 cm	sediment	DNA, enrichment	160904	73.3013	118.5404	-	46	77-78
LE16-19	Terpai Tumus	deep sediment 12-14 cm	sediment	DNA, enrichment	160904	73.3013	118.5404	-	57	77-78
LE16-19	Terpai Tumus	deep sediment 14-18 cm	sediment	DNA, enrichment	160904	73.3013	118.5404	-	67	77-78
LE16-19	Terpai Tumus	bottom sediment 0-2 cm	sediment	methane	160904	73.3013	118.5404	-	77	77-78
LE16-19	Terpai Tumus	deep sediment 2-4 cm	sediment	methane	160904	73.3013	118.5404	-	7	77-78
LE16-19	Terpai Tumus	deep sediment 4-6 cm	sediment	methane	160904	73.3013	118.5404	-	12	100
LE16-19	Terpai Tumus	deep sediment 6-8 cm	sediment	methane	160904	73.3013	118.5404	-	17	100
LE16-19	Terpai Tumus	deep sediment 14-18 cm	sediment	methane	160904	73.3013	118.5404	-	23	100
LE16-19	Terpai Tumus	cDOM	water	cDOM	160904	73.3013	118.5404	-	34.5	100
LE16-19	Terpai Tumus	cDOM	water	cDOM	160904	73.3013	118.5404	-	46	100
LE16-19	Terpai Tumus	cDOM	water	cDOM	160904	73.3013	118.5404	-	56	100

Station	Location	Sample ID	Sample type	Analysis	Sample date [yymmdd]	Latitude N	Longitude E	Depth Water	Depth Sediment	[cm] Permafrost (b.s.b.)
LE16-19	Terpai Tumus	cDOM	water	cDOM	160904	73.3013	118.5404	-	66	100
LE16-19	Terpai Tumus	ions	water	ions	160904	73.3013	118.5404	-	76	100
LE16-19	Terpai Tumus	ions	water	ions	160904	73.3013	118.5404	-	86	100
LE16-19	Terpai Tumus	ions	water	ions	160904	73.3013	118.5404	-	98	100
LE16-19	Terpai Tumus	ions	water	ions	160904	73.3013	118.5404	-	12	100
LE16-19	Terpai Tumus	ions	water	ions	160904	73.3013	118.5404	-	17	77-78
LE16-19	Terpai Tumus	isotopes	water	isotopes analysis	160904	73.3013	118.5404	-	23	77-78
LE16-19	Terpai Tumus	isotopes	water	isotopes analysis	160904	73.3013	118.5404	-	34.5	77-78
LE16-19	Terpai Tumus	isotopes	water	isotopes analysis	160904	73.3013	118.5404	-	46	77-78
LE16-19	Terpai Tumus	isotopes	water	isotopes analysis	160904	73.3013	118.5404	-	57	77-78
LE16-19	Terpai Tumus	1105	water	methane	160904	73.3013	118.5404	-	67	77-78
LE16-19	Terpai Tumus	1106	water	methane	160904	73.3013	118.5404	-	77	77-78
LE16-19	Terpai Tumus	1107	water	methane	160904	73.3013	118.5404	-	7	77-78
LE16-19	Terpai Tumus	1108	water	methane	160904	73.3013	118.5404	-	12	100
LE16-19	Terpai Tumus	1109	water	methane	160904	73.3013	118.5404	-	17	100
LE16-19	Terpai Tumus	1110	water	methane	160904	73.3013	118.5404	-	23	100
LE16-19	Terpai Tumus	1111	water	methane	160904	73.3013	118.5404	-	34.5	100
LE16-19	Terpai Tumus	1112	water	methane	160904	73.3013	118.5404	-	46	100
LE16-19	Terpai Tums	?	water	plankton	160904	73.3013	118.5404	-	56	100
LE16-22	Mamontov Klyk	air sample	air	methane	160905	73.71058	117.17025	-	66	100
LE16-22	Mamontov Klyk	cDOM	water	cDOM	160905	73.71058	117.17025	-	76	100

Station	Location	Sample ID	Sample type	Analysis	Sample date [yymmdd]	Latitude N	Longitude E	Depth [cm]		
								Water	Sedi-ment	Perma-frost (b.s.b.)
LE16-22	Mamontov Klyk	cDOM	water	cDOM	160905	73.71058	117.17025	-	86	100
LE16-22	Mamontov Klyk	cDOM	water	cDOM	160905	73.71058	117.17025	-	98	100
LE16-22	Mamontov Klyk	cDOM	water	cDOM	160905	73.71058	117.17025	-	10-20	100
LE16-22	Mamontov Klyk	ions	water	ions	160905	73.71058	117.17025	-	20-30	-
LE16-22	Mamontov Klyk	ions	water	ions	160905	73.71058	117.17025	-	30-40	-
LE16-22	Mamontov Klyk	ions	water	ions	160905	73.71058	117.17025	-	40-50	-
LE16-22	Mamontov Klyk	ions	water	ions	160905	73.71058	117.17025	-	50-60	-
LE16-22	Mamontov Klyk	ions	water	ions	160905	73.71058	117.17025	-	60-70	-
LE16-22	Mamontov Klyk	ions	water	ions	160905	73.71058	117.17025	-	10-20	-
LE16-22	Mamontov Klyk	ions	water	ions	160905	73.71058	117.17025	-	20-30	-
LE16-22	Mamontov Klyk	ions	water	ions	160905	73.71058	117.17025	-	30-40	-
LE16-22	Mamontov Klyk	isotopes	water	isotopes analysis	160905	73.71058	117.17025	-	40-50	-
LE16-22	Mamontov Klyk	isotopes	water	isotopes analysis	160905	73.71058	117.17025	-	50-60	-
LE16-22	Mamontov Klyk	isotopes	water	isotopes analysis	160905	73.71058	117.17025	-	60-70	-
LE16-22	Mamontov Klyk	isotopes	water	isotopes analysis	160905	73.71058	117.17025	120	-	-
LE16-22	Mamontov Klyk	1113	water	methane	160905	73.71058	117.17025	480	-	-
LE16-22	Mamontov Klyk	1114	water	methane	160905	73.71058	117.17025	256	-	-
LE16-22	Mamontov Klyk	1115	water	methane	160905	73.71058	117.17025	1024	-	-
LE16-22	Mamontov Klyk	1116	water	methane	160905	73.71058	117.17025	100	-	-
LE16-22	Mamontov Klyk	1117	water	methane	160905	73.71058	117.17025	400	-	-
LE16-22	Mamontov Klyk	1118	water	methane	160905	73.71058	117.17025	53	-	-

Station	Location	Sample ID	Sample type	Analysis	Sample date [yymmdd]	Latitude N	Longitude E	Depth [cm]		
								Water	Sedi-ment	Perma-frost (b.s.b.)
LE16-22	Mamontov Klyk	1119	water	methane	160905	73.71058	117.17025	125	-	-
LE16-22	Mamontov Klyk	1120	water	methane	160905	73.71058	117.17025	500	-	-
LE16-22	Mamontov Klyk	?	water	plankton	160905	73.71058	117.17025	634	-	-
LE16-23	Transect MK to LD	isotopes	water	isotopes analysis	160905	73.6316	118.9889	53	-	-
LE16-23	Transect MK to LD	1121	water	methane	160905	73.6316	118.9889	90	-	-
LE16-23	Transect MK to LD	1122	water	methane	160905	73.6316	118.9889	340	-	-
LE16-23	Transect MK to LD	?	water	plankton	160905	73.6316	118.9889	432	-	-
LE16-24	Olenyokskaya channel	air sample	air	methane	160906	72.29042	126.08268	53	-	-
LE16-24	Olenyokskaya channel	cDOM	water	cDOM	160906	72.29042	126.08268	140	-	-
LE16-24	Olenyokskaya channel	cDOM	water	cDOM	160906	72.29042	126.08268	500	-	-
LE16-24	Olenyokskaya channel	cDOM	water	cDOM	160906	72.29042	126.08268	616	-	-
LE16-24	Olenyokskaya channel	cDOM	water	cDOM	160906	72.29042	126.08268	922	-	-
LE16-24	Olenyokskaya channel	ions	water	ions	160906	72.29042	126.08268	53	-	-
LE16-24	Olenyokskaya channel	ions	water	ions	160906	72.29042	126.08268	170	-	-
LE16-24	Olenyokskaya channel	ions	water	ions	160906	72.29042	126.08268	700	-	-
LE16-24	Olenyokskaya channel	ions	water	ions	160906	72.29042	126.08268	840	-	-

Station	Location	Sample ID	Sample type	Analysis	Sample date [yymmdd]	Latitude N	Longitude E	Depth [cm]		
								Water	Sedi-ment	Perma-frost (b.s.b.)
LE16-24	Olenyokskaya channel	ions	water	ions	160906	72.29042	126.08268	53	-	-
LE16-24	Olenyokskaya channel	ions	water	ions	160906	72.29042	126.08268	200	-	-
LE16-24	Olenyokskaya channel	ions	water	ions	160906	72.29042	126.08268	840	-	-
LE16-24	Olenyokskaya channel	ions	water	ions	160906	72.29042	126.08268	935	-	-
LE16-24	Olenyokskaya channel	isotopes	water	isotopes analysis	160906	72.29042	126.08268	53	-	-
LE16-24	Olenyokskaya channel	isotopes	water	isotopes analysis	160906	72.29042	126.08268	250	-	-
LE16-24	Olenyokskaya channel	isotopes	water	isotopes analysis	160906	72.29042	126.08268	1000	-	-
LE16-24	Olenyokskaya channel	isotopes	water	isotopes analysis	160906	72.29042	126.08268	53	-	-
LE16-24	Olenyokskaya channel	1123	water	methane	160906	72.29042	126.08268	165	-	-
LE16-24	Olenyokskaya channel	1124	water	methane	160906	72.29042	126.08268	640	-	-
LE16-24	Olenyokskaya channel	1125	water	methane	160906	72.29042	126.08268	832	-	-
LE16-24	Olenyokskaya channel	1126	water	methane	160906	72.29042	126.08268	53	-	-
LE16-24	Olenyokskaya channel	1127	water	methane	160906	72.29042	126.08268	368	-	-
LE16-24	Olenyokskaya channel	1128	water	methane	160906	72.29042	126.08268	-	5	-
LE16-24	Olenyokskaya channel	1129	water	methane	160906	72.29042	126.08268	-	15	65

Station	Location	Sample ID	Sample type	Analysis	Sample date [yymmdd]	Latitude N	Longitude E	Depth [cm]		
								Water	Sedi-ment	Perma-frost (b.s.b.)
LE16-24	Olenyokskaya channel	1130	water	methane	160906	72.29042	126.08268	-	20-30	65
LE16-24	Olenyokskaya channel	botle 9 turbidity	water	turbidity	160906	72.29042	126.08268	-	30-40	65
LE16-24	Olenyokskaya channel	bottle 12 turbidity	water	turbidity	160906	72.29042	126.08268	-	40-50	65
LE16-24	Olenyokskaya channel	bottle 10 turbidity	water	turbidity	160906	72.29042	126.08268	-	50-55	65
LE16-24	Olenyokskaya channel	bottle 18 turbidity	water	turbidity	160906	72.29042	126.08268	-	55-60	65
LE16-24	Olenyokskaya channel	?	water	plankton	160906	72.29042	126.08268	-	60-65	65
LE16-25	Bykovsky channel	ions	water	ions	160907	72.41058	126.88885	-	5	65
LE16-25	Bykovsky channel	ions	water	ions	160907	72.41058	126.88885	-	10	57.5
LE16-25	Bykovsky channel	ions	water	ions	160907	72.41058	126.88885	-	15	57.5
LE16-25	Bykovsky channel	ions	water	ions	160907	72.41058	126.88885	-	20	57.5
LE16-25	Bykovsky channel	ions	water	ions	160907	72.41058	126.88885	-	25	57.5
LE16-25	Bykovsky channel	ions	water	ions	160907	72.41058	126.88885	-	30	57.5
LE16-25	Bykovsky channel	ions	water	ions	160907	72.41058	126.88885	-	33	57.5
LE16-25	Bykovsky channel	ions	water	ions	160907	72.41058	126.88885	-	5	57.5
LE16-25	Bykovsky channel	isotopes	water	isotopes analysis	160907	72.41058	126.88885	-	15	39

Station	Location	Sample ID	Sample type	Analysis	Sample date [yymmdd]	Latitude N	Longitude E	Depth Water	Depth Sediment	[cm] Permafrost (b.s.b.)
LE16-25	Bykovsky channel	isotopes	water	isotopes analysis	160907	72.41058	126.88885	-	25	39
LE16-25	Bykovsky channel	isotopes	water	isotopes analysis	160907	72.41058	126.88885	-	30	39
LE16-25	Bykovsky channel	isotopes	water	isotopes analysis	160907	72.41058	126.88885	-	39	39
LE16-25	Bykovsky channel	1131	water	methane	160907	72.41058	126.88885	-	5	39
LE16-25	Bykovsky channel	1132	water	methane	160907	72.41058	126.88885	-	15	50
LE16-25	Bykovsky channel	1133	water	methane	160907	72.41058	126.88885	-	25	50
LE16-25	Bykovsky channel	1134	water	methane	160907	72.41058	126.88885	-	35	50
LE16-25	Bykovsky channel	1135	water	methane	160907	72.41058	126.88885	-	45	50
LE16-25	Bykovsky channel	1136	water	methane	160907	72.41058	126.88885	-	7.5	50
LE16-25	Bykovsky channel	1137	water	methane	160907	72.41058	126.88885	-	15	48
LE16-25	Bykovsky channel	1138	water	methane	160907	72.41058	126.88885	-	25	48
LE16-25	Bykovsky channel	air sample	water	methane	160907	72.41058	126.88885	-	35	48
LE16-25	Bykovsky channel	bottle 29 turbidity	water	turbidity	160907	72.41058	126.88885	-	5	48
LE16-25	Bykovsky channel	bottle 30 turbidity	water	turbidity	160907	72.41058	126.88885	-	15	45
LE16-26	Bykovsky channel	air sample	methane	methane	160907	72.23118	127.96187	-	25	45

Station	Location	Sample ID	Sample type	Analysis	Sample date [yymmdd]	Latitude N	Longitude E	Depth [cm]		
								Water	Sedi-ment	Perma-frost (b.s.b.)
LE16-26	Bykovsky channel	ions	water	ions	160907	72.23118	127.96187	-	35	45
LE16-26	Bykovsky channel	ions	water	ions	160907	72.23118	127.96187	-	43.5	45
LE16-26	Bykovsky channel	ions	water	ions	160907	72.23118	127.96187	-	5	45
LE16-26	Bykovsky channel	ions	water	ions	160907	72.23118	127.96187	-	10	50
LE16-26	Bykovsky channel	ions	water	ions	160907	72.23118	127.96187	-	20	50
LE16-26	Bykovsky channel	ions	water	ions	160907	72.23118	127.96187	-	30	50
LE16-26	Bykovsky channel	isotopes	water	isotopes analysis	160907	72.23118	127.96187	-	37	50
LE16-26	Bykovsky channel	isotopes	water	isotopes analysis	160907	72.23118	127.96187	-	40	50
LE16-26	Bykovsky channel	isotopes	water	isotopes analysis	160907	72.23118	127.96187	53	-	50
LE16-26	Bykovsky channel	1139	water	methane	160907	72.23118	127.96187	53	-	-
LE16-26	Bykovsky channel	1140	water	methane	160907	72.23118	127.96187	120	-	-
LE16-26	Bykovsky channel	1141	water	methane	160907	72.23118	127.96187	120	-	-
LE16-26	Bykovsky channel	1142	water	methane	160907	72.23118	127.96187	480	-	-
LE16-26	Bykovsky channel	1143	water	methane	160907	72.23118	127.96187	480	-	-
LE16-26	Bykovsky channel	1144	water	methane	160907	72.23118	127.96187	600	-	-

Station	Location	Sample ID	Sample type	Analysis	Sample date [yymmdd]	Latitude N	Longitude E	Depth [cm]		
								Water	Sedi-ment	Perma-frost (b.s.b.)
LE16-26	Bykovsky channel	bottle 25 turbidity	water	turbidity	160907	72.23118	127.96187	600	-	-
LE16-26	Bykovsky channel	bottle 20 turbidity	water	turbidity	160907	72.23118	127.96187	600	0-2	-
LE16-27	Bykovsky Mys	air sample	air	methane	190608	72.00485	129.09566	600	0-2	-
LE16-27	Bykovsky Mys	deep sediment 0-2 cm	sediment	methane	190608	72.00485	129.09566	-100	-	-
LE16-27	Bykovsky Mys	deep sediment 0-2 cm	sediment	methane	190608	72.00485	129.09566	53	-	-
LE16-27	Bykovsky Mys	bottom sediment	sediment	pore size	160908	72.00485	129.09566	53	-	-
LE16-27	Bykovsky Mys	ions	water	ions	160908	72.00485	129.09566	100	-	-
LE16-27	Bykovsky Mys	ions	water	ions	160908	72.00485	129.09566	100	-	-
LE16-27	Bykovsky Mys	ions	water	ions	160908	72.00485	129.09566	400	-	-
LE16-27	Bykovsky Mys	ions	water	ions	160908	72.00485	129.09566	400	-	-
LE16-27	Bykovsky Mys	ions	water	ions	160908	72.00485	129.09566	522	-	-
LE16-27	Bykovsky Mys	ions	water	ions	160908	72.00485	129.09566	522	-	-
LE16-27	Bykovsky Mys	ions	water	ions	160908	72.00485	129.09566	522	0-2	-
LE16-27	Bykovsky Mys	ions	water	ions	160908	72.00485	129.09566	522	0-2	-
LE16-27	Bykovsky Mys	isotopes	water	isotopes analysis	160908	72.00485	129.09566	-100	-	-
LE16-27	Bykovsky Mys	isotopes	water	isotopes analysis	160908	72.00485	129.09566	53	-	-
LE16-27	Bykovsky Mys	isotopes	water	isotopes analysis	160908	72.00485	129.09566	53	-	-
LE16-27	Bykovsky Mys	isotopes	water	isotopes analysis	160908	72.00485	129.09566	125	-	-
LE16-27	Bykovsky Mys	1145	water	methane	160908	72.00485	129.09566	125	-	-

Station	Location	Sample ID	Sample type	Analysis	Sample date [yymmdd]	Latitude N	Longitude E	Depth [cm]		
								Water	Sedi-ment	Perma-frost (b.s.b.)
LE16-27	Bykovsky Mys	1146	water	methane	160908	72.00485	129.09566	500	-	-
LE16-27	Bykovsky Mys	1147	water	methane	160908	72.00485	129.09566	500	-	-
LE16-27	Bykovsky Mys	1148	water	methane	160908	72.00485	129.09566	634	-	-
LE16-27	Bykovsky Mys	1149	water	methane	160908	72.00485	129.09566	634	-	-
LE16-27	Bykovsky Mys	1150	water	methane	160908	72.00485	129.09566	634	0-2	-
LE16-27	Bykovsky Mys	1151	water	methane	160908	72.00485	129.09566	634	0-2	-
LE16-27	Bykovsky Mys	1152	water	methane	160908	72.00485	129.09566	634	14-16	-
LE16-27	Bykovsky Mys	bottle 27 turbidity	water	turbidity	160908	72.00485	129.09566	634	14-16	-
LE16-27	Bykovsky Mys	bottle 28 turbidity	water	turbidity	160908	72.00485	129.09566	53	-	-
LE16-27	Bykovsky Mys	?	water	plankton	160908	72.00485	129.09566	53	-	-
LE16-29	Ivashkina lagoon	Core 1	sediment	DNA	160909	71.73411	129.41125	90	-	-
LE16-29	Ivashkina lagoon	Core 1	sediment	DNA	160909	71.73411	129.41125	90	-	-
LE16-29	Ivashkina lagoon	Core 1	sediment	DNA	160909	71.73411	129.41125	340	-	-
LE16-29	Ivashkina lagoon	Core 1	sediment	DNA	160909	71.73411	129.41125	340	-	-
LE16-29	Ivashkina lagoon	Core 1	sediment	DNA	160909	71.73411	129.41125	432	-	-
LE16-29	Ivashkina lagoon	Core 1	sediment	DNA	160909	71.73411	129.41125	432	-	-
LE16-29	Ivashkina lagoon	Core 1	sediment	DNA	160909	71.73411	129.41125	432	0-2	-
LE16-29	Ivashkina lagoon	Core 1	sediment	DNA	160909	71.73411	129.41125	432	2-4	-

Station	Location	Sample ID	Sample type	Analysis	Sample date [yymmdd]	Latitude N	Longitude E		Depth [cm]	
								Water	Sedi-ment	Perma-frost (b.s.b.)
LE16-29	Ivashkina lagoon	Core 2	sediment	DNA	160909	71.73512	129.40875	432	4-6	-
LE16-29	Ivashkina lagoon	Core 2	sediment	DNA	160909	71.73512	129.40875	432	6-8	-
LE16-29	Ivashkina lagoon	Core 2	sediment	DNA	160909	71.73512	129.40875	432	14-18	-
LE16-29	Ivashkina lagoon	Core 2	sediment	DNA	160909	71.73512	129.40875	-100	-	-
LE16-29	Ivashkina lagoon	Core 2	sediment	DNA	160909	71.73512	129.40875	53	-	-
LE16-29	Ivashkina lagoon	Core 2	sediment	DNA	160909	71.73512	129.40875	53	-	-
LE16-29	Ivashkina lagoon	Core 2	sediment	DNA	160909	71.73512	129.40875	140	-	-
LE16-29	Ivashkina lagoon	Core 1	sediment	DNA, enrichment	160909	71.73411	129.41125	140	-	-
LE16-29	Ivashkina lagoon	Core 1	sediment	DNA, enrichment	160909	71.73411	129.41125	500	-	-
LE16-29	Ivashkina lagoon	Core 1	sediment	DNA, enrichment	160909	71.73411	129.41125	500	-	-
LE16-29	Ivashkina lagoon	Core 1	sediment	DNA, enrichment	160909	71.73411	129.41125	616	-	-
LE16-29	Ivashkina lagoon	Core 1	sediment	DNA, enrichment	160909	71.73411	129.41125	616	-	-
LE16-29	Ivashkina	Core 1	sediment	DNA,	160909	71.73411	129.41125	-100	-	-

Station	Location	Sample ID	Sample type	Analysis	Sample date [yymmdd]	Latitude N	Longitude E	Depth [cm]		
								Water	Sedi-ment	Perma-frost (b.s.b.)
	lagoon			enrichment						
LE16-29	Ivashkina lagoon	Core 1	sediment	DNA, enrichment	160909	71.73411	129.41125	53	-	-
LE16-29	Ivashkina lagoon	Core 1	sediment	DNA, enrichment	160909	71.73411	129.41125	53	-	-
LE16-29	Ivashkina lagoon	Core 2	sediment	DNA, enrichment	160909	71.73512	129.40875	53	-	-
LE16-29	Ivashkina lagoon	Core 2	sediment	DNA, enrichment	160909	71.73512	129.40875	53	-	-
LE16-29	Ivashkina lagoon	Core 2	sediment	DNA, enrichment	160909	71.73512	129.40875	170	-	-
LE16-29	Ivashkina lagoon	Core 2	sediment	DNA, enrichment	160909	71.73512	129.40875	170	-	-
LE16-29	Ivashkina lagoon	Core 2	sediment	DNA, enrichment	160909	71.73512	129.40875	700	-	-
LE16-29	Ivashkina lagoon	Core 2	sediment	DNA, enrichment	160909	71.73512	129.40875	700	-	-
LE16-29	Ivashkina lagoon	Core 2	sediment	DNA, enrichment	160909	71.73512	129.40875	840	-	-
LE16-29	Ivashkina lagoon	Core 2	sediment	DNA, enrichme	160909	71.73512	129.40875	840	-	-

Station	Location	Sample ID	Sample type	Analysis	Sample date [yymmdd]	Latitude N	Longitude E	Depth		[cm]
								Water	Sedi-ment	Perma-frost (b.s.b.)
				nt						
LE16-29	Ivashkina lagoon	Core 2	sediment	DNA, enrichment	160909	71.73512	129.40875	-100	-	-
LE16-29	Ivashkina lagoon	Core 1	sediment	methane	160909	71.73411	129.41125	53	-	-
LE16-29	Ivashkina lagoon	Core 1	sediment	methane	160909	71.73411	129.41125	53	-	-
LE16-29	Ivashkina lagoon	Core 1	sediment	methane	160909	71.73411	129.41125	200	-	-
LE16-29	Ivashkina lagoon	Core 1	sediment	methane	160909	71.73411	129.41125	200	-	-
LE16-29	Ivashkina lagoon	Core 1	sediment	methane	160909	71.73411	129.41125	830	-	-
LE16-29	Ivashkina lagoon	Core 1	sediment	methane	160909	71.73411	129.41125	830	-	-
LE16-29	Ivashkina lagoon	Core 1	sediment	methane	160909	71.73411	129.41125	935	-	-
LE16-29	Ivashkina lagoon	Core 1	sediment	methane	160909	71.73411	129.41125	935	-	-
LE16-29	Ivashkina lagoon	Core 2	sediment	methane	160909	71.73512	129.40875	-100	-	-
LE16-29	Ivashkina lagoon	Core 2	sediment	methane	160909	71.73512	129.40875	53	-	-
LE16-29	Ivashkina lagoon	Core 2	sediment	methane	160909	71.73512	129.40875	53	-	-
LE16-29	Ivashkina lagoon	Core 2	sediment	methane	160909	71.73512	129.40875	250	-	-
LE16-29	Ivashkina lagoon	Core 2	sediment	methane	160909	71.73512	129.40875	250	-	-

Station	Location	Sample ID	Sample type	Analysis	Sample date [yymmdd]	Latitude N	Longitude E	Depth [cm]		
								Water	Sedi-ment	Perma-frost (b.s.b.)
LE16-29	Ivashkina lagoon	Core 2	sediment	methane	160909	71.73512	129.40875	1000	-	-
LE16-29	Ivashkina lagoon	Core 2	sediment	methane	160909	71.73512	129.40875	1000	-	-
LE16-29	Ivashkina lagoon	Core 2	sediment	methane	160909	71.73512	129.40875	-100	-	-
LE16-29	Ivashkina lagoon	Core 2	sediment	methane	160909	71.73512	129.40875	53	-	-
LE16-29	Ivashkina lagoon	Core 2	sediment	methane	160909	71.73512	129.40875	53	-	-
LE16-29	Ivashkina lagoon	Core 2	sediment	methane	160909	71.73512	129.40875	165	-	-
LE16-29	Ivashkina lagoon	Core 2	sediment	methane	160909	71.73512	129.40875	165	-	-
LE16-29	Ivashkina lagoon	Core 1	water	Fe2+	160909	71.73411	129.41125	640	-	-
LE16-29	Ivashkina lagoon	Core 1	water	Fe2+	160909	71.73411	129.41125	640	-	-
LE16-29	Ivashkina lagoon	Core 1	water	Fe2+	160909	71.73411	129.41125	832	-	-
LE16-29	Ivashkina lagoon	Core 1	water	Fe2+	160909	71.73411	129.41125	832	-	-
LE16-29	Ivashkina lagoon	Core 1	water	Fe2+	160909	71.73411	129.41125	832	0-2	-
LE16-29	Ivashkina lagoon	Core 1	water	Fe2+	160909	71.73411	129.41125	832	0-2	-
LE16-29	Ivashkina lagoon	Core 1	water	Fe2+	160909	71.73411	129.41125	-100	-	-
LE16-29	Ivashkina lagoon	Core 1	water	Fe2+	160909	71.73411	129.41125	-	0-10	-

Station	Location	Sample ID	Sample type	Analysis	Sample date [yymmdd]	Latitude N	Longitude E	Depth [cm]		
								Water	Sedi-ment	Perma-frost (b.s.b.)
LE16-29	Ivashkina lagoon	Core 2	water	Fe2+	160909	71.73512	129.40875	-	10-20	
LE16-29	Ivashkina lagoon	Core 2	water	Fe2+	160909	71.73512	129.40875	-	20-30	
LE16-29	Ivashkina lagoon	Core 2	water	Fe2+	160909	71.73512	129.40875	-	30-40	
LE16-29	Ivashkina lagoon	Core 2	water	Fe2+	160909	71.73512	129.40875	-	40-50	
LE16-29	Ivashkina lagoon	Core 2	water	Fe2+	160909	71.73512	129.40875	-	60-50	
LE16-29	Ivashkina lagoon	Core 2	water	Fe2+	160909	71.73512	129.40875	-	70-60	
LE16-29	Ivashkina lagoon	Core 2	water	Fe2+	160909	71.73512	129.40875	-	70-75	
LE16-29	Ivashkina lagoon	Core 2	water	Fe2+	160909	71.73512	129.40875	-	0-15	
LE16-29	Ivashkina lagoon	Core 2	water	Fe2+	160909	71.73512	129.40875	-	15-25	
LE16-29	Ivashkina lagoon	Core 2	water	Fe2+	160909	71.73512	129.40875	-	25-30	
LE16-29	Ivashkina lagoon	Core 2	water	Fe2+	160909	71.73512	129.40875	-	30-45	
LE16-29	Ivashkina lagoon	Core 1	water	ions (anions)	160909	71.73411	129.41125	-	45-50	
LE16-29	Ivashkina lagoon	Core 1	water	ions (anions)	160909	71.73411	129.41125	-	50-55	
LE16-29	Ivashkina lagoon	Core 1	water	ions (anions)	160909	71.73411	129.41125	-	55-60	
LE16-29	Ivashkina lagoon	Core 1	water	ions (anions)	160909	71.73411	129.41125	-	60-65	

Station	Location	Sample ID	Sample type	Analysis	Sample date [yymmdd]	Latitude N	Longitude E	Water	Depth	[cm]
									Sedi-ment	Perma-frost (b.s.b.)
LE16-29	Ivashkina lagoon	Core 1	water	ions (anions)	160909	71.73411	129.41125	-	65-70	
LE16-29	Ivashkina lagoon	Core 1	water	ions (anions)	160909	71.73411	129.41125	-	70-80	
LE16-29	Ivashkina lagoon	Core 1	water	ions (anions)	160909	71.73411	129.41125	-	80-90	
LE16-29	Ivashkina lagoon	Core 1	water	ions (anions)	160909	71.73411	129.41125	5	-	
LE16-29	Ivashkina lagoon	Core 2	water	ions (anions)	160909	71.73512	129.40875	5	-	-
LE16-29	Ivashkina lagoon	Core 2	water	ions (anions)	160909	71.73512	129.40875	53	-	-
LE16-29	Ivashkina lagoon	Core 2	water	ions (anions)	160909	71.73512	129.40875	53	-	-
LE16-29	Ivashkina lagoon	Core 2	water	ions (anions)	160909	71.73512	129.40875	368	-	-
LE16-29	Ivashkina lagoon	Core 2	water	ions (anions)	160909	71.73512	129.40875	368	-	-
LE16-29	Ivashkina lagoon	Core 2	water	ions (anions)	160909	71.73512	129.40875	-	0-10	-
LE16-29	Ivashkina lagoon	Core 2	water	ions (anions)	160909	71.73512	129.40875	-	10-20	76
LE16-29	Ivashkina lagoon	Core 2	water	ions (anions)	160909	71.73512	129.40875	-	20-30	76
LE16-29	Ivashkina lagoon	Core 2	water	ions (anions)	160909	71.73512	129.40875	-	30-35	76
LE16-29	Ivashkina lagoon	Core 2	water	ions (anions)	160909	71.73512	129.40875	-	35-40	76
LE16-29	Ivashkina lagoon	Core 2	water	ions (anions)	160909	71.73512	129.40875	-	40-45	76

Station	Location	Sample ID	Sample type	Analysis	Sample date [yymmdd]	Latitude N	Longitude E	Depth		[cm]
								Water	Sedi-ment	Perma-frost (b.s.b.)
LE16-29	Ivashkina lagoon	Core 1	water	ions (cations)	160909	71.73411	129.41125	-	45-50	76
LE16-29	Ivashkina lagoon	Core 1	water	ions (cations)	160909	71.73411	129.41125	-	50-55	76
LE16-29	Ivashkina lagoon	Core 1	water	ions (cations)	160909	71.73411	129.41125	-	55-60	76
LE16-29	Ivashkina lagoon	Core 1	water	ions (cations)	160909	71.73411	129.41125	-	60-65	76
LE16-29	Ivashkina lagoon	Core 1	water	ions (cations)	160909	71.73411	129.41125	-	65-70	76
LE16-29	Ivashkina lagoon	Core 1	water	ions (cations)	160909	71.73411	129.41125	-	70-76	76
LE16-29	Ivashkina lagoon	Core 1	water	ions (cations)	160909	71.73411	129.41125	0-600	-	76
LE16-29	Ivashkina lagoon	Core 1	water	ions (cations)	160909	71.73411	129.41125	0-522	-	-
LE16-29	Ivashkina lagoon	Core 2	water	ions (cations)	160909	71.73512	129.40875	0-634	-	-
LE16-29	Ivashkina lagoon	Core 2	water	ions (cations)	160909	71.73512	129.40875	0-432	-	-
LE16-29	Ivashkina lagoon	Core 2	water	ions (cations)	160909	71.73512	129.40875	0-616	-	-
LE16-29	Ivashkina lagoon	Core 2	water	ions (cations)	160909	71.73512	129.40875	0-922	-	-
LE16-29	Ivashkina lagoon	Core 2	water	ions (cations)	160909	71.73512	129.40875	0-840	-	-
LE16-29	Ivashkina lagoon	Core 2	water	ions (cations)	160909	71.73512	129.40875	0-832	-	-
LE16-29	Ivashkina lagoon	Core 2	water	ions (cations)	160909	71.73512	129.40875	0-368	-	-

Station	Location	Sample ID	Sample type	Analysis	Sample date [yymmdd]	Latitude N	Longitude E	Depth [cm]		
								Water	Sedi-ment	Perma-frost (b.s.b.)
LE16-29	Ivashkina lagoon	Core 2	water	ions (cations)	160909	71.73512	129.40875	600	0-5	-
LE16-29	Ivashkina lagoon	Core 2	water	ions (cations)	160909	71.73512	129.40875	522	0-5	-
LE16-29	Ivashkina lagoon	Core 2	water	ions (cations)	160909	71.73512	129.40875	634	0-5	-
LE16-29	Ivashkina lagoon	Core 2	water	ions (cations)	160909	71.73512	129.40875	832	0-4	-
LE16-29	Ivashkina lagoon	Core 1	water	ions (cations)	160909	71.73411	129.41125	-	0-10	-
LE16-29	Ivashkina lagoon	Core 1	water	ions (cations)	160909	71.73411	129.41125	-	10-20	-
LE16-29	Ivashkina lagoon	Core 1	water	ions (cations)	160909	71.73411	129.41125	-	20-30	-
LE16-29	Ivashkina lagoon	Core 1	water	ions (cations)	160909	71.73411	129.41125	-	30-40	-
LE16-29	Ivashkina lagoon	Core 1	water	ions (cations)	160909	71.73411	129.41125	-	40-50	-
LE16-29	Ivashkina lagoon	Core 1	water	ions (cations)	160909	71.73411	129.41125	-	50-60	-
LE16-29	Ivashkina lagoon	Core 1	water	ions (cations)	160909	71.73411	129.41125	-	60-70	-
LE16-29	Ivashkina lagoon	Core 1	water	ions (cations)	160909	71.73411	129.41125	120	-	-
LE16-29	Ivashkina lagoon	Core 2	water	ions (cations)	160909	71.73512	129.40875	120	-	-
LE16-29	Ivashkina lagoon	Core 2	water	ions (cations)	160909	71.73512	129.40875	480	-	-
LE16-29	Ivashkina lagoon	Core 2	water	ions (cations)	160909	71.73512	129.40875	480	-	-

Station	Location	Sample ID	Sample type	Analysis	Sample date [yymmdd]	Latitude N	Longitude E	Depth		[cm]
								Water	Sedi-ment	Perma-frost (b.s.b.)
LE16-29	Ivashkina lagoon	Core 2	water	ions (cations)	160909	71.73512	129.40875	256	-	-
LE16-29	Ivashkina lagoon	Core 2	water	ions (cations)	160909	71.73512	129.40875	256	-	-
LE16-29	Ivashkina lagoon	Core 2	water	ions (cations)	160909	71.73512	129.40875	1024	-	-
LE16-29	Ivashkina lagoon	Core 2	water	ions (cations)	160909	71.73512	129.40875	1024	-	-
LE16-29	Ivashkina lagoon	Core 2	water	ions (cations)	160909	71.73512	129.40875	100	-	-
LE16-29	Ivashkina lagoon	Core 2	water	ions (cations)	160909	71.73512	129.40875	100	-	-
LE16-29	Ivashkina lagoon	Core 2	water	ions (cations)	160909	71.73512	129.40875	400	-	-
LE16-29	Ivashkina lagoon	Core 2	water	ions (cations)	160909	71.73512	129.40875	400	-	-
LE16-29	Ivashkina lagoon	Core 1	water	volatile fatty acids	160909	71.73411	129.41125	170	-	-
LE16-29	Ivashkina lagoon	Core 1	water	volatile fatty acids	160909	71.73411	129.41125	170	-	-
LE16-29	Ivashkina lagoon	Core 1	water	volatile fatty acids	160909	71.73411	129.41125	700	-	-
LE16-29	Ivashkina lagoon	Core 1	water	volatile fatty acids	160909	71.73411	129.41125	700	-	-
LE16-29	Ivashkina lagoon	Core 1	water	volatile fatty	160909	71.73411	129.41125	200	-	-

Station	Location	Sample ID	Sample type	Analysis	Sample date [yymmdd]	Latitude N	Longitude E	Depth [cm]		
								Water	Sedi-ment	Perma-frost (b.s.b.)
				acids						
LE16-29	Ivashkina lagoon	Core 1	water	volatile fatty acids	160909	71.73411	129.41125	840	-	-
LE16-29	Ivashkina lagoon	Core 1	water	volatile fatty acids	160909	71.73411	129.41125	250	-	-
LE16-29	Ivashkina lagoon	Core 1	water	volatile fatty acids	160909	71.73411	129.41125	1000	-	-
LE16-29	Ivashkina lagoon	Core 2	water	volatile fatty acids	160909	71.73512	129.40875	165	-	-
LE16-29	Ivashkina lagoon	Core 2	water	volatile fatty acids	160909	71.73512	129.40875	640	-	-
LE16-29	Ivashkina lagoon	Core 2	water	volatile fatty acids	160909	71.73512	129.40875	-	10	-
LE16-29	Ivashkina lagoon	Core 2	water	volatile fatty acids	160909	71.73512	129.40875	-	30	65
LE16-29	Ivashkina lagoon	Core 2	water	volatile fatty acids	160909	71.73512	129.40875	-	50	65
LE16-29	Ivashkina lagoon	Core 2	water	volatile fatty acids	160909	71.73512	129.40875	-	55	65
LE16-29	Ivashkina lagoon	Core 2	water	volatile fatty	160909	71.73512	129.40875	-	23	65

Station	Location	Sample ID	Sample type	Analysis	Sample date [yymmdd]	Latitude N	Longitude E	Depth Water	Depth Sediment	[cm] Permafrost (b.s.b.)
				acids						
LE16-29	Ivashkina lagoon	Core 2	water	volatile fatty acids	160909	71.73512	129.40875	-	34.5	57.5
LE16-29	Ivashkina lagoon	Core 2	water	volatile fatty acids	160909	71.73512	129.40875	-	46	57.5
LE16-29	Ivashkina lagoon	Core 2	water	volatile fatty acids	160909	71.73512	129.40875	-	57	57.5
LE16-29	Ivashkina lagoon	Core 2	water	volatile fatty acids	160909	71.73512	129.40875	-	7	57.5
LE16-29	Ivashkina lagoon	Core 1	water	water (pore) back up	160909	71.73411	129.41125	-	12	39
LE16-29	Ivashkina lagoon	Core 1	water	water (pore) back up	160909	71.73411	129.41125	-	23	39
LE16-29	Ivashkina lagoon	Core 1	water	water (pore) back up	160909	71.73411	129.41125	-	34.5	39
LE16-29	Ivashkina lagoon	Core 1	water	water (pore) back up	160909	71.73411	129.41125	-	37.5	39
LE16-29	Ivashkina lagoon	Core 1	water	water (pore) back up	160909	71.73411	129.41125	-	7	39
LE16-29	Ivashkina lagoon	Core 1	water	water (pore)	160909	71.73411	129.41125	-	12	50

Station	Location	Sample ID	Sample type	Analysis	Sample date [yymmdd]	Latitude N	Longitude E		Depth	[cm]
								Water	Sedi-ment	Perma-frost (b.s.b.)
				back up						
LE16-29	Ivashkina lagoon	Core 1	water	water (pore) back up	160909	71.73411	129.41125	-	23	50
LE16-29	Ivashkina lagoon	Core 1	water	water (pore) back up	160909	71.73411	129.41125	-	34.5	50
LE16-29	Ivashkina lagoon	Core 2	water	water (pore) back up	160909	71.73512	129.40875	-	46	50
LE16-29	Ivashkina lagoon	Core 2	water	water (pore) back up	160909	71.73512	129.40875	-	50	50
LE16-29	Ivashkina lagoon	Core 2	water	water (pore) back up	160909	71.73512	129.40875	-	17	50
LE16-29	Ivashkina lagoon	Core 2	water	water (pore) back up	160909	71.73512	129.40875	-	23	48
LE16-29	Ivashkina lagoon	Core 2	water	water (pore) back up	160909	71.73512	129.40875	-	34.5	48
LE16-29	Ivashkina lagoon	Core 2	water	water (pore) back up	160909	71.73512	129.40875	-	46	48
LE16-29	Ivashkina lagoon	Core 2	water	water (pore) back up	160909	71.73512	129.40875	-	48	48
LE16-29	Ivashkina lagoon	Core 2	water	water (pore)	160909	71.73512	129.40875	1	-	48

Station	Location	Sample ID	Sample type	Analysis	Sample date [yymmdd]	Latitude N	Longitude E	Depth		[cm]
								Water	Sedi-ment	Perma-frost (b.s.b.)
				back up						
LE16-29	Ivashkina lagoon	Core 2	water	water (pore) back up	160909	71.73512	129.40875	-	7	50
LE16-29	Ivashkina lagoon	Core 2	water	water (pore) back up	160909	71.73512	129.40875	-	12	45
LE16-29	Ivashkina lagoon	Core 2	water	water (pore) back up	160909	71.73512	129.40875	-	23	45
LE16-30	Ivashkina Lagoon	1153	water	methane	160909	71.74457	129.40224	-	34.5	45
LE16-30	Ivashkina Lagoon	1154	water	methane	160909	71.74457	129.40224	-	45	45
LE16-31	Ivashkina Lagoon	ions	water	ions	160909	71.72868	129.41249	-	12	45
LE16-31	Ivashkina Lagoon	ions	water	ions	160909	71.72868	129.41249	-	17	50
LE16-31	Ivashkina Lagoon	ions	water	ions	160909	71.72868	129.41249	-	23	50
LE16-31	Ivashkina Lagoon	ions	water	ions	160909	71.72868	129.41249	-	34.5	50
LE16-31	Ivashkina Lagoon	isotopes	water	isotopes analysis	160909	71.72868	129.41249	-	46	50
LE16-31	Ivashkina Lagoon	isotopes	water	isotopes analysis	160909	71.72868	129.41249	-	50	50
LE16-31	Ivashkina Lagoon	1155	water	methane	1609010	71.72868	129.41249	1	-	50
LE16-31	Ivashkina Lagoon	1156	water	methane	1609010	71.72868	129.41249	1	-	-

Station	Location	Sample ID	Sample type	Analysis	Sample date [yymmdd]	Latitude N	Longitude E	Depth [cm]		
								Water	Sedi-ment	Perma-frost (b.s.b.)
LE16-31	Ivashkina Lagoon	1157	water	methane	1609010	71.72868	129.41249			-
LE16-31	Ivashkina Lagoon	1158	water	methane	1609010	71.72868	129.41249			
LE16-31	Ivashkina Lagoon	?	water	plankton	160909	71.72868	129.41249	-	12	
LE16-33	Muostakh island		sediment	DNA	160910	71.60451	129.95845	-	17	77-78
LE16-33	Muostakh island		sediment	DNA	160910	71.60451	129.95845	-	23	77-79
LE16-33	Muostakh island		sediment	DNA	160910	71.60451	129.95845	-	34.5	77-80
LE16-33	Muostakh island		sediment	DNA	160910	71.60451	129.95845	-	46	77-81
LE16-33	Muostakh island		sediment	DNA	160910	71.60451	129.95845	-	57	77-82
LE16-33	Muostakh island		sediment	DNA	160910	71.60451	129.95845	-	67	77-83
LE16-33	Muostakh island		sediment	DNA	160910	71.60451	129.95845	-	77	77-84
LE16-33	Muostakh island		sediment	DNA	160910	71.60451	129.95845	-	7	77-85
LE16-33	Muostakh island		sediment	DNA	160910	71.60451	129.95845	-	12	100
LE16-33	Muostakh island		sediment	DNA	160910	71.60451	129.95845	-	17	100
LE16-33	Muostakh island		sediment	DNA	160910	71.60451	129.95845	-	23	100
LE16-33	Muostakh island		sediment	DNA	160910	71.60451	129.95845	-	34.5	100
LE16-33	Muostakh island		sediment	DNA, enrichment	160910	71.60451	129.95845	-	46	100
LE16-33	Muostakh island		sediment	DNA, enrichment	160910	71.60451	129.95845	-	56	100
LE16-33	Muostakh island		sediment	DNA, enrichment	160910	71.60451	129.95845	-	66	100

Station	Location	Sample ID	Sample type	Analysis	Sample date [yymmdd]	Latitude N	Longitude E	Depth [cm]		
								Water	Sedi-ment	Perma-frost (b.s.b.)
LE16-33	Muostakh island		sediment	DNA, enrichment	160910	71.60451	129.95845	-	76	100
LE16-33	Muostakh island		sediment	DNA, enrichment	160910	71.60451	129.95845	-	86	100
LE16-33	Muostakh island		sediment	DNA, enrichment	160910	71.60451	129.95845	-	98	100
LE16-33	Muostakh island		sediment	DNA, enrichment	160910	71.60451	129.95845	-	10-20	100
LE16-33	Muostakh island		sediment	DNA, enrichment	160910	71.60451	129.95845	-	20-30	76
LE16-33	Muostakh island		sediment	DNA, enrichment	160910	71.60451	129.95845	-	30-40	76
LE16-33	Muostakh island		sediment	DNA, enrichment	160910	71.60451	129.95845	-	40-50	76
LE16-33	Muostakh island		sediment	DNA, enrichment	160910	71.60451	129.95845	-	50-60	76
LE16-33	Muostakh island		sediment	DNA, enrichment	160910	71.60451	129.95845	-	60-70	76
LE16-33	Muostakh island	-	sediment	methane	160910	71.60451	129.95845	-	-	76
LE16-33	Muostakh island	-	sediment	methane	160910	71.60451	129.95845	-	-	-
LE16-33	Muostakh island	-	sediment	methane	160910	71.60451	129.95845	-	-	-

Station	Location	Sample ID	Sample type	Analysis	Sample date [yymmdd]	Latitude N	Longitude E	Depth	[cm]	
								Water	Sedi-ment	Perma-frost (b.s.b.)
LE16-33	Muostakh island	-	sediment	methane	160910	71.60451	129.95845	-	-	-
LE16-33	Muostakh island	-	sediment	methane	160910	71.60451	129.95845	-	-	-
LE16-33	Muostakh island	-	sediment	methane	160910	71.60451	129.95845	-	-	-
LE16-33	Muostakh island	-	sediment	methane	160910	71.60451	129.95845	-	-	-
LE16-33	Muostakh island	-	sediment	methane	160910	71.60451	129.95845	-	-	-
LE16-33	Muostakh island	-	sediment	methane	160910	71.60451	129.95845	-	-	-
LE16-33	Muostakh island	-	sediment	methane	160910	71.60451	129.95845	-	-	-
LE16-33	Muostakh island	-	sediment	methane	160910	71.60451	129.95845	-	-	-
LE16-33	Muostakh island	-	sediment	methane	160910	71.60451	129.95845	-	-	-
LE16-33	Muostakh island		sediment	pore size	160910	71.60451	129.95845	-	-	-
LE16-33	Muostakh island		sediment	pore size	160910	71.60451	129.95845	-	-	-
LE16-33	Muostakh island		sediment	pore size	160910	71.60451	129.95845	-	-	-
LE16-33	Muostakh island		sediment	pore size	160910	71.60451	129.95845	-	-	-
LE16-33	Muostakh island		sediment	pore size	160910	71.60451	129.95845	-	-	-
LE16-33	Muostakh island		sediment	pore size	160910	71.60451	129.95845	-	-	-
LE16-33	Muostakh island		sediment	pore size	160910	71.60451	129.95845	-	-	-
LE16-33	Muostakh island		water	Fe2+	160910	71.60451	129.95845	-	-	-
LE16-33	Muostakh island		water	Fe2+	160910	71.60451	129.95845	-	-	-
LE16-33	Muostakh island		water	Fe2+	160910	71.60451	129.95845	-	-	-
LE16-33	Muostakh island		water	Fe2+	160910	71.60451	129.95845	-	-	-
LE16-33	Muostakh island		water	Fe2+	160910	71.60451	129.95845	-	-	-
LE16-33	Muostakh island		water	Fe2+	160910	71.60451	129.95845	-	-	-
LE16-33	Muostakh island		water	ions	160910	71.60451	129.95845	-	-	-

Station	Location	Sample ID	Sample type	Analysis	Sample date [yymmdd]	Latitude N	Longitude E	Depth [cm]		
								Water	Sedi-ment	Perma-frost (b.s.b.)
				(anions)						
LE16-33	Muostakh island		water	ions (anions)	160910	71.60451	129.95845	-	-	-
LE16-33	Muostakh island		water	ions (anions)	160910	71.60451	129.95845	-	-	-
LE16-33	Muostakh island		water	ions (anions)	160910	71.60451	129.95845	-	-	-
LE16-33	Muostakh island		water	ions (anions)	160910	71.60451	129.95845	-	-	-
LE16-33	Muostakh island		water	ions (anions)	160910	71.60451	129.95845	-	-	-
LE16-33	Muostakh island		water	ions (cations)	160910	71.60451	129.95845	-	-	-
LE16-33	Muostakh island		water	ions (cations)	160910	71.60451	129.95845	-	-	50
LE16-33	Muostakh island		water	ions (cations)	160910	71.60451	129.95845	-	-	-
LE16-33	Muostakh island		water	ions (cations)	160910	71.60451	129.95845	-	-	-
LE16-33	Muostakh island		water	ions (cations)	160910	71.60451	129.95845	-	12	-
LE16-33	Muostakh island		water	ions (cations)	160910	71.60451	129.95845	-	17	-
LE16-33	Muostakh island		water	ions (cations)	160910	71.60451	129.95845	-	23	-
LE16-33	Muostakh island		water	ions (cations)	160910	71.60451	129.95845	-	34.5	-
LE16-33	Muostakh island		water	ions (cations)	160910	71.60451	129.95845	-	46	-
LE16-33	Muostakh island		water	ions	160910	71.60451	129.95845	-	57	-

Station	Location	Sample ID	Sample type	Analysis	Sample date [yymmdd]	Latitude N	Longitude E	Depth [cm]		
								Water	Sedi-ment	Perma-frost (b.s.b.)
				(cations)						
LE16-33	Muostakh island		water	ions (cations)	160910	71.60451	129.95845	-	67	-
LE16-33	Muostakh island		water	ions (cations)	160910	71.60451	129.95845	-	77	-
LE16-33	Muostakh island		water	volatile fatty acids	160910	71.60451	129.95845	-	7	-
LE16-33	Muostakh island		water	volatile fatty acids	160910	71.60451	129.95845	-	12	-
LE16-33	Muostakh island		water	volatile fatty acids	160910	71.60451	129.95845	-	17	-
LE16-33	Muostakh island		water	volatile fatty acids	160910	71.60451	129.95845	-	23	-
LE16-33	Muostakh island		water	volatile fatty acids	160910	71.60451	129.95845	-	34.5	-
LE16-33	Muostakh island		water	volatile fatty acids	160910	71.60451	129.95845	-	46	-
LE16-33	Muostakh island		water	water (pore) back up	160910	71.60451	129.95845	-	56	-
LE16-33	Muostakh island		water	water (pore) back up	160910	71.60451	129.95845	-	66	-
LE16-33	Muostakh island		water	water	160910	71.60451	129.95845	-	76	-

Station	Location	Sample ID	Sample type	Analysis	Sample date [yymmdd]	Latitude N	Longitude E		Depth	[cm]
								Water	Sedi-ment	Perma-frost (b.s.b.)
				(pore) back up						
LE16-8	Samoylov Island	Methanosarc. Solig. 5 cm	sediment	DNA, enrichment	160827	72.21662	129.4951	-	86	-
LE16-8	Samoylov Island	Methanosarc. Solig. 10 cm	sediment	DNA, enrichment	160827	72.21662	129.4951	-	98	-
LE16-8	Samoylov Island	Methanosarc. Solig. 15 cm	sediment	DNA, enrichment	160827	72.21662	129.4951	-	40-50	-
LE16-8	Samoylov Island	Methanosarc. Solig. 20 cm	sediment	DNA, enrichment	160827	72.21662	129.4951	-	50-60	-
LE16-8	Samoylov Island	Methanosarc. Solig. 25 cm	sediment	DNA, enrichment	160827	72.21662	129.4951	-	60-70	-
LE16-8	Samoylov Island	Methanosarc. Solig. 30 cm	sediment	DNA, enrichment	160827	72.21662	129.4951			-

Table A 3.1.-3: List of measurements performed at station LE16-1.

Station Name	Activity	Lat	Lon	Date	Time	Record ID	Samples
LE16-1-L1	Landstations Seismic	71.61203	129.94066	24.08.16	06:44:00	705	
LE16-1-L10	Landstations Seismic	71.60638	129.95477	24.08.16	05:00:00	699	
LE16-1-L11	Landstations Seismic	71.60852	129.94964	24.08.16	06:00:00	704	
LE16-1-L12	Landstations Seismic	71.61066	129.94700	24.08.16	06:29:00	707	
LE16-1-L13	Landstations Seismic	71.60853	129.95551	24.08.16	07:20:00	703	
LE16-1-L14	Landstations Seismic	71.60626	129.96160	24.08.16	07:33:00	702	
LE16-1-L15	Landstations Seismic	71.60325	129.97001	24.08.16	07:51:00	706	
LE16-1-L2	Landstations Seismic	71.61047	129.95174	24.08.16	06:15:00	708	
LE16-1-L3	Landstations Seismic	71.60853	129.95932	24.08.16	04:44:00	698	
LE16-1-L4	Landstations Seismic	71.60592	129.96802	24.08.16	04:32:00	694	
LE16-1-L5	Landstations Seismic	71.60284	129.97707	24.08.16	03:52:00	697	
LE16-1-L6	Landstations Seismic	71.59936	129.98659	24.08.16	03:37:00	695	
LE16-1-L7	Landstations Seismic	71.59696	129.97655	24.08.16	03:22:00	701	
LE16-1-L8	Landstations Seismic	71.60052	129.96960	24.08.16	04:07:00	696	
LE16-1-L9	Landstations Seismic	71.60354	129.96169	24.08.16	04:20:00	700	
LE16-1-MI1	Sediment Core	71.61104	129.94315	24.08.16	06:00:00		DNA, methane, Fe2+, ions (anions), volatile fatty acids
LE16-1-CR1	Coastal Erosion Misha	71.61104	129.94315	24.08.16	06:00:00		
LE16-1-CR2	Coastal Erosion Misha	71.61104	129.94315	24.08.16	06:00:00		
LE16-1-CR3	Coastal Erosion Misha	71.61104	129.94315	24.08.16	06:00:00		
LE16-1-CR4	Coastal Erosion Misha	71.61104	129.94315	24.08.16	06:00:00		
LE16-1-CR5	Coastal Erosion Misha	71.61104	129.94315	24.08.16	06:00:00		
LE16-1-CR6	Coastal Erosion Misha	71.61104	129.94315	24.08.16	06:00:00		

Table A 3.1.-4: List of measurements performed at station LE16-2

Station Name	Activity	Lat	Lon	Date	Time	Waterdepth (m)	OBS Name
LE16-2-1	OBS Deployment	71.60388	129.94640	24.08.16	02:15:00	3.1	A3T
LE16-2-2	OBS Deployment	71.59758	129.95123	24.08.16	02:29:00	2.7	A3X
LE16-2-3	OBS Deployment	71.60014	129.92736	24.08.16	02:42:00	5.8	A3V+CTD (108)
LE16-2-4	OBS Deployment	71.60805	129.92948	24.08.16	02:57:00	3.8	A47
LE16-2-5	OBS Deployment	71.61146	129.91195	24.08.16	03:08:00	4.3	A3Z
LE16-2-6	OBS Deployment	71.61823	129.91644	24.08.16	03:20:00	3.5	A3W
LE16-2-7	OBS Deployment	71.61708	129.93661	24.08.16	03:31:00	5.5	A44
LE16-2-8	OBS Deployment	71.61499	129.95275	24.08.16	03:41:00	4.9	A48
LE16-2-9	OBS Deployment	71.61139	129.96274	24.08.16	03:50:00	4.9	A40
LE16-2-10	OBS Deployment	71.60824	129.98717	24.08.16	04:01:00	6.0	A42
LE16-2-11	OBS Deployment	71.60681	130.00442	24.08.16	04:09:00	6.5	A45
LE16-2-12	OBS Deployment	71.61582	129.99887	24.08.16	04:25:00	6.2	A3S
LE16-2-13	OBS Deployment	71.61417	129.97754	24.08.16	04:43:00	6.0	A3R+CTD (107)
LE16-2-14	OBS Deployment	71.61874	129.96647	24.08.16	04:53:00	5.5	A43
LE16-2-15	OBS Deployment	71.62400	129.98344	24.08.16	05:03:00	6.5	A3U
LE16-2-16	OBS Deployment	71.62147	129.95363	24.08.16	05:17:00	5.5	A41
LE16-2-17	OBS Deployment	71.62502	129.93586	24.08.16	05:25:00	4.9	A46

Table A 3.1.-5: List of measurements performed at station LE16-3.

Station Name	Activity	Lat	Lon	Date	Time	Waterdepth (m)
LE16-3-1	CTD	71.60187	129.94280	24.08.16	09:07:00	4.1
LE16-3-2	CTD	71.60531	129.83275	24.08.16	10:52:00	7.2
LE16-3-3	CTD	71.61294	129.59419	24.08.16	11:29:00	10.57
LE16-3-4	CTD	71.61783	129.18450	24.08.16	12:31:00	11

Table A 3.1.-6: LE16-4

Station Name	Activity	Lat	Lon	Date	Time	Waterdepth (m)	Record ID
LE16-4-MOBSI1	MOBSI	71.78900	129.43045	25.08.16	07:24:21	no depth	4
LE16-4-CTD1	CTD	71.80073	129.46159	25.08.16	08:04:32	4.15	
LE16-4-MOBSI2	MOBSI	71.80075	129.46158	25.08.16	08:04:58	4.12	6
LE16-4-CTD2	CTD	71.80076	129.46164	25.08.16	08:06:18	4.12	
LE16-4-MOBSI3	MOBSI	71.81236	129.48987	25.08.16	08:33:08	5.58	7
LE16-4-CTD3	CTD	71.81236	129.48987	25.08.16	08:33:08		

Table A 3.1.-7: LE16-5

Station Name	Activity	Lat	Lon	Date	Time
LE16-5-1CR	Cliff Erosion rate Measurement	71.78380	129.41241	25.08.16	09:00:00

Table A 3.1.-8: LE16-6

Station Name	Activity	Lat	Lon	Date	Time	Comment
LE16-6-CR1	Cliff Erosion rate Measurement	126.50485	72.36724	26.08.16	20:00:00	10.19m from house corner to cliff

Table A 3.1.-9: LE16-7

Station Name	Activity	Lat	Lon	Time	Date	Record ID	Waterdepth (m)	Comment
LE16-7-CTD1	CTD	72.37808	126.43944	27.08.16	01:55:46		2.03	
LE16-7-MOBSI1	MOBSI	72.37805	126.43945	27.08.16	01:57:56	8	2.03	
LE16-7-CTD2	CTD	72.37675	126.44299	27.08.16	02:41:45		4.31	
LE16-7-MOBSI2	MOBSI	72.37680	126.44324	27.08.16	02:44:00	9	2.00	
LE16-7-PERMAFROSTDEPTH1	Permafrost probing	72.37711	126.44302	27.08.16	03:01:24			
LE16-7-MOBSI3	MOBSI	72.37712	126.44296	27.08.16	03:16:06	10	2.00	196 cm permafrost BSB
LE16-7-PERMAFROSTDEPTH2	Permafrost probing	72.37785	126.44054	27.08.16	03:34:13			
LE16-7-MOBSI4	MOBSI	72.37783	126.44056	27.08.16	03:41:32	12	4.90	
LE16-7-MOBSI5	MOBSI	72.38005	126.43990	27.08.16	04:23:53	13	7.2	drift on sensor
LE16-7-CTD3	CTD	72.37971	126.43746	27.08.16	05:52:03		5.39	
LE16-7-MOBSI6	MOBSI	72.37970	126.43752	27.08.16	05:55:12	14	5.7	
LE16-7-CTD4	CTD	72.38144	126.43590	27.08.16	06:14:12		11.73	
LE16-7-MOBSI7	MOBSI	72.38156	126.43673	27.08.16	06:18:25	15	11.7	
LE16-7-CTD5	CTD	72.38295	126.43281	27.08.16	06:46:36		6.19	
LE16-7-CTD6	CTD	72.38193	126.43726	27.08.16	07:00:33		12.93	
LE16-7-MOBSI8	MOBSI	72.38198	126.43791	27.08.16	07:04:05	16	12.9	
LE16-7-CTD7	CTD	72.38099	126.43688	27.08.16	07:23:02		9.51	
LE16-7-CTD8	CTD	72.38047	126.43806	27.08.16	07:42:16		9.25	
LE16-7-MOBSI9	MOBSI	72.38052	126.43820	27.08.16	07:44:19	19	9.22	
LE16-7-MOBSI10	MOBSI	72.37915	126.43933	27.08.16	08:03:53	20	4.7	
LE16-7-PERMDEPTH3	Permafrost probing	72.37883	126.44750	27.08.16	08:23:48		0.975	

Table A 3.1.-10: LE16-9

Station Name	Activity	Lat	Lon	Date	Time	Sample Depths	Permafrost b.s.b. (m)	Samples
LE16-8-1	Methanosarcina soligelidi site	72.36757	126.47530	27.08.16	13:29:00	5-30cm (5,10,15,20,25,30)	0.77	DNA, enrichment

Table A 3.1.-11: LE16-9

Station Name	Activity	Lat	Long	Date	Time	Waterdepth (m)	Permafrost b.s.b. (m)	Record ID	Comment
LE16-9-3	Permafrost probing	72.36816	126.48525	28.08.16	03:20:05		0.6		Start Profile 1
LE16-9-5	MOBSI	72.36819	126.48527	28.08.16	03:26:06	0.6		21	No CTD
LE16-9-6a	Permafrost probing	72.36836	126.48537	28.08.16	03:36:44	2.4	1.07		
LE16-9-6b	MOBSI	72.36836	126.48537	28.08.16	03:36:44	2.4		22	No CTD
LE16-9-7a	MOBSI	72.36855	126.48549	28.08.16	03:46:30	4.86		23	
LE16-9-7b	CTD	72.36872	126.48560	28.08.16	02:48:25	4.8463			
LE16-9-8a	MOBSI	72.36872	126.48560	28.08.16	03:54:51	4.53		24	
LE16-9-8b	CTD	72.36872	126.48560	28.08.16	02:55:32	4.5297			
LE16-9-9a	MOBSI	72.36889	126.48566	28.08.16	04:04:28	3.77		25	
LE16-9-9b	CTD	72.36889	126.48566	28.08.16	03:07:06	3.7735			
LE16-9-10a	MOBSI	72.36905	126.48572	28.08.16	04:15:15	3.98		26	
LE16-9-10b	CTD	72.36905	126.48572	28.08.16	03:15:44	3.9504			
LE16-9-11	Waypoint	72.36942	126.48575	28.08.16	04:57:16				End of Profile 1
LE16-9-13a	Permafrost probing	72.36819	126.48637	28.08.16	05:31:52	0.36	0.81		
LE16-9-13b	MOBSI	72.36819	126.48637	28.08.16	05:31:52	0.36		28	No CTD
LE16-9-17a	Permafrost probing	72.36830	126.48645	28.08.16	05:56:41	2.48	2.72		
LE16-9-17b	MOBSI	72.36830	126.48645	28.08.16	05:56:41	2.48		31	
LE16-9-17c	CTD	72.36830	126.48645	28.08.16	04:58:32	2.4784			
LE16-9-18a	MOBSI	72.36839	126.48662	28.08.16	06:22:30	2.76		32	
LE16-8-18b	CTD	72.36839	126.48662	28.08.16	05:21:51	2.729			
LE16-9-19a	MOBSI	72.36854	126.48660	28.08.16	06:34:01	3.97		33	
LE16-9-19b	CTD	72.36854	126.48660	28.08.16	05:34:55	3.9412			
LE16-9-20a	MOBSI	72.36872	126.48661	28.08.16	06:44:33	3.99		34	
LE16-9-20b	CTD	72.36872	126.48661	28.08.16	05:45:02	3.9878			
LE16-9-21a	MOBSI	72.36890	126.48665	28.08.16	06:55:01	3.95		36	
Station Name	**Activity**	**Lat**	**Long**	**Date**	**Time**	**Waterdepth (m)**	**Permafrost b.s.b. (m)**	**Record ID**	**Comment**

LE16-9-21b	CTD	72.36890	126.48665	28.08.16	05:55:37	3.9436			
LE16-9-22a	MOBSI	72.36897	126.48672	28.08.16	07:05:31	4.11		37	
LE16-9-22b	CTD	72.36897	126.48672	28.08.16	06:06:27	4.0835			
LE16-9-23	Waypoint	72.36928	126.48682	28.08.16	07:28:45				End of Profile 2
LE16-9-25a	Permafrost probing	72.36822	126.48814	28.08.16	07:57:22	0.4	0.83		
LE16-9-25b	MOBSI	72.36822	126.48814	28.08.16	07:57:22	0.4		38	No CTD
LE16-9-26a	Permafrost probing	72.36831	126.48813	28.08.16	08:01:27	0.7	0.93		
LE16-9-26b	MOBSI	72.36831	126.48813	28.08.16	08:01:27	0.7		39	No CTD
LE16-9-27a	Permafrost probing	72.36841	126.48828	28.08.16	08:17:17	1.13	0.97		
LE16-9-27b	MOBSI	72.36841	126.48828	28.08.16	08:17:17	1.13		41	
LE16-9-27c	CTD	72.36841	126.48828	28.08.16	07:20:40	1.1361			
LE16-9-28a	Permafrost probing	72.36848	126.48839	28.08.16	08:31:20	1.27	0.92		
LE16-9-28b	MOBSI	72.36848	126.48839	28.08.16	08:31:20	1.27		42	
LE16-9-28c	CTD	72.36848	126.48839	28.08.16	07:38:18	1.2542			
LE16-9-29a	Permafrost probing	72.36857	126.48839	28.08.16	08:44:30	1.07	0.93		
LE16-9-29b	MOBSI	72.36857	126.48839	28.08.16	08:44:30	1.07		43	
LE16-9-29c	CTD	72.36857	126.48839	28.08.16	07:50:46	1.0468			
LE16-9-30a	Permafrost probing	72.36869	126.48840	28.08.16	08:53:51	0.91	0.99		
LE16-9-30b	MOBSI	72.36869	126.48840	28.08.16	08:53:51	0.91		44	
LE16-9-30c	CTD	72.36869	126.48840	28.08.16	08:00:33	0.09025			
LE16-9-31a	Permafrost probing	72.36878	126.48842	28.08.16	09:03:49	0.81	0.99		
LE16-9-31b	MOBSI	72.36878	126.48842	28.08.16	09:03:49	0.81		45	
LE16-9-31c	CTD	72.36878	126.48842	28.08.16	08:10:13	0.804			
Station Name	**Activity**	**Lat**	**Long**	**Date**	**Time**	**Waterdepth (m)**	**Permafrost b.s.b. (m)**	**Record ID**	**Comment**
LE16-9-32a	Permafrost probing	72.36884	126.48850	28.08.16	09:12:36	0.92	1.05		
LE16-9-32b	MOBSI	72.36884	126.48850	28.08.16	09:12:36	0.92		46	

LE16-9-32c	CTD	72.36884	126.48850	28.08.16	08:19:38	0.8971			
LE16-9-33a	Permafrost probing	72.36898	126.48851	28.08.16	09:22:17	0.53	1.13		
LE16-9-33b	MOBSI	72.36898	126.48851	28.08.16	09:22:17	0.53		47	
LE16-9-33c	CTD	72.36898	126.48851	28.08.16	08:28:15	0.511			
LE16-9-34a	MOBSI	72.36925	126.48561	28.08.16	10:10:01	2.05		48	
LE16-9-34b	CTD	72.36925	126.48561	28.08.16	09:09:46	0.2473			
LE16-9-35a	MOBSI	72.36934	126.48572	28.08.16	10:13:58	0.58		49	
Le16-9-35b	CTD	72.36934	126.48572	28.08.16	09:21:05	0.5619			
LE16-9-36a	MOBSI	72.36926	126.48692	28.08.16	10:31:41	0.65		50	
LE16-9-36b	CTD	72.36926	126.48692	28.08.16	09:32:20	0.6284			
LE16-9-37a	MOBSI	72.36905	126.48670	28.08.16	10:37:32	3.8		51	
LE16-9-37b	CTD	72.36905	126.48670	28.08.16	09:45:10	3.8041		51	

Table A 3.1.-12: LE16-10

Station Name	Activity	Lat	Lon	Date	Depth (m)	Comment	Samples
LE16-10-1	Sediment Core	72.37021	126.47942	27.08.16	0 - 0.33	AKS9 Rim	DNA, enrichment; Fe2+; ions (anions); ions (cations); methane; volatile fatty acids; water (pore) back up
LE16-10-2	Sediment Core	72.37021	126.47942	27.08.16	0 - 0.39	AKS9 CP	DNA, enrichment; Fe2+; ions (anions); ions (cations); methane; volatile fatty acids; water (pore) back up
LE16-10-3	Sediment Core	72.36995	126.48256	28.08.16	0 - 0.35	AKS0 Rim	DNA, enrichment; Fe2+; ions (anions); ions (cations); methane; volatile fatty acids; water (pore) back up
LE16-10-4	Sediment Core	72.36995	126.48256	28.08.16	0 - 0.50	AKS0 CP	DNA, enrichment; Fe2+; ions (anions); ions (cations); methane; volatile fatty acids; water (pore) back up
LE16-10-5	Water Sample	72.36995	126.48256	28.08.16	0.01	AKS0	DNA; DNA, enrichment; Fe2+; ions (anions); ions (cations); volatile fatty acids; water back up
LE16-10-6	Sediment Core	72.36983	126.47791	28.08.16	0 - 0.40	AKS11 Rim	DNA, enrichment; Fe2+; ions (anions); ions (cations); methane; volatile fatty acids; water (pore) back up
LE16-10-7	Sediment Core	72.36983	126.47791	28.08.16	0 - 0.35	AKS11 CP	DNA, enrichment; Fe2+; ions (anions); ions (cations); methane; volatile fatty acids; water (pore) back up
LE16-10-8	Water Sample	72.36757	126.47530	30.08.16	0.01	Lena River	DNA; DNA, enrichment; Fe2+; ions (anions); ions (cations); volatile fatty acids; water back up

Table A 3.1.-13: LE16-11

Station Name	Activity	Lat	Long	Date	Comment	Samples
LE16-11-MW-P2	Moos sample, Porewater	72.56838	127.20632	29.08.16	Pond1	DNA, enrichment; Fe2+; ions (anions); ions (cations); volatile fatty acids; water back up
LE16-11-MW-P3	Moos sample, Porewater	72.57157	127.24133	29.08.16	Pond2	DNA, enrichment; Fe2+; ions (anions); ions (cations); volatile fatty acids; water back up

Table A 3.1.-14: LE16-12

Station Name	Activity	Lat	Long	Date	Time	Record ID	Distance (m)	Comment
LE16-12-1	MOBSI	72.36711	126.48429	30.08.16	09:34:00	5, 6	10	Hammerschlag
LE16-12-2	MOBSI	72.36711	126.48429	30.08.16	09:36:00	7, 8	9.5	Hammerschlag
LE16-12-3	MOBSI	72.36711	126.48429	30.08.16	09:38:00	9, 10	9	Hammerschlag
LE16-12-4	MOBSI	72.36711	126.48429	30.08.16	09:40:00	11, 12	8.5	Hammerschlag
LE16-12-5	MOBSI	72.36711	126.48429	30.08.16	09:42:00	13, 14	8	Hammerschlag
LE16-12-6	MOBSI	72.36711	126.48429	30.08.16	09:44:00	15, 16	7.5	Hammerschlag
LE16-12-7	MOBSI	72.36711	126.48429	30.08.16	09:46:00	17, 18	7	Hammerschlag
LE16-12-8	MOBSI	72.36711	126.48429	30.08.16	09:48:00	19, 20	6.5	Hammerschlag
LE16-12-9	MOBSI	72.36711	126.48429	30.08.16	09:50:00	21, 22	6	Hammerschlag
LE16-12-10	MOBSI	72.36711	126.48429	30.08.16	09:52:00	23, 34	5.5	Hammerschlag
LE16-12-11	MOBSI	72.36711	126.48429	30.08.16	09:54:00	25, 26	5	Hammerschlag
LE16-12-12	MOBSI	72.36711	126.48429	30.08.16	09:56:00	27, 28	4.5	Hammerschlag
LE16-12-13	MOBSI	72.36711	126.48429	30.08.16	09:58:00	29, 30	4	Hammerschlag
LE16-12-14	MOBSI	72.36711	126.48429	30.08.16	10:00:00	31, 32	3.5	Hammerschlag
LE16-12-15	MOBSI	72.36711	126.48429	30.08.16	10:02:00	33, 34	3	Hammerschlag
LE16-12-16	MOBSI	72.36711	126.48429	30.08.16	10:04:00	35, 37	2.5	Hammerschlag
LE16-12-17	MOBSI	72.36711	126.48429	30.08.16	10:06:00	38, 39	2	Hammerschlag
LE16-12-18	MOBSI	72.36711	126.48429	30.08.16	10:08:00	40, 41	1.5	Hammerschlag
LE16-12-19	MOBSI	72.36711	126.48429	30.08.16	10:10:00	42, 43	1	Hammerschlag
LE16-12-20	MOBSI	72.36711	126.48429	30.08.16	10:12:00	44, 45	0.5	Hammerschlag
LE16-12-21	MOBSI	72.36711	126.48429	30.08.16	10:14:00	46		Noise

Table A 3.1.-15: LE16-13

Station Name	Activity	Lat	Long	Date	Time	Record ID	Waterdepth (m)	Permafrost b.s.b. (m)	Comment	Samples
LE16-13-1	Water Sampling	72.33682	125.74561	31.08.16	06:49:00		0			methane; plankton
LE16-13-2	Water Sampling	72.33682	125.74561	31.08.16	06:49:00		1.2			methane; plankton; cDOM; ions; isotopes; turbidity
LE16-13-3	Water Sampling	72.33682	125.74561	31.08.16	06:49:00		4.8			methane; plankton; cDOM; ions; isotopes analysis; turbidity
LE16-13-4a	Water Sampling	72.33682	125.74561	31.08.16	06:49:00		6			methane; plankton
LE16-13-4b	Sediment Core	72.33682	125.74561	31.08.16	06:49:00				0 - 2 cm	14C; methane; pore size
LE16-13-5	Air	72.33682	125.74561	31.08.16	06:49:00		-1			methane
LE16-13-6	MOBSI	72.34131	125.76138	31.08.16	06:49:32	48		1.22	Shore	
LE16-13-7a	MOBSI	72.34101	125.76059	31.08.16	07:01:13	49	2.1	1.34		
LE16-13-7b	CTD	72.34101	125.76059	31.08.16	06:01:00		2.1			
LE16-13-8a	MOBSI	72.34063	125.75755	31.08.16	07:26:58	50	3.21			
LE16-13-8b	CTD	72.34063	125.75755	31.08.16	06:26:00		3.21			
LE16-13-9a	MOBSI	72.34084	125.75826	31.08.16	07:50:23	51	2.46			
LE16-13-9b	CTD	72.34084	125.75826	31.08.16	06:50:00		2.46			
LE16-13-10a	MOBSI	72.34038	125.75547	31.08.16	08:04:01	52	3.56			
LE16-13-10b	CTD	72.34038	125.75547	31.08.16	07:01:00		3.56			
LE16-13-11a	MOBSI	72.33989	125.75291	31.08.16	08:15:00	53	4.72			
LE16-13-11b	CTD	72.33989	125.75291	31.08.16	07:14:00		4.72			
LE16-13-12a	MOBSI	72.33939	125.74981	31.08.16	08:31:44	54	5.12			
LE16-13-12b	CTD	72.33939	125.74981	31.08.16	07:30:00		5.12			
LE16-13-13a	MOBSI	72.33867	125.74719	31.08.16	08:42:24	55	4.62			
LE16-13-13b	CTD	72.33867	125.74719	31.08.16	07:42:00		4.62			
LE16-13-14a	MOBSI	72.33808	125.74403	31.08.16	08:53:09	56	4.88			
LE16-13-14b	CTD	72.33808	125.74403	31.08.16	07:53:00		4.88			

Station Name	Activity	Lat	Long	Date	Time	Record ID	Waterdepth (m)	Permafrost b.s.b. (m)	Comment	Samples
LE16-13-15a	MOBSI	72.33766	125.74010	31.08.16	09:04:41	57	6.95			
LE16-13-15b	CTD	72.33766	125.74010	31.08.16	08:04:00		6.95			
LE16-13-16a	MOBSI	72.33731	125.73681	31.08.16	11:28:56	58	7.7			
LE16-13-16b	CTD	72.33731	125.73681	31.08.16	10:28:00		7.7			
LE16-13-17a	MOBSI	72.33674	125.73378	31.08.16	11:31:58	59	6.75			
LE16-13-17b	CTD	72.33674	125.73378	31.08.16	10:47:00		6.75			
LE16-13-18a	MOBSI	72.33659	125.72968	31.08.16	12:00:52	60	5.92			
LE16-13-18b	MOBSI	72.33659	125.72968	31.08.16	11:02:00		5.92			
LE16-13-19a	MOBSI	72.33641	125.72732	31.08.16	12:13:03	61	4.25			
LE16-13-19b	CTD	72.33641	125.72732	31.08.16	11:13:00		4.25			
LE16-13-20a	MOBSI	72.33630	125.72643	31.08.16	12:21:41	62	5.14			
LE16-13-20b	CTD	72.33630	125.72643	31.08.16	11:22:00		5.14			
LE16-13-21a	MOBSI	72.33610	125.72572	31.08.16	12:41:16	63	0.58	0.9		
LE16-13-21b	CTD	72.33610	125.72572	31.08.16	11:42:00		0.58	0.9		
LE16-13-22	MOBSI	72.33588	125.72543	31.08.16	12:54:14	64		0.85	Shore	
LE16-13-23	CTD	72.33686	125.74542	31.08.16	09:25:00		6.27			

Table A 3.1.-16: LE16-14

Station Name	Activity	Lat	Lon	Date	Permafrost b.s.b. (m)	Waterdepth (m)	Comment
LE16-14-1	Permafrost probing	72.33110	125.77635	01.09.16	0.95	0.15	
LE16-14-2	Permafrost probing	72.33095	125.77612	01.09.16	1.07		Shoreline, northern, sand bar
LE16-14-3	Permafrost probing	72.33098	125.77595	01.09.16	1.17		
LE16-14-4	Permafrost probing	72.33097	125.77587	01.09.16	1.02		
LE16-14-5	Permafrost probing	72.33080	125.77533	01.09.16	0.98		
LE16-14-6	Permafrost probing	72.33072	125.77483	01.09.16	1.03		
LE16-14-7	Permafrost probing	72.33053	125.77425	01.09.16	0.9		
LE16-14-8	Permafrost probing	72.33040	125.77378	01.09.16	1		
LE16-14-9	Permafrost probing	72.33025	125.77313	01.09.16	0.97		
LE16-14-10	Permafrost probing	72.33012	125.77262	01.09.16	0.85		
LE16-14-11	Permafrost probing	72.33002	125.77227	01.09.16	0.69		
LE16-14-12	Permafrost probing	72.32997	125.77207	01.09.16	0.87		
LE16-14-13	Permafrost probing	72.32993	125.77183	01.09.16	0.85		
LE16-14-14	Permafrost probing	72.32980	125.77110	01.09.16	1.05	0.33	
LE16-14-15	Permafrost probing	72.32962	125.77092	01.09.16	0.62	0.86	
LE16-14-16	Permafrost probing	72.32958	125.77033	01.09.16	0.51	0.95	
LE16-14-17	Permafrost probing	72.32938	125.76960	01.09.16	0.74	1.06	
LE16-14-18	Permafrost probing	72.32943	125.76967	01.09.16	0.67	1.11	
LE16-14-19	Permafrost probing	72.32928	125.76888	01.09.16	0.59	0.97	
LE16-14-20	Permafrost probing	72.32922	125.76828	01.09.16	0.45	0.9	
LE16-14-21	Permafrost probing	72.32908	125.76815	01.09.16	0.54	0.68	
LE16-14-22	Permafrost probing	72.32892	125.76797	01.09.16	0.47	0.38	
LE16-14-23	Permafrost probing	72.32892	125.76783	01.09.16	0.7	0.15	
LE16-14-24	Permafrost probing	72.32886	125.76769	01.09.16	0.63		Shoreline mainland (S side, Chay tumus)
LE16-14-25	Permafrost probing	72.32881	125.76742	01.09.16	0.82		
LE16-14-26	Permafrost probing	72.32986	125.77164	01.09.16	0.8		2 m from shoreline
LE16-14-27	Permafrost probing	72.32986	125.77153	01.09.16	0.8		Shoreline, southern, sand bar

Station Name	Activity	Lat	Lon	Date	Permafrost b.s.b. (m)	Waterdepth (m)	Comment
LE16-14-28	Permafrost probing	72.32983	125.77128	01.09.16	0.78	0.2	
LE16-14-29	Permafrost probing	72.32983	125.77131	01.09.16	0.63	0.39	
LE16-14-30	Permafrost probing	72.32978	125.77111	01.09.16	0.6	0.58	

Table A 3.1.-17: LE16-15

Station Name	Activity	Lat	Long	Date	Time	Waterdepth (m)	Samples
LE16-15-1	CTD	72.51120	125.27130	01.09.16	07:39:00	12.8	
LE16-15-2	Watersampling	72.51120	125.27130	01.09.16		2.56	2l turbidity; cDOM; ions; isotopes; pH; conductivity
LE16-15-3	Watersampling	72.51120	125.27130	01.09.16		10.24	2l turbidity; cDOM; ions; isotopes; pH; conductivity

Table A 3.1.-18: LE16-17

Station Name	Activity	Lat	Long	Date	Time	Waterdepth (m)	Comment	Samples
LE16-17-1	CTD	72.873037	123.321642	02.09.16	02:44:00	5.18	Air Temp 16 °C	
LE16-17-2	Watersampling	72.873037	123.321642	02.09.16	02:44:00	surface		methane
LE16-17-3	Watersampling	72.873037	123.321642	02.09.16	02:44:00	1		cDOM; ions; isotopes; methane; turbidity
LE16-17-4	Watersampling	72.873037	123.321642	02.09.16	02:44:00	4		cDOM; ions; isotopes; methane; turbidity
LE16-17-5a	Sediment core	72.873037	123.321642	02.09.16	02:44:00	5.22		methane; pore size;
LE16-17-5b	Watersampling	72.873037	123.321642	02.09.16	02:44:00	5.22		methane
LE16-17-6	Methane Airsampling	72.873037	123.321642	02.09.16	02:44:00			methane
LE16-17-7	Plankton	72.873037	123.321642	02.09.16	02:44:00	0-5,22		plankton

Table A 3.1.-19: LE16-18

Station Name	Activity	Lat	Long	Date	Time	Waterdepth (m)	Record ID	Samples
LE16-18-1	CTD	73.24270	118.95830	03.09.16	05:14:00	6.34		
LE16-18-2	Watersampling	73.24270	118.95830	03.09.16		surface		methane; ion; isotopes; cDOM; conductivity; pH
LE16-18-3	Watersampling	73.24270	118.95830	03.09.16		1.25		methane; ion; isotopes; cDOM; conductivity; pH
LE16-18-4	Watersampling	73.24270	118.95830	03.09.16		5		methane; ion; isotopes; cDOM; conductivity; pH
LE16-18-5	Watersampling	73.24270	118.95830	03.09.16		6.34		methane; ion; isotopes; cDOM; conductivity; pH
LE16-18-6	Gravitiy Corer	73.24270	118.95830	03.09.16				4 x methane, 8 x sediment samples (0-16cm bsb)
LE16-18-7	Gravitiy Corer	73.24270	118.95830	03.09.16	06:14:00			Sediment (0-2, 2-4, 4-6cm) for 14C
LE16-18-8	Plankton net	73.24270	118.95830	03.09.16				0-6,34m ca. 20degree angle
LE16-18-9	MOBSI	73.24270	118.95830	03.09.16			65	

Table A 3.1.-20: LE16-19

Station Name	Activity	Lat	Lon	Date	Time	Waterdepth (m)	Sediment-depth (cm)	Samples
LE16-19-1	CTD	73.30131	118.54043	04.09.16	00:36:00	4.32	-	
LE16-19-2	Watersampling	73.30131	118.54043	04.09.16	00:36:00	0.53	-	methane; ion; isotopes; cDOM; conductivity, pH
LE16-19-3	Watersampling	73.30131	118.54043	04.09.16	00:36:00	0.90	-	methane; ion; isotopes; cDOM; conductivity, pH
LE16-19-4	Watersampling	73.30131	118.54043	04.09.16	00:36:00	3.40	-	methane; ion; isotopes; cDOM; conductivity, pH
LE16-19-5	Watersampling	73.30131	118.54043	04.09.16	00:36:00	4.32	-	methane; ion; isotopes; cDOM; conductivity, pH
LE16-19-6	Gravitiy Corer	73.30131	118.54043	04.09.16	00:36:00	4.32	0-18	5 x methane, 8 x sediment samples (0-16cm bsb)
LE16-19-7	Gravitiy Corer	73.30131	118.54043	04.09.16	00:36:00	4.32	0-5	Sediment upper 4-5 cm for 14C
LE16-19-8	Plankton net	73.30131	118.54043	04.09.16	00:36:00	4.32	-	

Table A 3.1.-21: LE16-20

Station Name	Activity	Lat	Lon	Date	Comment
LE16-20-CR1	Coastline Retreat Rate	73.60630	117.17736	04.09.16	Mamm Klyk

Table A 3.1.-22: LE16-21

Station Name	Activity	Lat	Lon	Date	Comment
LE16-21-1	Borehole	73.60630	117.17736	04.09.16	Temp Chain broke after last deployment

Table A 3.1.-23: LE16-22

Station Name	Activity	Lat	Lon	Date	Time	Record ID	Waterdepth (m)	Comment	Samples
LE16-22-MOBSI1	MOBSI	73.63164	117.16832	05.09.16	00:15:17	67	4.6	ship echolot	
LE16-22-MOBSI2	MOBSI	73.62680	117.17004	05.09.16	01:00:20	68	4.1	ship echolot	
LE16-22-MOBSI3	MOBSI	73.62204	117.16891	05.09.16	01:44:19	69	3.3	ship echolot	
LE16-22-CTD1	CTD	73.65535	117.17114	05.09.16	02:35:00		5.45		
LE16-22-MOBSI4	MOBSI	73.65535	117.17114	05.09.16	02:35:01	70	5.45		
LE16-22-CTD2	CTD	73.67241	117.17039	05.09.16	03:06:00		5.82		
LE16-22-MOBSI5	MOBSI	73.67241	117.17039	05.09.16	03:06:00	71	5.82		
LE16-22-CTD3	CTD	73.69159	117.17005	05.09.16	03:37:00		5.74		
LE16-22-MOBSI6	MOBSI	73.69159	117.17005	05.09.16	03:36:48	72	5.74		
LE16-22-Watersampling1	Watersampling	73.71058	117.17025	05.09.16	04:14:11		surface		ions; isotopes; methane
LE16-22-Watersampling2	Watersampling	73.71058	117.17025	05.09.16	04:14:11		1.4		cDOM; ions; isotopes; methane
LE16-22-Watersampling3	Watersampling	73.71058	117.17025	05.09.16	04:14:11		5		cDOM; ions; isotopes; methane
LE16-22-Watersampling4	Watersampling	73.71058	117.17025	05.09.16	04:14:11		6.16		cDOM; ions; isotopes; methane
LE16-22-CTD4	CTD	73.71058	117.17025	05.09.16	04:11:00		6.16		
LE16-22-MOBSI7	MOBSI	73.71058	117.17025	05.09.16	04:14:11	73.74	6.16	seal on cable	
LE16-22-CTD5	CTD	73.73880	117.16602	05.09.16	06:34:00		9.61		
LE16-22-MOBSI8	MOBSI	73.73880	117.16602	05.09.16	06:34:06	75	9.61		
LE16-22-CTD6	CTD	73.76513	117.16378	05.09.16	07:18:00		10.1		
LE16-22-MOBSI9	MOBSI	73.76513	117.16378	05.09.16	07:17:40	76	10.1		
LE16-22-Air	Methane Airsampling	73.71058	117.17025	05.09.16	04:14:11		-1		methane

Table A 3.1.-24: LE16-23

Station Name	Activity	Lat	Lon	Date	Time	Waterdepth (m)	Samples
LE16-23-1	CTD	73.63160	118.98890	05.09.2016	11:47:00	9.22	
LE16-23-2	Plankton	73.63160	118.98890	05.09.2016	11:55:00	9.22	isotopes, methane
LE16-23-3	Watersampling	73.63160	118.98890	05.09.2016	11:59:00	surface	methane

Table A 3.1.-25: LE16-24

Station Name	Activity	Lat	Lon	Date	Time	Waterdepth (m)	Comment	Samples
LE16-24-CTD1	CTD	72.29042	126.08268	06:09.2016	10:50:00	1.4	Temp 10.45 °C	
LE16-24-Watersampling1	Watersampling	72.29042	126.08268	06:09.2016	10:50:00	surface		cDOM; ions; isotopes; methane
LE16-24-Watersampling2	Watersampling	72.29042	126.08268	06:09.2016	10:50:00	1.7		cDOM; ions; isotopes; methane
LE16-24-Watersampling3	Watersampling	72.29042	126.08268	06:09.2016	10:50:00	7		cDOM; ions; isotopes; methane
LE16-24-Watersampling4	Watersampling	72.29042	126.08268	06:09.2016	10:50:00	8.4		cDOM; ions; isotopes; methane
LE16-24-Air	Methane Air sampling	72.29042	126.08268	06:09.2016	10:50:00	-1		methane
LE16-24-Plankton	Plankton	72.29042	126.08268	06:09.2016	10:50:00	0 - 8.4		plankton

Table A 3.1.-26: LE16-25

Station Name	Activity	Lat	Lon	Date	Time	Waterdepth (m)	Samples
LE16-25-CTD1	CTD	72.41058	126.88885	07.09.16	07:09:00	10.27	
LE16-25-Watersampling1	Watersample	72.41058	126.88885	07.09.16	07:09:00	surface	ions; isotopes; methane
LE16-25-Watersampling2	Watersample	72.41058	126.88885	07.09.16	07:09:00	2	ions; isotopes; methane; turbidity
LE16-25-Watersampling3	Watersample	72.41058	126.88885	07.09.16	07:09:00	8.4	ions; isotopes; methane; turbidity
LE16-25-Watersampling4	Watersample	72.41058	126.88885	07.09.16	07:09:00	9.35	ions; isotopes; methane
LE16-25-Air	Methane Airsampling	72.41058	126.88885	07.09.16	07:09:00	-1	methane

Table A 3.1.-27: LE16-26

Station Name	Activity	Lat	Lon	Date	Time	Waterdepth (m)	Comment	Samples
LE16-26-CTD1	CTD	72.23118	127.96187	07.09.16	10:24:00	12.47		
LE16-26-Watersampling1	Water Sample	72.23118	127.96187	07.09.16	10:24:00	surface		ions; isotopes; methane
LE16-26-Watersampling2	Water Sample	72.23118	127.96187	07.09.16	10:24:00	2.5		ions; isotopes; methane; turbidity
LE16-26-Watersampling3	Water Sample	72.23118	127.96187	07.09.16	10:24:00	10	strong drift	ions; isotopes; methane; turbidity
LE16-26-Air	Methane Air Sampling	72.23118	127.96187	07.09.16	10:24:00	-1		methane

Table A 3.1.-28: LE16-27

Station Name	Activity	Lat	Lon	Date	Time	Waterdepth (m)	Samples
LE16-27-CTD1	CTD	72.00485	129.09566	07.09.16	23:57:00		
LE16-27-Watersampling1	Water Sample	72.00485	129.09566	07.09.16	23:57:00	surface	ions; isotopes; methane
LE16-27-Watersampling2	Water Sample	72.00485	129.09566	07.09.16	23:57:00	1.65	ions; isotopes; methane; turbidity
LE16-27-Watersampling3	Water Sample	72.00485	129.09566	07.09.16	23:57:00	6.45	ions; isotopes; methane; turbidity
LE16-27-Watersampling4	Water Sample	72.00485	129.09566	07.09.16	23:57:00	8.32	ions; isotopes; methane
LE16-27-Sediment	Sediment	72.00485	129.09566	07.09.16	23:57:00	8.32	methane; pore size
LE16-27-Air	Methane Air Sampling	72.00485	129.09566	07.09.16	23:57:00	-1	methane

Table A 3.1.-29: LE16-28

Station Name	Activity	Lat	Lon	Date	Permafrost b.s.b. (cm)	Waterdepth (cm)
LE16-28-1	Permafrost probing	71.73424	129.40972	08.09.16	110	
LE16-28-2	Permafrost probing	71.73430	129.40979	08.09.16	150	
LE16-28-3	Permafrost probing	71.73439	129.40984	08.09.16	110	
LE16-28-4	Permafrost probing	71.73445	129.40989	08.09.16	90	
LE16-28-5	Permafrost probing	71.73451	129.40991	08.09.16	75	
LE16-28-6	Permafrost probing	71.73453	129.41003	08.09.16	80	
LE16-28-7	Permafrost probing	71.73467	129.41030	08.09.16	97	
LE16-28-8	Permafrost probing	71.73472	129.41050	08.09.16	95	
LE16-28-9	Permafrost probing	71.73481	129.41069	08.09.16	102	
LE16-28-10	Permafrost probing	71.73490	129.41087	08.09.16	120	
LE16-28-11	Permafrost probing	71.73493	129.41098	08.09.16	97	15
LE16-28-12	Permafrost probing	71.73506	129.41121	08.09.16	103	
LE16-28-13	Permafrost probing	71.73507	129.41125	08.09.16	95	
LE16-28-14	Permafrost probing	71.73532	129.41116	08.09.16	101	
LE16-28-15	Permafrost probing	71.73536	129.41158	08.09.16	95	55

Table A 3.1.-30: LE16-29

Station Name	Activity	Lat	Lon	Date	Time	comment	Samples
LE16-29-1	sediment core	71.73411	129.41125	09.09.16	01:28:51	8x methane, 8x sediment samples	DNA; DNA, enrichment; methane
LE16-29-2	porewater samples	71.73411	129.41125	09.09.16	01:28:51	8 depths	Fe2+; ions (anions); ions (cations); volatile fatty acids; water (pore) back up
LE16-29-3	sediment core	71.73512	129.40875	09.09.16	01:28:51	11x methane, 9x sediment samples	DNA; DNA, enrichment; methane
LE16-29-4	porewater samples	71.73512	129.40875	09.09.16	01:28:51	8 depths	Fe2+; ions (anions); ions (cations); volatile fatty acids; water (pore) back up

Table A 3.1.-31: LE16-30

Station Name	Activity	Lat	Lon	Date	Date Time	Record ID	Waterdepth (m)	Comment
LE16-30-CTD1	CTD	71.75318	129.38641	09.09.16	01:30:00		0.4	
LE16-30-25	MOBSI	71.75318	129.38641	09.09.16	01:28:51	1		1m offshore
LE16-30-CTD2	CTD	71.75276	129.38715	09.09.16	01:47:00		1.5	
LE16-30-26	MOBSI	71.75276	129.38715	09.09.16	01:45:13	2		
LE16-30-CTD3	CTD	71.75233	129.38767	09.09.16	01:54:00		1.24	
LE16-30-27	MOBSI	71.75233	129.38767	09.09.16	01:54:26	3		
LE16-30-CTD4	CTD	71.75191	129.38820	09.09.16	02:04:00		1.17	
LE16-30-28	MOBSI	71.75191	129.38820	09.09.16	02:04:45	4		
LE16-30-CTD5	CTD	71.75150	129.38869	09.09.16	02:12:00		1.31	
LE16-30-29	MOBSI	71.75150	129.38869	09.09.16	02:13:11	5		
LE16-30-CTD6	CTD	71.75070	129.39024	09.09.16	02:24:00		2.43	
LE16-30-30	MOBSI	71.75070	129.39024	09.09.16	02:22:16	7, 6		
LE16-30-CTD7	CTD	71.75027	129.39089	09.09.16	02:37:00		1.99	
LE16-30-31	MOBSI	71.75027	129.39089	09.09.16	02:37:03	8		
LE16-30-CTD8	CTD	71.74925	129.39338	09.09.16	02:51:00		2.77	
LE16-30-32	MOBSI	71.74925	129.39338	09.09.16	02:49:25	9		
LE16-30-CTD9	CTD	71.74801	129.39567	09.09.16	03:01:00		2.68	
LE16-30-33	MOBSI	71.74801	129.39567	09.09.16	03:01:05	10		
LE16-30-CTD10	CTD	71.74650	129.39924	09.09.16	03:13:00		2.57	
LE16-30-34	MOBSI	71.74650	129.39924	09.09.16	03:12:22	11		
LE16-30-CTD11	CTD	71.74457	129.40224	09.09.16	03:23:00		2.78	
LE16-30-Methane	Water Methane	71.74457	129.40224	09.09.16				
LE16-30-35	MOBSI	71.74457	129.40224	09.09.16	03:23:05	12		
LE16-30-CTD12	CTD	71.74253	129.40533	09.09.16	03:41:00		2.55	
LE16-30-36	MOBSI	71.74253	129.40533	09.09.16	03:41:17	13		

Station Name	Activity	Lat	Lon	Date	Date Time	Record ID	Waterdepth (m)	Comment
LE16-30-CTD13	CTD	71.74047	129.40908	09.09.16	03:53:00		2.78	
LE16-30-37	MOBSI	71.74047	129.40908	09.09.16	03:57:20	15		
LE16-30-CTD14	CTD	71.73941	129.41078	09.09.16	04:11:00		2.66	
LE16-30-38	MOBSI	71.73941	129.41078	09.09.16	04:10:49	16		
LE16-30-CTD15	CTD	71.73840	129.41292	09.09.16	04:22:00		2.63	
LE16-30-39	MOBSI	71.73840	129.41292	09.09.16	04:20:52	17		
LE16-30-CTD16	CTD	71.73787	129.41428	09.09.16	04:32:00		2.71	
LE16-30-40	MOBSI	71.73787	129.41428	09.09.16	04:30:15	18		
LE16-30-CTD17	CTD	71.73723	129.41626	09.09.16	04:47:00		2.71	
LE16-30-41	MOBSI	71.73723	129.41626	09.09.16	04:42:01	19		
LE16-30-CTD18	CTD	71.73625	129.41731	09.09.16	04:53:00		2.37	
LE16-30-42	MOBSI	71.73625	129.41731	09.09.16	04:52:29	20		
LE16-30-CTD19	CTD	71.73553	129.41793	09.09.16	05:00:00		0.38	
LE16-30-43	MOBSI	71.73553	129.41793	09.09.16	05:00:06	21		Permafrost: 0,65 bsb at shoreline
LE16-30-44	MOBSI	71.73541	129.41814	09.09.16	05:06:49	22		Permafrost: 0,85 bsb at shore
LE16-30-45	MOBSI	71.58868	129.83727	09.09.16	05:06:49	23	3.68	CTD Time: 10:35:00

Table A 3.1.-32: LE16-31

Station Name	Activity	Lat	Lon	Date	Time	Waterdepth (m)	Samples
LE16-31-CTD1	CTD	71.72868	129.41249	09.09.16	10:35:00	3.68	
LE16-31-2	water sampling	71.72868	129.41249	09.09.16	05:06:49	0.53	methane; isotopes; ions
LE16-31-3	water sampling	71.72868	129.41249	09.09.16	05:06:49	3.68	methane; isotopes; ions
LE16-31-4	air sampling	71.72868	129.41249	09.09.16	05:06:49	-1	methane

Table A 3.1.-33: LE16-32

Station Name	Activity	Lat	Lon	Date	Time	Record ID	Waterdepth (m)
LE16-32-CTD1	CTD	71.58868	129.83726	09.09.16	22:45:00		8.06
LE16-32-45	MOBSI	71.58868	129.83726	09.09.16	22:42:23	24	
LE16-32-CTD2	CTD	71.61200	129.82428	09.09.16	23:06:00		5.93
LE16-32-46	MOBSI	71.61200	129.82428	09.09.16	23:05:07	25	
LE16-32-CTD3	CTD	71.64262	129.91602	09.09.16	23:39:00		4.23
LE16-32-47	MOBSI	71.64262	129.91602	09.09.16	23:38:01	26	
LE16-32-CTD4	CTD	71.64126	129.99011	10.09.16	00:15:00		6.02
LE16-32-49	MOBSI	71.64126	129.99011	10.09.16	00:15:02	27	
LE16-32-CTD5	CTD	71.63189	130.04829	10.09.16	00:37:00		7.73
LE16-32-50	MOBSI	71.63189	130.04829	10.09.16	00:35:23	28	

Table A 3.1.-34: LE16-33

Station Name	Activity	Lat	Lon	Date	Time	Samples
LE16-33-1	Sediment Core	71.60451	129.95845	10.09.16	09:03:12	DNA; DNA, enrichment; methane, pore size;
LE16-33-2	Sediment for porewater	71.60451	129.95845	10.09.16	09:03:12	Fe2+; ions (anions); ions (cations); volatile fatty acids, water (pore) back up

A 4.1.-1: Lake and Permafrost

sample ID	Lat	long	core length [m]	water depth [m]	notes
BSC-LS-01	71.0606500°	121.7029333°	0.22	4.5	BSC-S-XX = sites
BSC-LS-02	71.0607667°	121.7030500°	0.3	4.5	BSC-LS-XX = lake
BSC-LS-03	71.0606500°	121.7029333°	0.22	4.5	BSC-W-XX = water
BSC-W-01	71.0606500°	121.7029333°		3.5	BSC-PS-XX = permafrost
BSC-W-02	71.0606500°	121.7029333°		3	
BSC-W-03	71.0606500°	121.7029333°		1	
BSC-W-04	71.025237°	121.680678°	Beenchime river water	0.1	
			top depth [m]	**bottom depth [m]**	
BSC-PS-01-01	71.0343333°	121.7059333°	0	0.05	BSC-S-05
BSC-PS-01-02	71.0343333°	121.7059333°	0.05	0.1	BSC-S-05
BSC-PS-01-03	71.0343333°	121.7059333°	0.15	0.2	BSC-S-05
BSC-PS-01-04	71.0343333°	121.7059333°	0.3	0.35	BSC-S-05
BSC-PS-01-05	71.0343333°	121.7059333°	0.45	0.5	BSC-S-05
BSC-PS-01-06	71.0343333°	121.7059333°	0.6	0.65	BSC-S-05
BSC-PS-01-07	71.0343333°	121.7059333°	0.75	0.8	BSC-S-05
BSC-PS-01-08	71.0343333°	121.7059333°	0.85	0.9	BSC-S-05
BSC-PS-01-09	71.0343333°	121.7059333°	1	1.15	BSC-S-05
BSC-PS-01-10	71.0343333°	121.7059333°	1.15	1.3	BSC-S-05
BSC-PS-01-11	71.0343333°	121.7059333°	1.3	1.4	BSC-S-05
BSC-PS-01-12	71.0343333°	121.7059333°	1.4	1.6	BSC-S-05
BSC-PS-01-13	71.0343333°	121.7059333°	1.6	1.65	BSC-S-05
BSC-PS-02-01	71.0469500°	121.6965833°	0	0.2	BSC-S-07
BSC-PS-02-02	71.0469500°	121.6965833°	0.2	0.3	BSC-S-07
BSC-PS-02-03	71.0469500°	121.6965833°	0.3	0.34	BSC-S-07
BSC-PS-02-04	71.0469500°	121.6965833°	0.34	0.4	BSC-S-07
BSC-PS-02-05	71.0469500°	121.6965833°	0.4	0.5	BSC-S-07

sample ID	Lat	long	core length [m]	water depth [m]	notes
BSC-PS-02-06	71.0469500°	121.6965833°	0.5	0.6	BSC-S-07
BSC-PS-02-07	71.0469500°	121.6965833°	0.6	0.75	BSC-S-07
BSC-PS-02-08	71.0469500°	121.6965833°	0.75	0.85	BSC-S-07
BSC-PS-02-09	71.0469500°	121.6965833°	0.85	0.92	BSC-S-07
BSC-PS-02-10	71.0469500°	121.6965833°	0.92	1.05	BSC-S-07
BSC-PS-02-11	71.0469500°	121.6965833°	1.05	1.12	BSC-S-07
BSC-PS-02-12	71.0469500°	121.6965833°	1.12	1.2	BSC-S-07
BSC-PS-02-13	71.0469500°	121.6965833°	1.2	1.25	BSC-S-07
BSC-PS-02-14	71.0469500°	121.6965833°	1.25	1.32	BSC-S-07
BSC-PS-02-15	71.0469500°	121.6965833°	1.32	1.4	BSC-S-07
BSC-PS-02-16	71.0469500°	121.6965833°	1.4	1.47	BSC-S-07
BSC-PS-02-17	71.0469500°	121.6965833°	1.47	1.52	BSC-S-07
BSC-PS-02-18	71.0469500°	121.6965833°	1.52	1.6	BSC-S-07
BSC-PS-02-19	71.0469500°	121.6965833°	1.6	1.7	BSC-S-07
BSC-PS-02-20	71.0469500°	121.6965833°	1.7	1.75	BSC-S-07
BSC-PS-03-01	71.0348833°	121.6872833°	0	0.03	BSC-S-08
BSC-PS-03-02	71.0348833°	121.6872833°	0.1	0.15	BSC-S-08
BSC-PS-03-03	71.0348833°	121.6872833°	0.26	0.3	BSC-S-08
BSC-PS-03-04	71.0348833°	121.6872833°	0.35	0.45	BSC-S-08
BSC-PS-03-05	71.0348833°	121.6872833°	0.55	0.6	BSC-S-08
BSC-PS-03-06	71.0348833°	121.6872833°	0.75	0.8	BSC-S-08
BSC-PS-04-01	71.0369333°	121.6948333°	0	0.05	BSC-S-09
BSC-PS-04-02	71.0369333°	121.6948333°	0.2	0.3	BSC-S-09
BSC-PS-04-03	71.0369333°	121.6948333°	0.5	0.6	BSC-S-09
BSC-PS-04-04	71.0369333°	121.6948333°	0.6	0.7	BSC-S-09
BSC-PS-04-05	71.0369333°	121.6948333°	0.8	0.85	BSC-S-09
BSC-PS-05A-01	71.0598000°	121.7061167°	0	0.03	BSC-S-10

sample ID	Lat	long	core length [m]	water depth [m]	notes
BSC-PS-05A-02	71.0598000°	121.7061167°	0.03	0.2	BSC-S-10
BSC-PS-05A-03	71.0598000°	121.7061167°	0.2	0.27	BSC-S-10
BSC-PS-05A-04	71.0598000°	121.7061167°	0.3	0.41	BSC-S-10
BSC-PS-05A-05	71.0598000°	121.7061167°	0.41	0.51	BSC-S-10
BSC-PS-05A-06	71.0598000°	121.7061167°	0.51	0.6	BSC-S-10
BSC-PS-05A-07	71.0598000°	121.7061167°	0.6	0.7	BSC-S-10
BSC-PS-05A-08	71.0598000°	121.7061167°	0.7	0.82	BSC-S-10
BSC-PS-05A-09	71.0598000°	121.7061167°	0.82	0.9	BSC-S-10
BSC-PS-05A-10	71.0598000°	121.7061167°	0.9	0.95	BSC-S-10
BSC-PS-05B-01	71.0598000°	121.7061167°	0	0.03	BSC-S-10
BSC-PS-05B-02	71.0598000°	121.7061167°	0.03	0.4	BSC-S-10
BSC-PS-05B-03	71.0598000°	121.7061167°	0.4	0.5	BSC-S-10
BSC-PS-05B-04	71.0598000°	121.7061167°	0.5	0.6	BSC-S-10
BSC-PS-05B-05	71.0598000°	121.7061167°	0.6	0.7	BSC-S-10

Table A 4.2.-1: Mineralogy

Sample ID	lat	long	ID extension	notes
BSC 16	71.0330833°	121.7585556°	1/1	breccia
BSC 17	71.0330833°	121.7585556°	1/2	breccia
BSC 18	71.0330833°	121.7585556°	1/3	breccia
BSC 19	71.0330833°	121.7585556°	1/4	breccia
BSC 20	71.0330833°	121.7585556°	1/5	breccia
BSC 21	71.0350000°	121.6830833°	2/1	sandstone
BSC 22	71.0350000°	121.6830833°	2/2	sandstone
BSC 23	71.0371111°	121.6039444°	3/1	limestone
BSC 24	71.0287778°	121.6801389°	4/1	sandstone, coarse-grained
BSC 25	71.0287778°	121.6801389°	4/2	sandstone, coarse-grained
BSC 26	71.0287778°	121.6801389°	4/3	sandstone, coarse-grained
BSC 27	71.0287778°	121.6801389°	4/5	sandstone, coarse-grained
BSC 28	71.0287778°	121.6801389°	4/6	sandstone, coarse-grained
BSC 29	71.0287778°	121.6801389°	4/7	sandstone, coarse-grained
BSC 30	71.0287778°	121.6801389°	4/9	sandstone, coarse-grained
BSC 31	71.0287778°	121.6801389°	4/10	sandstone, coarse-grained
BSC 32	71.0293611°	121.6788333°	5/1	breccia w/ ferrugination
BSC 33	71.0293611°	121.6788333°	5/2	breccia w/ ferrugination
BSC 34	71.0293611°	121.6788333°	5/3	breccia w/ ferrugination
BSC 35	71.0294167°	121.6749722°	6/1	limestone
BSC 36	71.0294167°	121.6749722°	6/2	limestone
BSC 37	71.0294167°	121.6749722°	6/3	limestone

Sample ID	lat	long	ID extension	notes
BSC 38	71.0293056°	121.6617778°	7/1	limestone
BSC 39	71.0293056°	121.6617778°	7/3	limestone
BSC 40	71.0296389°	121.6488889°	8/1	limestone
BSC 41	71.0296389°	121.6488889°	8/2	limestone
BSC 42	71.0295556°	121.6419167°	9/1	limestone
BSC 43	71.0295556°	121.6419167°	9/2	limestone
BSC 44	71.0285000°	121.6797500°	10/1	sandstone
BSC 45	71.0285000°	121.6797500°	10/2	sandstone
BSC 46	71.0285000°	121.6797500°	10/3	sandstone
BSC 47	71.0285000°	121.6797500°	10/4	sandstone
BSC 48	71.0285000°	121.6797500°	10/5	sandstone
BSC 49	71.0285000°	121.6797500°	10/6	sandstone
BSC 50	71.0186111°	121.7134722°	11/1	unknown
BSC 51	71.0186111°	121.7134722°	11/2	unknown
BSC 52	71.0558889°	121.7882778°	12/1	limestone
BSC 53	71.0558889°	121.7882778°	12/2	limestone
BSC 54	71.0607778°	121.7782778°	13/1	breccia
BSC 55	71.0607778°	121.7782778°	13/2	breccia
BSC 56	71.0607778°	121.7782778°	13/4	breccia
BSC 57	71.0607778°	121.7782778°	13/5	breccia
BSC 58	71.0607778°	121.7782778°	13/6	sandstone
BSC 59	71.0607778°	121.7782778°	13/7	unknown
BSC 60	71.0607778°	121.7782778°	13/8	breccia
BSC 61	71.0607778°	121.7782778°	13/9	breccia
BSC 62	71.0607778°	121.7782778°	13/10	breccia
BSC 63	71.0384444°	121.5673889°	14/1	breccia
BSC 64	71.0384444°	121.5673889°	14/2	breccia

Sample ID	lat	long	ID extension	notes
BSC 65	71.0384444°	121.5673889°	14/3	breccia
BSC 66	71.0384444°	121.5673889°	14/4	breccia
BSC 67	71.0433889°	121.5603889°	15/1	unknown
BSC 68	71.0433889°	121.5603889°	15/2	unknown
BSC 69	71.0491389°	121.5557778°	16/1	breccia
BS16	71.0210000°	121.7046111°	1	sediment sample
BS16	71.0183611°	121.7435833°	2	sediment sample
BS16	71.0292778°	121.6183333°	3	sediment sample
BS16	71.0297778°	121.7056389°	4	sediment sample
BS16	71.0205556°	121.6750833°	5	sediment sample
BS16	71.0235556°	121.6415278°	6	sediment sample
BS16	71.0186111°	121.7134722°	7/1	sediment sample
BS16	71.0186111°	121.7134722°	7/2	sediment sample
BS16	71.0620000°	121.5637778°	8/1	sediment sample
BS16	71.0620000°	121.5637778°	8/2	sediment sample

Table A 4.4.-1: Bedrock

Sample ID			sampling	sample description
1.1				camp
2.1	71.0453056°	121.7766389°	yes	bedding limestone eastern crater rim
2.2	71.0395278°	121.7687778°	yes	dolomite
2.3	71.0320556°	121.7620833°	no	dolomite
2.4	71.0330833°	121.9085278°	yes 2x	dolomitic breccia, polymictic breccia
3.1	71.0248889°	121.6741389°	no	red bedding limestone to the south
3.2	71.0238889°	121.6733889°	no	100 m to south at the slope
3.3			no	15 m downhill
3.4	71.0237222°	121.6707500°	no	around the cliff, ca. 40 m thick limestone banks
3.5	71.0241667°	121.6580556°	no	cliffs
3.6	71.0269167°	121.6781944°	no	red limestone
3.7			no	slightly tilted limestone
3.8	71.0275556°	121.6781389°	no	slightly tilted limestone
3.9			no	10 m to north
3.10			no	20 m to north
3.11	71.0286111°	121.6756944°	no	northflank, low dip angle, rotated
3.12	71.0350000°	121.6831667°	yes	ca. 400 m to north, autigenic breccia? small piece of sandstone
3.13	71.0405833°	121.6584167°	no	no breccia
4.1	71.0273056°	121.6407500°	no	400 m west from the camp, red limestones
4.2	71.0293611°	121.6184722°	no	red bedding limestones
4.3	71.0358611°	121.5923889°	no	search for allogenic breccia
4.4	71.0371111°	121.6039444°	no	plateau downhill, limestone event, brecciated
4.5	71.0509139°	121.6797472°	no	nothing at the inner crater wall
5.1	71°01´31.5´´	121°41´56,4´´	no	limestone opposite to the camp in eastern direction to the dolomites
5.2			yes	top of the carbonte hill, fine bedding, limestone breccia

Sample ID			sampling	sample description
5.3				
5.4	71.0333333°	121.7575556°	yes	dolomitic breccia
6.1	71.0293333°	121.6786944°	yes	limestone breccia at the house hill
6.2	71.0284722°	121.6799722°	yes	sandstone breccia block of Kesusinski suite
6.3	71.0299722°	121.7669167°	no	search for old drill hole
6.4	71.0297778°	121.7056389°	no	
7.1	71.0348833°	121.6872833°	yes	1. pit, country rock on top of sandbank, 2x impact melt, 1x striation, 1x polymictic impact beccia
7.2	71.0369333°	121.6948333°	no	2. pit
8.1	71.0355556°	121.7762500°	no	red bedding limestone at the white river
8.2			no	fossil erosion cut of river, red limestones
8.3	71.0558889°	121.7882778°	no	search for autigenic breccia at the top of the huge hill
8.4	71.0607500°	121.7784444°	yes	sandstone and sandstone breccia, limestone breccia, 1x sandstone; 1x large piece limestone breccia, 2x river polymictic breccia
9.1	71.0284722°	121.6799722°	yes	sandstone breccia at the north flank of our hill, transition sandstone to limestone
10.1			yes	limestone breccia from the SW hill southern flank
10.2			yes	breccia from the SW hill, northern flank
11.1	71.0250556°	121.6822583°	yes	riverside near camp surface sample bag
11.2	71.0250583°	121.6822611°	yes	riverside near camp surface sample bag

Table A 5.1.-1: Details on visited field locations for vegetation analyses. Values in grey were estimated for missing slopes or aspects from GPS points taken at the plot or for microrelief and vegetation cover from pictures. Vegetation cover in percent and '+' meaning some individuals and 'r' 1-2 individuals both without significant coverage <<1%.

ID	Lati-tude	Longitude	Elevation	Type	Grid size	Slope [m/10 m]	As-pect	Mikro-relief	*Al-nus*	*Pinus*	*Larix*	*Salix*
V 01	67,3 618	168,25 42	492	plot	r=15 m	2,50	S	40	<1	0	10	<1
V 02	67,3 660	168,23 66	559	plot	r=15 m	1,67	S	100	1	r	4	1
V 03	67,3 664	168,294 8	485	inten sive grid	24x2 6 m	5,00	SW	60	*0*	r	*8*	*0*
V 04	67,3 736	168,31 00	509	plot	r=15 m	2,57	SSW	50	0	5 0	6	0
V 05	67,3 769	168,31 22	584	plot	r=15 m	*6,89*	*SSO*	50	<1	2 0	2	<1
V 06	67,3 500	168,18 85	593	plot	r=15 m	3,00	N	50	3	3	*5*	3
V 07	67,3 456	168,18 42	692	plot	r=15 m	2,22	*WS W*	15	*0*	*0*	*0*	*0*
V 08	67,3 449	168,18 02	672	plot	r=15 m	1,67	SW	40	r	< 1	r	r
V 09	67,3 538	168,21 57	488	plot	r=15 m	0,67	SO	30	3	0	r	3
V 10	67,3 452	168,20 13	547	plot	r=15 m	5,14	SSO	50	0	1 0	4	0
V 11	67,3 500	168,20 09	600	plot	r=15 m	1,00	NOO	30	0	8	10	0
V 12	67,3 531	168,22 64	465	plot	r=15 m	0,67	*WS W*	60	r	0	7	r
V 13	66,9 731	163,41 77	134	grid	10x5 m	0,00		*20*	*0*	*0*	*70*	*0*
V 14	66,9 874	163,39 81	217	plot	r=15 m	0,10	S	*10*	20	0	3	35
V 15	66,9 914	163,38 43	249	plot	r=15 m	0,00		20	50	0	r	5
V 16	66,9 715	163,40 21	133	plot	r=15 m	0,00		35	0	0	7	20
V 17	66,9 869	163,45 50	153	inten sive grid	20x2 4 m	0,00		60	0	0	25	2
V 18	66,9 699	163,38 45	131	grid	10x5 m	0,00		50	0	0	50	<1
V 19	66,9 706	163,39 48	125	plot	r=15 m	0,50	*S*	50	0	0	20	5
V 20	65,9 249	166,36 09	662	plot	r=15 m	0,40	S	20	0	r	10	1
V 21	65,9 260	166,36 09	674	plot	r=15 m	0,40	S	20	6	r	5	<1
V 22	65,9 352	166,39 05	754	plot	r=15 m	3,00	S	50	3	5 0	<1	r
V	65,9	166,39	733	plot	r=15	6,67	SSO	20	1	6	0	0

ID	Lati-tude	Longitude	Elevation	Type	Grid size	Slope [m/10 m]	As-pect	Mikro-relief	*Al-nus*	*Pinus*	*Larix*	*Salix*
23	352	33			m					0		
V 24	65,9 365	166,38 90	788	plot	r=15 m	2,83	SW	20	0	r	0	0
V 25	65,9 372	166,39 06	804	plot	r=15 m	3,33	O	20	0	0	0	0
V 26	65,9 369	166,38 61	751	plot	r=15 m	2,50	W	10	0	1 0	20	0
V 27	65,9 369	166,38 50	733	plot	r=15 m	3,60	W	30	0	4	12	r
V 28	65,9 231	166,36 83	648	inten sive grid	36x3 6 m	0,67	S	*10*	*0*	*0*	*7*	*1*
V 29	65,9 252	166,38 82	666	plot	r=15 m	1,00	SSW	40	0	2, 5 0	5	2
V 30	65,9 579	166,33 33	719	plot	r=15 m	0,85	SW	60	0	0	r	10
V 31	65,9 585	166,33 68	746	plot	r=15 m	0,93	SW	50	0	0	r	3
V 32	65,9 468	166,35 61	737	plot	r=15 m	0,36	SO	10	0	0	1	1
V 33	65,9 459	166,35 77	722	plot	r=15 m	0,81	SOO	40	0	0	0	4
V 34	65,9 415	166,34 86	716	plot	r=15 m	1,06	SW	20	0	0	30	r
V 35	65,9 329	166,26 18	694	plot	r=15 m	3,09	WW S	30	0	r	30	1
V 36	65,9 294	166,29 10	781	plot	r=15 m	1,18	O	30	0	0	r	1
V 37	65,9 002	166,41 90	511	inten sive grid	24x2 4 m	0,00		60	0	r	20	4
V 38	65,9 003	166,41 68	511	plot	r=15 m	0,00		60	0	0	20	0
V 39	65,9 217	166,31 39	720	plot	r=15 m	1,07	WS W	50	0	1	20	2
V 40	67,7 969	168,70 96	644	plot	r=15 m	0,20	NW	30	0	0	0	0
V 41	67,8 171	168,68 65	657	plot	r=15 m	0,75	SW	30	0	0	0	0
V 42	67,8 171	168,68 85	657	plot	r=15 m	0,83	SO	40	0	0	0	0
V 43	67,8 195	168,69 76	646	plot	r=15 m	0,50	S	100	0	0	0	0
V 44	67,8 196	168,69 63	649	plot	r=15 m	0,20	SW	50	0	0	0	0
V 45	67,8 200	168,71 40	619	plot	r=15 m	0,00		25	0	0	0	1
V 46	67,8 199	168,71 15	622	plot	r=15 m	0,00		20	0	0	0	2
V 47	67,8 048	168,70 37	621	plot	r=15 m	1,00	*0NO*	10	0	0	0	15
V	67,8	168,63	748	plot	r=15	0,50	SO	40	0	0	0	2

ID	Lati-tude	Longitude	Elevation	Type	Grid size	Slope [m/10 m]	As-pect	Mikro-relief	*Al-nus*	*Pinus*	*Larix*	*Salix*
48	002	79			m							
V 49	67,8 026	168,63 59	786	plot	r=15 m	4,00	SSW	30	0	0	0	0
V 50	67,8 051	168,62 97	850	plot	r=15 m	3,33	SSO	25	0	0	0	+
V 51	67,8 055	168,63 27	910	plot	r=15 m	10,00	SW	50	0	0	0	0
V 52	67,8 069	168,63 11	920	plot	r=15 m	4,00	NNW	50	0	0	0	0
V 53	67,8 079	168,63 23	892	plot	r=15 m	13,33	NNW	40	0	0	0	r
V 54	67,8 096	168,62 99	873	plot	r=15 m	3,25	SW	40	0	0	0	r
V 55	67,8 091	168,63 36	863	plot	r=15 m	3,33	NNO	10	0	0	0	0
V 56	67,8 082	168,63 55	897	plot	r=15 m	4,22	N	10	0	0	0	0
V 57	67,8 076	168,64 50	736	plot	r=15 m	1,00	O	55	0	0	0	+
V 58	67,8 086	168,64 50	728	plot	r=15 m	0,56	O	30	0	0	0	+

Table A 5.1.-2: Details on sampled lakes. Additional information can be found in the online version of this table.

Lakes	Lat (°N)	Long (°E)	Max. dept (m)	Lake size (m x m)	Short cores	Long cores
16-KP-01-L01	67.37601	168.25443	4.7	700x600	16-KP-01-L01 Core A	16-KP-01-L01 Long 1
16-KP-01-L02-A	67.34148	168.30443	37	12000x2600	16-KP-01-L02 Core A, B, C	16-KP-01-L02 Long1
16-KP-01-L02-B	67.37798	168.35133	37	12000x2600	16-KP-01-L02core D,E,F	/
16-KP-01-L03	67.35303	168.18231	4.6	200x100	16-KP-01-L03 core A, B	/
16-KP-01-L04	67.35300	168.18230	3.2	150x80	16-KP-01-L04 core A	16-KP-01-L04 Long 1
16-KP-01-L05	67.35300	168.17249	6.1	50x50	16-KP-01-L05 Core A, B	/
16-KP-02-L06	66.96977	163.42265	2.3	200x200	16-KP-02-L06 Core A	16-KP-02-L06 Long 1
16-KP-02-L07	66.96423	163.40186	1.7	1000x500	16-KP-02-L07 core A	16-KP-02-L07 Long 1
16-KP-02-L08	66.97119	163.4425	4	300x300	16-KP-02-L08 Core A, B	/
16-KP-02-L09	66.97327	163.46121	2.4	500x500	/	/
16-KP-03-L10	65.93208	166.35152	57	6500x1500	16-KP-03-L10 core A, B,C,D,E	16-KP-03-L10 Long 1
16-KP-02-L11	65.93019	166.37842	17.5	300x300	16-KP-03-L11 core A	16-KP-03-L11 Long 1
16-KP-02-L12	65.92297	166.32713	28.7	100x200	/	/
16-KP-02-L13	65.91169	166.30676	20.7	700x200	16-KP-03-L13 core A	/
16-KP-02-L14	65.91650	166.29563	31m	3000x1000	/	/
16-KP-02-L15	65.894889	166.29208	14.6	200x200	16-KP-03-L15 Core A	/
16-KP-02-L16	65.90243	166.32498	20	200x150	/	/
16-KP-02-L17	65.90219	166.33243	21	200x150	16-KP-03-L17 core A	/
16-KP-02-L18	65.90616	166.34116	12.2	150x150	/	/
16-KP-02-L19	67.78876	168.73837	31	4000x1500	16-KP-04-L19 Core A, B, C, D	16-KP-04-L19 Long I, II
16-KP-02-L20	67.81298	168.71523	4	100x100	16-KP-04-L20 core A	16-KP-04-L20 Long I
16-KP-02-L21	67.80087	168.69608	5	150x150	16-KP-04-L21 Core A	/

Lakes	Lat (°N)	Long (°E)	Max. dept (m)	Lake size (m x m)	Short cores	Long cores
16-KP-02-L22	67.80452	168.69910	7.6	200x100	16-KP-04-L22 Core A	/

Table A 6.1.-1: Lake sediment samples retrieved during Expedition Yakutia 2016. Gear code: Grav UWITEC gravity corer; Rus Russian Peat Corer; Grab HYDRO-BIOS sediment grabber; Push UWITEC Push-tube.

Lake	Site/Core ID	Core Length ID	measured from	sample date	N (DecDeg)	E (DecDeg)	Gear	Water Depth (m)
Bety	PG2350	0-1 cm	sediment	2016-09-02	64.488	122.722033	Grab	1.6
Bety	PG2351	0-1 cm	sediment	2016-09-02	64.488067	122.7318	Grab	0.5
Bety	PG2352	0-1 cm	sediment	2016-09-02	64.488067	122.730567	Grab	0.8
Bety	PG2353	0-1 cm	sediment	2016-09-02	64.4919	122.723667	Grab	0.6
Bety	PG2354	0-1 cm	sediment	2016-09-02	64.492117	122.723517	Grab	0.6
Bety	PG2355	0-1 cm	sediment	2016-09-02	64.487367	122.712867	Grab	0.5
Bety	PG2356	0-1 cm	sediment	2016-09-02	64.487483	122.713467	Grab	0.6
Bety	PG2357	0-1 cm	sediment	2016-09-02	64.484717	122.72135	Grab	0.7
Bety	PG2358	0-1 cm	sediment	2016-09-02	64.485017	122.721267	Grab	0.4
Beti	PG2360-1	0-41 cm	sediment	2016-09-02	64.48795	122.72229	Grav	1.5
Beti	PG2360-2	0-60 cm	sediment	2016-09-02	64.48795	122.72229	Grav	1.5
Beti	PG2360-3	1.5-2.5 m	water surface	2016-09-02	64.48795	122.72229	Rus	1.5
Beti	PG2360-4	2.3-3.3 m	water surface	2016-09-02	64.48795	122.72229	Rus	1.5
Beti	PG2360-5	2.81-3.81 m	water surface	2016-09-02	64.48795	122.72229	Rus	1.5
Satagay	PG2361-1	0-34 cm	sediment	2016-09-03	64.4675	122.719833	Grav	1.5
Satagay	PG2361-2	0-41 cm	sediment	2016-09-03	64.4675	122.719833	Grav	1.5

Lake	Site/Core ID	Core Length ID	measured from	sample date	N (DecDeg)	E (DecDeg)	Gear	Water Depth (m)
Satagay	PG2361-1/12	1.5-9.7 m	water surface	2016-09-03	64.4675	122.719833	Rus	1.5
Satagay	PG2362	0-1 cm	sediment	2016-09-03	64.472	122.717367	Grab	0.7
Satagay	PG2362-1	0-100, 100-149 m	sediment	2016-09-04	64.467517	122.7168	Push	1.4
Satagay	PG2362-2/14	1.5-11.91 m	water surface	2016-09-04	64.467517	122.7168	Rus	1.4
Satagay	PG2363	0-1 cm	sediment	2016-09-03	64.472333	122.717683	Grab	0.5
Satagay	PG2363-1/12	1.5-11.25 m	water surface	2016-09-04	64.467633	122.71665	Rus	1.4
Satagay	PG2364	0-1 cm	sediment	2016-09-03	64.46715	122.696267	Grab	0.7
Satagay	PG2364-1	0-100, 100-126 cm	sediment	2016-09-04	64.4677	122.716867	Push	1.4
Satagay	PG2364-2	0-100, 100-136 cm	sediment	2016-09-04	64.4677	122.716867	Push	1.4
Satagay	PG2365	0-57 cm	sediment	2016-09-04	64.472033	122.720733	Rus	0
Satagay	PG2365	0-1 cm	sediment	2016-09-03	64.467183	122.695533	Grab	0.5
Satagay	PG2366	0-63 cm	sediment	2016-09-04	no value	no value	Rus	0
Satagay	PG2366	0-1 cm	sediment	2016-09-03	64.464183	122.724267	Grab	0.5
Satagay	PG2367	0-1 cm	sediment	2016-09-03	64.464733	122.7251	Grab	0.8
Liunkju	PG2367-1	0-60 cm	sediment	2016-09-05	64.55355	122.729683	Grav	11.5

Lake	Site/Core ID	Core Length ID	measured from	sample date	N (DecDeg)	E (DecDeg)	Gear	Water Depth (m)
Liunkju	PG2367-2	0-100, 100-133 cm	sediment	2016-09-05	64.55355	122.729683	Push	
Satagay	PG2368	0-1 cm	sediment	2016-09-03	64.470767	122.733567	Grab	0.7
Satagay	PG2369	0-1 cm	sediment	2016-09-03	64.470867	122.733467	Grab	0.7
Grav: UWITEC gravity corer	Rus: Russian Peat Corer		Grab: HYDRO-BIOS sediment grabber		Push: UWITEC Push-tube			

Table A 6.1.-2: Parameters of lakes studied during Expedition Yakutia 2016

Paramter/Lake	Satagay	Bety	Liunkju
Coordinates	64.4713 N, 122,7317 E	64.4880 N, 122,7220 E	64.5523 N, 122,7290 E
Elevation, m	178	181	202
Max Water Depth, m	1.6	1.6	16.0
Mean Water Depth, m	1	0.6	8.5
Length, km	2.3	1.27	0.32
Lake area, km^2	2	0.86	0.05
Origin	Thermokarst	Thermokarst	Crater ?
Catchment vegetation	*Larix dahurica Betula pendula* *Cyperaceae, Poaceae, Phragmites australis, Sphagnum*	*Larix dahurica, Betula pendula.* Coastal swamp. Dominance *Cyperaceae, Poaceae, Phragmites australis, Scolochloa festucácea, Sphagnum*	*Larix dahurica, Betula nana, Ledum palustre/ Rhododendron tomentosum, Phragmites australis, Sphagnum*
Mean $T_{January}$, °C	- 38		
Mean T_{July}, °C	+17.5		
Ice-free period	130 days		
Annual precipitation	250 mm		

Die **Berichte zur Polar- und Meeresforschung** (ISSN 1866-3192) werden beginnend mit dem Band 569 (2008) als Open-Access-Publikation herausgegeben. Ein Verzeichnis aller Bände einschließlich der Druckausgaben (ISSN 1618-3193, Band 377-568, von 2000 bis 2008) sowie der früheren **Berichte zur Polarforschung** (ISSN 0176-5027, Band 1-376, von 1981 bis 2000) befindet sich im electronic Publication Information Center **(ePIC)** des Alfred-Wegener-Instituts, Helmholtz-Zentrum für Polar- und Meeresforschung (AWI); see http://epic.awi.de. Durch Auswahl “Reports on Polar- and Marine Research“ (via “browse”/”type”) wird eine Liste der Publikationen, sortiert nach Bandnummer, innerhalb der absteigenden chronologischen Reihenfolge der Jahrgänge mit Verweis auf das jeweilige pdf-Symbol zum Herunterladen angezeigt.

The **Reports on Polar and Marine Research** (ISSN 1866-3192) are available as open access publications since 2008. A table of all volumes including the printed issues (ISSN 1618-3193, Vol. 377-568, from 2000 until 2008), as well as the earlier **Reports on Polar Research** (ISSN 0176-5027, Vol. 1-376, from 1981 until 2000) is provided by the electronic Publication Information Center **(ePIC)** of the Alfred Wegener Institute, Helmholtz Centre for Polar and Marine Research (AWI); see URL http://epic.awi.de. To generate a list of all Reports, use the URL http://epic.awi.de and select “browse”/ ”type” to browse ”Reports on Polar and Marine Research”. A chronological list in declining order will be presented, and pdf-icons displayed for downloading.

Zuletzt erschienene Ausgaben:

Recently published issues:

709 (2017) Russian-German Cooperation: Expeditions to Siberia in 2016, edited by Pier Paul Overduin, Franziska Blender, Dmitry Y. Bolshiyanov, Mikhail N. Grigoriev, Anne Morgenstern, Hanno Meyer

708 (2017) The role of atmospheric circulation patterns on the variability of ice core constitutents in coastal Dronning Maud Land, Antarctica, by Kerstin Schmidt

707 (2017) Distribution patterns and migratory behavior of Antarctic blue whales, by Karolin Thomisch

706 (2017) The Expedition PS101 of the Research Vessel POLARSTERN to the Arctic Ocean in 2016, edited by Antje Boetius and Autun Purser

705 (2017) The Expedition PS100 of the Research Vessel POLARSTERN to the Fram Strait in 2016, edited by Torsten Kanzow

704 (2016) The Expeditions PS99.1 and PS99.2 of the Research Vessel POLARSTERN to the Fram Strait in 2016, edited by Thomas Soltwedel

703 (2016) The Expedition PS94 of the Research Vessel POLARSTERN to the central Arctic Ocean in 2015, edited by Ursula Schauer

702 (2016) The Expeditions PS95.1 and PS95.2 of the Research Vessel POLARSTERN to the Atlantic Ocean in 2015, edited by Rainer Knust and Karin Lochte

701 (2016) The Expedition PS97 of the Research Vessel POLARSTERN to the Drake Passage in 2016, edited by Frank Lamy

700 (2016) The Expedition PS96 of the Research Vessel POLARSTERN to the southern Weddell Sea in 2015/2016, edited by Michael Schröder

699 (2016) Die Tagebücher Alfred Wegeners zur Danmark-Expedition 1906/08, herausgegeben von Reinhard A. Krause

ALFRED-WEGENER-INSTITUT
HELMHOLTZ-ZENTRUM FÜR POLAR-
UND MEERESFORSCHUNG

BREMERHAVEN

Am Handelshafen 12
27570 Bremerhaven
Telefon 0471 4831-0
Telefax 0471 4831-1149
www.awi.de

HELMHOLTZ
GEMEINSCHAFT